THE UNIVERSITY OF MICHIGAN

COLLEGE OF ENGINEERING
Department of Meteorology and Oceanography

Technical Report

PARTICLE SIZE DISTRIBUTIONS OF TRACE ELEMENTS IN POLLUTION AEROSOLS

Gordon D. Nifong

John W. Winchester
Project Director

ORA Project 08903

under contract with:

U. S. ATOMIC ENERGY COMMISSION
CHICAGO OPERATIONS OFFICE
CONTRACT NO. AT(11-1)-1705
ARGONNE, ILLINOIS

administered through:

OFFICE OF RESEARCH ADMINISTRATION ANN ARBOR

August 1970

TABLE OF CONTENTS

		Page
LIST OF TABLES		v
LIST OF FIGURES		vii
CHAPTER I	INTRODUCTION	1
CHAPTER II	EXPERIMENTAL DESIGN	15
CHAPTER III	SAMPLING APPARATUS AND ANALYTICAL PROCEDURES	23
	A. SAMPLE COLLECTION	23
	B. NEUTRON ACTIVATION ANALYSIS	32
	C. ATOMIC ABSORPTION SPECTROSCOPY	37
	D. COMPARISON OF METHODS	40
CHAPTER IV	RESULTS AND THEIR INTERPRETATION	56
	A. INTRODUCTION	56
	B. GROUPINGS BY PARTICLE SIZE DISTRIBUTIONS	58
	1. Iron, Manganese, Chromium, Cobalt, Scandium, and Thorium	58
	2. Zinc, Antimony, Arsenic, and Indium	84
	3. Copper	106
	4. Calcium, Magnesium, Titanium	113
	5. Aluminum and Rare Earths	123
	6. Bromine, Gallium, Potassium	136

TABLE OF CONTENTS (continued)

		Page
	7. Sodium and Chlorine	148
	8. Vanadium	160
	9. Miscellaneous Elements	167
	10. Total Aerosol Samples	169
	C. PROPERTIES AND USES OF ELEMENTS	172
	D. ATMOSPHERIC RESIDENCE TIMES	174
	E. TRACERS	179
CHAPTER V	CONCLUSIONS	195
SELECTED BIBLIOGRAPHY		202
APPENDIX		207
	A. Data	208
	B. Water Pollution in Lake Michigan by Trace Elements from Pollution Aerosol Fallout (Abstract)	263

LIST OF TABLES

Table		Page
1	Concentration and Size of Certain Metals in Ambient Aerosols	3
2	Comparison of Air Pollution Inventory with River Inflow of Trace Elements to Lake Michigan	14
3	Calibration of the Andersen Sampler 50% Cut Off Diameters	28
4	Percent of Total Mass vs. Andersen Sampler Stage for the "Junge" Distribution	28
5	Atomic Absorption Spectrophotometer Operating Parameters	39
6	Mass and Mass Ratio by Duplicate Analysis	42
7	Mass and Mass Ratio by Different Counting Times	43
8	Mass and Mass Ratio by Analytical Method	44
9	Mass and Mass Ratio by Duplicate Sample Run	45
10	Average Mass of Elements as Per Cent of Total Aerosol Mass	171
11	Classification of Elements by Size, Chemical Properties, and Uses	173
12	Melting Points and Solubilities in Water for Common Compounds	175
13	Elemental Settling Times	178
14	Details of Sample Runs	208
15	Meteorological Conditions for Sample Runs	210
16	Impactor Stage and Filter Materials Used	211
17	Impactor Stage and Filter Impurity Levels	212
18	Nuclear Properties and Measurement of Short-Lived Isotopes	213
19	Nuclear Properties and Measurement of Long-Lived Isotopes	214

LIST OF TABLES (continued)

Table		Page
20	**Limits of Detection for Determination of Trace Elements in Aerosols**	216
21	Open Hearth Vicinity	217
22	Sinter Plant Vicinity	221
23	Blast Furnace Vicinity	224
24	Central Fire Station, East Chicago, Indiana	225
25	Markstown Park, East Chicago, Indiana	232
26	Field School, East Chicago, Indiana	237
27	Wirt School, Gary, Indiana	240
28	Gary Airport, Gary, Indiana	242
29	Central Fire Station, Gary, Indiana	248
30	City Hall, Hammond, Indiana	250
31	Lake Michigan	252
32	School of Public Health, The University of Michigan, Ann Arbor, Michigan	256
33	"High Volume" Sample Runs	259

LIST OF FIGURES

Figure		Page
1	Urban Sampling Locations in Northwest Indiana	22
2	Schematic view of Andersen Sampler, Model 0203	25
3	Duplicate Analyses by Atomic Absorption Spectroscopy, Run 29	46
4	Duplicate Analyses by Neutron Activation, Run 4	47
5	Duplicate Analyses by Neutron Activation, Run 4	48
6	Duplicate Analyses by Neutron Activation, Run 43	49
7	Duplicate Analyses by Analytical Method, by 4000-sec. Neutron Activation and by Atomic Absorption, Run 22	50
8	Duplicate Analyses by Analytical Method, by 2000- and 4000-sec. Neutron Activation, and by Atomic Absorption, Run 22	51
9	Duplicate Samples, Run 21	52
10	Duplicate Samples, Run 21	53
11	Duplicate Samples, Run 35	54
12	Duplicate Samples, Run 35	55
13	Run 19, East Chicago Central Fire Station	67
14	Run 22, East Chicago Markstown Park	68
15	Run 19, East Chicago Central Fire Station, and Run 22, East Chicago Markstown Park	69
16	Run 27, Gary Wirt School	70
17	Run 49, Ann Arbor	71
18	Run 49, Ann Arbor	72
19	Runs 42, 43 & 44, Lake Michigan	73

LIST OF FIGURES (continued)

Figure		Page
20	Runs 2 & 4, Open Hearth Vicinity	74
21	Run 2, Open Hearth Vicinity; and Run 7, Sinter Plant Vicinity	75
22	Runs 7-9, Sinter Plant Vicinity	76
23	Runs 7-9, Sinter Plant Vicinity	77
24	Runs 31-35, Gary Airport	78
25	Runs 31-35, Gary Airport	79
26	Runs 31-34, Gary Airport	80
27	Runs 17 & 18, East Chicago Central Fire Station	81
28	Runs 23-25, East Chicago Field School	82
29	Runs 20 & 21, East Chicago Markstown Park	83
30	Run 19, East Chicago Central Fire Station	91
31	Run 22, East Chicago Markstown Park	92
32	Run 19, East Chicago Central Fire Station	93
33	Run 27, Gary Wirt School	94
34	Run 42, Lake Michigan	95
35	Run 43, Lake Michigan	96
36	Run 44, Lake Michigan	97
37	Runs 2-4, Open Hearth Vicinity	98
38	Runs 7-10, Sinter Plant Vicinity	99
39	Runs 23-26, East Chicago Field School	100
40	Runs 20 & 21, East Chicago Markstown Park	101
41	Runs 15-18, East Chicago Central Fire Station	102
42	Runs 36 & 38, Gary Central Fire Station	103

LIST OF FIGURES (continued)

Figure		Page
43	Runs 31-35, Gary Airport	104
44	Runs 45 & 49, Ann Arbor	105
45	Runs 42-44, Lake Michigan	111
46	Runs 20 & 21, East Chicago Markstown Park; and Runs 31 & 35, Gary Airport	112
47	Run 19, East Chicago Central Fire Station	116
48	Run 22, East Chicago Markstown Park	117
49	Run 9, Sinter Plant Vicinity	118
50	Run 4, Open Hearth Vicinity	119
51	Run 27, Gary Wirt School	120
52	Runs 33 & 35, Gary Airport	121
53	Runs 42 & 43, Lake Michigan	122
54	Run 27, Gary Wirt School	126
55	Run 19, East Chicago Central Fire Station	127
56	Run 22, East Chicago Markstown Park	128
57	Runs 2-4, Open Hearth Vicinity	129
58	Runs 7-10, Sinter Plant Vicinity	130
59	Runs 20 & 21, East Chicago Markstown Park	131
60	Runs 23-26, East Chicago Field School	132
61	Runs 15-17, East Chicago Central Fire Station	133
62	Runs 31-35, Gary Airport	134
63	Run 49, Ann Arbor	135
64	Run 19, East Chicago Central Fire Station	140
65	Run 22, East Chicago Markstown Park	141
66	Run 27, Gary Wirt School	142

LIST OF FIGURES (continued)

Figure		Page
67	Runs 2-4, Open Hearth Vicinity	143
68	Runs 7-10, Sinter Plant Vicinity	144
69	Run 21, East Chicago Markstown Park	145
70	Runs 15-18, East Chicago Central Fire Station	146
71	Runs 36 & 38, Gary Central Fire Station; and Runs 42 & 43, Lake Michigan	147
72	Run 19, East Chicago Central Fire Station	151
73	Run 22, East Chicago, Markstown Park	152
74	Run 27, Gary Wirt School	153
75	Runs 33 & 35, Gary Airport	154
76	Runs 17 & 18, East Chicago Central Fire Station	155
77	Run 20, East Chicago Markstown Park; and Run 25, East Chicago Field School	156
78	Run 4, Open Hearth Vicinity; and Run 9, Sinter Plant Vicinity	157
79	Runs 42 & 44, Lake Michigan	158
80	Run 4, Open Hearth Vicinity; Run 7, Sinter Plant Vicinity; Run 27, Gary Wirt School; and Run 30, Gary Airport	159
81	Run 27, Gary Wirt School; Runs 31-35, Gary Airport	162
82	Run 19, East Chicago Central Fire Station; and Run 22, East Chicago Markstown Park	163
83	Runs 20 & 21, East Chicago Markstown Park; and Run 23, East Chicago Field School	164
84	Runs 42 & 44, Lake Michigan	165
85	Runs 15, 17 & 18, East Chicago Central Fire Station	166
86	Run 19, East Chicago Central Fire Station	168

LIST OF FIGURES (continued)

Figure		Page
87	Iron, total aerosol averages	184
88	Manganese, total aerosol averages	185
89	Copper, total aerosol averages	186
90	Zinc, total aerosol averages	187
91	Aluminum, total aerosol averages	188
92	Chlorine, total aerosol averages	189
93	Potassium, total aerosol averages	190
94	Vanadium, total aerosol averages	191
95	Antimony-to-Zinc ratios—(A) Run 19, East Chicago Central Fire Station; (B) Runs 2-4, Open Hearth Vicinity; (C) Run 27, Gary Wirt School	192
96	Manganese-to-Iron ratios—(A) Run 27, Gary Wirt School; (B) Run 4, Open Hearth Vicinity; (C) Run 7, Sinter Plant Vicinity; (D) Run 19, East Chicago Central Fire Station	193
97	Chloride-to-Sodium ratios—(A) Run 9, Sinter Plant Vicinity; (B) Run 33, Gary Airport; (C) Run 4, Open Hearth Vicinity; (D) Run 25, East Chicago Field School	194

CHAPTER I

INTRODUCTION

Aerosols are suspensions of liquid or solid airborne particles, important because they may influence cloud and rain formation by nucleating cloud-droplets and ice crystals (Fletcher, 1962), may affect visibility and air temperature by absorbing and scattering radiation (U.S. Department of Health, Education, and Welfare, 1969), may present a health hazard upon being deposited in the respiratory tree (Cadle, 1965), and may cause economic loss through damage to livestock, plants, and materials. To better understand these roles, aerosol concentration, composition, and particle size distribution must be considered.

Considerable interest has arisen in recent years among persons involved in the study of urban air pollution about the composition of aerosol particles. But most aerosol measurements performed involve simply a determination of total particulate concentration by weight as collected on some type of filter, despite the fact that such "high-volume sample" results are dominated by the larger particle sizes, whereas smaller sizes are often of more interest from an effects standpoint. A strong interest exists in the area of particle-size distribution of aerosols, and this field is under intensive study (Whitby, 1969). Measurements of composition usually involve the determination of certain trace metals by emission spectroscopy upon total suspended particulate matter (U.S. Department of Health,

Education, and Welfare, 1966). But links between these two types of measurements have been scarce, despite the fact that such observations might prove quite valuable to toxicologists in better understanding possible public health hazards associated with urban air pollution, for an element carried by particles of respirable size may have toxicity effects which depend on particle size and indirectly on water solubility and ambient relative humidity. Also, such observations should prove equally valuable in identifying source processes and evaluating their contribution to local air pollution levels, in better understanding changes occurring in aerosols during their residence in the atmosphere, and, finally, in considering mechanisms by which aerosols are removed from the atmosphere. Thus a measure of distributions by mass of specific elemental components of aerosols according to particle size-fraction should prove valuable in evaluating aerosol generation processes, "life cycle," and effects. It has been the purpose of this research project to perform such measurements and to use the data obtained in order to better understand the aerosol in the ways discussed above.

As has been mentioned, current knowledge of the relationship between composition and particle size of atmospheric aerosols, especially close to a large industrial area source, is definitely limited. In addition to data on metal components of <u>total</u> suspended particulate matter in the atmosphere, such as that reported by the U. S. Public Health Service (1966), investigators such as Junge (1963) and

Friedlander (1960) have remarked extensively on the particle size distribution of aerosols. Work linking the two concepts is not extensive. Lee, Patterson, and Wagman (1968) of the National Air Pollution Control Administration used the Andersen Cascade Impactor to sample for aerosols in the cities of Cincinnati and Fairfax, Ohio. Atomic absorption spectroscopy was used to determine concentrations of 6 metals—iron, lead, cadmium, magnesium, copper, and chromium—in the air. They reported total concentration of each metal in the atmosphere, and presented graphs showing concentration over each size range. Also calculated for each metal were mass median diameters for aerodynamically equivalent spheres of unit density. Results of their study are shown in Table 1.

TABLE 1

CONCENTRATION AND SIZE OF CERTAIN METALS IN AMBIENT AEROSOLS (after Lee et al., 1968).

	Cincinnati, Ohio		Fairfax, Ohio	
	$\mu g/m^3$	MMD, μm	$\mu g/m^3$	MMD, μm
Fe	3.12	3.7	1.15	1.4
Cd	0.08	3.1	0.02	10
Mg	7.21	4.5	0.42	7.2
Cr	0.31	1.5	0.28	1.9
Pb	2.78	0.18	0.69	0.42
Cu	0.19	1.2	0.04	--

A major limitation of these data was the limited sensitivity of atomic absorption spectroscopy. Another limitation was in the small number of sampling locations available, with a resulting lack of data on areas of varying

commercial and industrial activities. Other investigators have indicated the need for information of aerosol composition as a function of particle size. Corn (1969), Whitby (1969), Mirsky (1969), Wagman (1966, 1967), and Faith (1964) all point out the great emphasis beginning to be placed on this particular type of air pollution research by governmental agencies and universities.

Junge (1963) and Wagman (1966) in particular have stressed the importance of composition of aerosols as a function of their size in understanding mechanisms of their formation and in characterizing their sources. For example, certain trace elements (silicon, calcium, magnesium) can be of natural origin, whereas others (lead, manganese, copper, zinc) are usually due to man-made pollution sources. A few (iron, aluminum) may arise from both. Particles of relatively large size tend to be generated as a result of mechanical forces, and are termed dispersion aerosols. Smaller-sized particles are usually products of combustion, arise by vapor condensation due to high supersaturation conditions, and are termed condensation aerosols. Dispersion aerosols are easily formed in sizes larger than about 1 μm, but only with difficulty in smaller sizes where surface free energy becomes appreciable and may inhibit further disintegration. Condensation aerosols, on the other hand, are usually less than 1 μm when formed. Thus, when an aerosol is very near its source, but airborne, the characteristics of the source largely determine the particle size distribution.

With respect to their sources and to the atmospheric processes which modify, often quite rapidly, elemental components of aerosols, particle size distribution is a key parameter. Junge (1963) has chosen to express the distribution as the number or volume of aerosol particles per unit logarithmic size-range. He has also recognized a "universal" mean distribution for atmospheric aerosols in populated continental areas. The "Junge distribution," n(r), can be approximated by

$$n(r) = \frac{dN}{d(\log r)} = C \cdot r^{-\beta} \qquad 0.1\ \mu m < r < 10\ \mu m$$

where N is the number of particles of radius less than r, C is a scaling factor, and the empirical constant $\beta \approx 3$.

This regularity of particle spectra in the atmosphere is applicable to the "stable" aerosol particle size range, including "large" particles 0.1 to 1 μm in radius and "giant" particles 1 to 10 μm in radius. Particles smaller than 0.1 μm coagulate rapidly, and in a sense serve as a source of larger-sized particles; particles greater than 10 μm fall out of the atmosphere rapidly, as the Stokes settling velocity for such sizes is generally greater than atmospheric turbulence motions.

Following Junge (1963), aerosol surface area and volume distributions are expressed as

$$s(r) = 4\pi r^2 n(r)$$

and

$$v(r) = \frac{4}{3}\pi r^3 n(r)$$

respectively. Then the "Junge surface area distribution" is

$$s(r) = 4\pi r^2 \cdot C \cdot r^{-3} = B \cdot r^{-1}$$

and the "Junge volume distribution" is

$$v(r) = \frac{4}{3}\pi r^3 \cdot C \cdot r^{-3} = B'$$

where B and B' are scaling factors. Hence the size distribution of aerosol surface area is observed to vary inversely with particle size while the size distribution of aerosol volume is observed to be constant with particle size. Since mass is a function of density times r^3, the "Junge mass distribution" is

$$m(r) = \frac{4}{3}\pi^3 \cdot d \cdot C \cdot r^{-3} = B'$$

where d = particle density.

Or, if density is constant,

$$\frac{dM}{d(\log r)} = \text{Constant},$$

where M is the mass concentration of particles less than size r.

Friedlander (1960) has offered a dimensional analysis similarity theory in explanation of the occurrence of the "Junge distribution." This theory involves dynamic

equilibrium between processes of formation and loss, or between coagulation and sedimentation of aerosol particles. Such a distribution shows an upper and lower size limit. The upper size limit, ≈ 10 μm, is largely determined by sedimentation, but this involves the density, hence the composition, of the particles, in addition to size. The lower size limit, ≈ 0.1 μm, is considered a result of coagulation, involving particle surface area, or size and shape, and possibly chemical reactions between particles, which are dependent on size and composition. Since the surface-to-mass ratio is greater for small particles than for large ones, coagulation is more likely to occur on small particles than on large. Also, smaller particles may be more reactive than the larger.

Junge (1969) suggests that such a dynamic equilibrium cannot generally be approached over the requisite size range, 0.1 to 10 μm, at a rate faster than the rate of change of meteorological conditions. Coagulation is rapid for particles < 0.1 μm, but slow for particles > 0.1 μm. The observed distribution arises not by heterogeneous coagulation so much as by the mixing (without coagulation) of aerosols from many independent sources both natural and man-made. The situation is such that the aerosol populations from each source may be distributed approximately log-normally in volume (as dispersion aerosols tend to be (Fletcher, 1962)), and that the resultant mixture might display a broad log-normal distribution, nearly constant over the stable

aerosol range. But there is a distinction between an expected "Junge distribution" for a multi-elemental aerosol distribution and a "Junge distribution" for any one of that aerosol's elemental components. The presence of a "Junge distribution" of total aerosol indicates the same distribution for one element in that aerosol only if the percentage of that element is constant within particles of all size ranges. Even though this is probably not the case for most elements, the "Junge distribution" can still serve as a useful index of comparison when considering elemental distribution according to particle size range.

Aerosol composition determines its water solubility, and solubility is exceedingly important to the future life of the aerosol. Junge (1963) has stated that as little as 1% or as much as 30% of continental aerosols may be water-soluble. Small water-soluble aerosols tend to grow, given proper relative humidity, and hence the "solute effect" is quite important in determining final size of an aerosol droplet. Such particles make excellent condensation nuclei. But if the particle is insoluble, no "solute effect" will exist, and essentially radius-of-curvature is predominant in determining final particle size (Fleagle and Businger, 1963; U.S. Department of Health, Education, and Welfare, 1969). In a region heavily polluted, such as the region studied during this project, it is likely that a large fraction of the total aerosol is inorganic in nature, perhaps resulting in a larger percentage of soluble material than

is often found. This idea is not in conflict with the high degree of adherence to the "Junge distribution" found for many elements.

Aerosol particles are eventually removed from the atmosphere by either dry or wet fallout. Wet fallout may occur by washout below the cloud (giant particles where $r > 1$ μm), by attachment to droplets within the cloud (Aitken particles), or by cloud-droplet nucleation and subsequent rainout. Rainout is likely the important process (Junge, 1963). In an area of strong pollution sources, considering that rainfall occurs only a small fraction of the time, gravitational settling may be an important mechanism of aerosol particle removal from the atmosphere, but perhaps for only giant ($r > 1$ μm) particles. Hewson (1964) states that for any specific plume, rainout is not important, and most particles undergo dry removal by turbulent impaction caused by small swirling eddies of air near the ground.

Dry removal, or dry fallout, may be by several mechanisms. For particles of diameters greater than 10 μm, Stokes settling may occur, but for smaller diameters, impaction, electrostatic forces, and turbulent air motions may all operate in a complex and poorly understood process (Slade, 1968). The Stokes settling velocity is defined as:

$$V_s = \frac{2 \cdot r^2 \cdot g \cdot \rho}{9 \cdot u}$$, where

V_s = Stokes settling velocity

r = particle radius

g = acceleration of gravity

ρ = particle density

μ = atmospheric dynamic viscosity

The above formula is for smooth spheres and neglects effects of buoyancy and slip flow. Irregular particle shape also reduces V_s by about two-thirds from that of spheres.

For particles about 10 μm in diameter, a settling velocity (V_s) $\approx$ 1 cm/sec is not unreasonable (Slade, 1968). If V_s < 1 cm/sec, the effect of sedimentation is negligible, and thus for particles < 10 μm diameter, other mechanisms of dry removal, turbulence and impaction, predominate. If V_s is between 1 and 100 cm/sec, diffusion equations may be used to predict a ground level concentration, and from this a removal rate calculated. Assuming that a particle is removed when it reaches the ground-air interface, an empirical deposition velocity can be estimated by

$$V_d = W/X$$

where W = amount removed per unit time per unit area,

V_d = deposition velocity due to all effects,

X = volumetric concentration of aerosols at surface.

In general, $V_d \geq V_s$. If V_s > 100 cm/sec, Stokes

settling is the dominant effect, turbulence much less so, and V_d and wind shear operate to produce a particle trajectory. However, at small V_s, V_d may be determined largely by other mechanisms, and this may be generally true for particles of diameter $d < 10$ μm.

Similarities in concentration and size distribution of aerosols suggest common types of source processes. Metal-to-metal correlations in size distributions, compared to source total emissions, may pinpoint a particular source process. In the data to follow, a striking similarity is noted between the size distributions of iron (Fe) and chromium (Cr), suggesting a common source process, the steel industry in this case. Also, zinc (Zn) and antimony (Sb) show similarities, both being condensation aerosols. Unlike Fe and Cr, which are contained in large particles, Zn and Sb are predominantly associated with smaller particles. Zinc appears on both large and small particles in the immediate vicinity of a steel manufacturing plant, and again in an urban, non-industrial, area. In the former case, an additional source process creating a Zn dispersion may be suspected. But in the urban area, growth of small particles by adsorption of Zn onto larger particles is possible, in addition to the presence of an unsuspected local source of Zn. These relationships are shown in the plots of the data presented in Chapter IV.

Thus it has been shown that a knowledge of composition of aerosols as a function of their particle size could contribute to an understanding of such aerosols in several ways-

in their formation, in transformations occurring during their residence times in the atmosphere, and in their removal, in addition to their possible health effects. In some cases, man-made pollution may be distinguished from pollution by natural sources, such as the re-entrainment of soil particles.

A goal of this research project is to characterize source processes and source conditions for various elements found in the sampling program, by examining through numeric and graphic techniques the relationships existing between size distributions of various elements, and by relating these in terms of source processes, based on local source conditions and meteorology. Also, changes in particle size spectra for elements during atmospheric "lifetimes" are to be established, and mechanisms by which such changes in size occur postulated. These data are then used to determine aerosol removal mechanisms and the possibility of using natural tracers to identify certain types of source processes.

The relation between air pollution generation in a source area and possible water pollution is considered. Also, recently, Winchester and Nifong (1969), and Winchester, Robbins and Dams (1969), raised the question of water pollution of Lake Michigan by trace elements from pollution aerosol fallout. Although pollution of lake water by dissolved inorganic substances, such as Cl^-, $SO_4^=$, Na^+, and Ca^{++}, may be due to surface water input, certain trace metals strongly associated with air pollution sources around the southern edge of Lake Michigan may be contributing

significantly to lake water pollution by an atmospheric route. Winchester and Nifong (1969) considered this question with the aid of an approximate materials balance. The pollution of the lake by a specific metal depends essentially on the amount of that metal emitted to the atmosphere by some source or sources, and its transport to, and fallout into, the lake.

Although transport and fallout processes are strongly affected by the particle size of aerosols, the size distribution of trace metals has not been measured for the southern Lake Michigan area. In fact, only for the cities of Cincinnati (Lee et al., 1968) and Los Angeles (Lundgren, 1969) have size distributions of trace metals in pollution aerosols been published.

In the materials balance mentioned above, only estimates of metals emitted to the atmosphere from sources around the southwestern shore of Lake Michigan could be made, and these were based on a consideration of total particulate emissions from the area, together with available elemental analyses of stack gas emissions from various industrial and combustion processes. Then, considering gross meteorology of the area, the fraction of the total emission to the atmosphere that might find its way into Lake Michigan was estimated. Ten per cent was chosen as a conservative estimate. A computer calculation performed later, and based on wind speed and direction, showed that the transfer efficiency of aerosols from Northwest Indiana to the Lake Michigan water

surface varied from 25 to 50% for realistic atmospheric residence times of 1 to 12 hours (Winchester, Robbins and Dams, 1969). Even with the lower estimate of 10%, amounts of some metals (notably Zn, Ni, and Cu) entering the lake from the atmosphere were significant when compared with lake content and surface water input. These amounts are shown in Table 2.

TABLE 2

COMPARISON OF AIR POLLUTION INVENTORY WITH RIVER INFLOW OF TRACE ELEMENTS TO LAKE MICHIGAN, METRIC UNITS (after Winchester and Nifong, 1969).

	Cu	Ni	Zn	Mn	Pb
Air pollution emission inventory, tons/year	3200	1000	3900	4600	2200
Mean concentration in Lake Michigan rivers, micrograms/liter	90	40	30	--	--
Inflow to Lake Michigan, tons/year	2700	760	500	--	--
Expected natural stream input to Lake Michigan, tons/year	230	10	650	230	100

Thus a study of aerosol size and composition from a heavily polluted source area around the southwestern shore of Lake Michigan, together with meteorological data, should prove useful in evaluating potential pollution of the lake, but, more important, provide data useful in studying the history of the aerosol. A final goal of the present work is to determine whether or not pollution of Lake Michigan by certain trace elements from aerosol fallout is significant, based on concentrations and particle sizes found in the source area.

CHAPTER II

EXPERIMENTAL DESIGN

In formulating an aerosol study, an initial consideration is the measurement of composition, concentration and particle size on each individual sample. The solution to this task is explained in detail in Chapter III. In this chapter sample locations, times, and lengths will be presented.

An equally important consideration was the decision of where to sample. Since the prevailing wind over Lake Michigan is from the south to southwest (U.S. Department of Interior, 1959), and lake pollution is of importance, the Chicago metropolitan area presented a good locale for investigation. The main purpose of the experiment was air pollution source characterization by the study of ambient aerosols; therefore, a region of strong pollution source potential was desired. The area of Northwest Indiana seemed ideal for this purpose. The cities of Gary, Hammond, and East Chicago were chosen in which to locate sample sites because they have a high population density, with attendant commercial sources of pollution, plus one of the densest industrial complexes anywhere in the nation. Two additional advantages soon appeared in the choice of Northwest Indiana. First, the three cities mentioned are located in close proximity to one another, and each has a governmental air pollution control agency, which subsequently proved most helpful. Second, by far the largest type of industrial process

in the area is the steel industry, and in Northwest Indiana admittance could be obtained to the premises of one such company in order to take ambient air samples as close as possible to specific source processes.

Contact was made with all parties concerned, and it was decided to utilize local community air sampling network stations for urban sampling points. It became necessary to establish sample points within the steel industry.

Three samples were taken on Lake Michigan by using a research vessel, the R/V Inland Seas, owned by The University of Michigan, and several samples were taken in the City of Ann Arbor, Michigan, for comparison with the Northwest Indiana samples. Descriptions of sample sites follow:

1. Open Hearth Vicinity

   Samples here were taken at the south side of a complex of open hearth furnaces. The sampling equipment was located 20 feet above ground on the roof of a small shed adjacent to the open hearth area. Three 24-hour samples and 2 shorter (4-5 hours) samples were obtained here.

2. Sinter Plant Vicinity

   Samples were obtained here at the south side of a sinter plant. The sampling apparatus was located 6 feet above ground, and 4 24-hour samples and 1 shorter (4 hours) sample obtained.

3. Blast Furnace Vicinity

Only 1 (5-hour) sample could be obtained at this location. It was taken 8 feet above ground on the roof of a maintenance building at the southern edge of the blast furnace area.

Stations 4-10 were established at sites used by the control agencies for ambient air sampling, and are shown in Figure 1 by number.

4. Central Fire Station, East Chicago, Indiana

This site is located at 450 East Columbus Drive in East Chicago. Eight samples—7 24-hour and 1 2-week—were collected on the fire station roof, 30 feet above ground. This site is ½ to 2 miles SSW of large steel operations. It is enclosed by industrial operations, with oil refining and oil storage to the north and west, a foundry to the southwest, a chemical company to the south, and a refractories operation to the east. Moreover, Columbus Drive is a major traffic artery.

5. Markstown Park, East Chicago, Indiana

Markstown Park at Broad and Pine Streets, East Chicago, is located in a small residential island surrounded by industry. Most of this is steel, although beyond the steel complex to the west, about ½ to 5 miles, are major oil refineries. A gypsum plant is located 1 mile south. Two 24-hour samples and 1 2-week sample were taken 10

feet off the ground on the roof of a small shelter in the park.

6. Field School, East Chicago, Indiana

Field School, at Block Avenue and James Place in East Chicago served as a sample site for 4 24-hour samples. These were taken on the school roof, about 50 feet above ground. The immediate vicinity around the school is residential, although a large steel industry stretches from the north to the west about ½ mile away.

7. Wirt School, Gary, Indiana

Wirt School is located at Grand Boulevard and Cypress Avenue in the northeastern part of Gary, Indiana. One 5-day sample was collected here, at an elevation of 25 feet above ground. The location is in a residential area, several miles east of industrial and commercial activities. This sample was used as a "control" against which to compare many of the others.

8. Gary Airport, Gary, Indiana

The Gary Airport is off Industrial Highway in northwest Gary, Indiana. A coal-fired power generating station and a large cement plant are located 2 miles north. One to two miles east lie oil storage and chemical operations, and a detinning company. Eight 24-hour samples were collected on the roof of the operations building,

about 12 feet above ground.

9. Central Fire Station, Gary, Indiana

The fire station is located in downtown Gary at the intersection of Fifth Avenue and Pennsylvania Street. The immediate vicinity is entirely commercial, with Fifth Avenue (as well as Fourth Avenue one block north) being a major traffic artery. One mile northwest, north, and northeast, lies a major steel complex. Three 24-hour samples were obtained on the fire station roof, about 15 feet above ground.

10. City Hall, Hammond, Indiana

Three 24-hour samples were taken at the City Hall in Hammond, located at Calumet Avenue and Highland Street in Hammond. These were collected on the building roof, 50 feet above ground. This area is commercial and residential, and about 5-6 miles SSW of the East Chicago steel complex. Calumet Avenue is a major traffic artery.

11. R/V Inland Seas, Lake Michigan

Three samples were taken on southern Lake Michigan on board The University of Michigan research vessel, the "Inland Seas." Sample #42 was taken near the middle of the southern third of the lake, starting at a point 20 miles offshore west of Holland (Lat. 42° 47' N, Long. 86° 33' W), and continuing southwest for 50 miles (Lat. 42°

16' N, Long. 87° 10' W). The other 2 samples were taken approximately 4-8 miles off the Chicago and northwestern Indiana shoreline—run #43 from a point 2 miles due east of Chicago Harbor to Lat. 41° 43' N, Long. 87° 21' W; and run #44 from Lat. 41° 43' N, Long. 87° 21' W to Lat. 42° 0' N, Long. 87° 28' W. All 3 samples were taken in the bow of the ship, as far forward as possible, about 15 feet above the water-line.

12. School of Public Health, The University of Michigan, Ann Arbor, Michigan

Six samples were taken for comparison purposes in Ann Arbor, Michigan. These samples were taken at roof level, about 60 feet above ground. This location is in a commercial-industrial area, but several power plant stacks are close by.

Eight field trips to Northwest Indiana and one to Lake Michigan were made to collect the data. Arrangements were made for sample sites during the Spring of 1969. Samples were collected during Summer and Fall, 1969, and Winter 1969-70.

Fifty runs were made with a cascade impactor sampler during the sampling program, two of which were paralleled by duplicate runs, for a total of 52 samples. Also 16 high-volume sample runs, 14 in parallel with impactor runs, were obtained. Details of each sample are reported in Table 14 of the Appendix.

Meteorological conditions were determined during the time of all sample runs made in Northwest Indiana. This is recorded in Table 15 of the Appendix. Values for wind speed and direction are averages from two meteorological stations, one located on the roof of the City Hall in downtown East Chicago, and the other located at Kaiser Aluminum, Incorporated, in western Gary. Winds from all quadrants except east were recorded during at least one day of sampling. Temperatures are those recorded in East Chicago. Relative humidity and precipitation are taken from records obtained at O'Hare Airport in Chicago, Illinois, and available from the National Weather Records Center in Asheville, North Carolina.

Figure 1. Urban Sampling Locations in Northwest Indiana

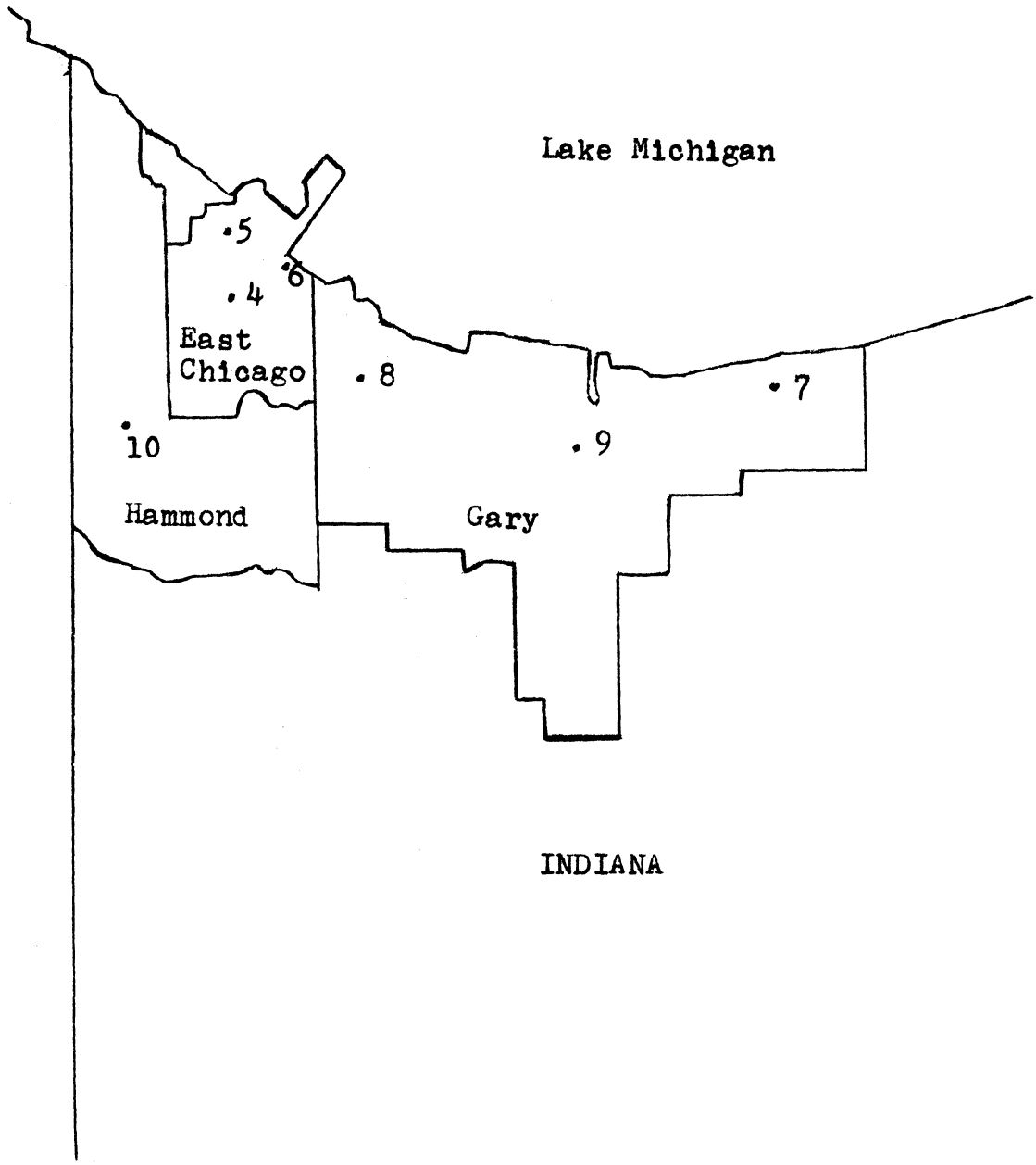

CHAPTER III

SAMPLING APPARATUS AND ANALYTICAL PROCEDURES

A. SAMPLE COLLECTION

In order to establish components, concentrations, and particle size distributions of any one aerosol sample, it was deemed best to collect the aerosol by size-fractions, then to analyze each size-fraction quantitatively for mass concentration of selected elements. Hence data for all size-fractions for any one sample would represent mass distributions of certain elemental components in an aerosol as a function of particle size. Such data do not indicate the "purity" of any one aerosol particle, but only the mass of an element associated with particles of a given size. In other words, if zinc (Zn) is found to equal 100 ng on particles 2-4 μm in radius, this may mean a small number of particles of that size have been collected, which are mostly Zn in composition. But far more likely, it means that a larger number of particles have been collected, and Zn content is a smaller fraction of each particle. The latter is stated to be the more likely, based on the work of Junge (1963) and the U.S. Public Health Service (1966, 1969).

This point is related to a point discussed in Chapter I, that if an aerosol is "Junge mass distributed," any one element will follow the same distribution only if its percent composition is uniform over all size particles.

The Andersen[1] sampler (Model 0203), modified by a seventh impaction stage and followed by an in-line filter, was used to collect the total aerosol and sort it by particle size-fractions. This device separates an aerosol into 7 size ranges, based on initial impaction, and an eighth size based on filtration. This last size-fraction is designated "stage 8" on all tables and figures in this report. Hence particle size expressed by data from the first 7 stages of the Andersen involve not only diameter, but also density and shape of the particles. The Andersen sampler (Figure 2) consists of 7 impaction plates in series, each plate preceded by a group of parallel air jets, of uniform size within that group. Air flows through the jets, and must then negotiate a 90° turn at an impaction plate, establishing streamlines. But an aerosol particle, based on its size and density, may have sufficient momentum to depart from the air streamline and impact on the collection plate. This is axial momentum, and is developed by the mass and velocity of the particle. But radial momentum, developed by the drag of the curved air flow, also acts on the particle, and only if axial momentum exceeds radial momentum, or drag, will a particle leave the air flow and impact. But if a particle does not impact on one stage (insufficient mass (density and size)) while traveling at a given velocity, it goes to a next stage, where conditions

---

[1]Andersen Air Samplers, Medi-Comp Research and Development, 1423 South 2nd West, Salt Lake City, Utah.

Figure 2. Schematic view of Andersen Sampler, Model 0203.

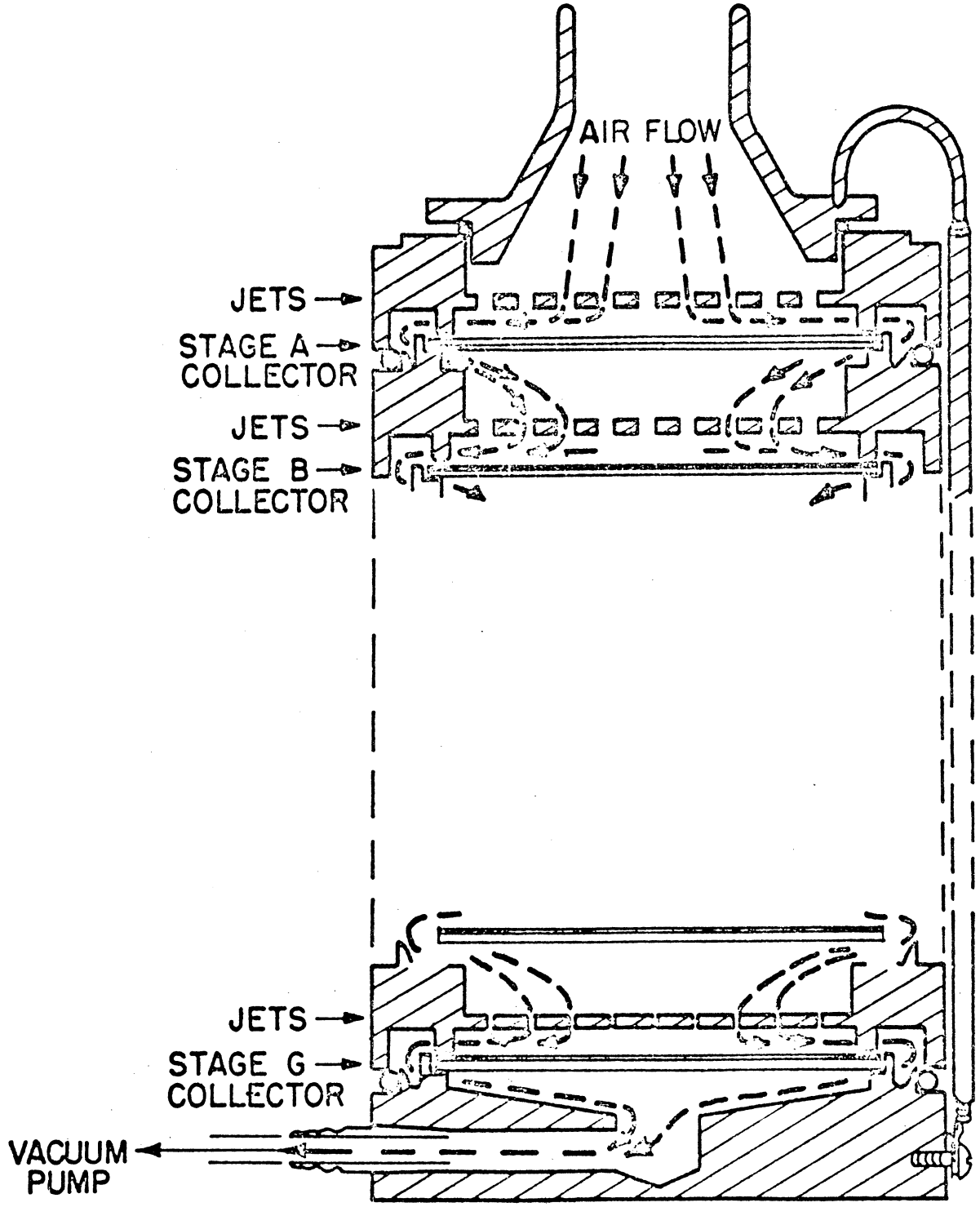

are the same, except that diameter of the air jets of that group has been reduced. This increases velocity of both air and particles, but increases axial momentum more so than radial momentum for the particle. Hence particles of smaller mass may impact here, while they followed the air flow on the preceding stage. The Andersen is composed of 7 such stages, each of decreasing air jet diameter (except stage 7, where the number of jets is reduced) such that in general, particles of a certain size and larger, impact on each stage. Finally, most particles that are small enough to escape impaction on all 7 stages are trapped by a back-up filter. Size as measured by the Andersen is related to true particle size only if uniform density and shape of the particles are assumed. A number of investigators have considered inertial impaction in detail. May (1945, 1962), Mercer (1963), Lundgren (1967), Ranz and Wong (1952), Wilcox (1953), and Davies and Aylward (1951) have treated the subject extensively. An inertial impaction parameter (K) has been established as:

$$K \approx \frac{\sigma \cdot d^2 \cdot V}{18 \cdot \mu \cdot D}$$

where

σ = particle density

μ = air viscosity

d = particle diameter

D = jet diameter

V = particle velocity

The larger K becomes, the more efficient impaction becomes. Clearly, impaction is proportional to particle mass (or size, if uniform density is assumed) and velocity.

Similar conditions lead to a means for calculating "cut-off diameter" for the impaction sampler. This is defined as that particle size for which 50% of the particles will be impacted at a given stage. "Cut-off diameter" is commonly used as the minimum diameter for particles collected on a particular stage.

$$D^2_{min} = \frac{36 \cdot \mu \cdot d}{\pi \cdot \sigma \cdot V}$$

D_{min} = minimum diameter

μ = air viscosity

σ = particle density

V = particle velocity

d = minimum width of air streamline

This enables one to calculate the size fraction that should be separated on any stage of the Andersen, a help since the 7th stage modification until very recently had not been calibrated by others.

Andersen (1966), Flesch et al. (1967), and May (quoted in Flesch et al., 1967) report experimental calibrations of the Andersen. A summary of their work is presented in Table 3.

TABLE 3

CALIBRATION OF THE ANDERSEN SAMPLER
50% CUT OFF DIAMETERS, μm

Stage	1	2	3	4	5	6	7
Andersen	9.2	5.5	3.3	2.0	1.0	--	--
Flesch (averaged)	--	5.35	3.28	1.76	.89	.54	--
May	--	5.5	3.5	2.6	1.1	--	--

The cut off diameter for stage 7 was calculated by Gillette (1970) using the method previously discussed and found to be 0.40 μm. One may now see that minimum diameters, or radii, for Andersen stages decrease by a factor roughly equal to $\sqrt{2}$ from one stage to the next. But the "Junge mass distribution" specifies a logrithmic radius interval. Therefore, an aerosol "Junge mass distributed" should also be distributed uniformly over the Andersen stages. This does not hold true for stage 1, which collects everything above a certain size, nor for stage 8, which collects everything below a certain size. Gillette (1970) has calculated how a "Junge distribution" should be impacted on successive Andersen stages. This is given in Table 4.

TABLE 4

PERCENT OF TOTAL MASS VS. ANDERSEN SAMPLER STAGE FOR THE "JUNGE" DISTRIBUTION (after Gillette, 1970).

A.S. Stage	Percent of Total Mass
1	25.0
2	9.8
3	9.8
4	9.8
5	11.1
6	9.8
7	8.4
8	16.4

This demonstrates that a "Junge distribution," itself a "straight line" distribution, should impact more or less uniformly over stages 2-7 of the Andersen, resulting in a horizontal straight line at some given concentration for stages 2 through 7, but with a peak at stage 1 and at the filter. Since a main technique for data interpretation in this work is the comparison of aerosol samples with the "Junge mass distribution," the Andersen Cascade Impactor was chosen to collect and separate by size-fraction those aerosols.

During the course of the project an especially interesting experiment was conducted with the Andersen impactor. Two aerosol samples were collected in Ann Arbor, each by 2 Andersens (runs #47 and #48). For run #47, 2 impactors were arranged in series, Andersen #2 sampling the ambient air, and Andersen #1 sampling the air that had just passed through the earlier impactor. No filter was used with the leading sampler. Results are shown in Table 32 of the Appendix, showing iron (Fe) and Zn analyzed by atomic absorption spectroscopy. It is quite evident that most aerosol particles of sufficient size to be impacted have done so in the leading Andersen.

For run #48, 2 impactors were dismantled, and reassembled such that except for stage 1, 2 identical stages were paired in series, a "13 stage" impactor. Again Fe and Zn were run by atomic absorption spectroscopy on the contents of each impaction plate. About 75% of material on each pair of identical stages was collected on the leading stage. Since cut-off diameter is not sharply defined, and each second

plate of a pair changed the size distribution of the aerosol entering plate 1 for the next smaller size range, 75% is a reasonable value and does not conflict with theory.

One final piece of work that should be described was a laboratory test of Andersen impaction efficiency. This was performed by generating a spherical test aerosol of known density and uniform, known, size. This was laboratory-sampled by an Andersen, and stages examined microscopically to find out if the bulk of the test aerosol had impacted on the proper stage. Two sizes of polystyrene latex particles[1] of density = 1.05 g/cc were used—6-14 μm diameter and 1.1 μm diameter. Microscopic examination showed the former to have impacted in about equal amounts on stages 1 and 2. For the latter size, a trace was found on stage 4, about two-thirds on stage 5, and one-third on stage 6. These distributions agree well with those found by the other investigators named, Andersen, Flesch et al., and Gillette.

During actual field sampling, each Andersen stage was covered with a washed, 1-mil polyethylene disc. At the completion of each run, the discs were removed and individually stored in clean petri dishes. Use of the plastic discs served two purposes—it facilitated handling and analysis of the sample, and it improved impactor collection efficiency by providing a slightly rougher impaction surface, compared with glass or metal discs.

Each run, except those for extended periods of time,

---

[1]Biological Products Division, Dow Chemical Company, Midland, Michigan.

was made with an in-line backup filter attached to the Andersen. A Millipore type AAWP025[1] membrane filter of pore size 0.8 μm was chosen. This choice was made on the basis of required air flow and trace element impurity characteristics of the filter. A similar, but larger filter (Millipore type AAWP047) was chosen for "high volume" sample runs. A description of sample media and impurity levels for all sampling media for those elements under test are listed in Table 16 and Table 17, respectively, of the Appendix.

Each Andersen sample, as well as each "high-volume" sample, was collected by use of a vacuum pump (Gast, Model 0740-V105[2]) and flowmeter (Dwyer, Series RMB, #53[3]). Each flowmeter was calibrated against a "primary" standard, a chain-compensated gasometer, in the laboratory before field use. In order to achieve proper air velocities through the Andersen impactor, it was necessary to operate it at 28 lpm (1 cfm) in the field. Therefore, calibrations of flowmeters included temperature corrections for the approximate ambient temperatures expected during each field trip. Impactors were housed in standard U. S. Weather Bureau meteorological shelters or "high volume" sample shelters during each run. Details of sample runs and meteorological conditions during

---

[1]Millipore Filter Corporation, Bedford, Massachusetts.

[2]Gast Manufacturing Corporation, Benton Harbor, Michigan.

[3]F. W. Dwyer Manufacturing Company, Incorporated, Michigan City, Indiana.

each run are given in the Appendix, Table 14 and Table 15, respectively.

Twenty-nine elements were quantitated with respect to particle size range by the use of two analytical techniques—neutron activation analysis with gamma-ray spectrometry, and atomic absorption spectroscopy. Since sample preparation and analytical techniques differed markedly between the two techniques, each will be discussed separately.

B. NEUTRON ACTIVATION ANALYSIS

For analysis by neutron activation and gamma detection, a portion of each polyethylene disc or membrane filter containing the impacted aerosol sample was irradiated in the Ford Reactor, Phoenix Memorial Laboratory, The University of Michigan. Each size-fraction of most samples was initially irradiated in a flux of approximately 2×10^{12} neutrons/cm^2/sec in a pneumatic tube system for a duration of 5 minutes. After 3 minutes of cooling, 5 elements were "counted" for a period of 400 seconds. "Counting" consists of recording counts, or the gamma-ray pulse height, over given energy (keV) ranges for the specified time, where time is live-time, rather than clock time. Fifteen minutes after irradiation, each sample was again counted, but for 1000 seconds, to obtain data on 7 additional elements. These 12 elements and their nuclear properties are listed in Table 18, "Nuclear Properties and Measurement of Short-Lived Isotopes," of the Appendix. Counts above background

over a given energy range for each element were then compared with a standard that had earlier been treated in an identical manner as the sample. Blanks were subtracted, and concentration and a standard deviation, the latter based on nuclear counting statistics, calculated for each element over each size range. Computer programs were written to assist in calculations.

Next, longer-lived isotopes were produced and measured, giving data on an additional 17 elements. Actually, 21 additional determinations were made on each sample size-fraction, but since two gamma energies were measured for each of 4 pollution elements, information was gained on only 17 different additional elements. The procedure for this work involved heat-sealing each sample fraction in a plastic vial, and irradiating it for 1-2 hours in the core of the reactor at a flux of 1.5×10^{13} neutrons/cm^2/sec. Then, after allowing the sample to decay for approximately 24 hours, each vial was cut open, its sample transferred to a clean glass vial, and 11 elements determined during a 2000-second count. The sample was allowed then to decay an additional 2-3 weeks and a 4000-second count taken, giving information on 10 elements. The decay periods were necessary in order to allow shorter-lived isotopes to die away, since their presence at times shortly after irradiation would give rise to large peaks, obscuring smaller peaks of the longer-lived material. These 21 determinations (i.e., 17 elements) and their nuclear properties are listed in

Table 19 of the Appendix, "Nuclear Properties and Measurement of Long-Lived Isotopes." Isotopes are grouped in the Appendix tables according to counting time (400- and 1000-second together), and ranked within groups in order of ascending atomic weight of the element sought. The counting equipment used for all neutron activation analyses was a 4096-channel gamma spectrometer[1], fitted with a high resolution Lithium-drifted Germanium detector. Gamma energies used for all 33 determinations of the 29 elements were selected from a tabulation of energies found with Ge(Li) Spectrometry by Dams and Adams (1968).

For the longer (1-2 hour) irradiations, a standard containing all elements of interest was irradiated with each group of size-fraction samples representing one run. Counts for each sample were compared with counts for the standard for each element, corrections made for differences in decay times, blank values subtracted, and appropriate concentrations and standard deviations calculated. Again, all computations but peak examination were computerized. For these longer counting times, certain samples were analyzed individually and others composited before analysis. Composites were necessary because of the large amounts of time needed to perform the 2000- and 4000-second counts. The decision of when to composite was made on the basis of sample location and knowledge of

---

[1]Nuclear Data, Incorporated, Chicago, Illinois.

meteorological conditions existing during sampling.

Spectrometer counts were usually printed out by channel on paper tape. In most cases (e.g. Cl, Br, Na, Zn) these were manually treated to determine peak sizes and standard deviations. This was done by summing counts in five channels at the peak, then subtracting five background channels located nearby. The standard deviation was calculated as the square root of the total counts in all ten channels. This method of data handling was especially necessary, often including graphs of peak height versus channel or energy, whenever spectra needed to be resolved because of close peak proximity for two elements. For a few elements, graphical treatment was essential, for one peak might be located on the side of a larger peak.

Essentially, analytical techniques and data processing involved in analysis by neutron activation were patterned after that outlined by Dams, Robbins, et al. (1970).

The limit of detection for each of the 29 elements is outlined in Table 20 of the Appendix. For most elements, limits of detection are well below those attained by other methods of analysis. It should be stressed that analysis of many of the less-common trace elements on one particular size-fraction has been achieved only because of the very low limits of detection attainable by neutron activation analysis. For some elements (Cl, Br, Na, Zn, e.g.), sample media impurities are the limiting factors. For many others, especially those having longer-lived isotopes,

the limit of detection is determined in part by the presence of the more abundant elements—Na, Br—which give rise to large amounts of radioactivity; hence the longer cooling time before counting of the longest-lived group of isotopes. For all elements, limit of detection is governed by:

1. Natural abundance of an isotope that can be activated to produce an isotope having a gamma ray.
2. The ease with which the isotope can be activated by thermal neutrons (atomic cross section).

These two factors, plus the half-life itself of an isotope produced by activation, largely determine the feasibility of analysis by this method.

These concepts may be shown theoretically by the equation:

$$W = \frac{A \times M}{6.02 \times 10^{23} \cdot I \cdot \sigma \cdot f \cdot S}$$

where $S = 1 - e^{-\lambda t}$

W = weight of the element

A = activity in disintegrations per second

M = atomic weight

I = neutron flux in neutrons/cm^2/second

σ = atomic cross section in barns

(1 barn = 10^{-24} cm^2)

f = fractional abundance of target nuclide

S = saturation factor

λ = radioisotope decay constant

t = time of irradiation

In practice, A, σ, and f in the above equation cannot be determined accurately, and the equations are not relied upon. Rather a sample and a standard are treated under identical conditions during irradiation and analysis and then comparisons made, which was the procedure followed during this work.

C. ATOMIC ABSORPTION SPECTROSCOPY

Each size fraction of each aerosol sample was also examined by atomic absorption spectroscopy. For a few samples taken early in the experiment, this means provided the only data available, as analysis by neutron activation for this specific work was in a stage of development.

Sample preparation for analysis by atomic absorption was quite different than that required for activation analysis. For this procedure, the aerosol fraction had to be removed from the polyethylene or filter disc, and the inorganic portion placed in solution. A number of possible techniques were considered, and a treatment of the sample with acid and ultrasonic vibrations was developed. This consisted of taking one-half of each disc (polyethylene or membrane) and cutting it into smaller sections. These sections were placed in a clean, acid-washed, glass vial. Five milliliters of 1 N reagent-grade hydrochloric acid were added, and the sample treated by ultrasonic vibrations for one hour. This process also warmed the sample solutions, due to the heat of dissipation of fluid motion, assisting in putting the elements into solution. Several strengths of

HCl, HNO_3, and mixtures of the two were evaluated for removal ability and effecting solution, but 1 N HCl seemed to give slightly better efficiencies. Longer times of vibration were also checked, but one hour was deemed sufficient. These efficiencies were evaluated in several ways—in microscopic evaluation of larger particles on stages before and after treatment, various parallel treatments of equal segments of individual samples, and by sequential treatments of individual samples, with analysis at each stage of the sequence. These tests, together with later comparisons of these data with that obtained by neutron activation analysis for the same samples, show that the procedure, as discussed, removed and placed in solution 85% $\pm$ 10% of the total mass present of the elements under test.

It should be mentioned here that all polyethylene discs were washed prior to field use by subjecting whole discs to ultrasonic vibrations in 1 N HCl, followed by three rinses in distilled, de-ionized, water.

During early work, consideration was given to the analysis of 6 metals—Zn, Fe, Cu, Mn, Cr, Pb—by atomic absorption spectroscopy. But lead was found to be present essentially on the filter for urban samples, and other investigators (Robinson, 1963; Gillette, 1970; Harrison, 1970) had been or were studying lead distributions extensively; hence Pb was omitted. Due to the very small mass involved in any one size fraction, or any one stage, data

for Cu, Mn, and Cr by atomic absorption spectroscopy were much less reliable than that produced by neutron activation for these elements. Hence recourse to the latter method was taken. But for Fe (because of its prevalence and better method sensitivity) and Zn (because of excellent method sensitivity) atomic absorption spectroscopy was used on each sample size fraction for quantitation. Atomic absorption spectroscopy serves equally well for Zn as neutron activation analysis does, and it is much superior regarding Fe. Sensitivities by atomic absorption spectroscopy are given in Table 20 of the Appendix.

A Jarrell-Ash Model 82-360 Atomic Absorption Spectrophotometer[1] equipped with recorder was used for analysis of each 5-ml sample of one size fraction. Operating parameters are given in Table 5.

TABLE 5

ATOMIC ABSORPTION SPECTROPHOTOMETER OPERATING PARAMETERS

	Lamp		Spectral Line	Fuel
	Mode	Current		
Fe	Normal	20 ma.	2483 Å	hydrogen-air
Zn	Hi-Intensity	6 ma.	2136 Å	hydrogen-air

Optimal lamp current, flame composition (fuel/air ratio), and flame position for each element were determined by plotting each variable against absorption to locate conditions for maximum absorption. Prior to each series of

---

[1]Jarrell-Ash Corporation, Newtonville, Massachusetts.

analyses, exact wavelength for maximum absorption was determined. Five dilutions of a multi-element standard were prepared and run frequently during sample analyses. From these a standard curve for each element was prepared, mass of element for each sample determined, and concentration calculated. A standard deviation for each sample was similarly calculated, based on absorption variability for each sample.

D. COMPARISON OF METHODS

The analyses of two metals—Fe and Zn—by both analytical techniques that have been discussed present an excellent opportunity to compare results from the two methods. Moreover, several samples were analyzed in duplicate by one or both methods, and on two occasions duplicate Andersen impactors were operated simultaneously in the field. Finally, as previously mentioned, several elements could be quantitated by two counts within the neutron activation procedure. Thus ample opportunity for various types of "cross-checking" exists, and will be discussed.

Duplicate analyses of an individual sample for Fe and Zn by atomic absorption spectroscopy usually differed by less than 10%, with one standard deviation being ≈ 10%. This is shown for run #29 in Figure 3. Duplicate analyses by neutron activation showed that agreement was usually within one standard deviation of concentration. This is illustrated by Figures 4, 5, and 6, showing respectively, Na and Cl for run #4, Al and Mn for run #4

and V and Br for run #43.

Masses and mass ratios for these duplicate analyses are listed in Table 6 for runs #4 and #29.

Copper, Zn, Sb and Br each were determined on two counts with the neutron activation procedure whenever longer-lived isotopes were determined. Copper from 400- and 2000-second counts, Br from 1000- and 2000-second counts and Zn and Sb each from 2000- and 4000-second counts could be compared. Zinc, Sb and Br provided better agreement than Cu, as can be seen in Table 7 (run #22).

A most interesting finding was the good agreement between analysis for Fe by 4000-second gamma counts and atomic absorption and for Zn by 2000-second gamma counts, 4000-second counts and atomic absorption. These results are tabulated in Table 8 and shown graphically in Figures 7 and 8 for run #22.

Finally, samples #21 and #35 were collected in duplicate. Results were within 20% of each other for most elements. Results and ratios for Al, Mn, Br, and Cl on run #21 and for Al, Mn, Na, and Cl on run #35 are presented graphically in Figures 9, 10, 11, and 12, with mass and mass ratio tabulated for run #21 in Table 9.

TABLE 6

MASS* AND MASS RATIO BY DUPLICATE ANALYSIS

	Stage							
	1	2	3	4	5	6	7	8
Run 29 (AA)								
Fe	1400	700	800	500	500	300	300	200
Fe (D)	1400	700	800	500	500	400	300	200
$\frac{Fe}{Fe\ (D)}$	1.0	1.0	1.0	1.0	1.0	0.75	1.0	1.0
Zn	56	29	69	74	220	160	220	290
Zn (D)	60	30	61	72	210	150	120	270
$\frac{Zn}{Zn\ (D)}$	0.94	0.97	1.13	1.03	1.05	1.07	1.83	1.07
Run 4								
Na	460	200	230	225	310	315	270	375
Na (D)	495	190	240	205	300	310	260	390
$\frac{Na}{Na\ (D)}$	0.93	1.05	0.96	1.10	1.04	1.02	1.04	0.96
Cl	690	300	365	285	390	690	530	790
Cl (D)	750	260	390	305	375	670	500	810
$\frac{Cl}{Cl\ (D)}$	0.92	1.15	0.93	0.93	1.04	1.03	1.06	0.97
Al	1950	1180	1110	1710	1830	478	116	35
Al (D)	1990	1020	1000	1605	1720	460	112	32
$\frac{Al}{Al\ (D)}$	0.98	1.16	1.11	1.07	1.07	1.04	1.04	1.10
Mn	415	147	113	118	113	118	131	151
Mn (D)	425	127	110	108	108	117	118	161
$\frac{Mn}{Mn\ (D)}$	0.97	1.15	1.03	1.10	1.05	1.01	1.11	0.94

* Mass expressed as concentration in ng/m^3.

TABLE 7

MASS* AND MASS RATIO BY DIFFERENT COUNTING TIMES

Run 22	Stage 1	2	3	4	5	6	7
Cu (400")	23	20	53	54	66	29	34
Cu (1000")	40	23	40	69	94	47	26
$\frac{\text{Cu (400")}}{\text{Cu (1000")}}$	0.58	0.88	1.32	0.78	0.70	0.62	1.30
Br (1000")	3.6	4.6	9.0	7.2	7.7	7.1	9.1
Br (2000")	5.8	6.8	9.5	11.0	10.1	10.7	26.0
$\frac{\text{Br (1000")}}{\text{Br (2000")}}$	0.62	0.68	0.95	0.66	0.76	0.67	0.35
Zn (2000")	15	27	44	82	161	107	70
Zn (4000")	23	23	39	78	135	86	54
$\frac{\text{Zn (2000")}}{\text{Zn (4000")}}$	0.65	1.18	1.11	1.04	1.19	1.23	1.28
Sb (2000")	1.1	0.6	0.9	1.6	2.8	2.4	1.9
Sb (4000")	0.8	0.7	1.2	1.4	4.5	1.4	4.7
$\frac{\text{Sb (2000")}}{\text{Sb (4000")}}$	1.4	0.9	0.8	1.1	0.6	1.7	0.4

* Mass expressed as concentration in ng/m^3.

TABLE 8

MASS* AND MASS RATIO BY ANALYTICAL METHOD

	Stage						
	1	2	3	4	5	6	7
Run 22							
Fe (4000")	920	565	460	235	210	40	40
Fe (AA)	790	400	390	300	280	190	70
$\frac{\text{Fe (4000")}}{\text{Fe (AA)}}$	1.16	1.41	1.18	0.79	0.76	0.21	0.57
Zn (2000")	15	27	44	82	161	107	70
Zn (4000")	23	23	39	78	135	86	54
Zn (AA)	21	28	45	90	173	102	77
$\frac{\text{Zn (2000")}}{\text{Zn (AA)}}$	0.72	0.97	0.98	0.91	0.93	1.05	0.91
$\frac{\text{Zn (4000")}}{\text{Zn (AA)}}$	1.10	0.83	0.87	0.87	0.78	0.85	0.70

* Mass expressed as concentration in ng/m^3.

TABLE 9

MASS* AND MASS RATIO BY DUPLICATE SAMPLE RUN

	Stage							
	1	2	3	4	5	6	7	8
Run 21								
Al	225	283	312	206	170	143	17	17
Al (D)	205	270	298	200	160	125	37	30
$\frac{Al}{Al\ (D)}$	1.10	1.05	1.05	1.03	1.06	1.14	0.46	0.60
Mn	13	11	16	14	26	27	15	14
Mn (D)	12	9	16	13	28	30	14	13
$\frac{Mn}{Mn\ (D)}$	1.07	1.22	1.00	1.07	0.93	0.90	1.07	1.07
Br (1000")	114	140	120	87	185	144	200	160
Br (D)	100	125	105	81	190	141	190	150
$\frac{Br}{Br\ (D)}$	1.14	1.12	1.14	1.07	0.98	1.02	1.05	1.06
Cl	53	95	56	73	140	135	92	120
Cl (D)	48	100	51	70	150	126	81	102
$\frac{Cl}{Cl\ (D)}$	1.10	0.95	1.09	1.04	0.93	1.07	1.13	1.17

* Mass expressed as concentration in ng/m^3.

Figure 3. Duplicate analyses by atomic absorption spectroscopy, run 29.

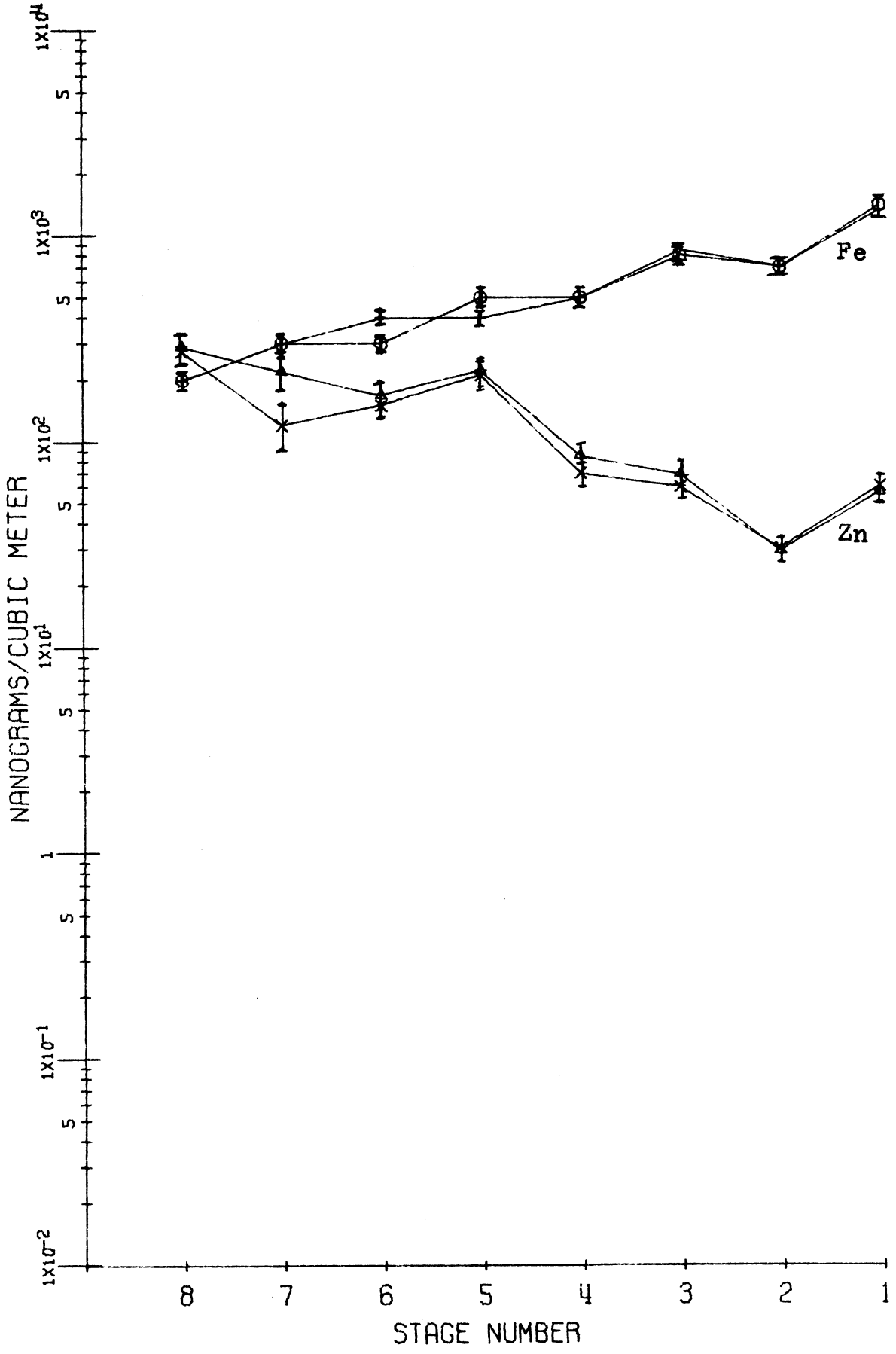

Figure 4. Duplicate analyses by neutron activation, run 4.

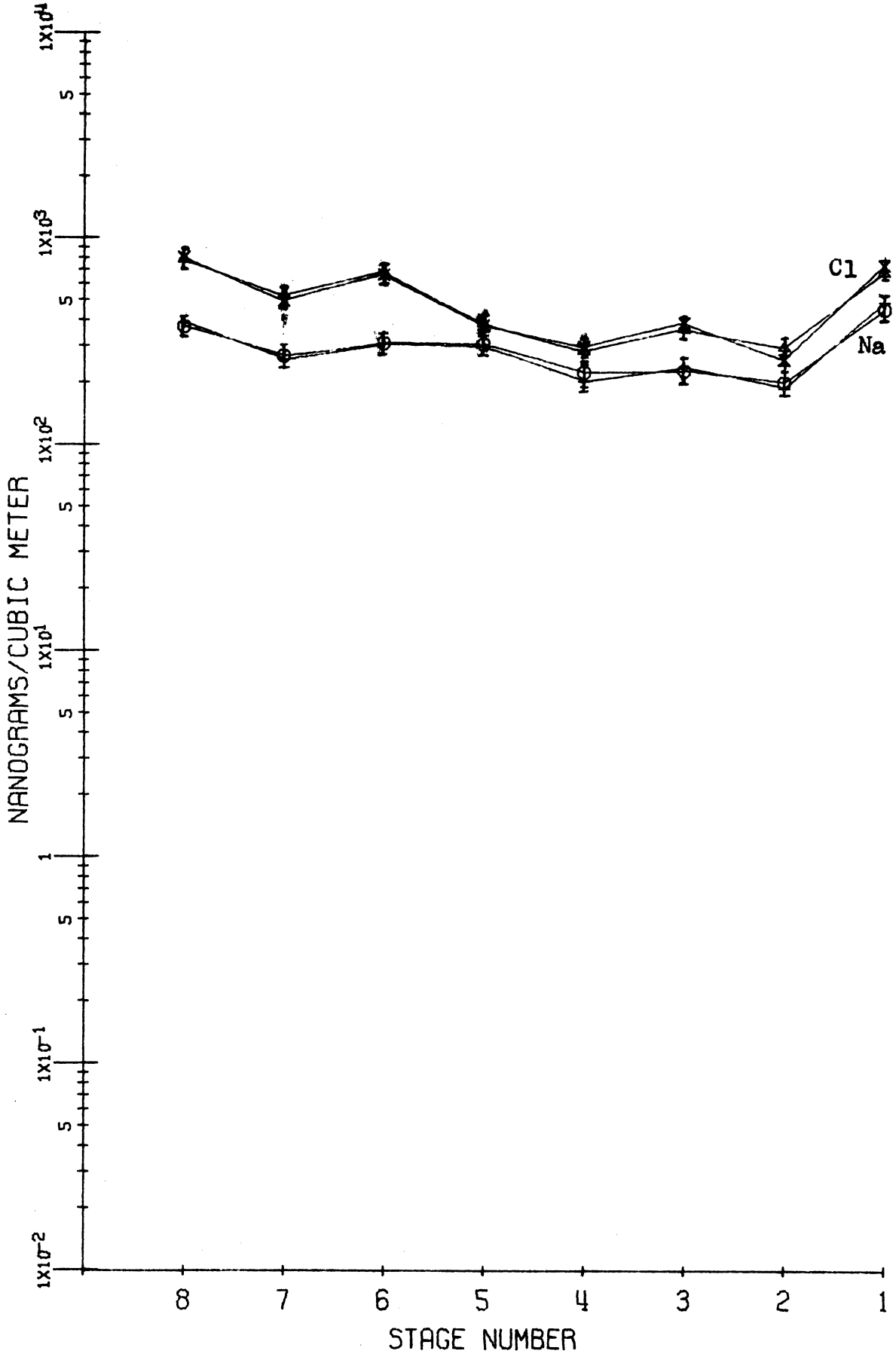

Figure 5. Duplicate analyses by neutron activation, run 4.

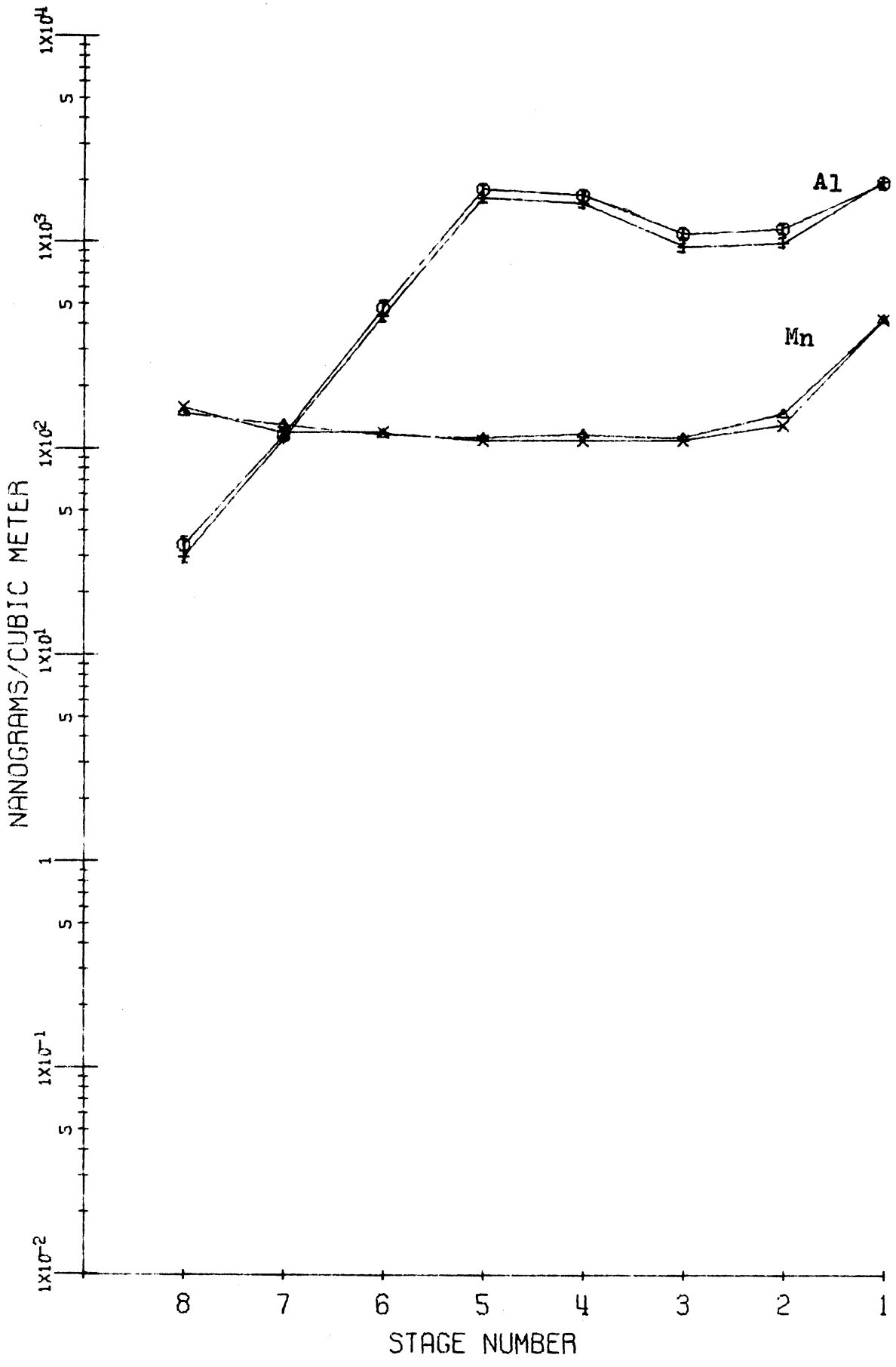

Figure 6. Duplicate analyses by neutron activation, run 43.

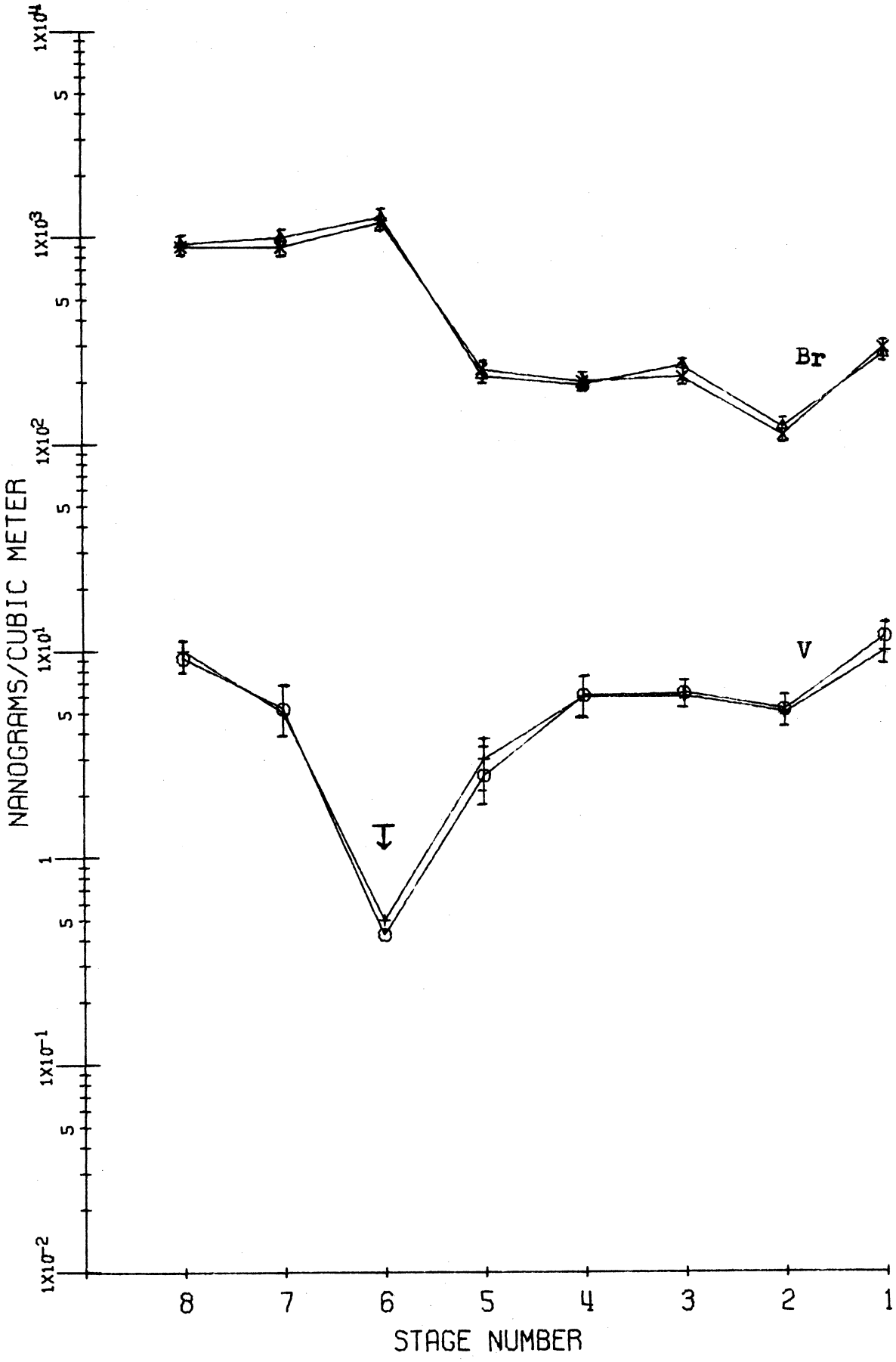

Figure 7. Duplicate analyses by analytical method, by 4000-sec. neutron activation and by atomic absorption, run 22.

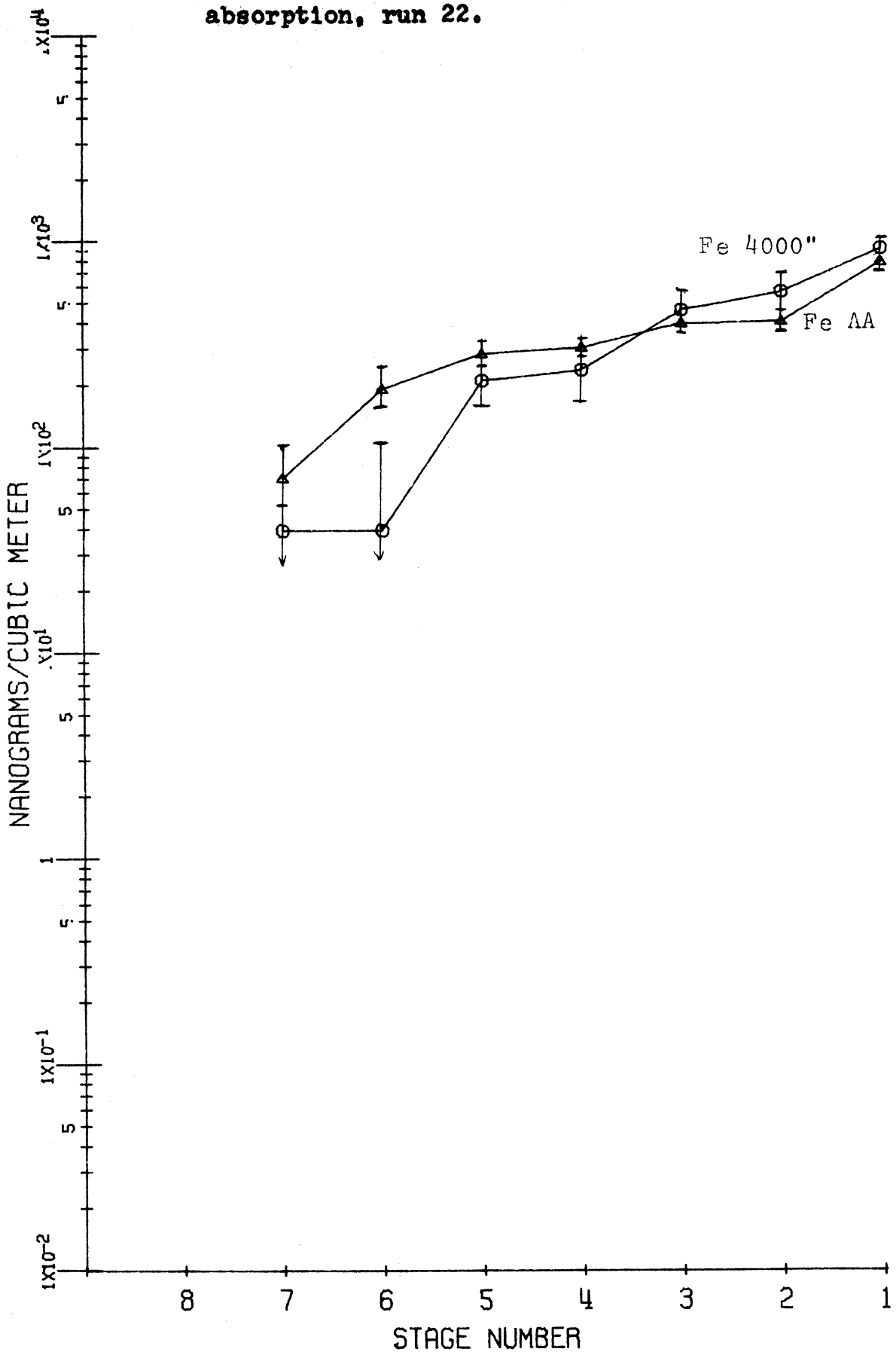

Figure 8. Duplicate analyses by analytical method, by 2000- and 4000-sec. neutron activation, and by atomic absorption, run 22.

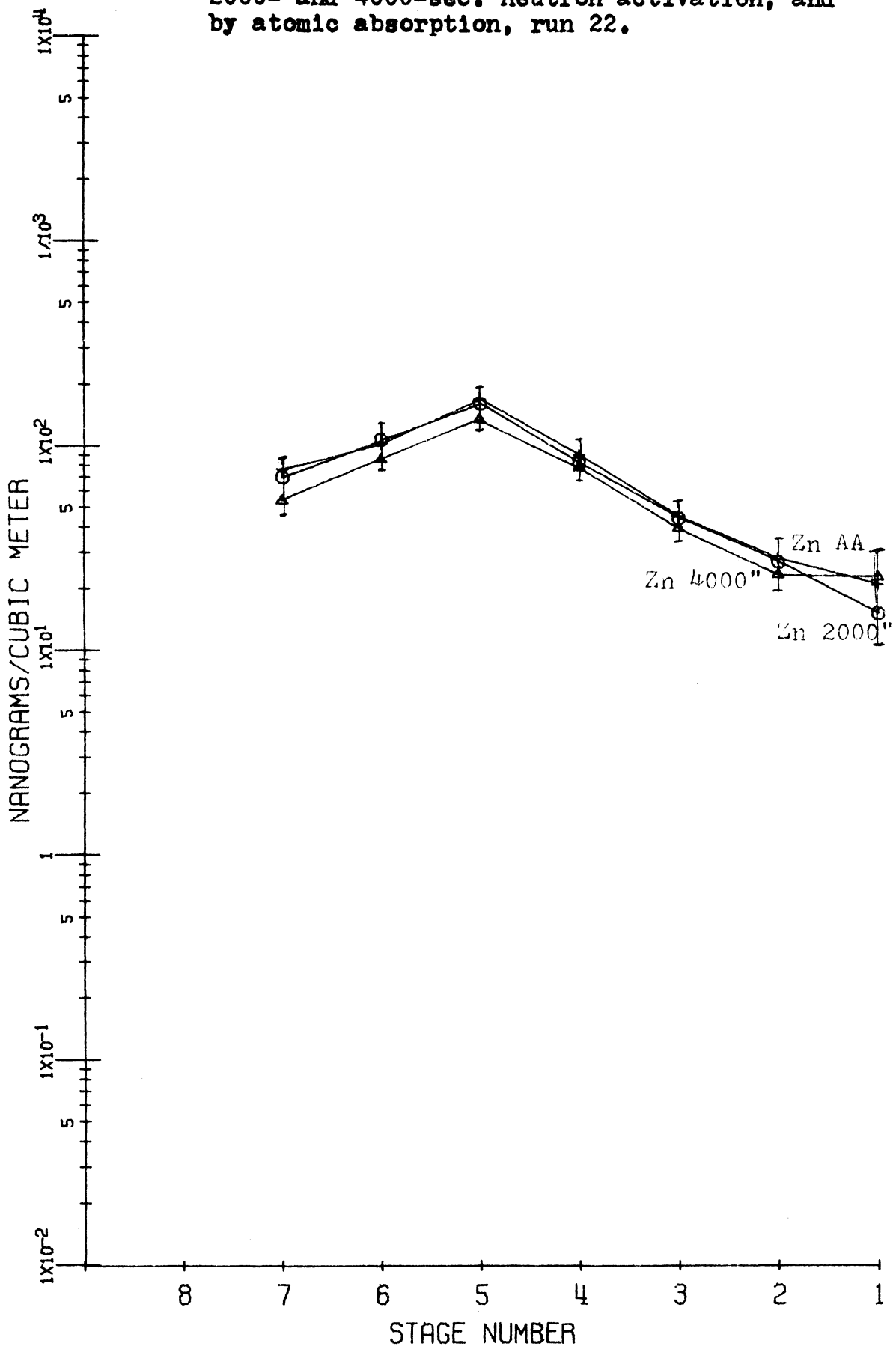

Figure 9. Duplicate samples, run 21.

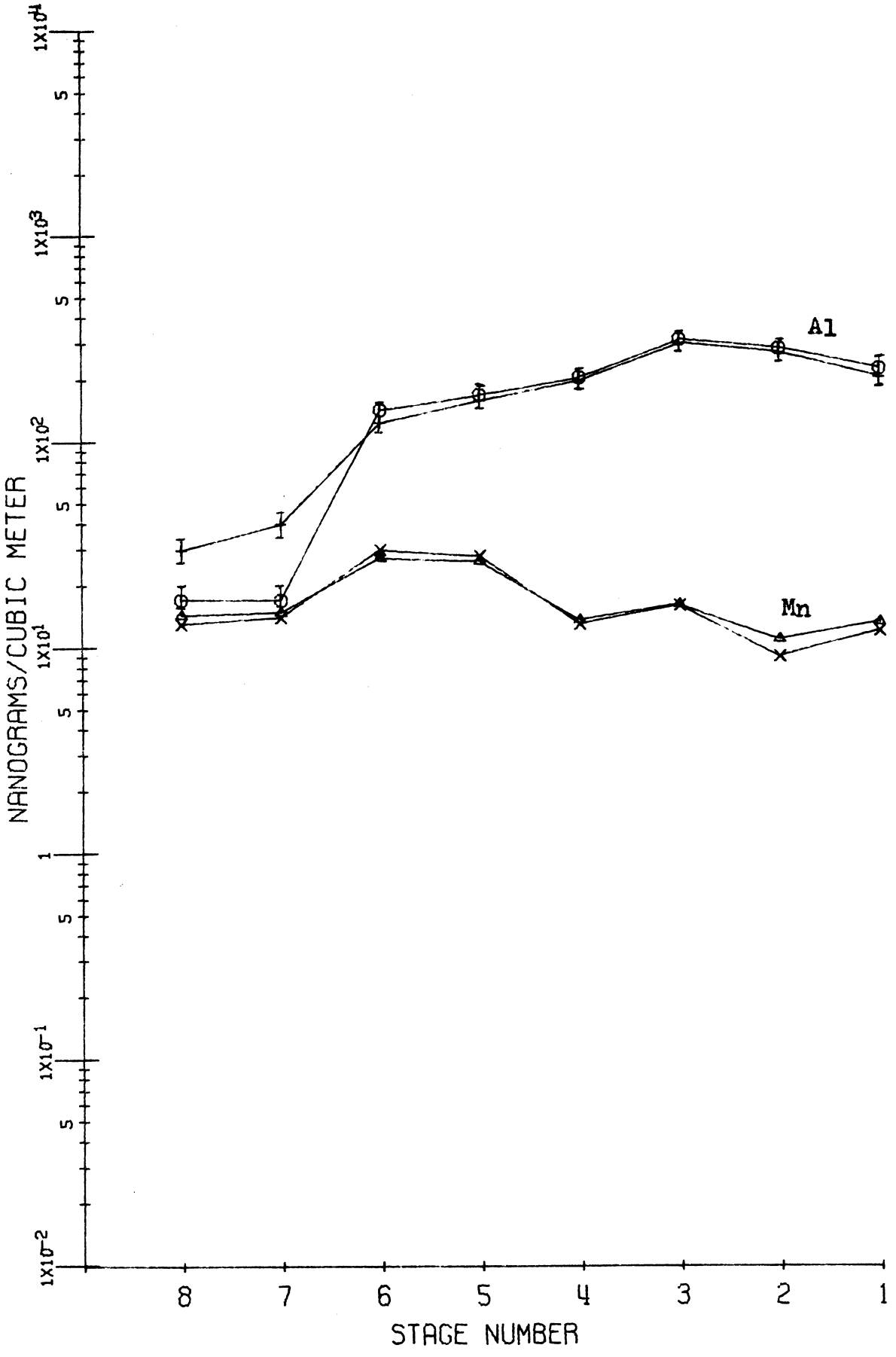

Figure 10. Duplicate samples, run 21.

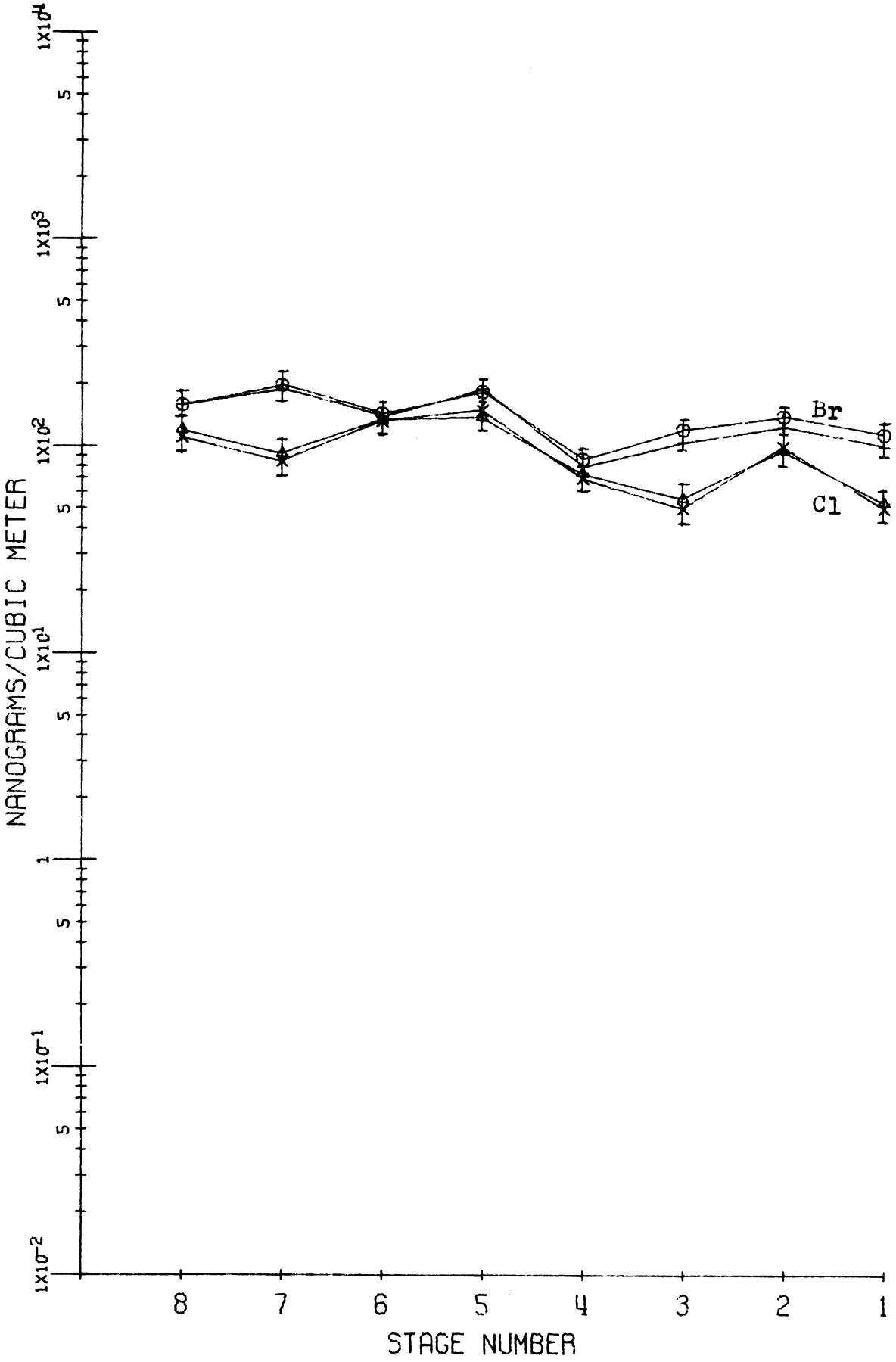

Figure 11. Duplicate samples, run 35.

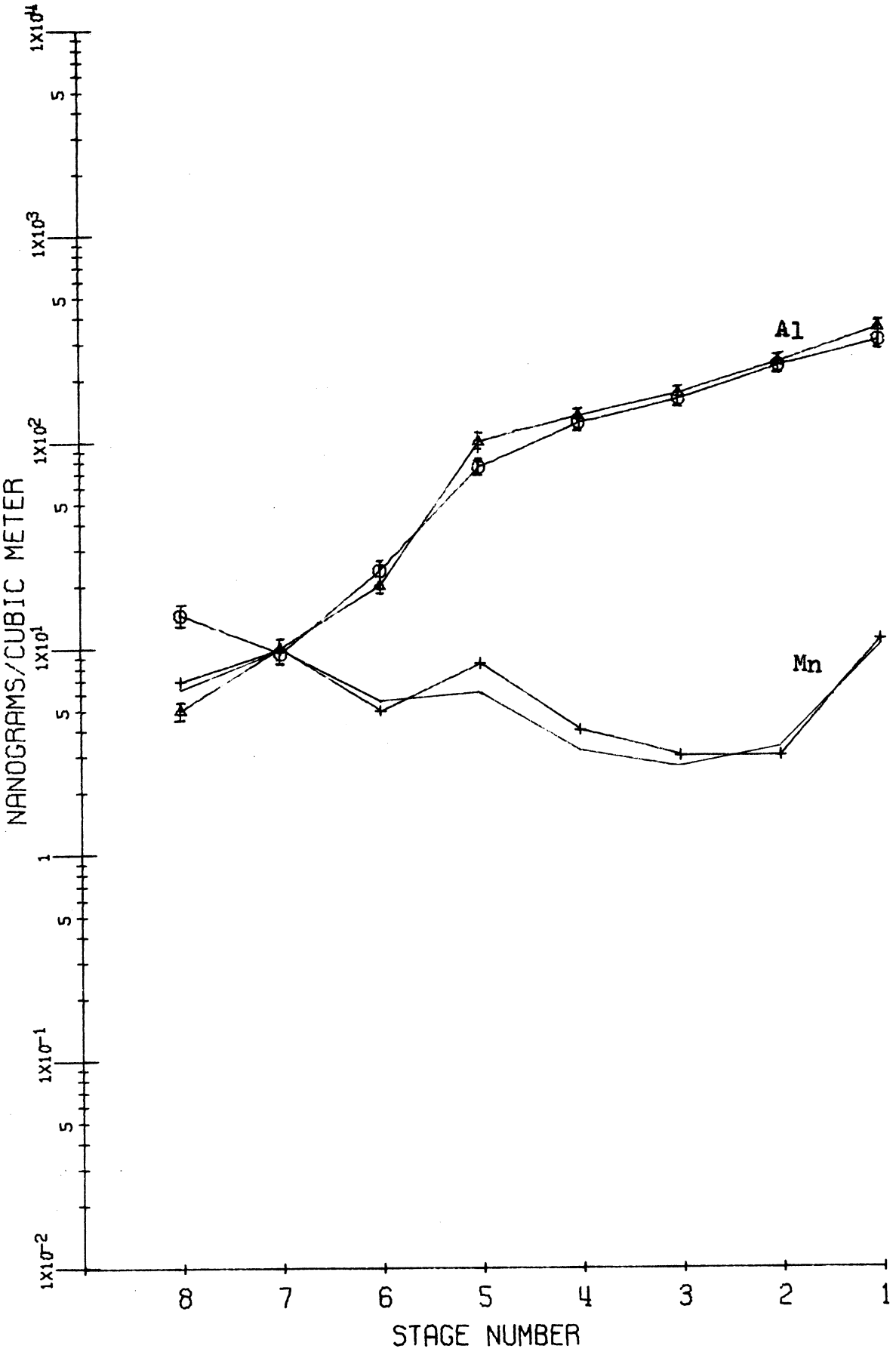

Figure 12. Duplicate samples, run 35.

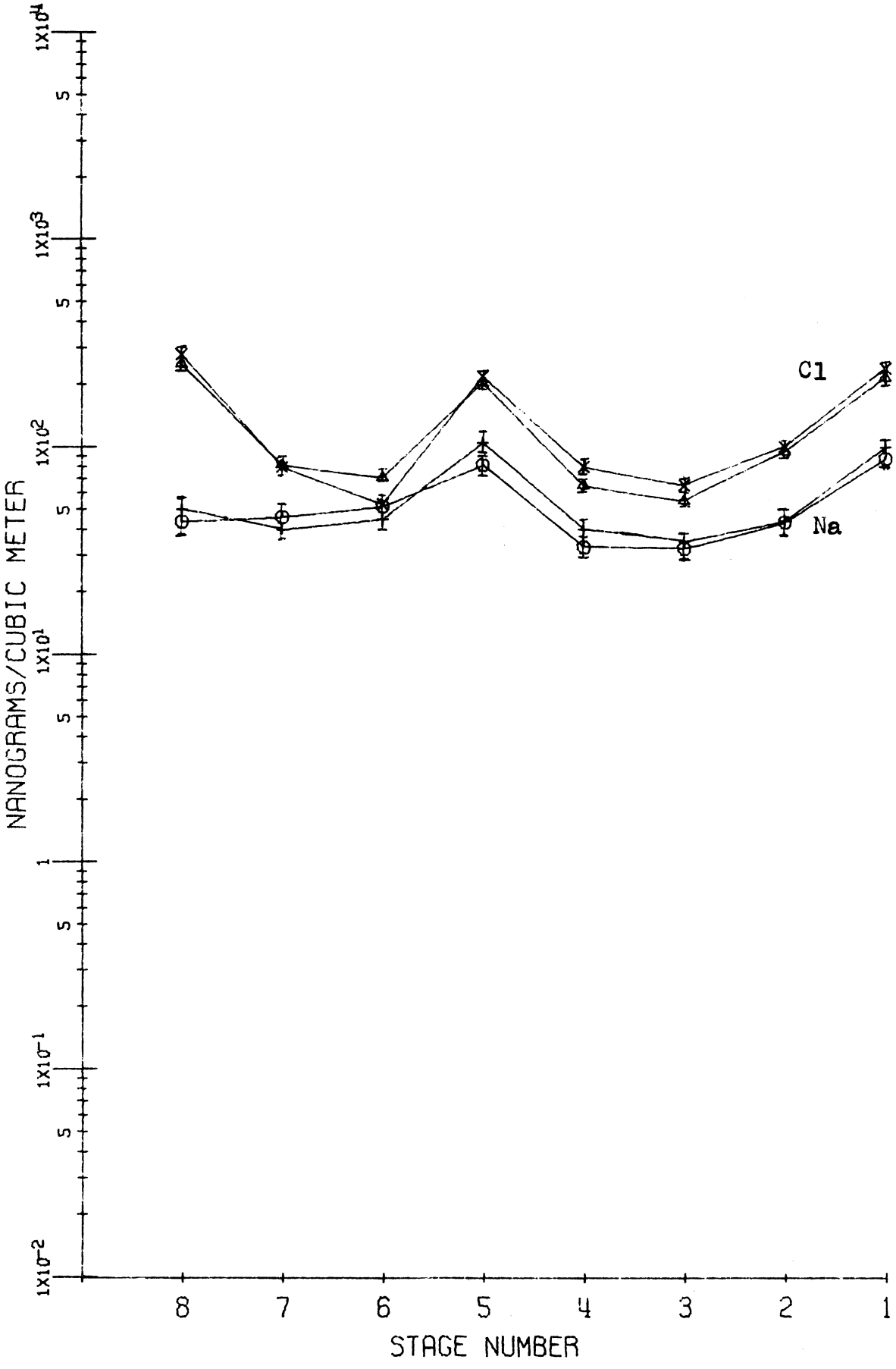

CHAPTER IV

RESULTS AND THEIR INTERPRETATION

A. INTRODUCTION

Results found for all 50 Andersen Impactor runs are included in the Appendix, Tables 21 through 32. Data have been organized such that all results from any one sample location are grouped on one table, with individual samples designated as runs. All 50 runs are numbered consecutively for ease in identification. Duplicate sample runs are given the same run number, but the second sample of the pair is designated "Duplicate" for identification purposes. Duplicate analyses are also labeled as such, and are grouped with original analyses.

For each datum point, one standard deviation is entered in parentheses immediately after the concentration figure. This error function is based on counting statistics for neutron activation data, and absorption peak variability for atomic absorption data. But for <u>all</u> samples, each concentration datum point is subject to an additional error of $\pm$ 10% of the value listed. This error arises due to possible errors in sample collection and in sample preparation, including such items as power fluctuations affecting flow rates, and sample disc aliquoting.

All 16 "high-volume" samples are arranged in a single table, Table 33, immediately following the Andersen data. Fourteen of these were taken in parallel with 14 of the

impactor samples, and these have been designated with the same run number as was assigned the parallel Andersen. Two "hi-vols" were taken when it was not possible to collect a size distribution sample; these are assigned runs #51 and #52. The format for entering the data is the same for these samples as was used for the impactor data. Standard deviations are based on the same considerations, and, again, an additional ± 10% error must be assigned to each concentration.

It has been found that of the 29 elements detected and quantitated by neutron activation and atomic absorption spectroscopy, 25 of these tend to fall into one of eight groups. This observation is made mainly on the basis of the size spectra, but it is also reinforced by total concentrations over all size ranges for a given element, and also by data obtained from high volume air sampling. Thus, it should prove useful to pick what seems to be an important single element in each group, based on abundance, to compare this with other elements in the same group, considering size spectra and concentrations, and to compare this group with other groups. It has proven most useful to compare each group's elements with the Junge distribution, $dM/d(\log r) = C$. Group 1 consists of metals associated with large aerosol particles arising from dispersion source processes, mainly associated with the ferrous metals industry, and includes iron (Fe), manganese (Mn), chromium (Cr), and cobalt (Co), in addition to scandium (Sc) and thorium (Th).

Group 2 includes elements found on very small, or "condensation," aerosol particles, again arising mainly from the steel industry, but from processes involving conditions of high supersaturation. Group 2 includes zinc (Zn), indium (In), antimony (Sb), and arsenic (As). Group 3 includes only copper (Cu) and seems to have source processes as mentioned for elements in both groups 1 and 2 above. Other apparent groupings from the data include elements associated also with large particles, such as group 4, including calcium (Ca), magnesium (Mg), and titanium (Ti); and group 5 including aluminum (Al), lanthanum (La), samarium (Sm), europium (Eu), and cerium (Ce). Elements associated more with smaller particles include group 6—bromine (Br), gallium (Ga), and potassium (K); and group 7—sodium (Na), and chlorine (Cl). As will be seen in the discussion, vanadium (V) seems to have a unique size pattern of its own. Because of extremely low concentrations involved, and/or erratic spectra obtained, tungsten (W), mercury (Hg), selenium (Se), and iodine (I) could not be adequately classified, although several comments about these 4 elements will be mentioned at the close of this discussion.

B. GROUPINGS BY PARTICLE SIZE DISTRIBUTIONS

1. Iron, Manganese, Chromium, Cobalt, Scandium, and Thorium

The "iron" group of elements, which includes Fe, Mn, Cr, Co, Sc, and Th, should first be considered. Essentially, these are obvious dispersion aerosols and their origin is mainly the ferrous and non-ferrous metals industries. The

link between this group and the second group is through Cu, where Cu seems to be emitted by both dispersion and condensation processes. Among the elements discussed, Fe shows the largest concentration of any element on particles of such a size as to be impacted on stage 1 of the Andersen Sampler, and decreases more or less gradually in concentration, depending on the sample location, toward the smaller sizes. The closer to a source, the higher the stage 1 concentration is relative to total Fe, and the steeper the slope of decreasing concentration. In other words, it would seem that in general a larger fraction of the Fe found close to source processes is associated with large particles than is true for more distant locations. Manganese is similar, generally having a large stage 1 size-fraction, but then a more uniform, or "flat" size distribution for particles impacted on stages 2 through the filter. This even distribution on smaller particles is not the case for Fe. Chromium, Sc, and Co tend more to parallel Fe. The relationship between Fe and Th is less distinct. Thus, looking for a moment at sample #19, taken over a two-week period at the East Chicago fire station (Figures 13 and 15), the Fe concentration is $\approx$ 700 ng/m^3 in the size fraction impacted on stage 1, drops to about 300 ng/m^3 at stage 5, and drops quite rapidly to less than 100 ng/m^3 at the filter. This is very similar to Cr and Sc where Cr is present to 1% of the Fe, and Sc 0.05%. It is not similar to Mn in that Mn has a more uniform concentration distribution, but

shows a strong peak associated with stage 1. Manganese at this location has a slightly rounded area around stages 6 and 7 similar to what will be shown to be the Zn pattern. This indicates some Mn on aged aerosol particles, or, Mn not necessarily local in origin. Manganese on other samples often approaches the Zn pattern except for a high stage 1 level, where stage 1 size Mn represents local dispersion sources. A number of other elements have size distribution patterns similar to Fe, and for sample run #19, include Mg and Ca. Also, Cl, Al, and Ti show a partial resemblance to Fe. These elements arise only partly from the area steel complex, and will be discussed in later sections.

Turning to the 2-week sample from Markstown, run #22 (Figures 14 and 15), Fe again shows a very even slope downward in concentration from stage 1 to stage 7, ranging from 800 to 100 ng/m^3 per size fraction. Thorium, Cr, Co, and Sc show similar distributions, but Mn again deviates in that it is more evenly distributed through all size ranges except the largest. These elements, except for Mn, are quite regular in their declining concentrations per stage from stage 1 to stage 7.

Contrast this with the next location, Wirt School in Gary, Indiana (Figure 16). The aerosol sampled here, run #27, shows an Fe pattern from large to small particles that slopes much more gradually than on previous samples, but, of course, concentration is still higher on larger particles. This pattern is also seen for Sc, Cr, and Co, as well as

for Ca, Ti, and Mg. Again, Mn is more evenly distributed among the stages. The magnitude of Fe at Wirt School is several hundred ng/m^3 per stage. Wirt School in Gary is located much further from the steel industry than is Field School or Markstown in East Chicago. This is reflected in the lower concentrations and more uniform size distribution for Fe found at Wirt than in East Chicago. But also notice ratios of elements. Fe/Mn is ≈ 10 for all particle sizes at Wirt, is ≈ 10 for small particles in East Chicago, but then rises to ≈ 50 for sample stage 2 in East Chicago. This shows dispersion Fe by steel industry pollution in East Chicago, with a small-particle background. Then Fe/Mn drops on stage 1, showing not an Fe decrease, but a sharp increase in large particle Mn pollution from steel industry sources.

On the Ann Arbor samples, runs #45-50, Fe shows the customary slope downward, somewhat steep, and the concentrations are on the order of as much as several hundred ng/m^3 down to less than a hundred ng/m^3 ranging from size 1 to the filter (Figure 17). Many other elements parallel it quite closely, including Zn, Cr, Al, Na, Ca, Ti, Cu, Cl, W, but not Sb. Manganese, Sc and Th show resemblance on larger sizes (Figure 18). A dispersion aerosol (fly ash from power generation) is strongly indicated for this area.

Considering samples taken on Lake Michigan, Mn is "Junge-distributed" far from shore, run #42, but strongly concentrated on those particles impacted on stages 1 and

2 where sampled close to the Gary shoreline, runs #43, 44 (Figure 19). In fact, the closest sample to Gary, run #43, shows a strong peak on stage 1 an order of magnitude greater than that on any other stage, but, on the next sample taken further away from Gary, run #44, Mn is predominantly stage 1 and stage 2-sized, then drops sharply in concentration to the other sizes. This would indicate that large particles containing most of the Mn mass are falling out. Note the decrease in stage 1 concentration from sample run #43 to run #42 for Al (Figure 19), Ca, Mg (Figure 53), Na, Cl (Figure 79), K (Figure 71), In and Cu (Figure 45), indicating greater pollution by dispersion aerosols of sample #43. Since only very small samples could be taken on Lake Michigan, it was not possible to accurately measure Fe.

Looking at the samples collected near open hearth operations, runs #1 through 5, Fe is present on all stages greater than a microgram/m^3 per stage, but it is 10 $\mu g/m^3$ on stage 1, dropping to about 2 to 5 $\mu g/m^3$ on most other stages. Chromium follows a very similar pattern, two orders of magnitude smaller. All samples for Fe bear this out; runs #2 and 4 have been plotted in Figure 20. Manganese also follows this pattern, and Sc (Figure 21), Na (Figure 78), Ca, Ti, and Mg (Figure 50) bear some resemblance. It appears as though the above mentioned elements are definitely associated with the steel industry, but that Ca, Mg, and Ti have other man-made and/or natural sources.

At the sinter plant, runs #6-10, a much stronger Fe

peak is found on stage 1 than existed at the open hearth (Figure 22). The composite sample yields 1 to 10 $\mu g/m^3$ in size ranges 2 through the filter, but as much as 30, 40, or 50 $\mu g/m^3$ on stage 1. Manganese shows a very similar pattern of being predominantly contained on stage 1, but then Mn on smaller sizes may become fairly evenly distributed (run #7), or fall off more rapidly in concentration (run #9). Sodium follows Fe, but Cl does not; Cl is fairly evenly distributed over all size-fractions except for a strong peak on the filter. Chromium quite closely parallels Fe, as does Cu, but Zn is somewhat different. The ratios Mn/Fe, Cr/Fe, and Na/Fe have been plotted (Figure 23).

The Gary Airport samples, runs #28-35, shows fairly steep Fe curves, but of much smaller magnitude than samples taken near steel operations (Figures 24, 25). Iron is present to the extent of 2000 ng/m^3 on stage 1, and declines to several hundred ng/m^3 throughout most of the size ranges for most samples. Chromium again is two orders of magnitude lower in concentration and very similar to Fe. Manganese shows peaks in concentration at stage 1 and usually also in the smaller size ranges. This indicates some local dispersion Mn is still present, but much of that on the larger sizes has fallen out. Hence a dip in concentration in stages 2, 3, and 4 results. Chromium is quite close to Mn in appearance, but Na and Cl tend to resemble Mn more so than they resemble Fe (Figure 75).

Element-to-element ratios have been plotted for Cr/Fe and Mn/Fe, and are shown in Figure 26. It is apparent that the fallout rate for large particles is much greater than it is for smaller particles. To elaborate, if an element is emitted on a dispersion aerosol and has a sharp excess in concentration in that size-fraction impacted on stage 1, as contrasted with size-fractions on stage 2 and smaller, then a sample collected at some distance downwind shows a loss of these largest stage 1 associated particles, loss to a smaller degree of particles that would impact on stages 2-4, and only slight loss of those in size ranges 5-filter. Hence the resulting curve shows an apparent dip in the distribution curve over size ranges 2, 3, and 4. But, if the element is associated with a dispersion aerosol, peaking in concentration on stage 1, but having a more gradual concentration decline as particle size decreases, then fallout results in a curve more nearly resembling a "Junge distribution." It should be emphasized that on a sampling trip during the first week in December of 1969, there was a large difference in Fe concentration between the first part of the week when the wind was from the north-northwest, and the last day of the week when it was from the southeast (Figure 24). On the last day Fe is much more evenly distributed over all sizes; the first 4 days it is steeper in slope and 2 to 3 times higher in concentration than on the last day. This should strengthen the hypothesis that the steel complex is the main source for Fe in that area. This same finding

is true for Mn. Note especially the difference in shape as well as magnitude for Mn between runs #33 and 35 (Figure 24). In general, the elements ascribed to steel industry sources are considerably lower in concentration at the airport when the wind is not from the mills than when the sample is located downwind from the source. This includes Zn, Cu, Sb, and Cr, in addition to Fe and Mn.

At the Gary fire station, samples #36-38 show high Fe values in the larger particle sizes, closely paralleled by Mn, and somewhat by Na. At the fire station the concentration of Mn is more elevated in the largest particle sizes with a north wind than it is with a south wind, although the magnitudes of the concentrations are not too different.

On samples from the East Chicago fire station, Fe again is much elevated in the stage 1-size range when there is a north wind, runs #15-17. Iron is much lower in magnitude and more uniform in size distribution when winds are not from the steel complex, run #18. Iron and Mn have different spectra between run #17 and run #18, as shown in Figure 27. Iron has a strong dip in concentration on run #18 on stage 2, which means that larger particles are falling out rapidly, lowering that part of the curve, but not that part representing smaller sizes. Chromium parallels Fe quite closely, Sc less so. Manganese concentrations are considerably lower on run #18 than on other samples, and somewhat more evenly distributed. Manganese is quite

"Junge-distributed" in many samples further from a suspected source. Again, Ca, Mg, and Ti, parallel Fe in part.

At Field School, the general pattern is repeated (Figure 28). But there is one difference, Fe is quite high on stage 1 for 2 samples, runs #23 and 24, 2-5 $\mu g/m^3$, then is almost "Junge-distributed" over other sizes, equal to approximately 1 $\mu g/m^3$ per stage, a fairly unusual finding. It seems that most local pollution Fe was of large particle sizes, but that there was extensive background Fe present on smaller particles. This finding also applies to Mn and Cr.

Considering last the Markstown station, on runs #20 and 21, Fe and Cr are related, but Mn less so (Figure 29). Iron is $\approx$ 1000 ng/m^3 per stage. Manganese may be emitted over a much wider range of particle sizes or, more probably, there is a natural background of Mn in the smaller size ranges. This agrees with local Mn pollution by larger-sized particles.

In summation, the 6 elements in this group, Fe, Mn, Cr, Co, Sc, and Th, are all essentially dispersion in origin. Undoubtedly all ferrous industries and non-ferrous metals industries emit all 6 to some degree, with the steel industry the prime source.

Figure 13. Run 19, East Chicago Central Fire Station.

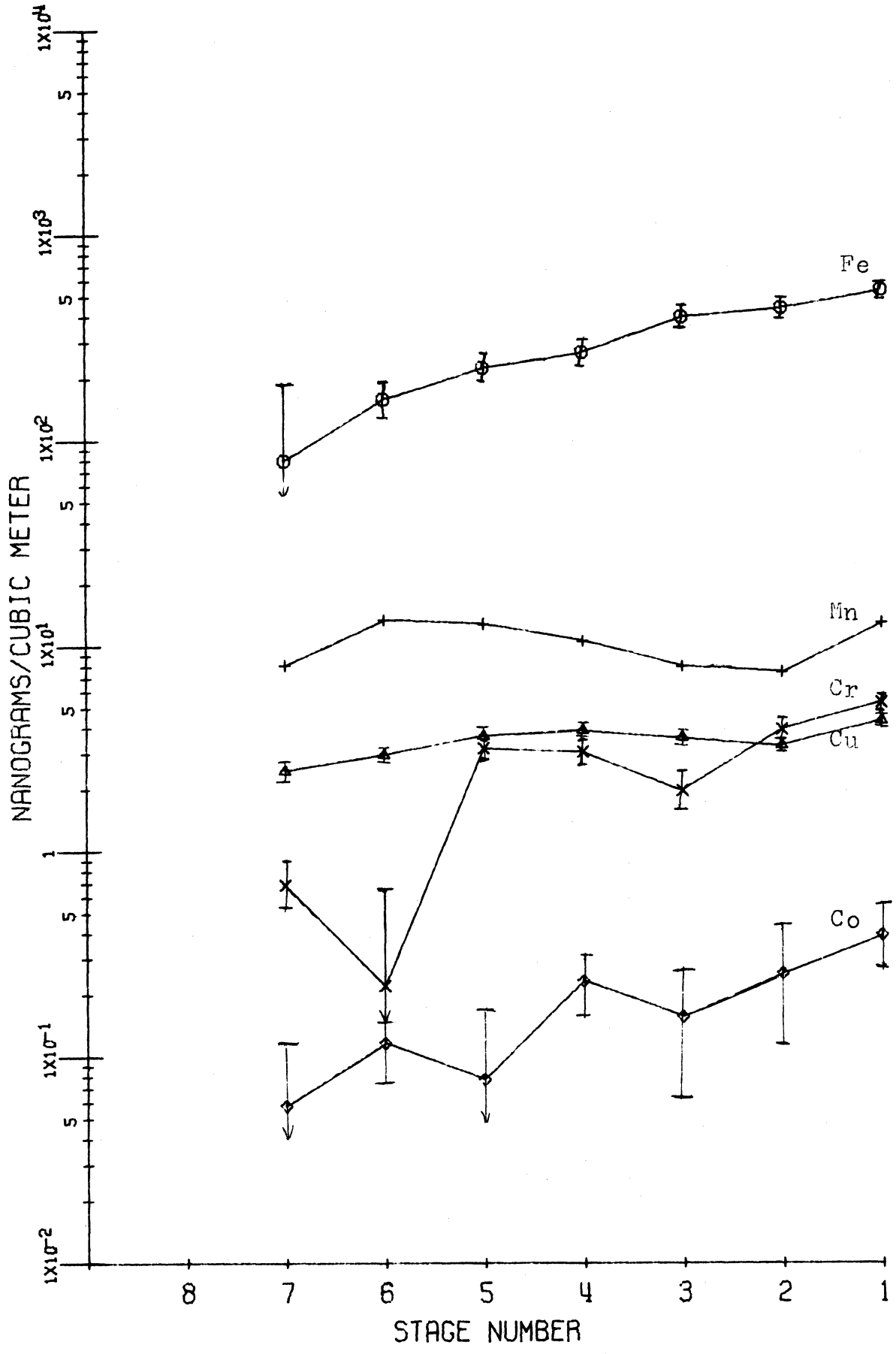

Figure 14. Run 22, East Chicago Markstown Park.

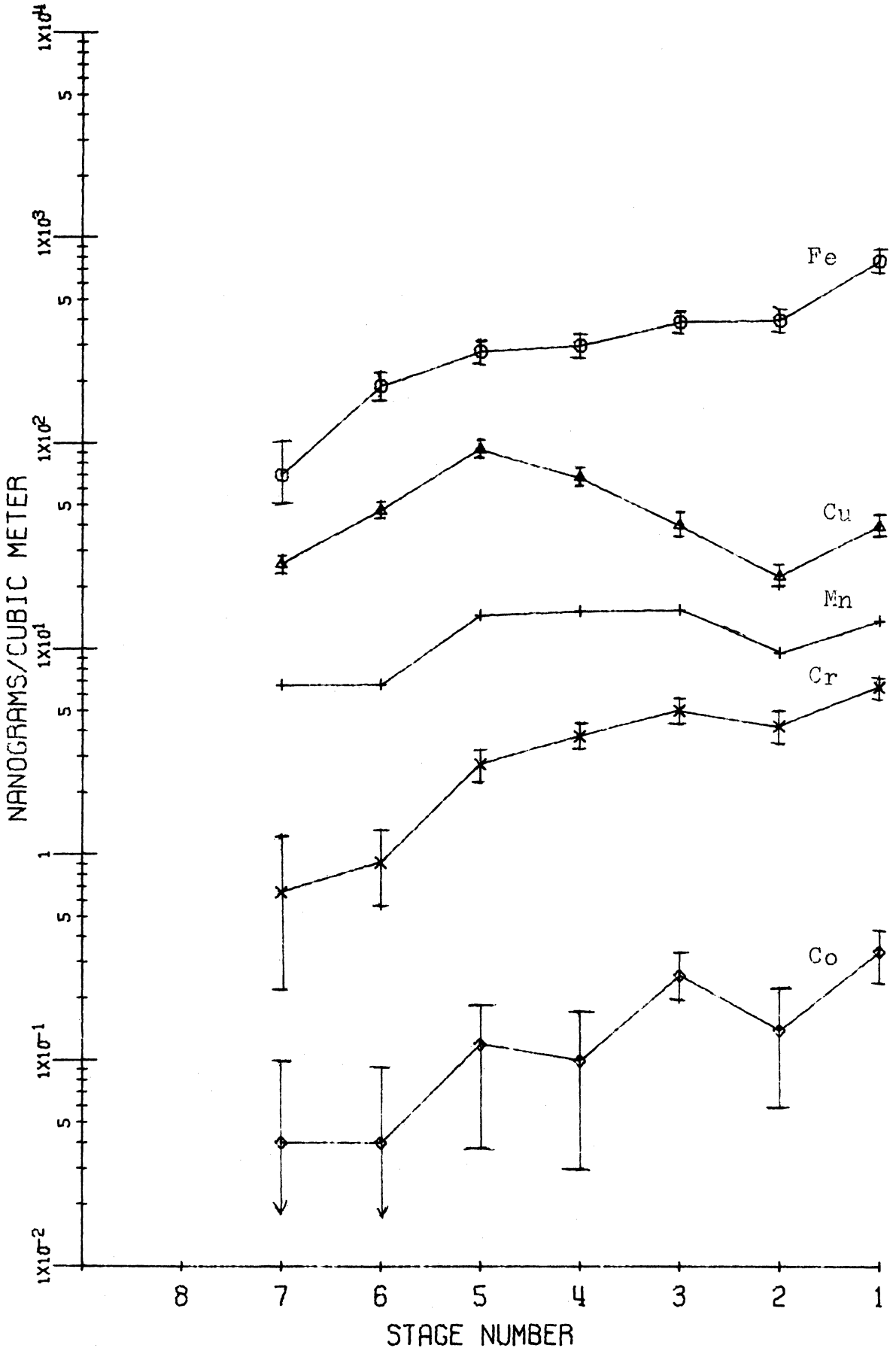

Figure 15. Run 19, East Chicago Central Fire Station; and Run 22, East Chicago Markstown Park.

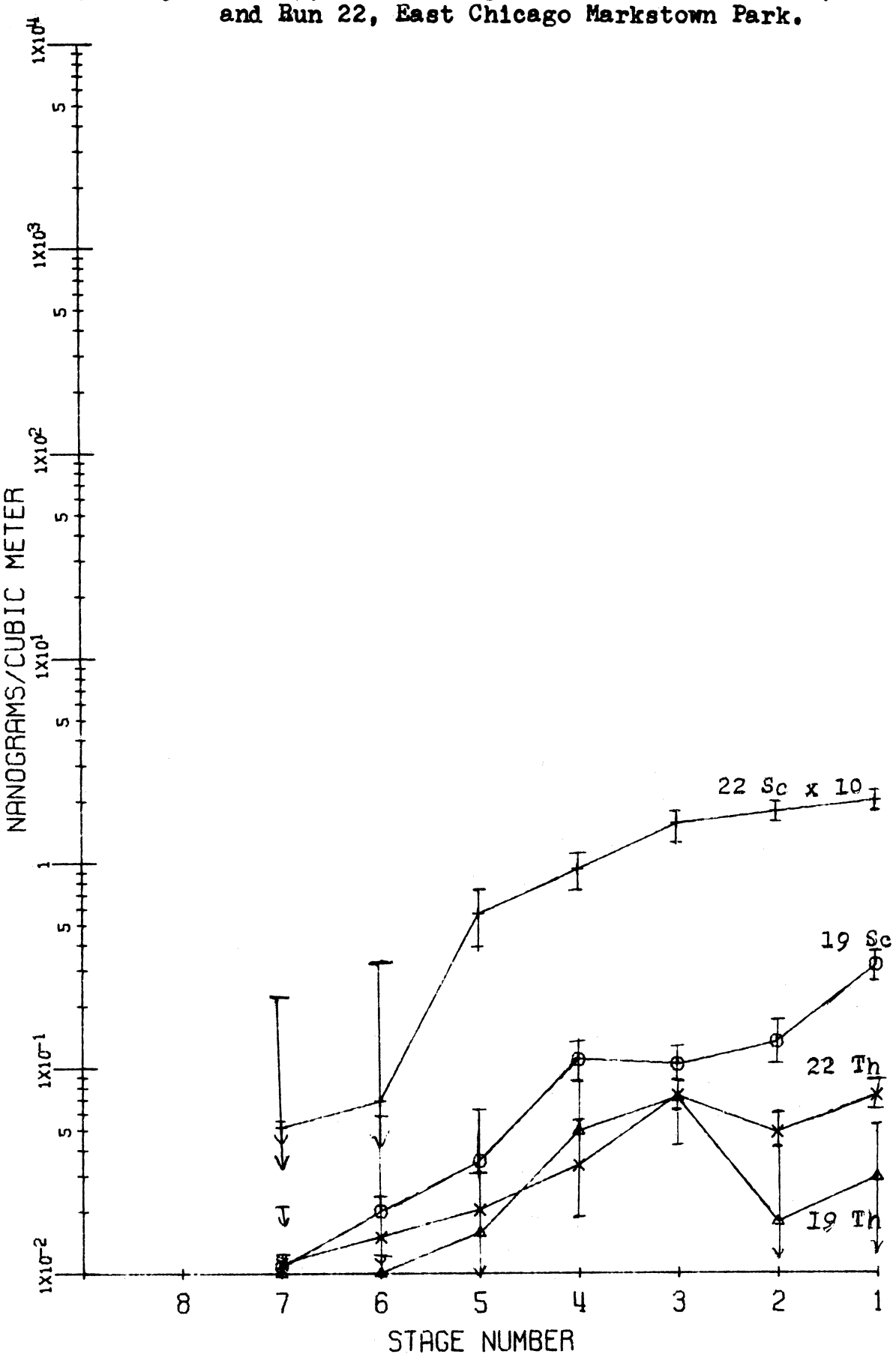

Figure 16. Run 27, Gary Wirt School.

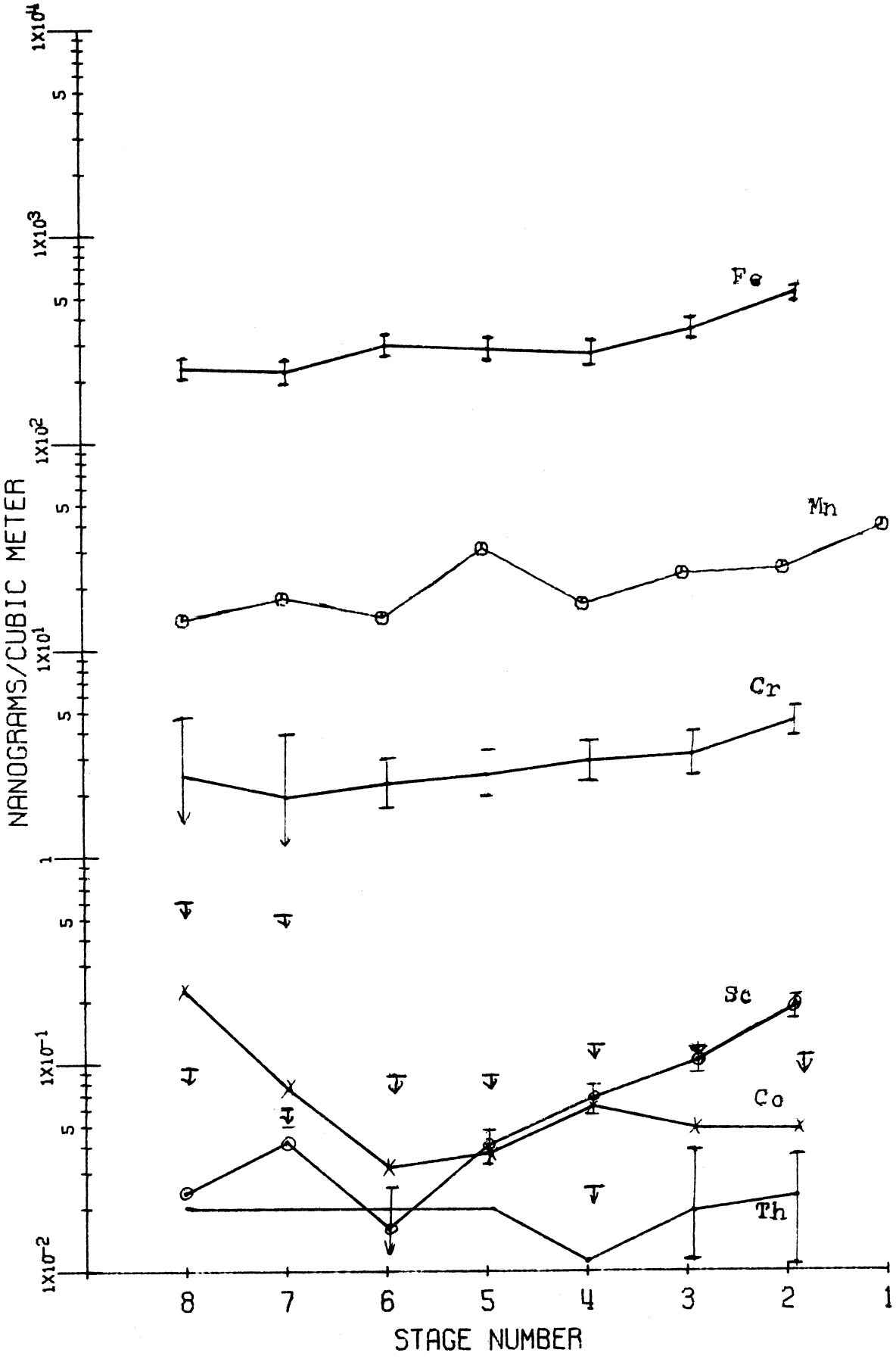

Figure 17. Run 49, Ann Arbor.

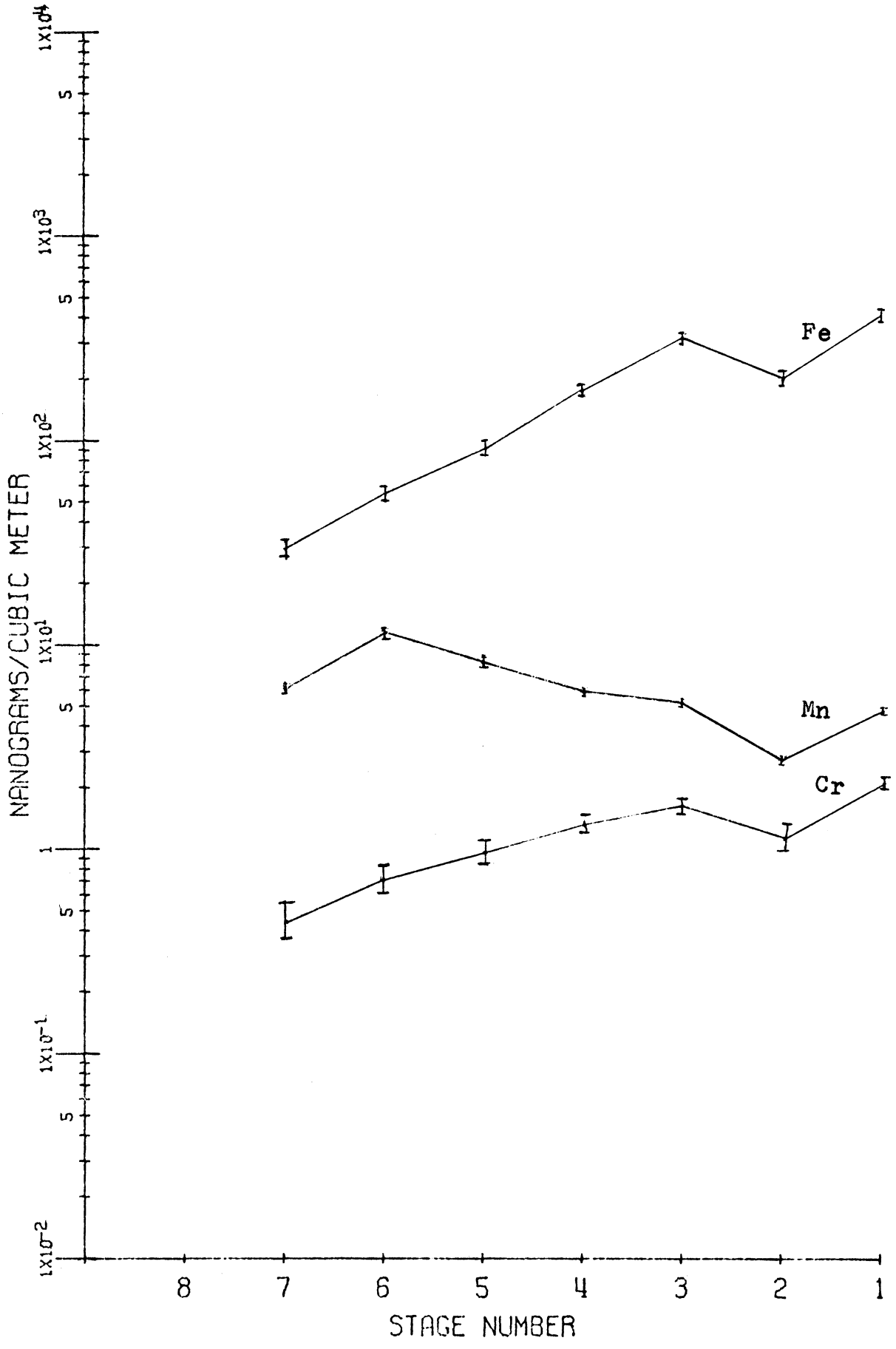

Figure 18. Run 49, Ann Arbor.

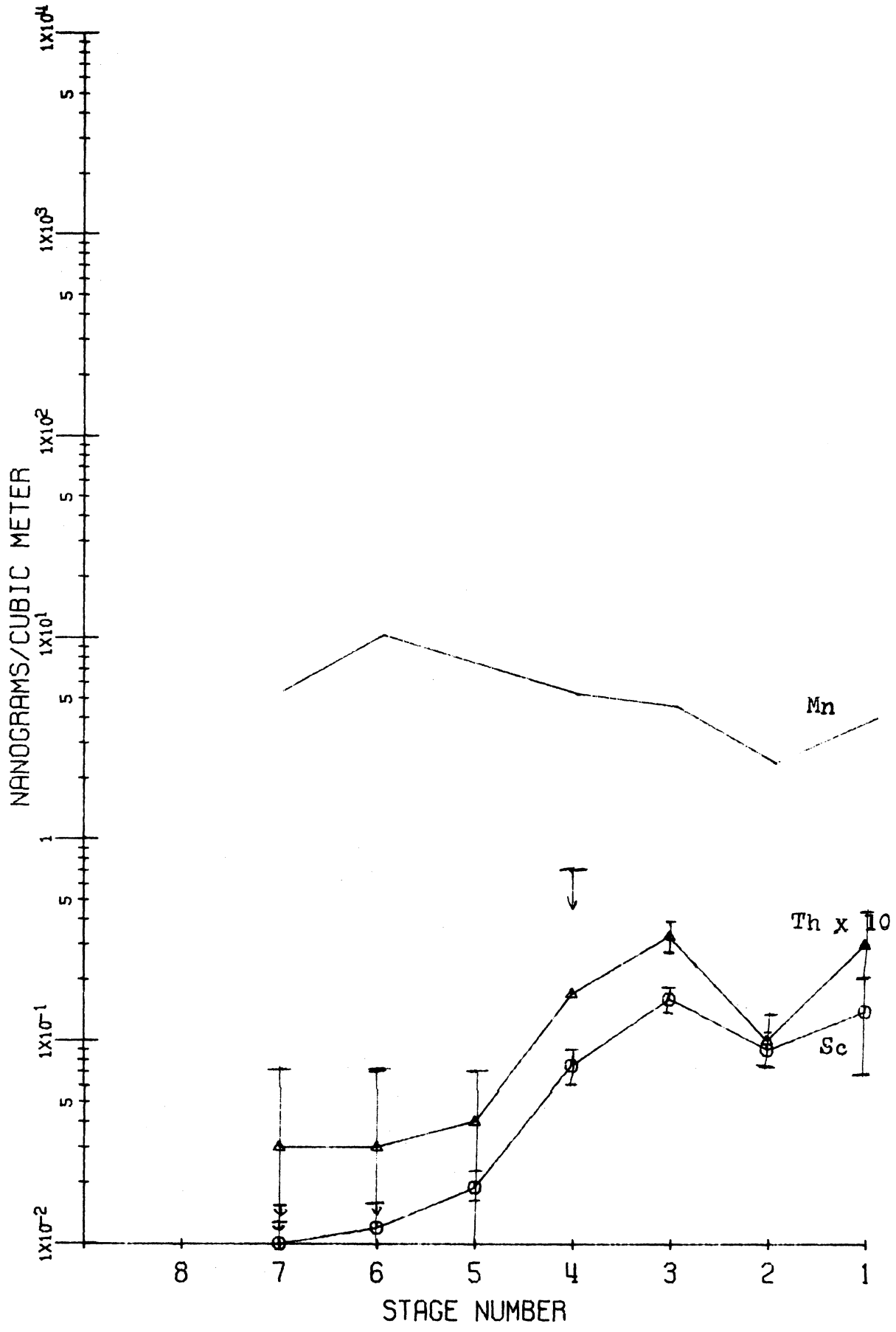

Figure 19. Runs 42, 43 & 44, Lake Michigan.

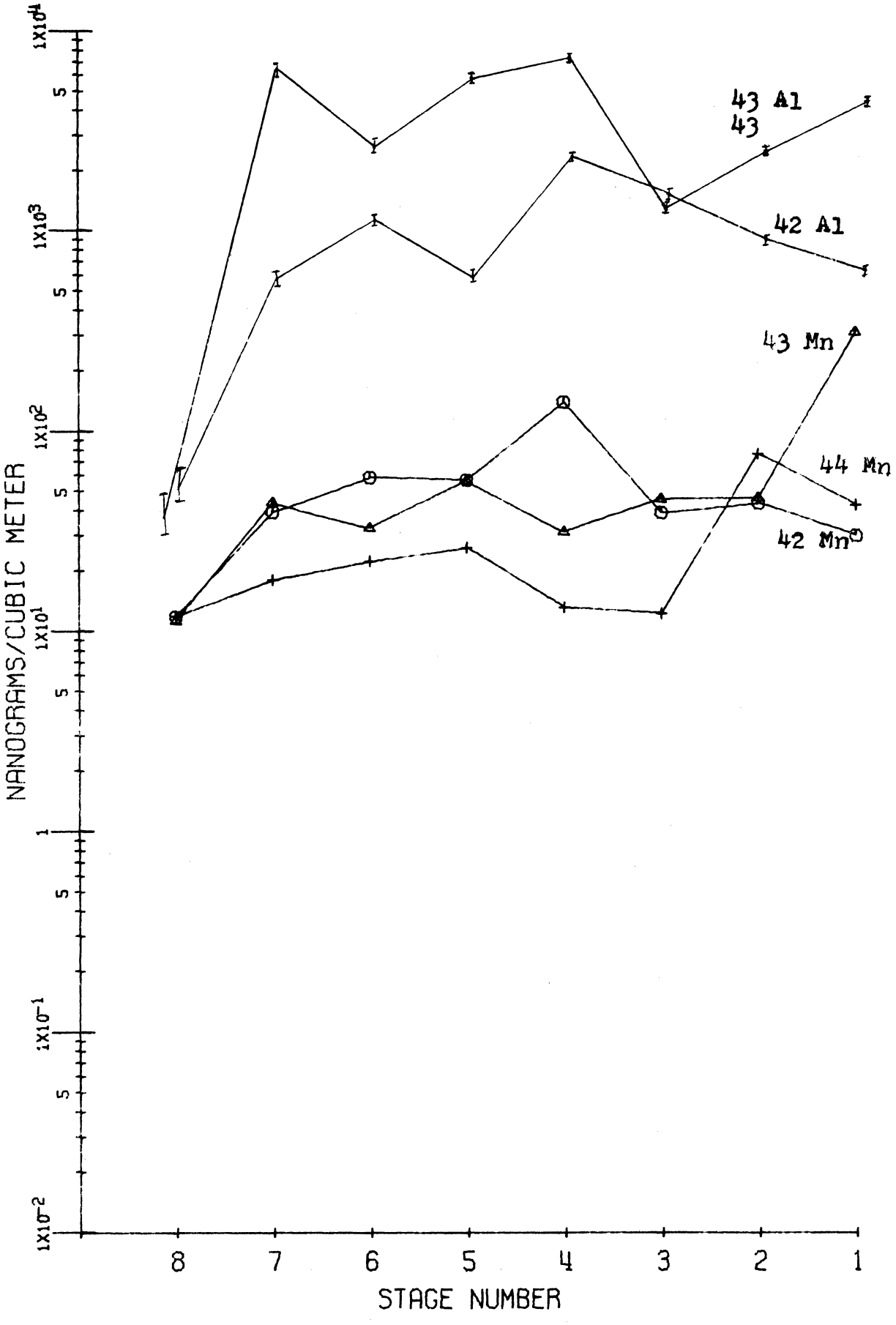

Figure 20. Runs 2 & 4, Open Hearth Vicinity.

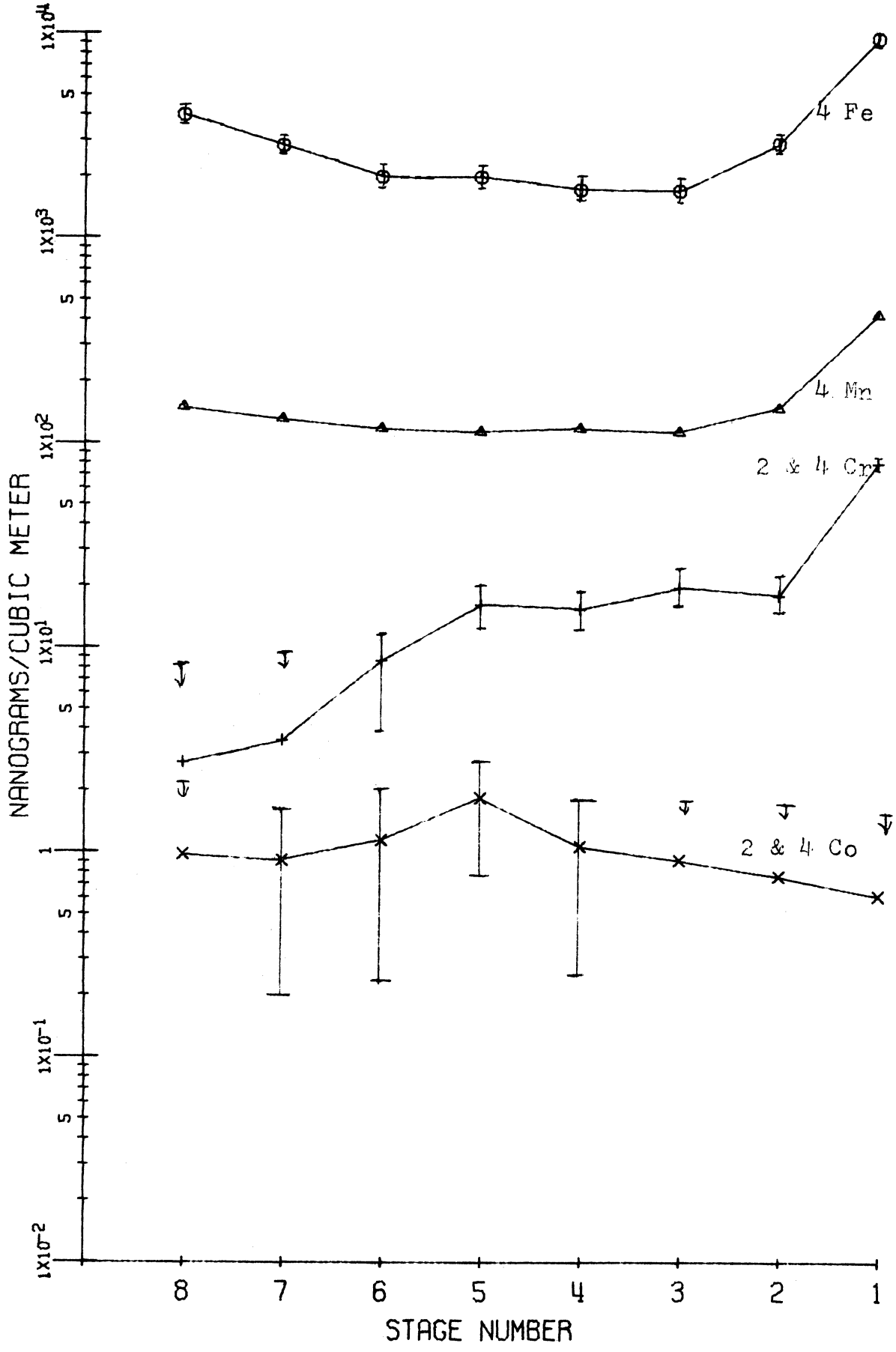

Figure 21. Run 2, Open Hearth Vicinity; and Run 7, Sinter Plant Vicinity.

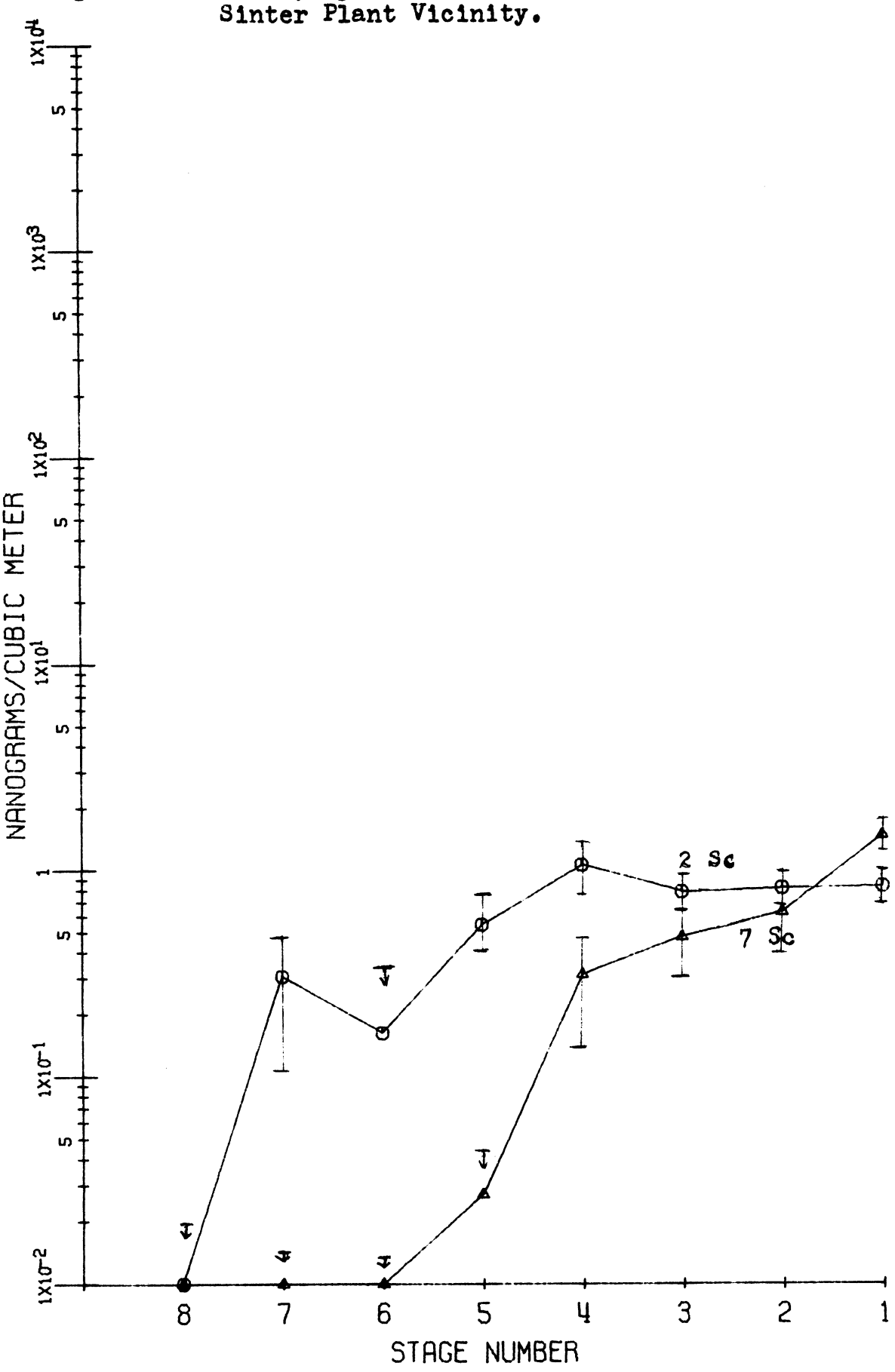

Figure 22. Runs 7-9, Sinter Plant Vicinity.

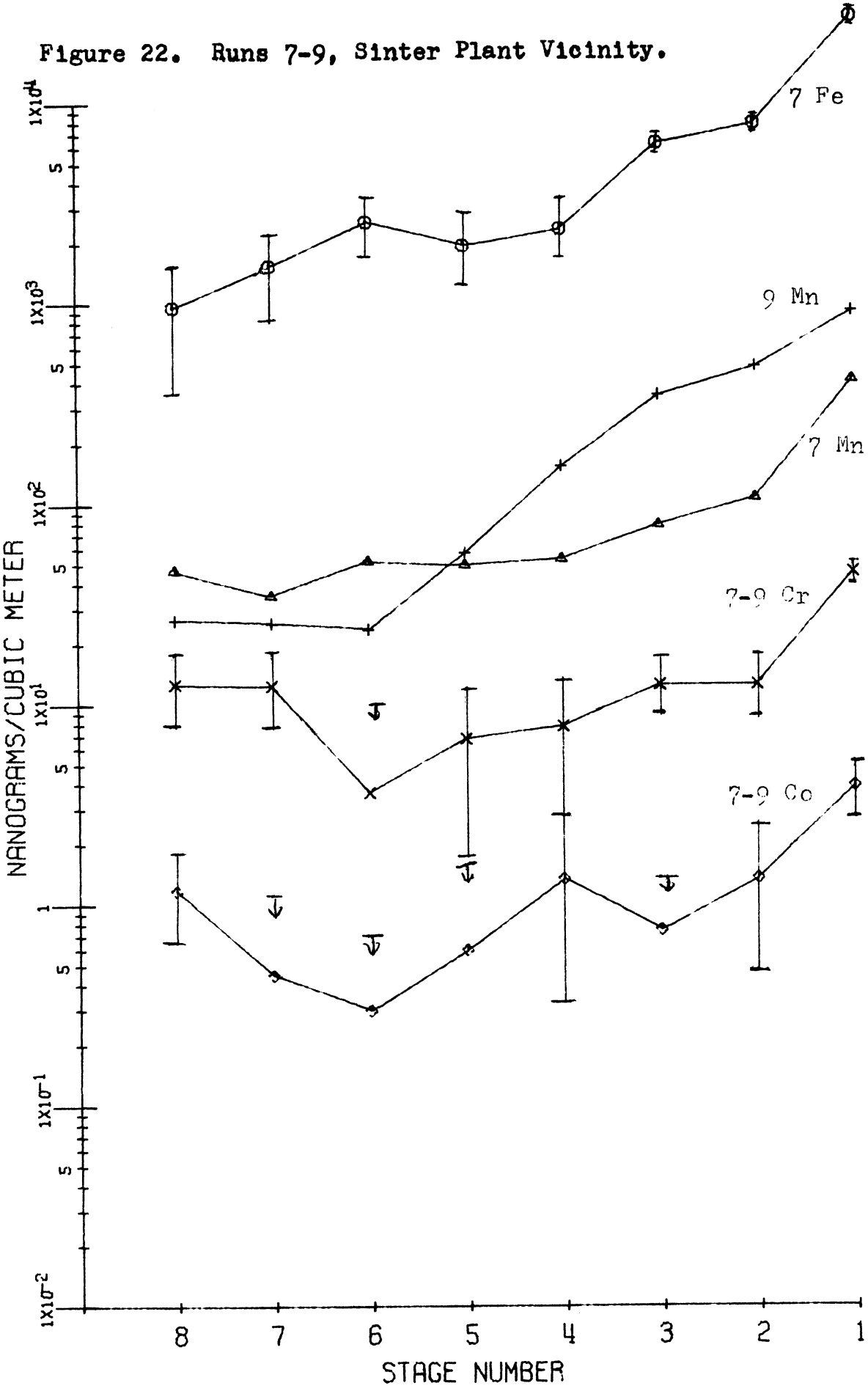

Figure 23. Runs 7-9, Sinter Plant Vicinity.

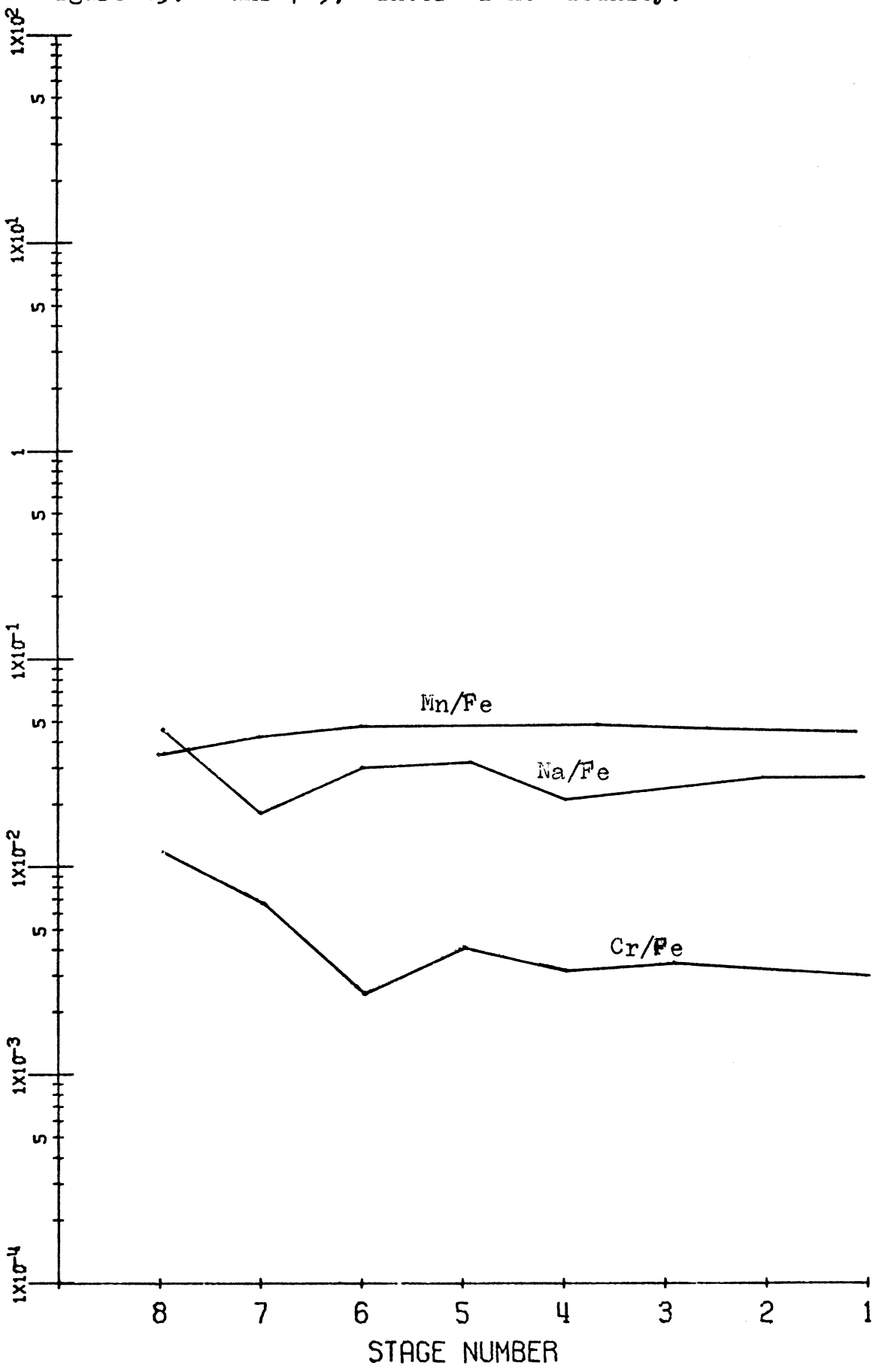

Figure 24. Runs 31-35, Gary Airport.

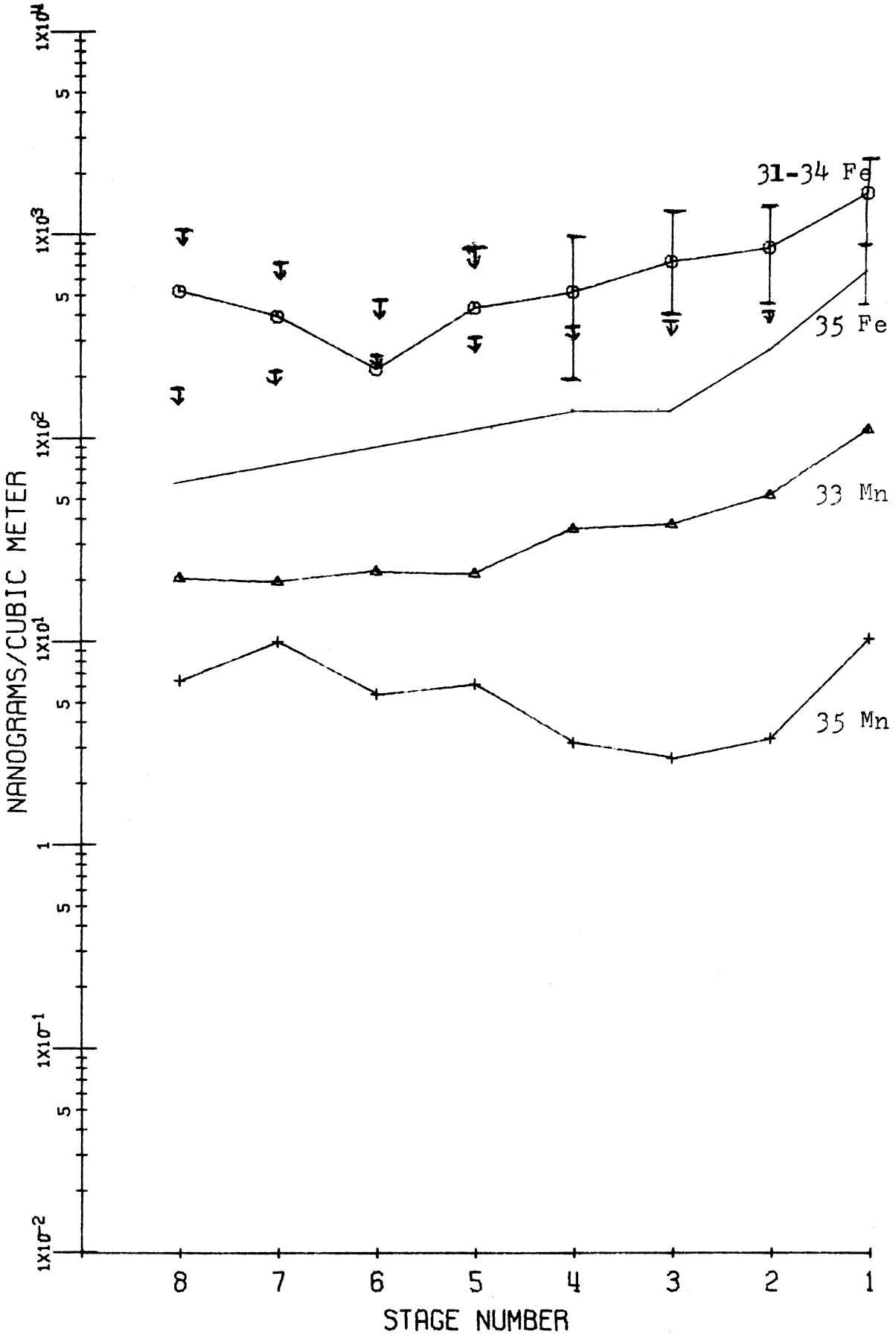

Figure 25. Runs 31-35, Gary Airport.

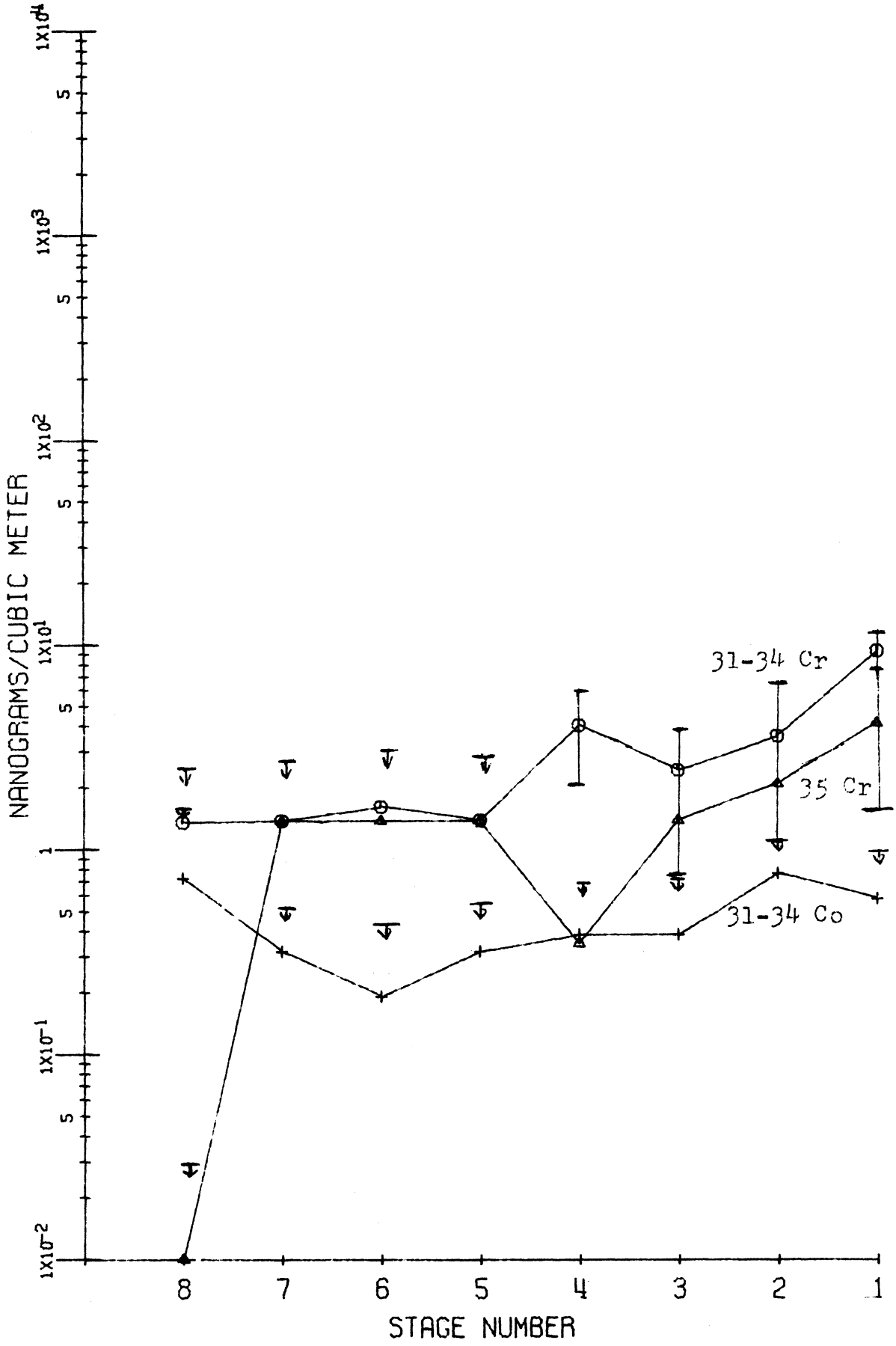

Figure 26. Runs 31-34, Gary Airport.

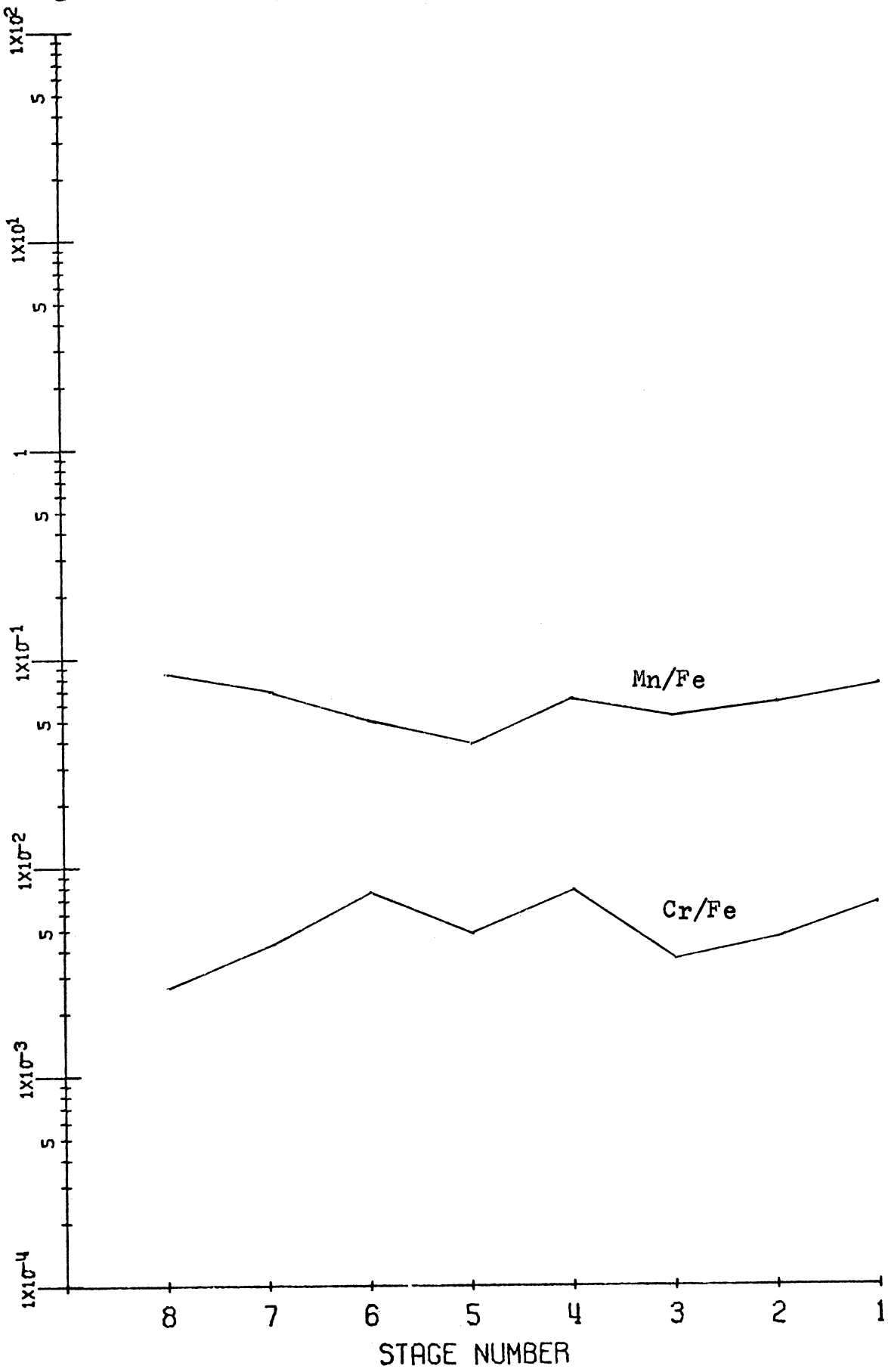

Figure 27. Runs 17 & 18, East Chicago Central Fire Station

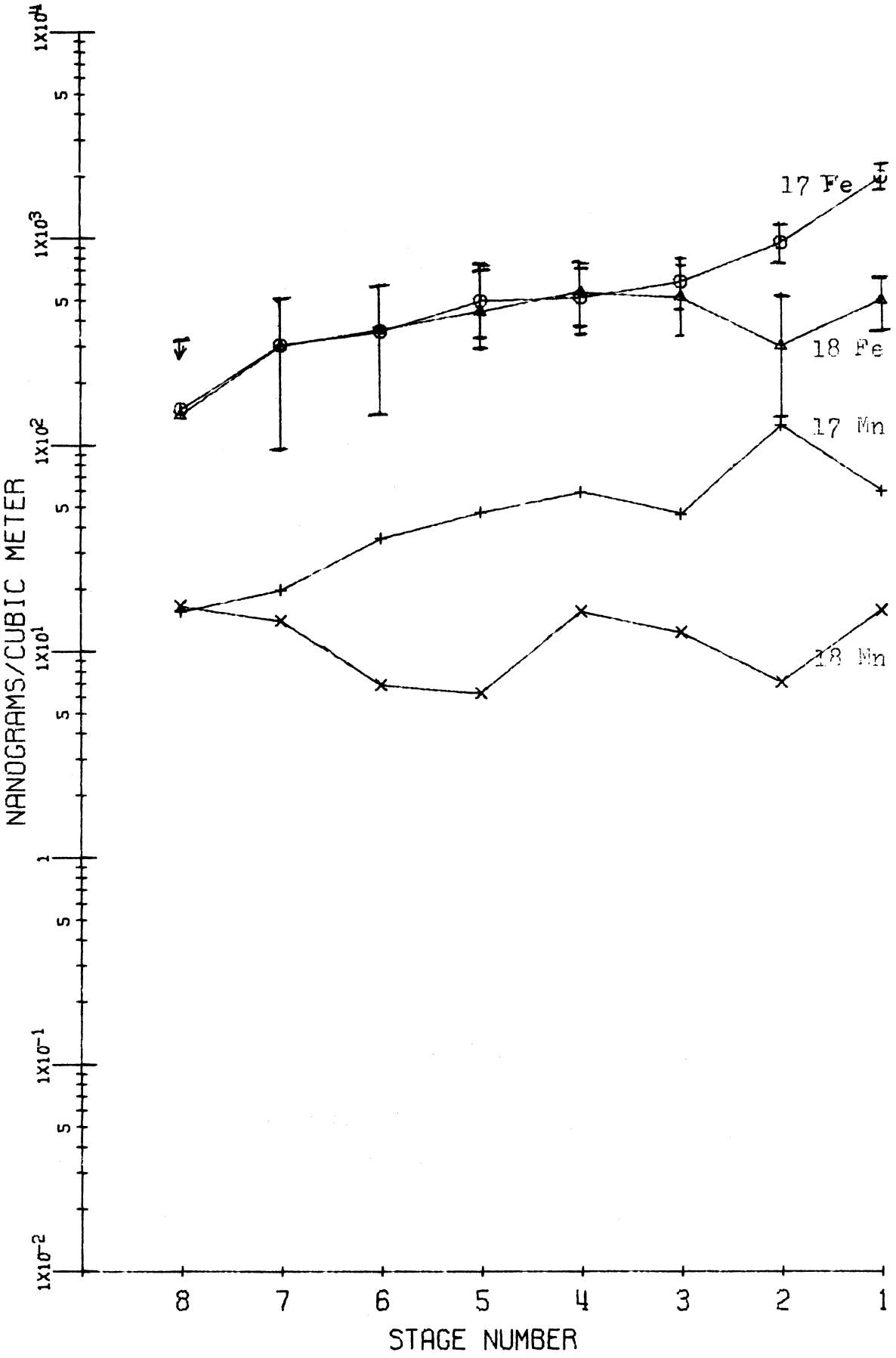

Figure 28. Runs 23-25, East Chicago Field School.

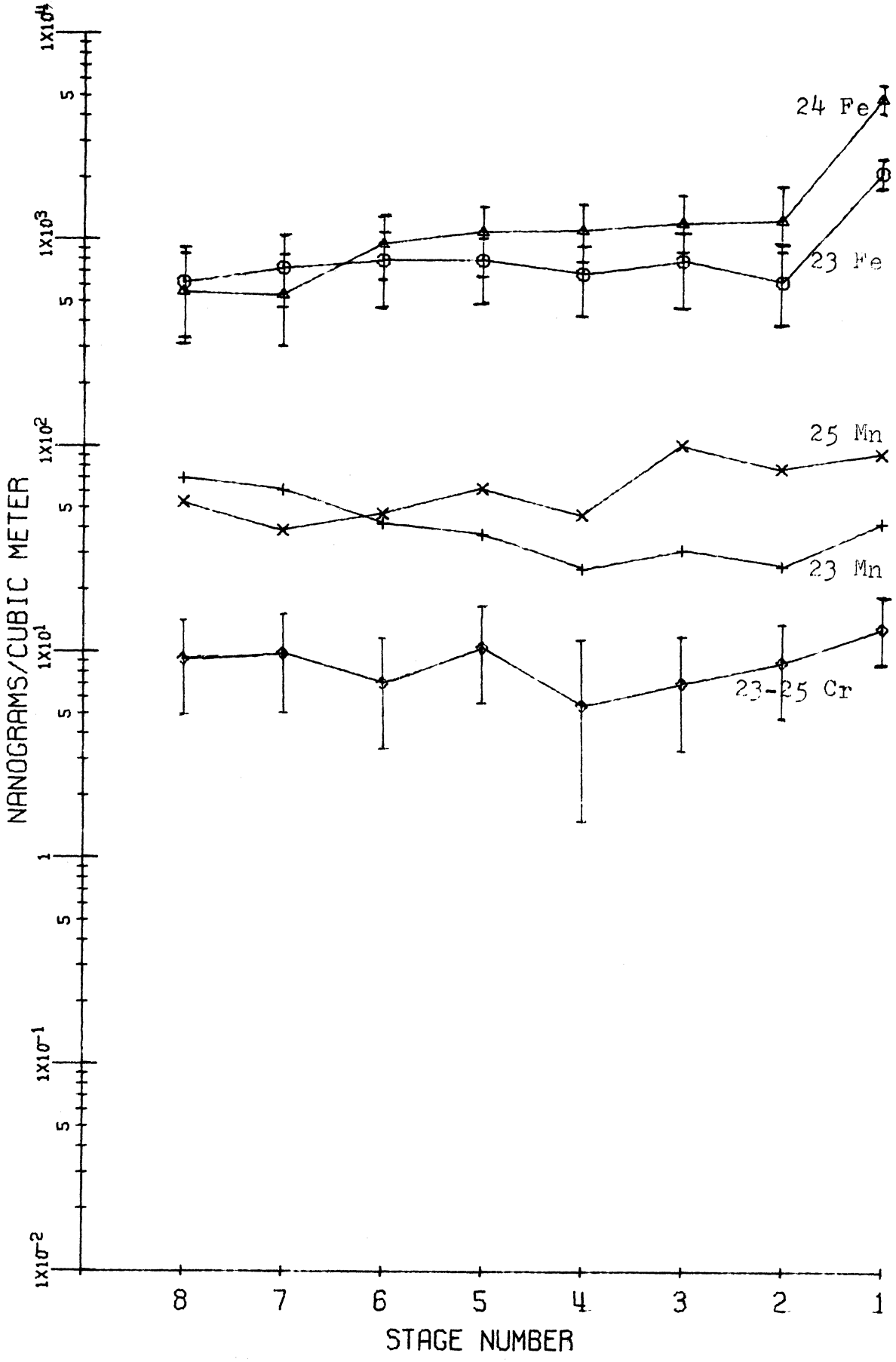

Figure 29. Runs 20 & 21, East Chicago Markstown Park.

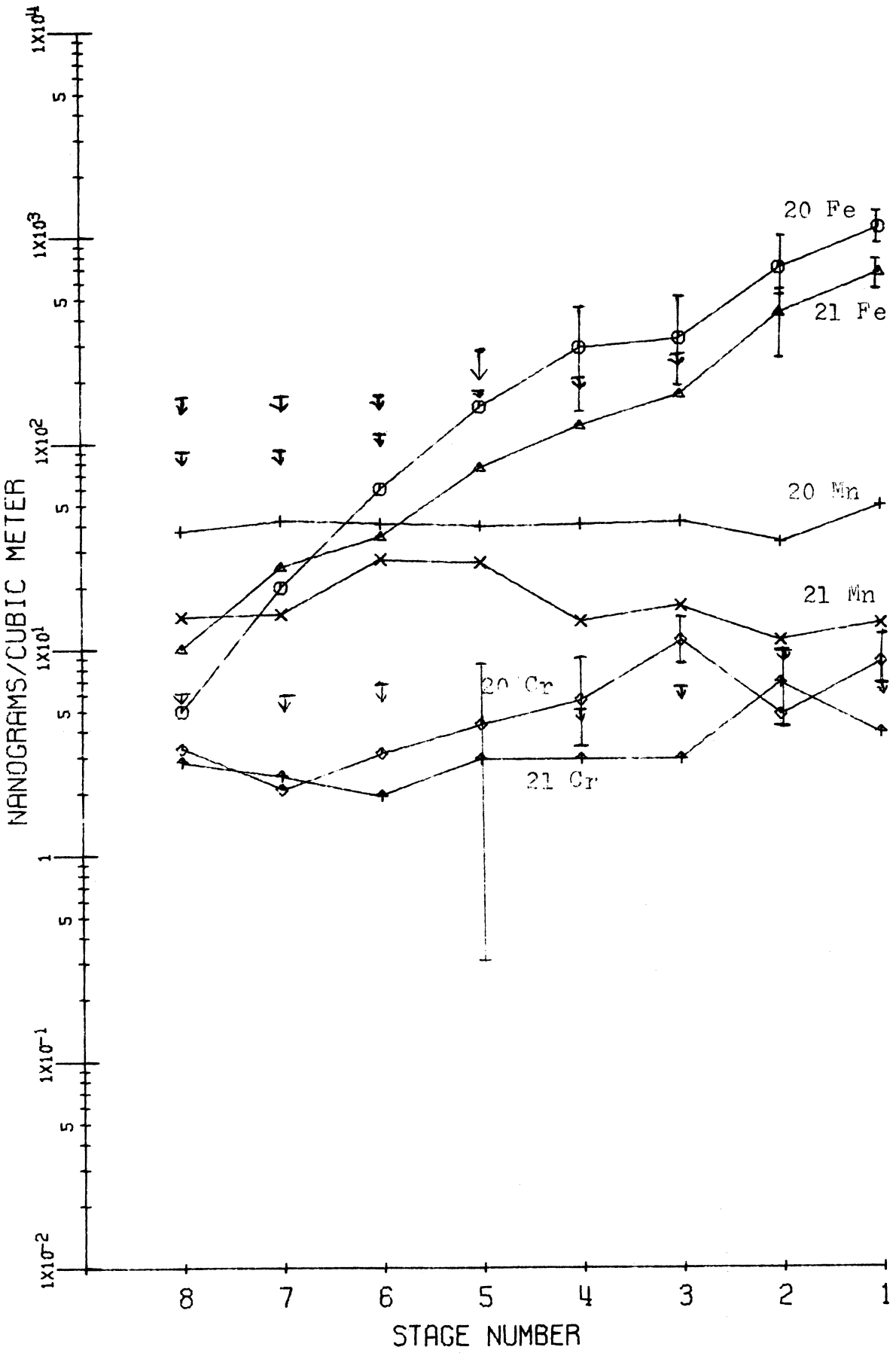

2. Zinc, Antimony, Arsenic, and Indium

Consider the second group mentioned, which might be called the "zinc" group. These elements seem to be largely associated with the steel industry in Northwest Indiana, and include In, Sb, and As, in addition to Zn. They are located on condensation aerosols from the steel industry. In many cases, however, their spectra do show large particle size components which resemble the large particle size components of dispersion aerosols from the same industry, pointing to two separate source processes.

Regarding the two samples taken in East Chicago for an extended period of time, runs #19 and 22, and considering Zn, this element has the general pattern of containing tens of nanograms/cubic meter per size-fraction on those aerosols of larger particle size as collected by the first several stages of the Andersen, but rising uniformly to a peak of about 200 ng/m^3 on aerosols collected on stage 5, and decreasing again through stage 7 (Figures 30 and 31). Related to Zn quite closely in both these sample runs are Sb, In, and As. In magnitude, Sb is 10-20%, As 5-10%, and In 0.01%, of the Zn. Antimony/Zn, In/Zn, and As/Zn ratios are shown for run #19 in Figure 32. In sample run #22, results are quite similar, but also Cu is closely related, especially to Sb.

When one looks at Wirt School in Gary, the same general pattern for Zn is seen (Figure 33). Here Sb, but not As, is related to Zn. Zinc concentrations range from 10's to 100

ng/m^3 per size fraction.

Over the south-central part of Lake Michigan, on run #42, the Zn concentration peaked on stages 6 and 8 of the Andersen. Offshore, but close to Gary, Indiana, run #43, Zn peaked on stages 1 and 8, then shifted to stages 3 and 8 somewhat further away from the shore, as shown by run #44. Total Zn rose from about 1 µg/m^3 in the first sample to 4½ µg/m^3 in the sample taken closest to Gary. Zinc was not especially related to Sb, As, or Cu; however, these three elements were related to each other. These relationships are shown in Figures 34, 35, and 36.

On the open hearth samples, runs #1-5, Zn showed a high concentration as sampled on stages 5 through 8 and on stage 1 of the Andersen sampler, as seen in Figure 37. Zinc is as high as 500 ng/m^3 on stage 1, falls to 150 ng/m^3 on stage 3, and rises to 750 ng/m^3 on the filter. Zinc is similar to Sb, although Sb peaks more sharply on the filter. This is also true for As. Antimony and Cu are strongly related at this location. Zinc is somewhat similar to Cu, but not to Fe, Cr, or Mn.

At the sinter plant, samples #6-10 show a strong Zn peak on stage 1, roughly 3000 ng/m^3, decreasing sharply to a stage 4 concentration of 350 ng/m^3, and rising somewhat on stages 5, 6, and 8. This pattern, as seen in Figure 38, indicates a strong dispersion Zn aerosol from the sinter plant, as contrasted with the condensation Zn aerosol from the open hearth. Antimony follows Zn fairly well at this

location, but has a higher filter and lower stage 2 content. Zinc follows Fe quite closely, indicating common origin by dispersion. Again, As and Sb appear more closely related to Cu.

Away from the immediate source vicinity, samples taken at Field School in East Chicago, Indiana, (runs #23-26) show slightly elevated Zn content in the largest particles, but more important, all runs except the last one show Zn as high as 800-1000 ng/m^3 on stages 5 through 8 (Figure 39). On the last run Zn drops as usual on the filter. Antimony and As parallel Zn except they exhibit rising filter levels, but they do not resemble Cu.

At Markstown Park in East Chicago, Indiana, sample #20 shows a peak in the concentration of Zn on stage 1 of 60 ng/m^3 (Figure 40). It is much higher on stage 6, 200 ng/m^3, and drops in concentration to 60 ng/m^3 on the filter. Sample run #21 shows no peak in stage 1, but has a high (160 ng/m^3) filter value. Since wind patterns are different, it seems that the first sample contains more steel industry dispersion Zn than the second. On the first sample Sb is of small size and follows the Zn pattern quite well except for the stage-1 Zn content. Antimony in the second sample follows Zn except for somewhat greater Sb on stages 1 and 2. Antimony does not follow the Cu pattern.

Samples collected at the Central Fire Station in East Chicago, Indiana, runs #12-18, show the customary Zn pattern (note run #15); however, one sample taken under a

different wind regime (#18) shows Zn decreasing gradually from stage 1 to the filter, but with a peak at stage 5. These points are illustrated in Figure 41. Total concentrations are similar to those found at Markstown. On samples #15-17 Sb and As resemble each other, but do not resemble Zn. Antimony and As peak slightly on stage 1 and strongly on the filter. On the last sample, #18, Sb is predominantly from condensation sources. Antimony, As and Cu are related well on run #15, although Cu is not especially high on the filter of the last sample.

At the Central Fire Station in Gary, runs #36-38, Zn peaks on both stages 1 and 5. Wind from the steel industry north of Gary emits Zn on aerosols of such size as to be impacted on Andersen stages 1, 7, and 8. Under other wind regimes Zn peaks as usual in aerosols impacted on stage 5, as shown in Figure 42.

At the Gary Airport Zn on samples #31, 32, 33, and 34 peaks on stage 5, with very small peaks also on stage 1. A last sample, #35, shows the stage 5 peak but not a stage 1 peak due to wind shift (Figure 43). Also, there is low Zn concentration on the filter. One other run, #30, shows a very flat Zn curve, falling off sharply on the filter. Here the wind was from the south. At this location Sb and As sometimes parallel Cu. On samples #31-34 Sb and As parallel Zn, but on sample #35 Sb does not follow the Zn so well, due to high Sb on smaller aerosol particle sizes.

At Ann Arbor, Michigan, runs #45-50, Zn is generally

quite erratic, is located on larger particles, and tends even to follow Fe in its size distribution (Figure 44). Only one sample shows the more characteristic shape (#45). On the samples taken over an extended period of time in Ann Arbor (#49, 50), Zn is paralleled closely by Ca, Na, and Ti, slightly by Cu and Cl, and not at all by Sb, As and In. Most Zn found in Ann Arbor aerosols is dispersion in form, from power plant and incinerator fly ash, and much probably arises by re-entrainment from the soil. Antimony, As, and In, closely related to each other, do not have dispersion source processes.

The conclusions arising from the size patterns outlined above are that in Northwest Indiana Zn arises primarily from the steel industry and is emitted by the industry in two size ranges: one is the large particle sizes that come predominantly from the sinter plant, the other is that fraction outlined by stage 5 through the filter of the Andersen, or the smaller sizes. These are the condensation aerosols from the open hearth and blast furnace areas, and are much greater in magnitude than is the dispersion Zn. There is a relatively fast fallout of the large-particle Zn, but the smallest particles of Zn, perhaps Zn fume, found near source processes on the filter and stage 7, tend to grow toward stages 6 and 5 by coagulation or surface adsorption onto other particles. For the aged aerosol, then, we have the customary shape. There are undoubtedly other sources of Zn in the area, which may emit particles even smaller in size than those from the

open hearth and blast furnace areas. This is especially well indicated by high concentrations of filter-sized Zn on samples taken when the wind was not from the direction of the steel industry, and probably arises from hot-melt processes such as galvanizing. These data are supported by the high volume data, which also indicate that near the open hearth area Zn is very closely paralleled in total concentration over several daily samples by Sb and As in the smallest size range, but at the sinter plant Zn parallels only Sb. Copper, although not closely related to Zn, resembles As and Sb in temporal distribution.

As one moves further away from the steel industry, these relationships grow less distinct, and are more altered by much smaller local sources, such as foundries. Thus it can be said that a large number of small sources, plus steel industry sintering operations, contribute Zn to the atmosphere on particles 4-10 μm in radius or larger. But a much greater Zn emission occurs from steel industry furnace operations and from other sources, such as galvanizing, for which the particle size is sub-micron, perhaps 0.1 μm or smaller in radius. As the pollution aerosol ages, larger particles fall out, and smaller particles increase their size by coagulation and/or adsorption onto larger particles, until finally a distribution is reached such that only a small fraction of Zn present in the atmosphere is on giant ($r > 1$ μm) particles. Particles ≈ 1 μm contain more Zn than

do other sizes, and Zn drops in concentration on both sides of this latter size.

Figure 30. Run 19, East Chicago Central Fire Station.

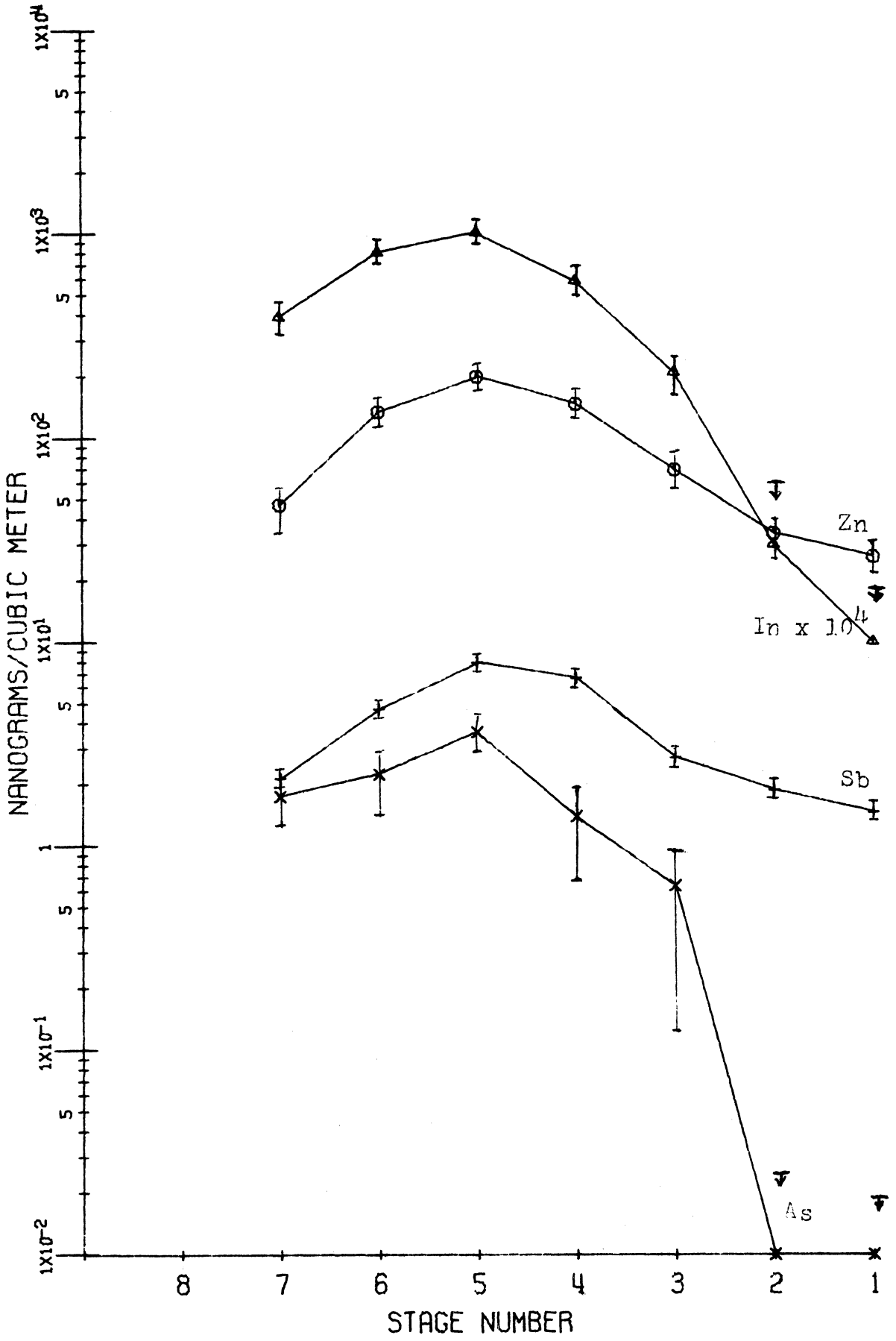

Figure 31. Run 22, East Chicago Markstown Park.

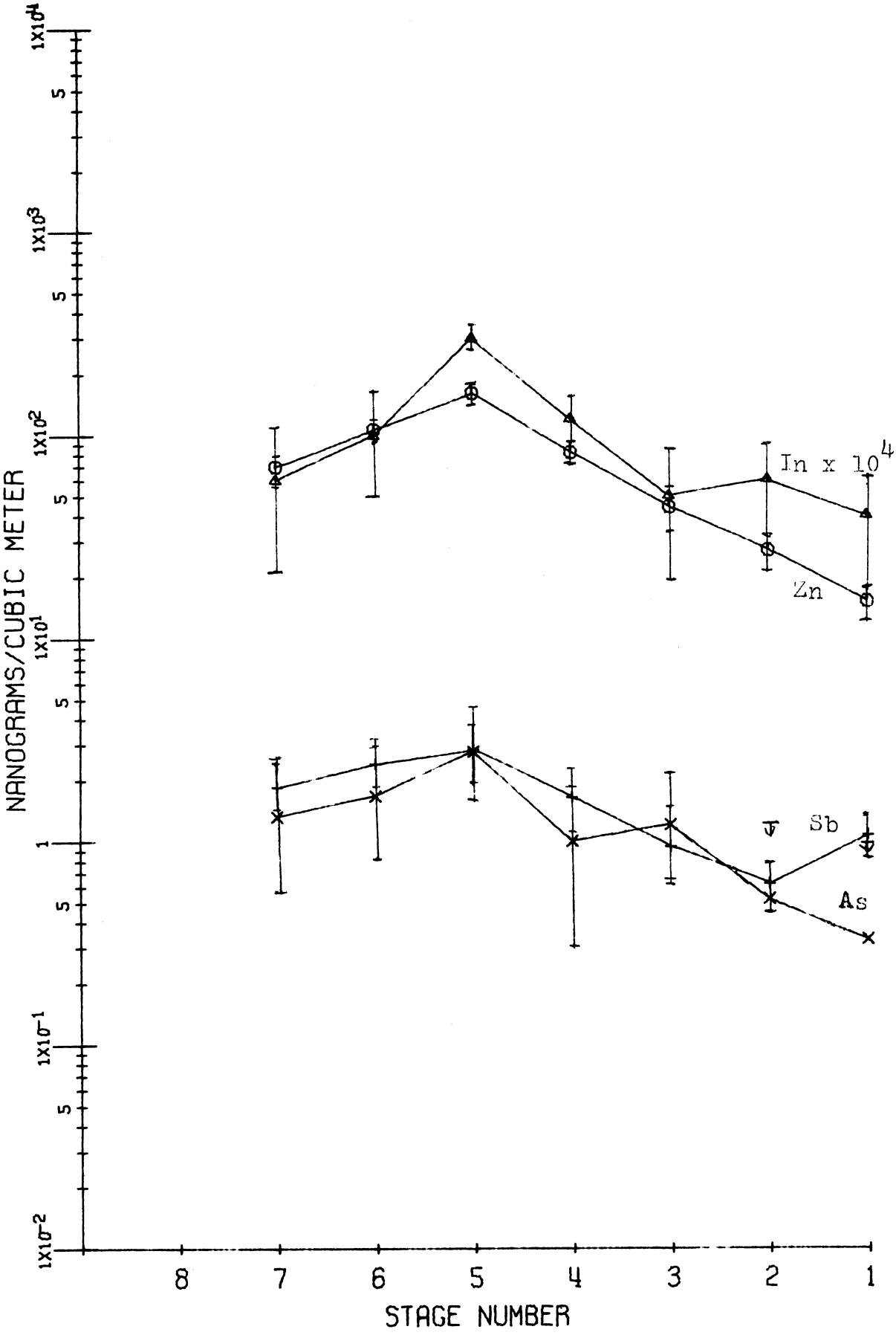

Figure 32. Run 19, East Chicago Central Fire Station.

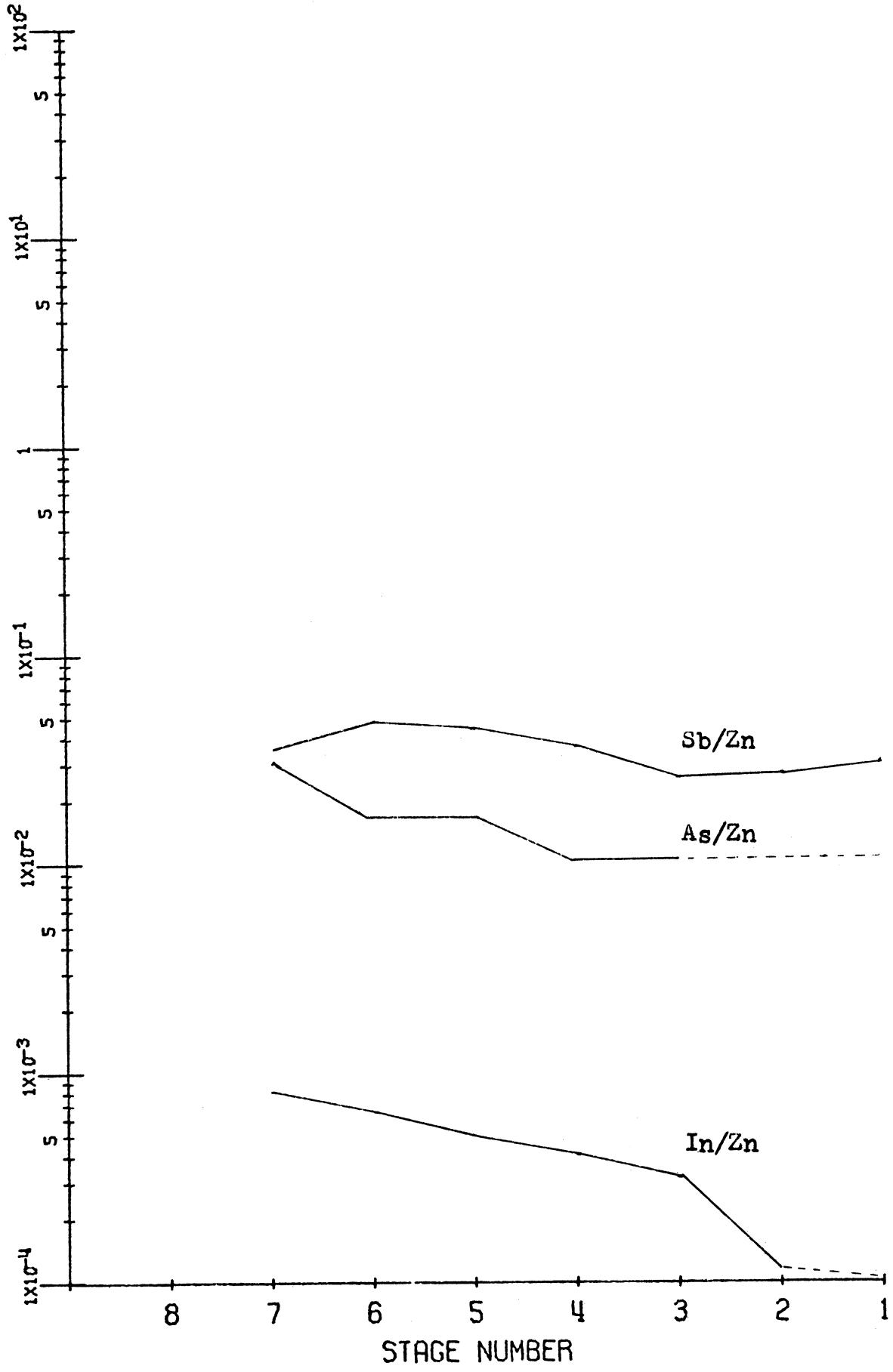

Figure 33. Run 27, Gary Wirt School.

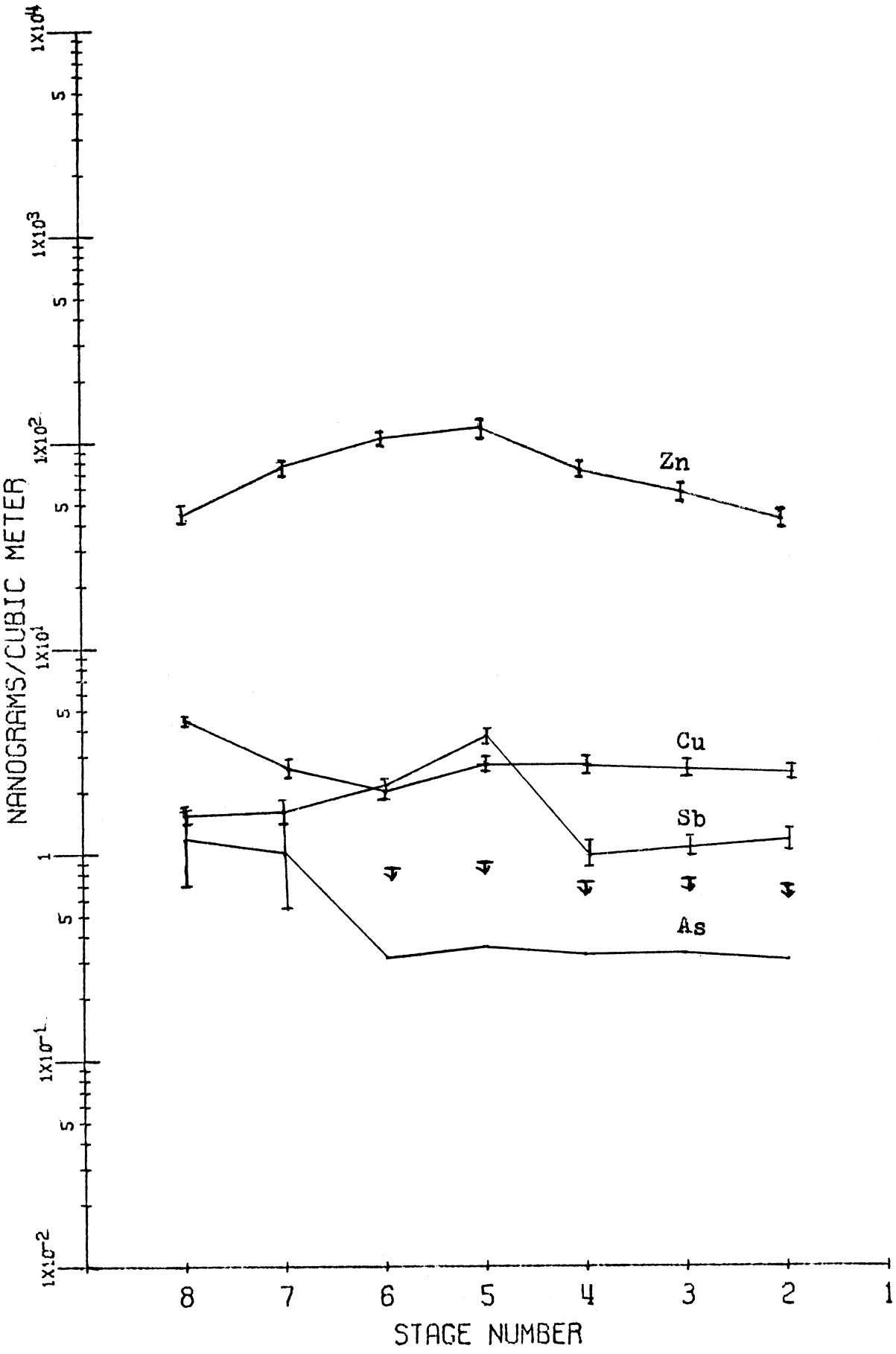

Figure 34. Run 42, Lake Michigan.

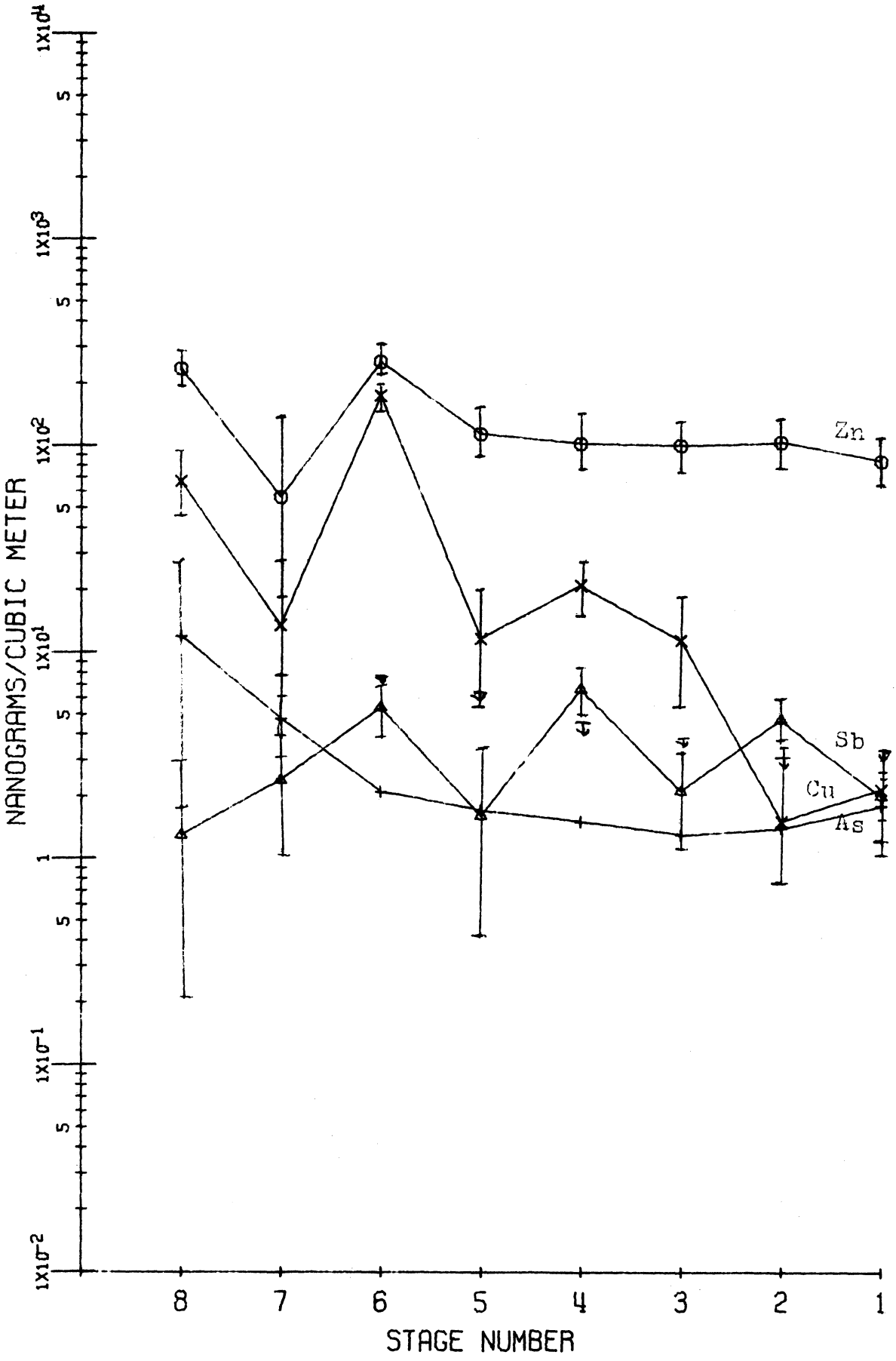

Figure 35. Run 43, Lake Michigan.

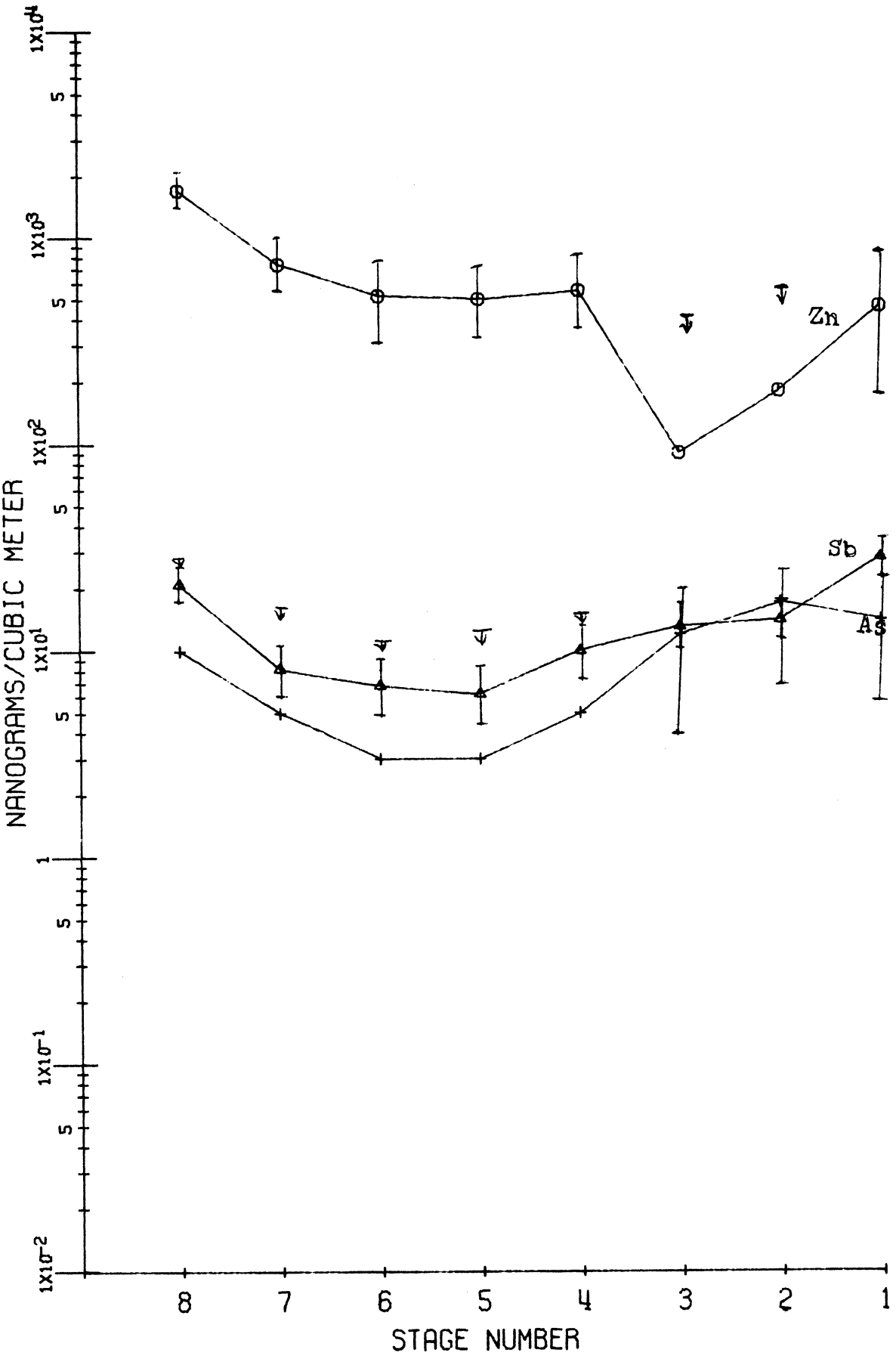

Figure 36. Run 44, Lake Michigan.

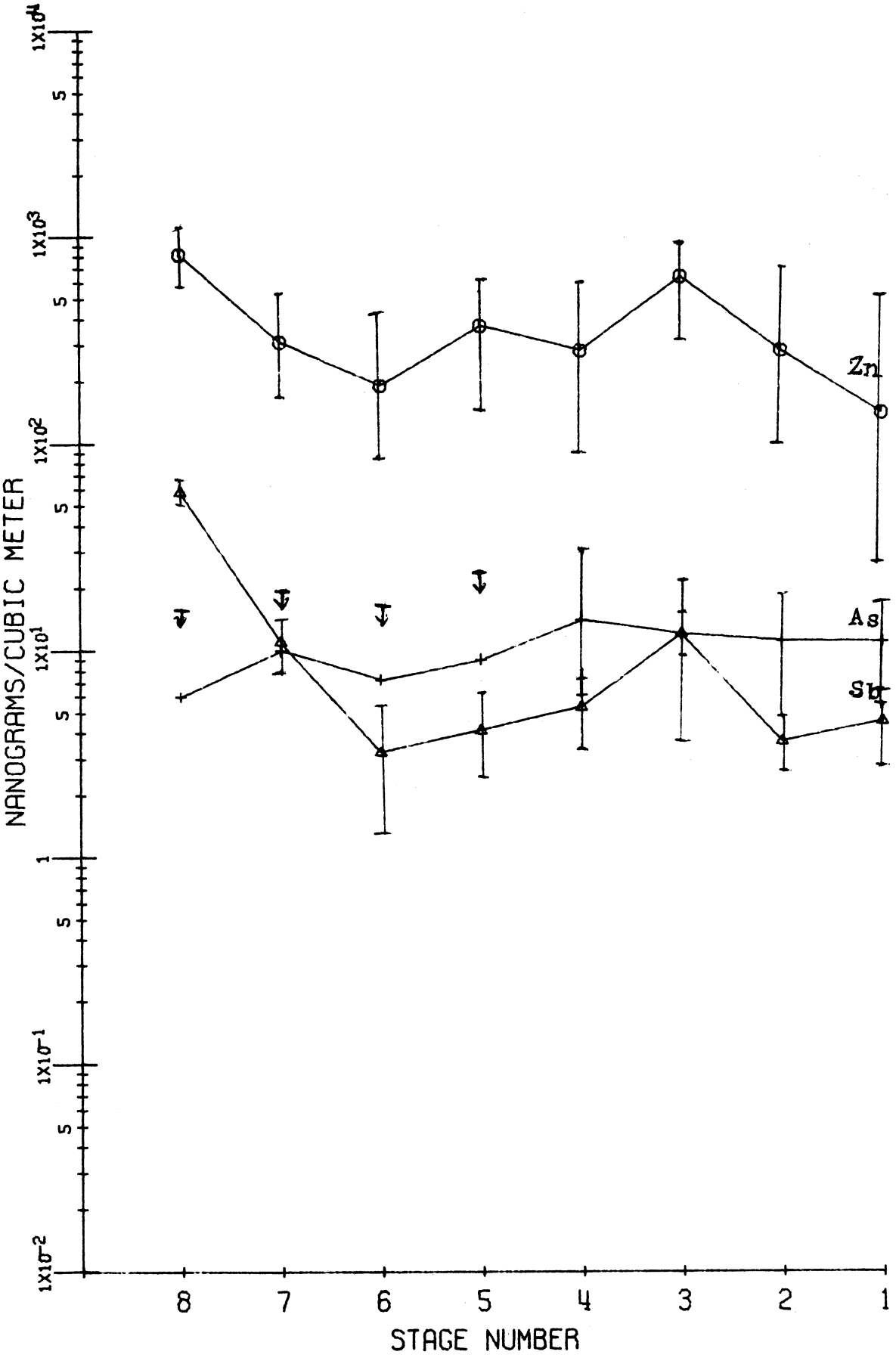

Figure 37. Runs 2-4, Open Hearth Vicinity.

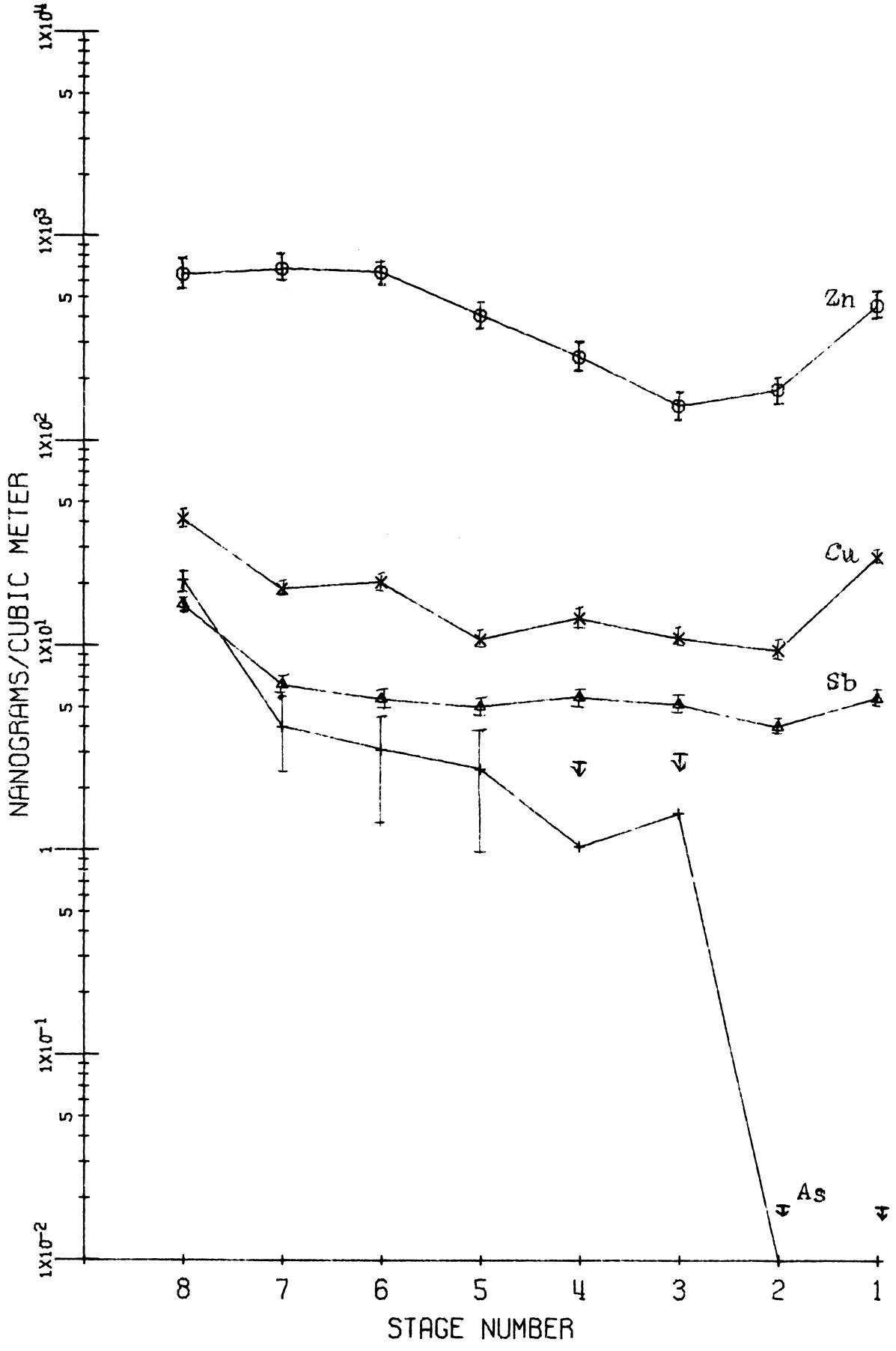

Figure 38. Runs 7-10, Sinter Plant Vicinity

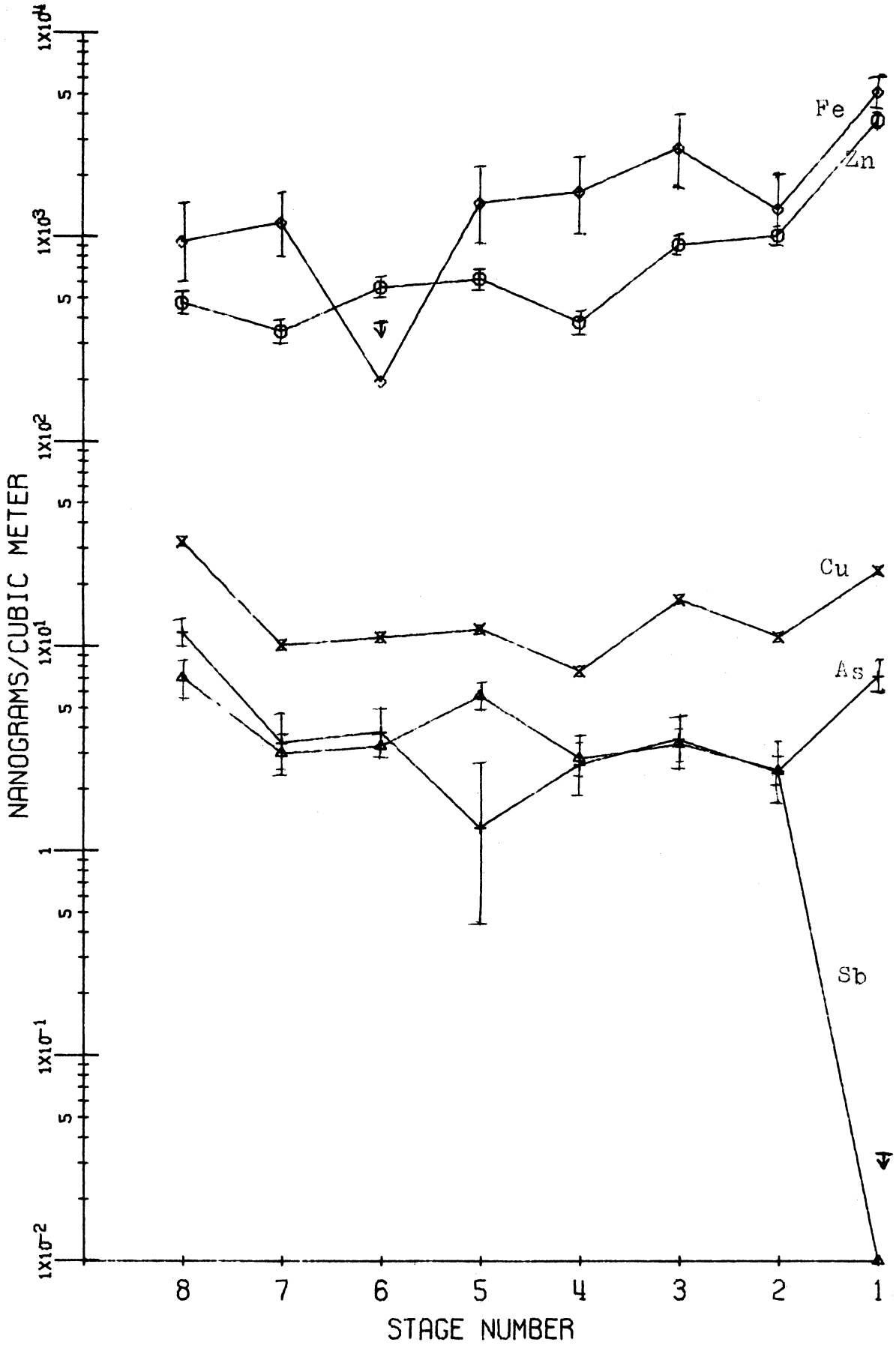

Figure 39. Runs 23-26, East Chicago Field School.

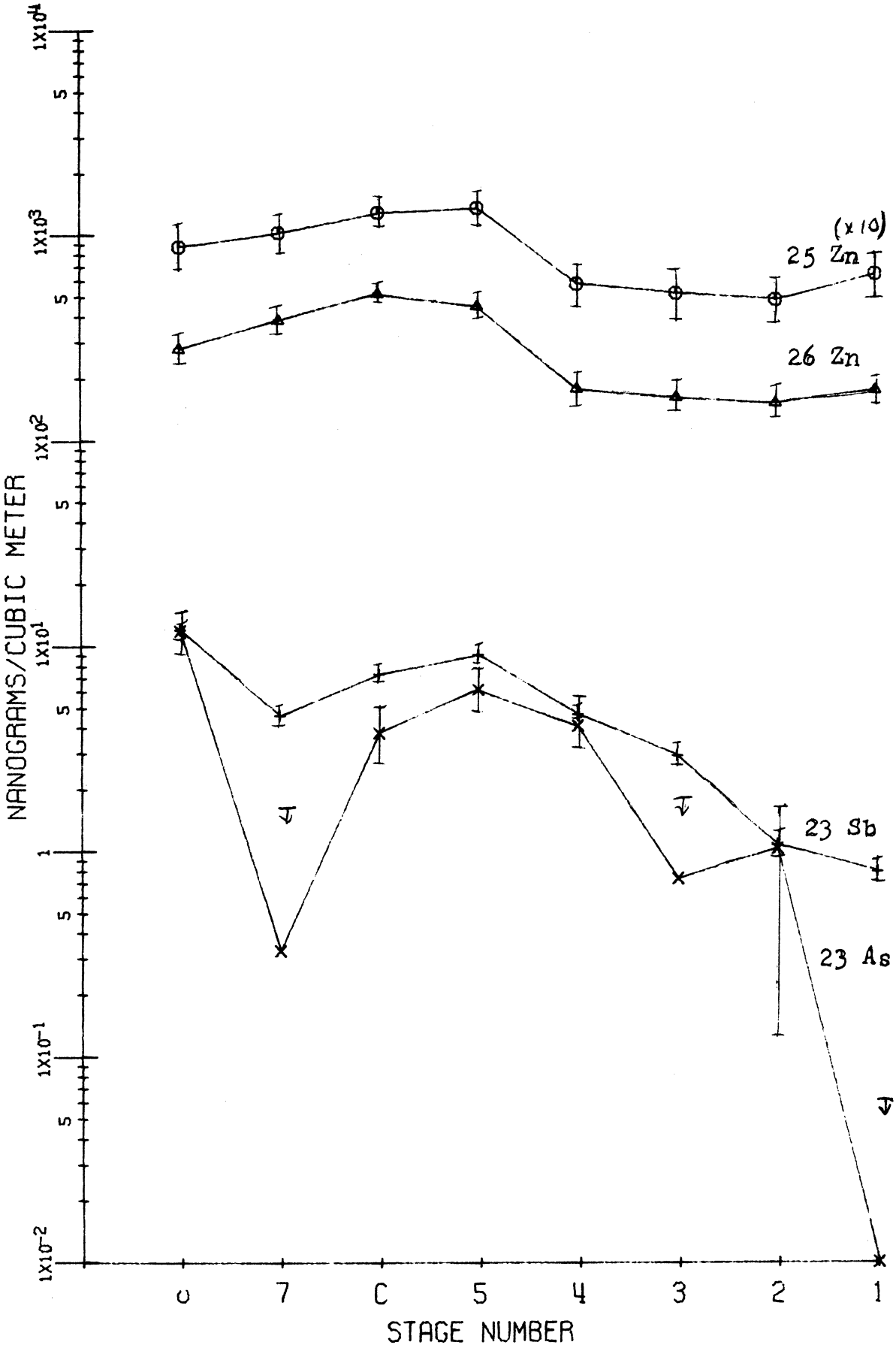

Figure 40. Runs 20 & 21, East Chicago Markstown Park.

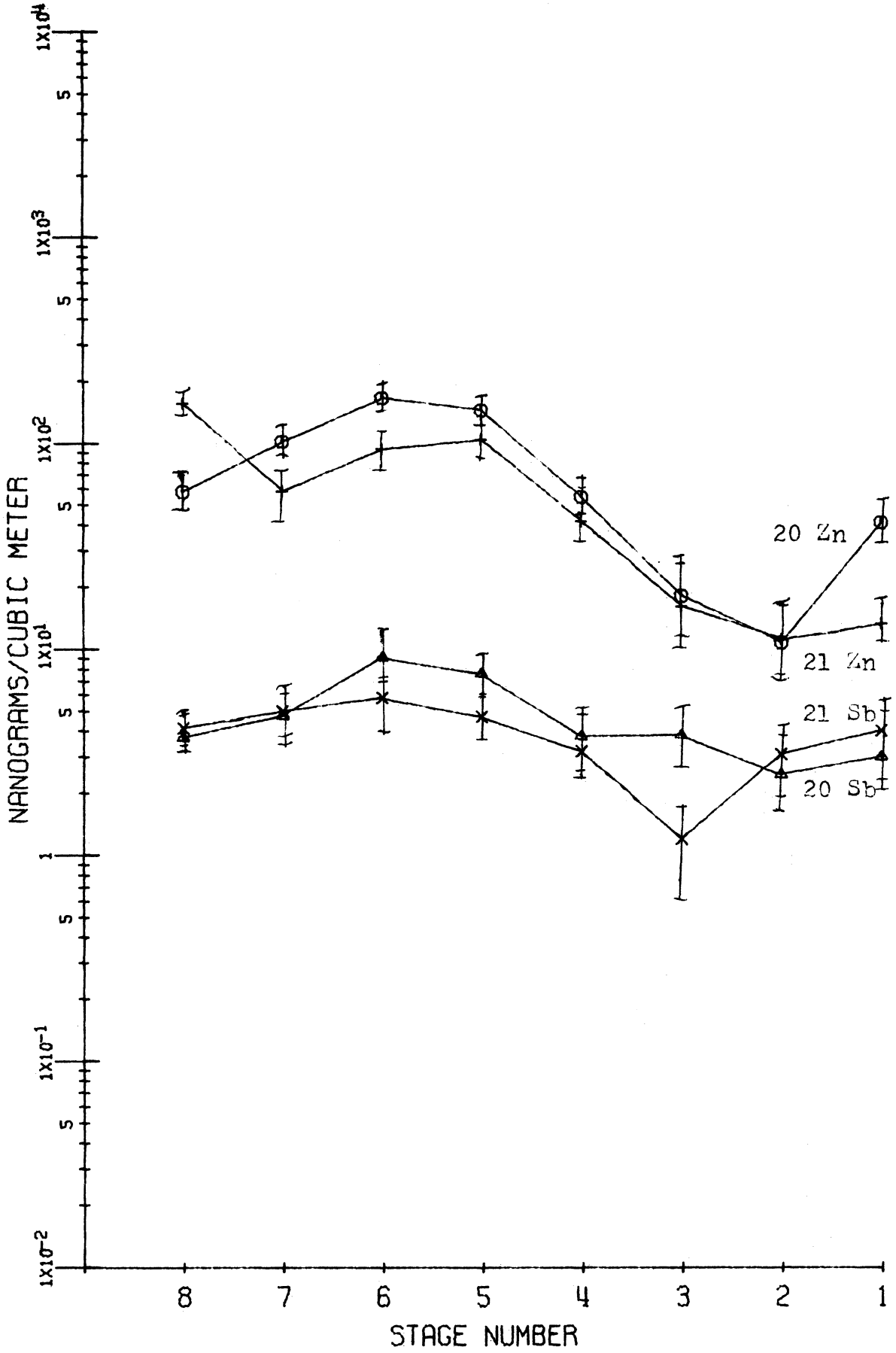

Figure 41. Runs 15-18, East Chicago Central Fire Station.

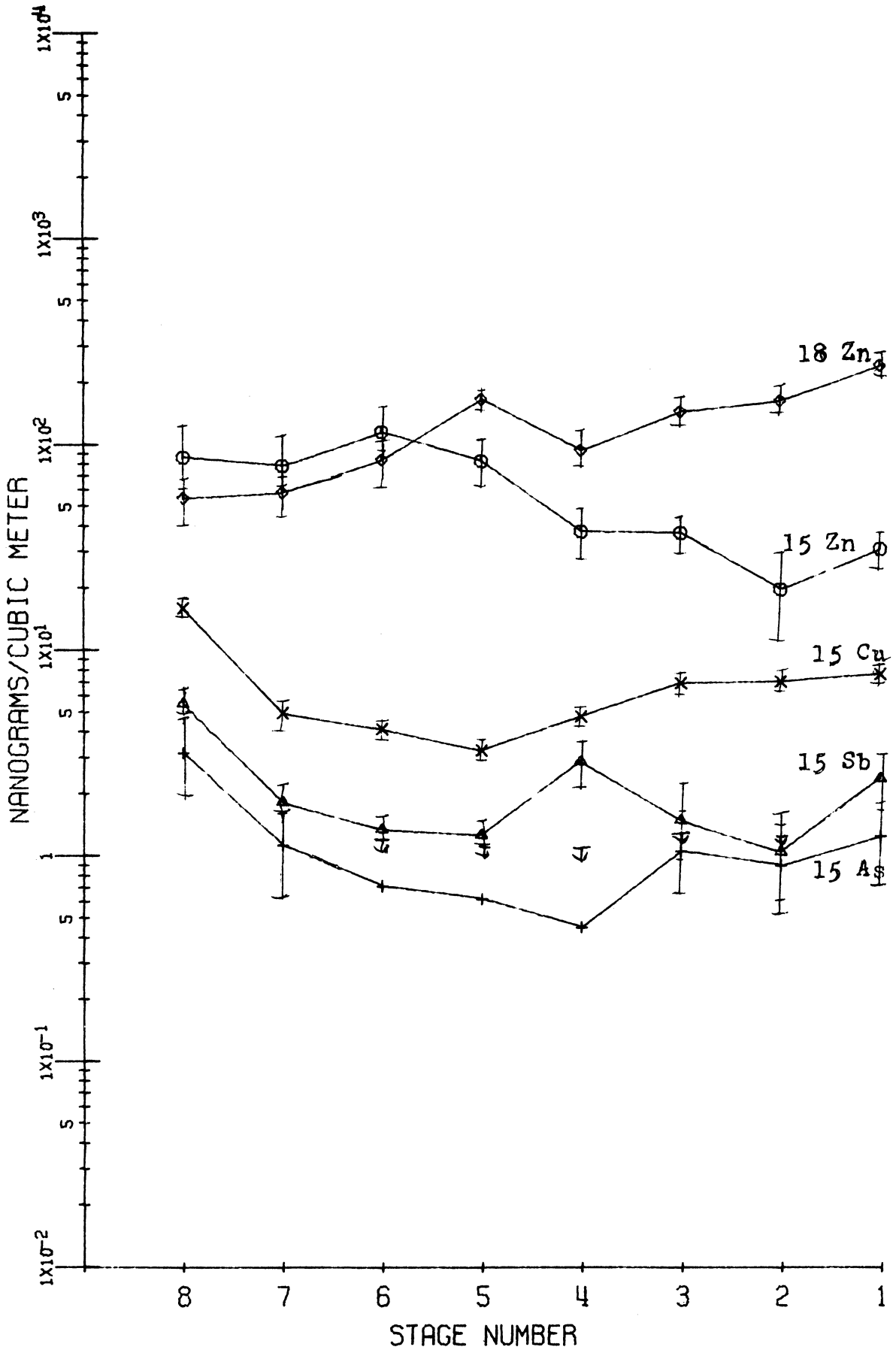

Figure 42. Runs 36 & 38, Gary Central Fire Station.

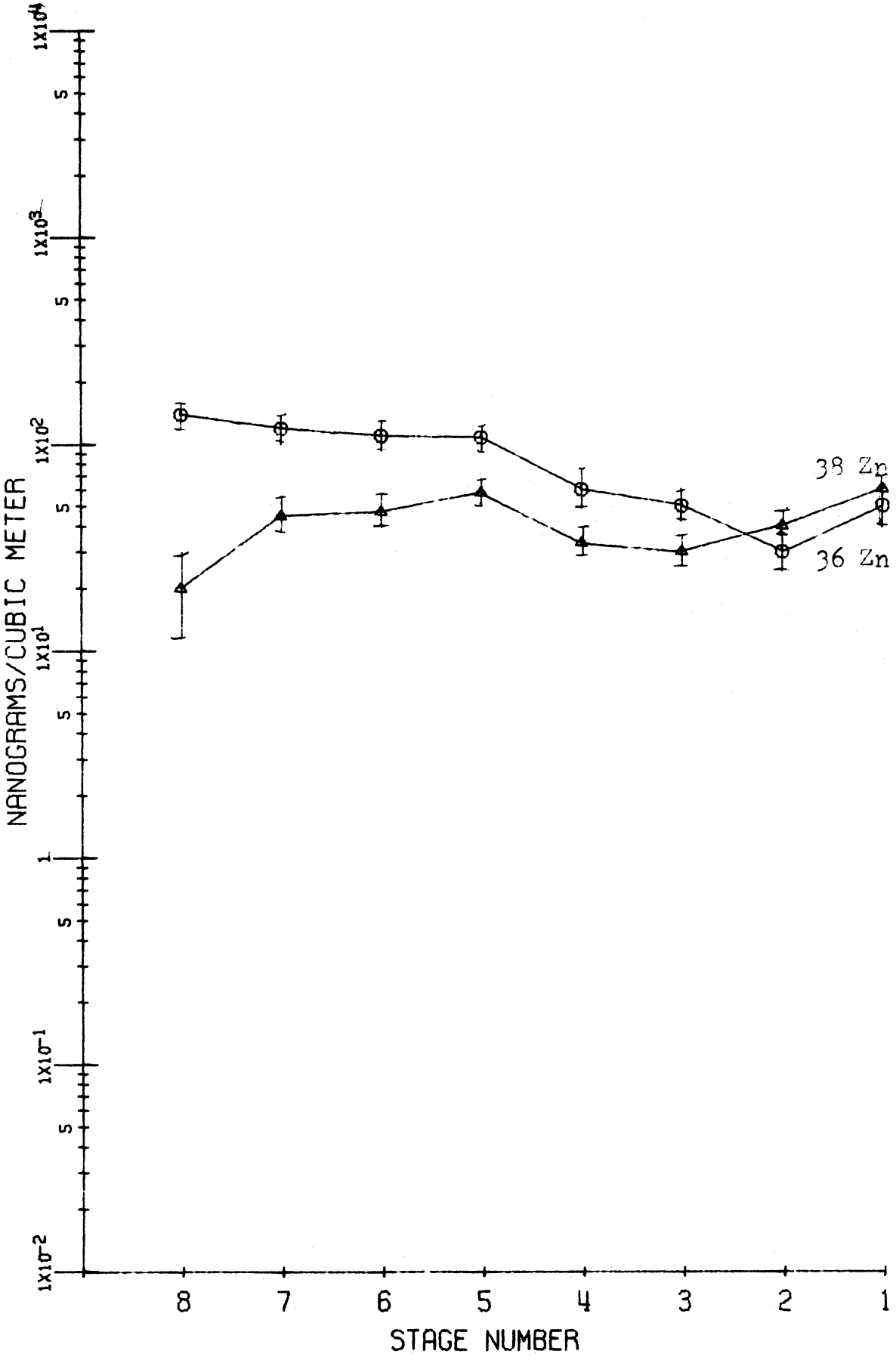

Figure 43. Runs 31-35, Gary Airport.

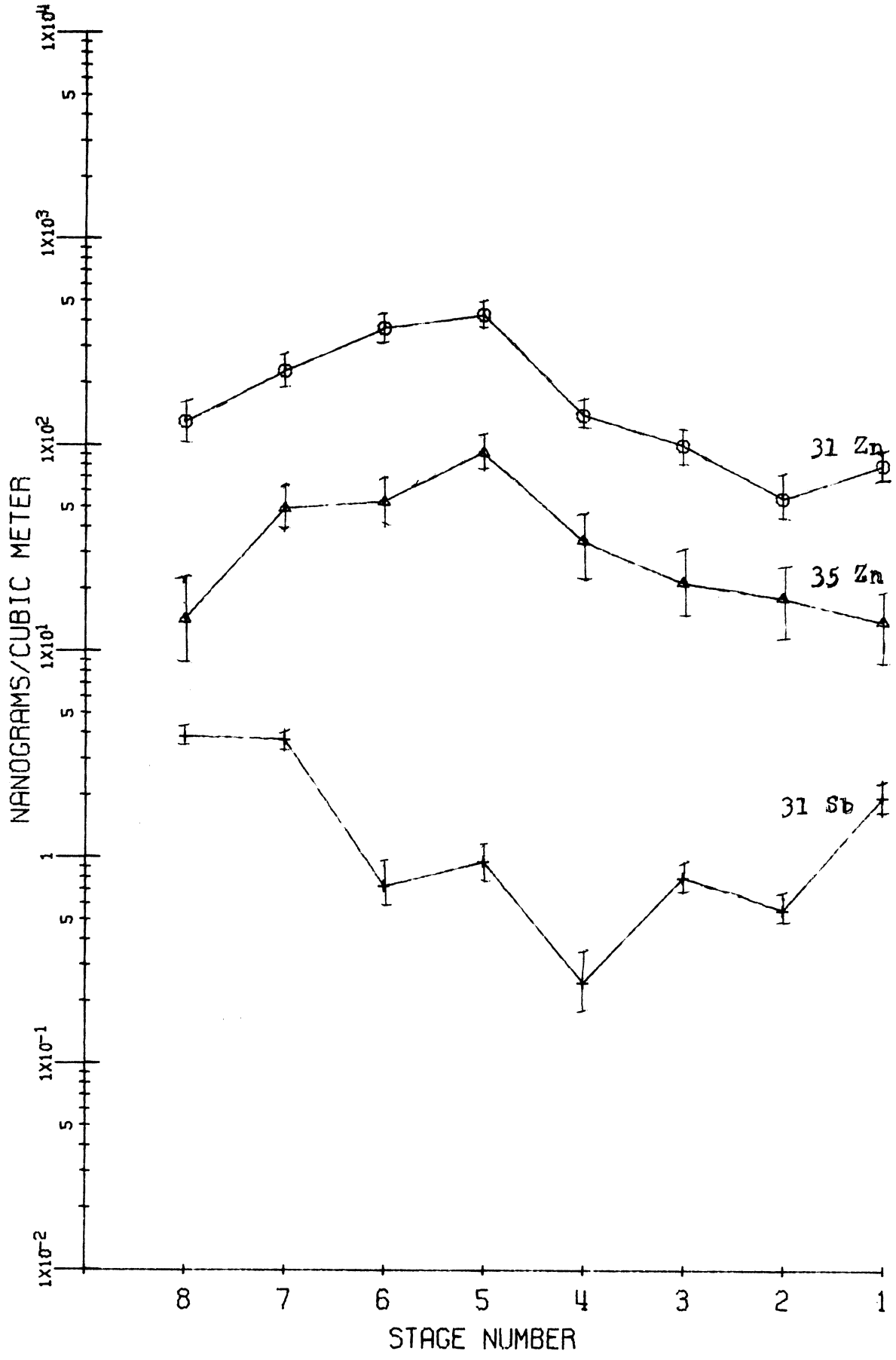

Figure 44. Runs 45 & 49, Ann Arbor.

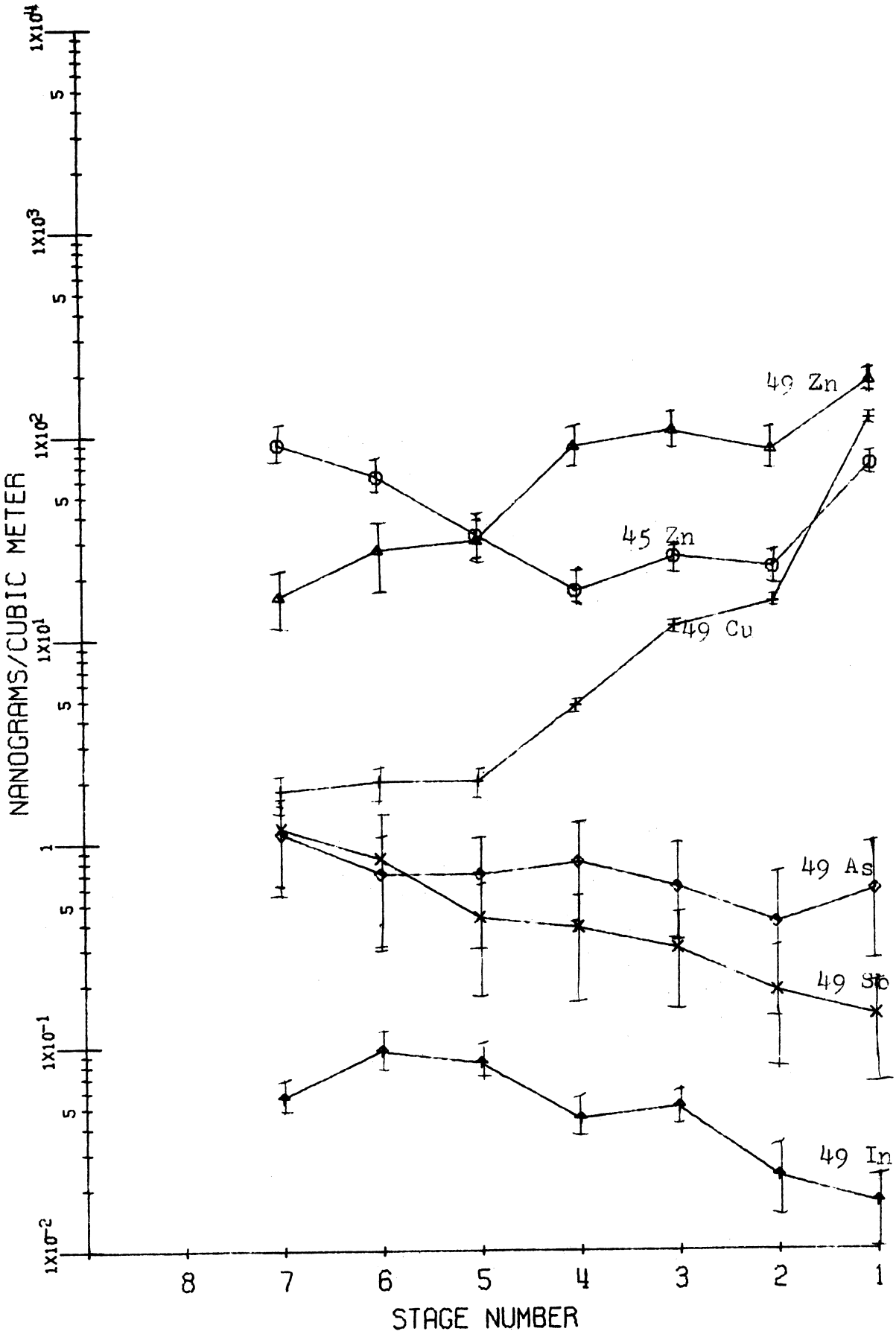

3. Copper

Copper has a distribution on many samples suggestive of both dispersion and condensation types of source processes. In the two-week sample from the East Chicago fire station, #19 (Figure 13), Cu is very nearly "Junge-distributed," having a slight peak in stage 1, a dip in stage 2, rising slightly in stage 4, but dropping off very gradually toward the filter. This pattern is paralleled very closely by Mn, slightly by K, slightly by Cr, and there seems to be some correlation with Co, Ce, Se, and Th. It is most important to consider that the average amount of Cu found here is approximately 3 to 4 ng per cubic meter per stage, for a total of about 30 ng per cubic meter.

In another large sample, #22 (Figure 14), taken at Markstown Park in East Chicago, Cu seems to follow in general the last sample described, but the peak on stage 1 is slightly more pronounced and there is a fairly strong peak on stage 5, declining toward stage 2 and stage 7. The magnitude of Cu is 20-100 ng/m^3 per stage, with total Cu equal to about 400 ug/m^3. Several elements tend to follow this pattern quite well; Sb does, and is present to about 5% the extent of Cu; Mn does to a certain extent, and is about 1/3 the magnitude of Cu. Samarium, Cr, and Ce also appear related to Cu.

At Wirt School in Gary, #27 (Figure 33), Cu is roughly 2 to 4 ng per cubic meter per stage, or a total of about 25 ng per cubic meter. It is fairly "Junge-distributed"

except for a small increase on stages 6 throught 8. The filter value is the highest. Only V seems to follow Cu fairly well at Wirt School; Sb, Ga, As, Zn, and Co show only slight similarities to Cu. This level appears to be a background level of Cu.

On Lake Michigan (Figure 45) Cu is somewhat erratic due to the small sample collected, but it should be pointed out that close to Northwest Indiana and Chicago, Cu has a small peak on stage 1 ≈ 30 ng/m^3, and a very large peak on stage 8 ≈ 300 ng/m^3. It is shown in both the samples taken close to the shore, #43 and 44. But when one gets further out over the lake, #42, the Cu has developed a large peak on stage 6 ≈ 200 ng/m^3, which was not present on the other two samples. There is also a smaller peak on the filter ≈ 60 ng/m^3. This suggests that Cu is growing in size by coagulation or adsorption onto larger aerosol particles. Zinc and Br parallel Cu on run #42 very well, indicating an aged aerosol. Antimony and As, but not Zn, resemble Cu in their size spectra when sampled close to Gary, suggesting local, but different, sources for Zn and Cu. Away from the shore Mn and Cu are fairly well related, but near Gary, Mn is not appreciably related to Cu. Close to Gary, most Mn is located on large particles—a dispersion source, but Cu is on small particles. Further offshore the Mn curve flattens, but Cu tends to concentrate on particles collected at stage 6. Mn varies much less with distance from the source than does Cu.

Samples #1-5 at the open hearth show a small (25 ng/m^3) value for Cu on stage 1 of the Andersen, a smaller value for Cu on stages 2-5, and a large Cu content (40 ng/m^3) on the filter (Figure 37). This trend in content generally parallels Sb, As, and Zn, and suggests a condensation aerosol. But the presence of a dispersion source is revealed by stage 1 Cu. The Mn distribution is similar except for the filter value, where Mn drops. Chloride, Br, and Fe are similar to Cu. Chromium and Ce, except that mass in the smaller size ranges, also resemble Cu.

Samples from the sinter plant show a similar distribution for Cu as does the open hearth, with elevated Cu ($\approx$ 30 ng/m^3) in particles collected on both stages 1 and 8, contrasted with 10-20 ng/m^3 on stages 2-7 (Figure 38). Potassium, Br, and As show this pattern. Antimony and Ga resemble Cu to a lesser degree. Manganese and Fe are essentially on large particles, Cl on much smaller particles. Within the steel industry, it seems likely that the major source of Cu is furnace operation, producing small particles, ($r < 1$ µm), or fume. A secondary source is sintering operations, but producing larger particles, $d > 4$ µm.

For the samples collected in Ann Arbor, #49 and 50, Cu very closely parallels Zn in that both elements are located on very large particles (Figure 44). Most Cu and most Zn particles have impacted on stage 1. Calcium, Al, Na, W, and Cl resemble Cu.

Now consider Cu found at the Gary Airport. Here Cu is

lower in magnitude on run #31-34, but otherwise the spectrum appears quite similar to those found for samples taken closer to the steel industry (Figure 46). Concentrations for the mid-size particles are about 5 ng/m^3 per stage, rising to 10 ng/m^3 on stage 1 and to 10-15 ng/m^3 on the filter. Antimony and As resemble Cu extremely closely on this sample, but Zn is not similar to Cu. In one sample from the Gary Airport, #55, Cu is more erratic, but is paralleled by Sb. Concentrations are lower in magnitude, without a large concentration on the filter, which may well be caused by a shifting of wind direction away from the steel industry toward the airport, thereby lowering the input of smaller particles.

At the East Chicago fire station, #15-18, Cu decreases from stage 1 toward stage 5, and most of the Cu is located on the filter (Figure 41). Antimony and As are quite similar in this case, but Zn is not.

At the Markstown Park station, runs #20-21, Cu shows a fairly different pattern; Cu drops in concentration from stage 1, reaching a minimum on the filter (Figure 46). This would seem to indicate Cu from a dispersion source, but wind direction does not indicate the steel industry as the only source. Copper is higher in the two samples from this station than at most community locations. Concentrations of 70-80 ng/m^3 on stage 1, dropping to 5-10 ng/m^3 on the filter, are found. This indicates dispersion Cu from non big-steel industry, perhaps a foundry, or metals fabrication.

Other elements which resemble the Cu at Markstown are rather few, possibly Fe and Cr, but Sb and Zn definitely vary from the Cu pattern. Hence there are other sources in addition to the steel industry emitting Cu, both by dispersion and condensation processes, but especially dispersion.

A last group of samples to consider are those collected at Field School in East Chicago, runs #23-26. Copper at this location is nearly "Junge-distributed" except for that Cu found on the filter, and is 10-30 ng/m^3 per stage in magnitude. The filter shows a large increase in Cu concentration, meaning small particle predominance. This strongly indicates an origin within the steel industry. This points out that the steel industry is responsible for most of the condensation Cu, and for at least a part of dispersion Cu. It is likely there are other sources of Cu generated on large particles nearby.

Figure 45, Runs 42-44, Lake Michigan.

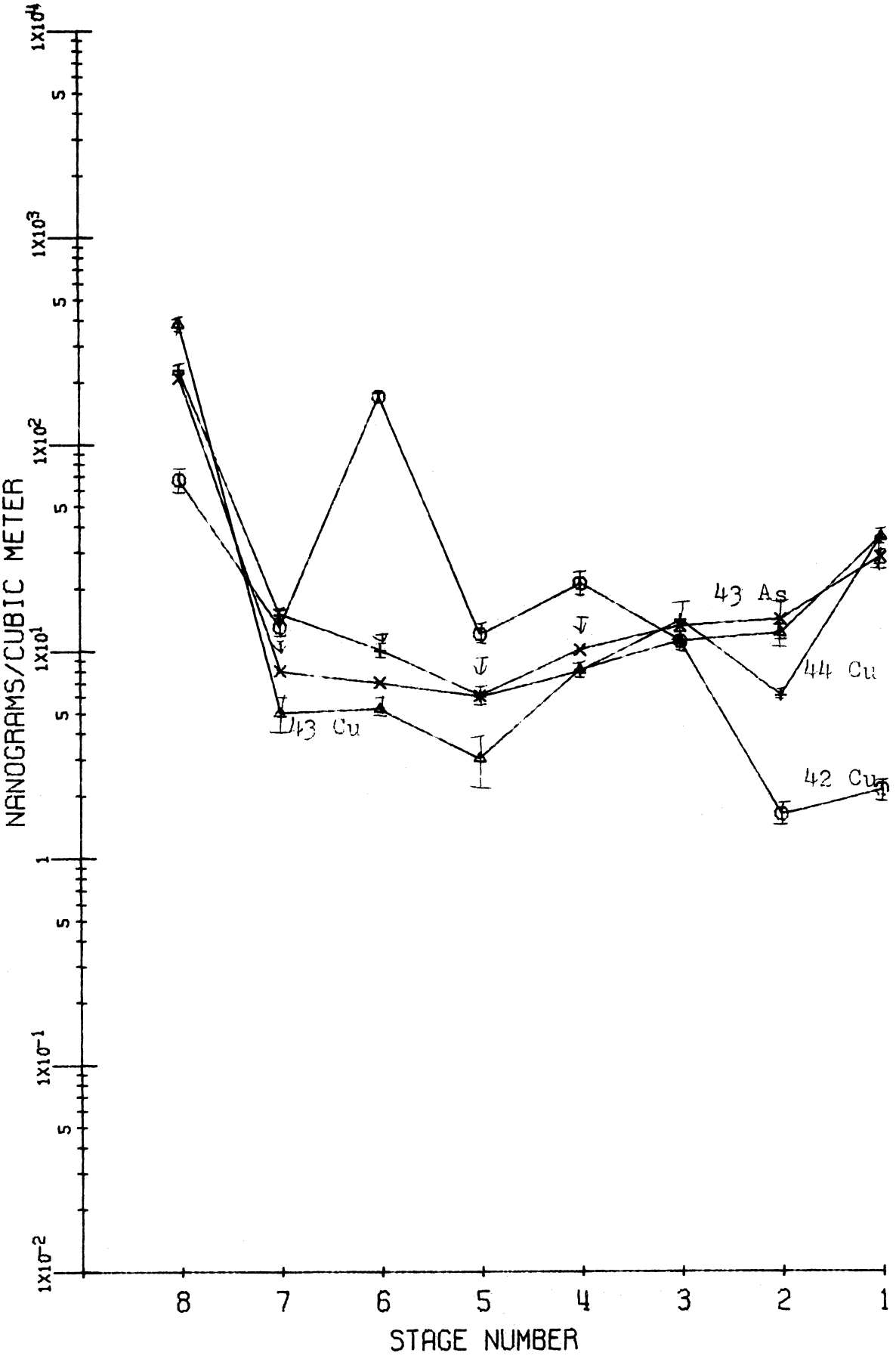

Figure 46. Runs 20 & 21, East Chicago Markstown Park; and Runs 31 & 35, Gary Airport.

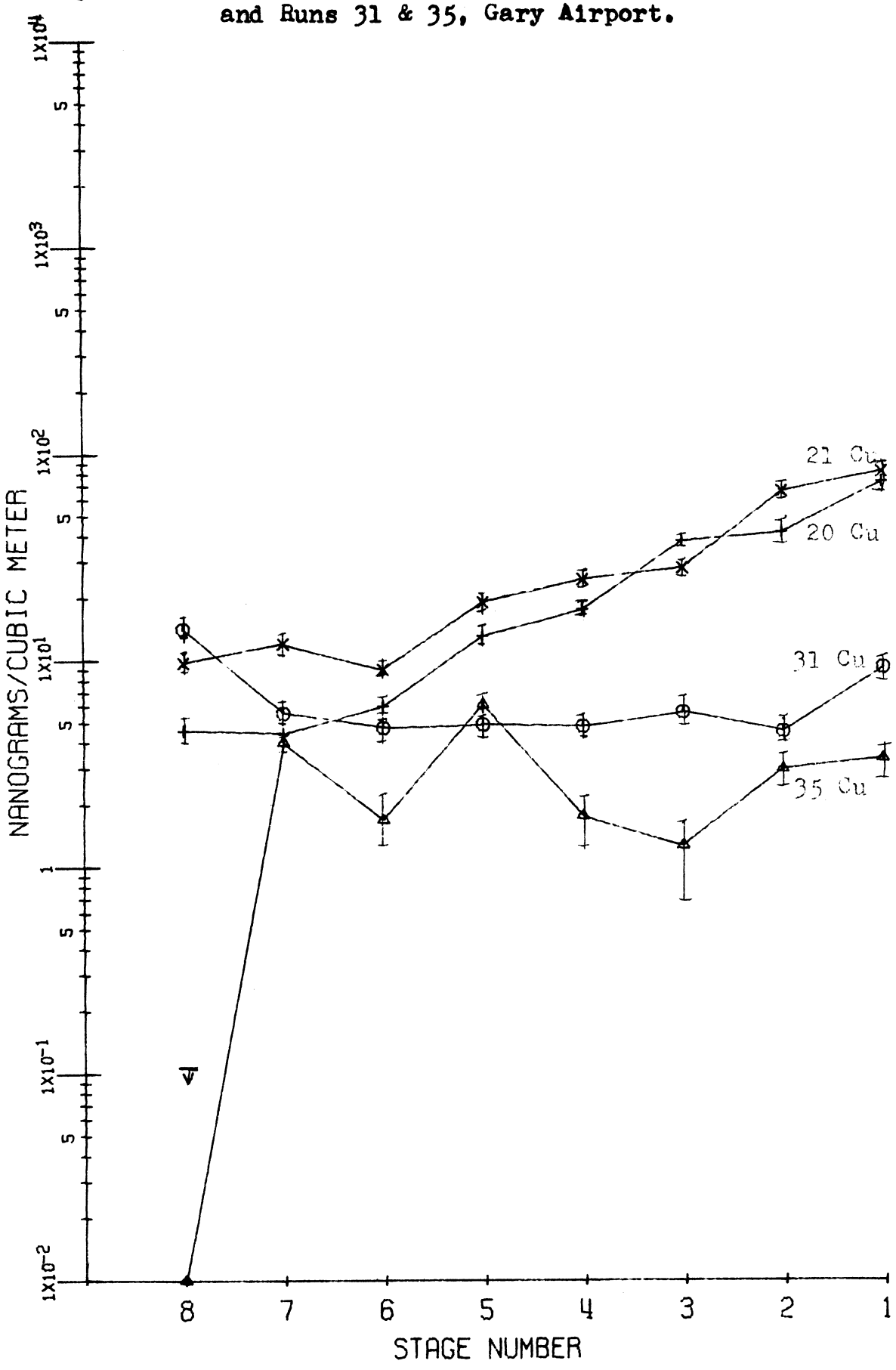

4. Calcium, Magnesium, Titanium

Calcium, Mg, and Ti group together not only because they have natural particle size distributions heavily favoring larger particles, but also because they have industrial pollution sources that generate particle size distributions very similar to, but higher in overall concentration, than the natural distribution. The data indicate that in Northwest Indiana Ca, Mg, and Ti arise mainly from the steel and the cement industries. Concentration of these three elements often reaches a value of an order of magnitude higher than that found in the background.

On the extended sample runs (#19, 22) (Figures 47, 48) taken in East Chicago, Ca has a concentration of about 0.4 $\mu g/m^3$ on stage 1 particles, dropping to less than 0.1 $\mu g/m^3$ at stage 5; Mg has a very similar pattern, with concentrations about 40% of that of Ca. Titanium has a similar distribution, with about 0.01 $\mu g/m^3$ at stage 1, and less than 0.005 $\mu g/m^3$ on stage 5. Titanium also shows small peaks at stages 2-3 in these samples. It was not possible to obtain samples close to a cement plant, but steel industry samples (open hearth and sinter plant) bear out the observation that pollution Ti is on slightly smaller particles than is Ca or Mg. Calcium is emitted by the sintering operation in quantities as high as 12 $\mu g/m^3$ on stage 1 sized particles (#9) (Figure 49), and decreases rapidly in concentration on smaller particles. Magnesium is quite similar, with about 4 $\mu g/m^3$ on particles impacting on

stage 1. Titanium is emitted also on large particles, but very much on those particles impacting on both stages 1 and 2. From open hearth operations (#4) (Figure 50) Ca and Mg have concentrations about half that found for sintering operations, and the decrease in concentrations for smaller size ranges is more gradual. Titanium values at the open hearth are higher than at the sintering plant ($\approx 0.5\ \mu g/m^3$ at stage 1). Thus the slight rise in Ti concentration at stages 2 and 3 found away from the industry is due to relatively more Ti produced in that size, when compared to Ca or Mg, plus the more rapid fallout of stage 1 size Ti when compared to fallout for smaller sizes (stages 2 and 3).

A sample at Wirt School in Gary, Indiana, shows similar patterns for these elements, but lower concentrations and more gradual decreases in concentration with decreasing particle size. ($Ca \leq 1\ \mu g/m^3$, $Mg \leq 0.2\ \mu g/m^3$, $Ti \leq .03\ \mu g/m^3$, per stage (Figure 51)).

Observations at other urban locations in Gary and East Chicago, Indiana, show results similar in distribution to Wirt School. Examination of runs #33 and 35 at the Gary Airport is fruitful (Figure 52). During run #33 winds were from the Northwest Indiana steel complex toward the sample. Note that all three elements are high in concentration in total, high on the first stage, and decrease rapidly with smaller particle size. On run #35, wind had shifted 180°, and results for all elements are an order of magnitude lower on larger particles, but dropping less

gradually to similar values for small particles. Hence in the latter samples the curves show a much less steep concentration drop-off with decreasing particle size.

Samples at Field School and Markstown Park in East Chicago and at the central fire stations in East Chicago and Gary show similar results. Samples on Lake Michigan, close to Northwest Indiana, with an offshore wind toward the sample point, also point out the importance of the large particle-size component of pollution Ca, Mg, and Ti. Sample #43, taken offshore from East Chicago, shows typical pollution Ca and Mg (Figure 53). Other samples from Ann Arbor, Michigan, reinforce the validity of this observation.

Figure 47. Run 19, East Chicago Central Fire Station.

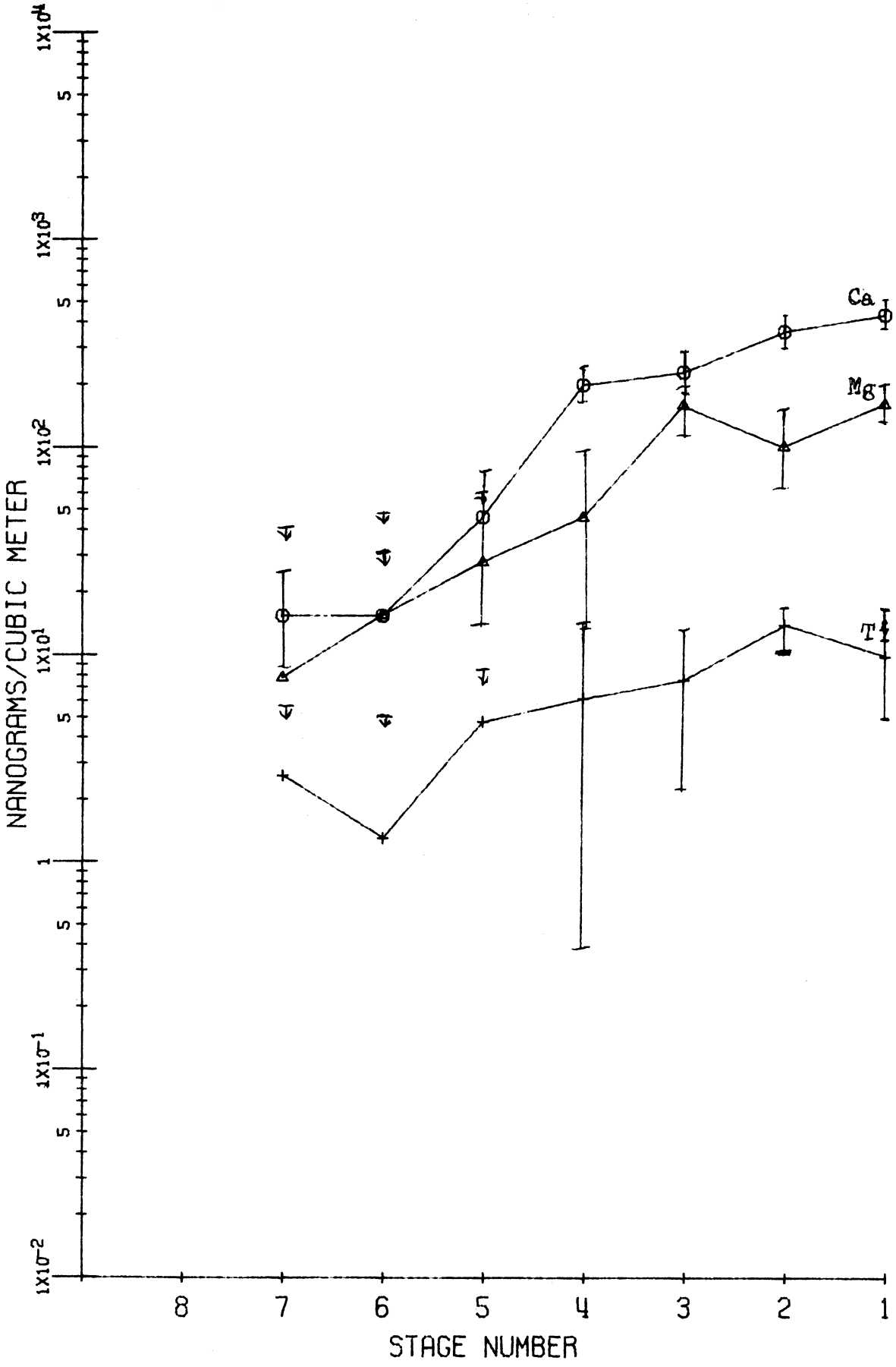

Figure 48. Run 22, East Chicago Markstown Park.

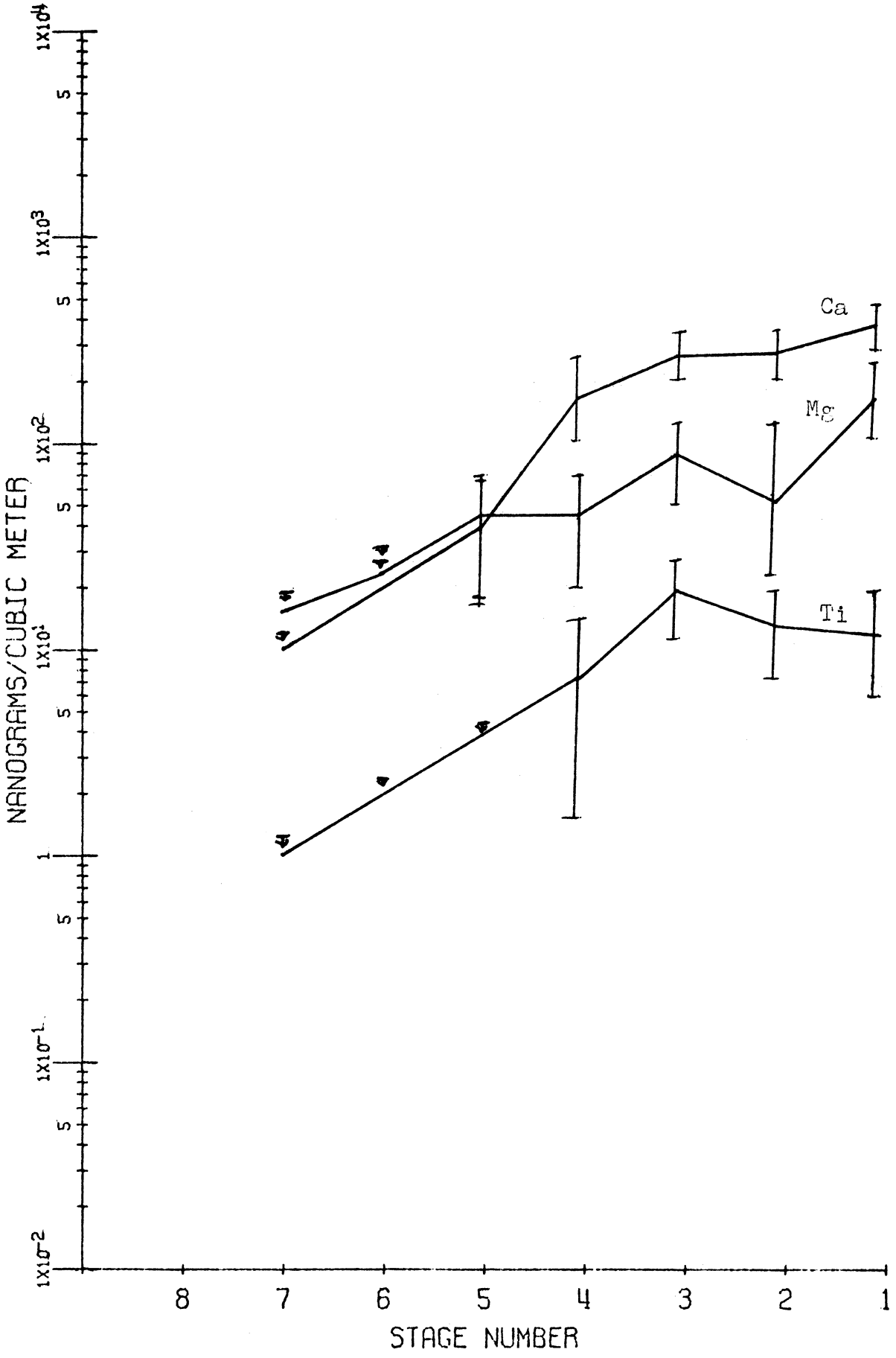

Figure 49. Run 9, Sinter Plant Vicinity.

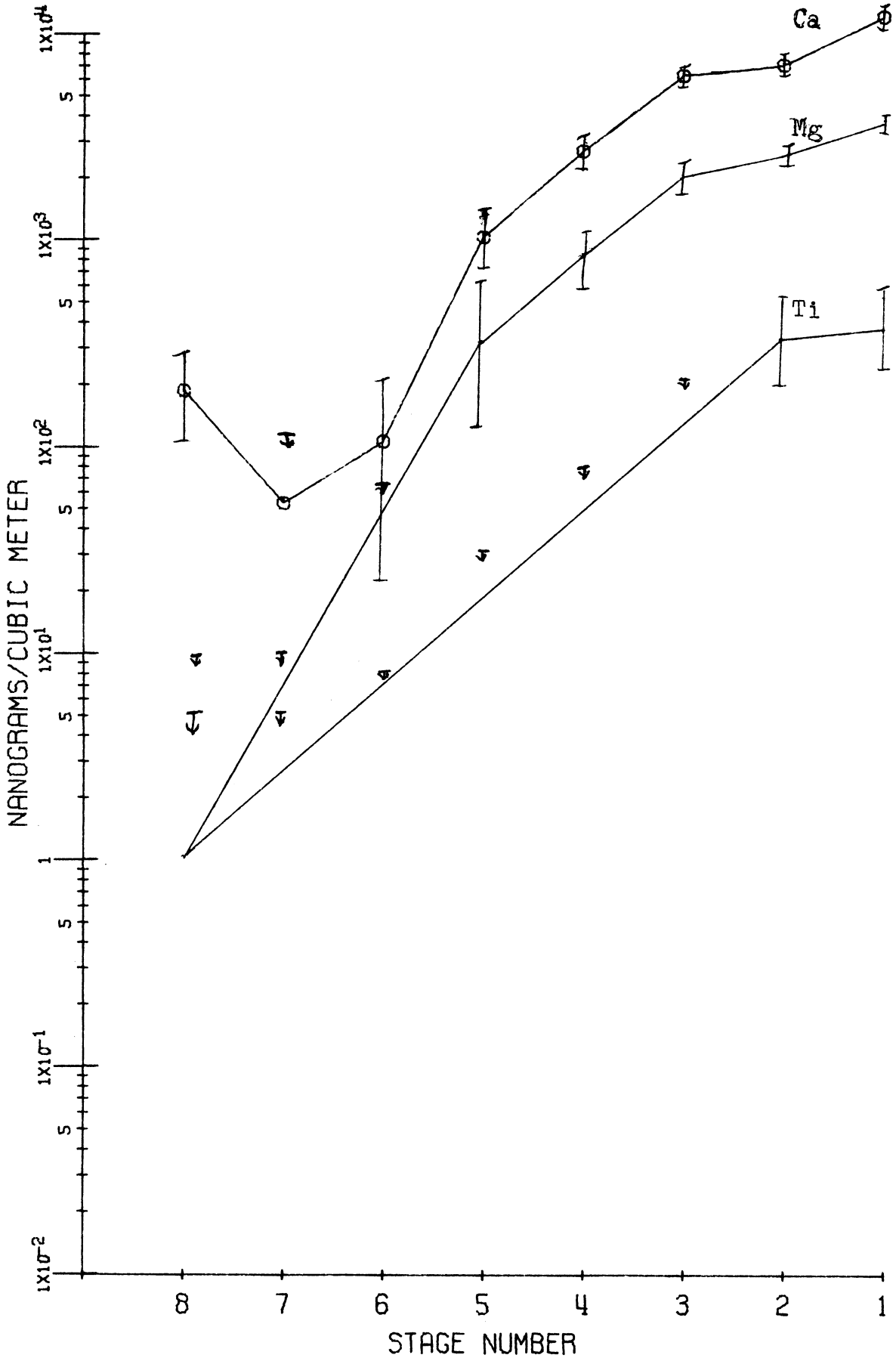

Figure 50. Run 4, Open Hearth Vicinity.

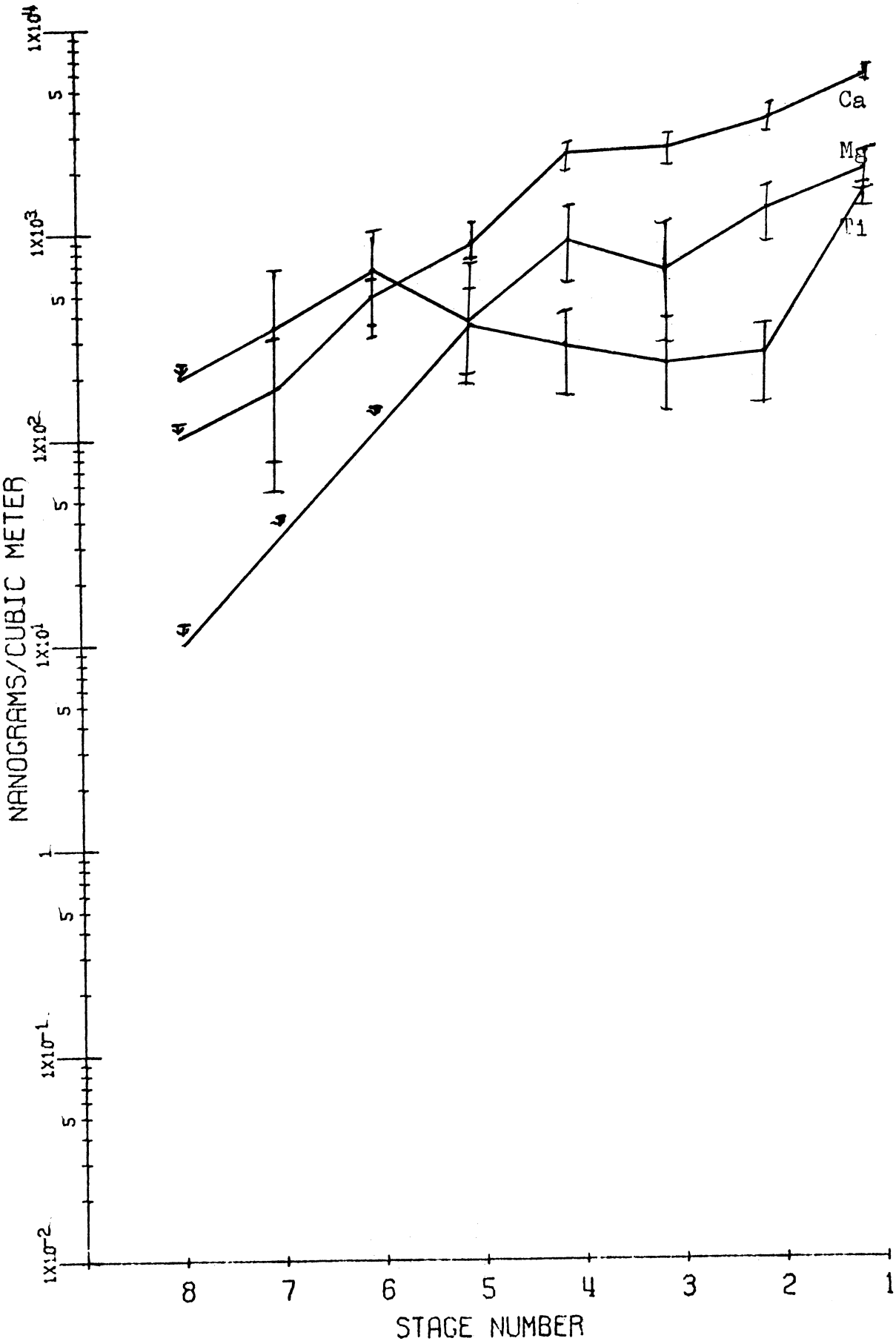

Figure 51. Run 27, Gary Wirt School.

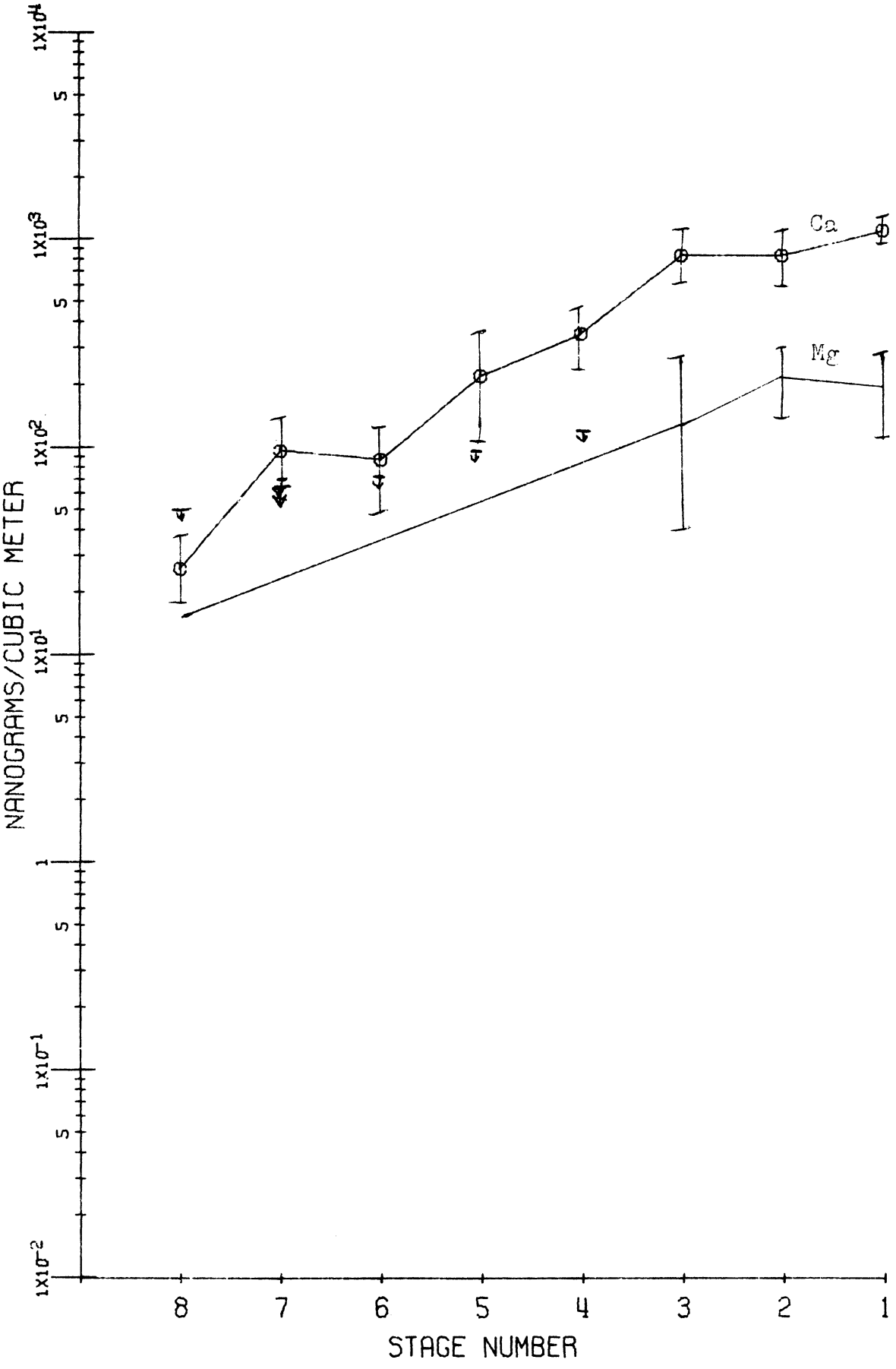

Figure 52. Runs 33 & 35, Gary Airport.

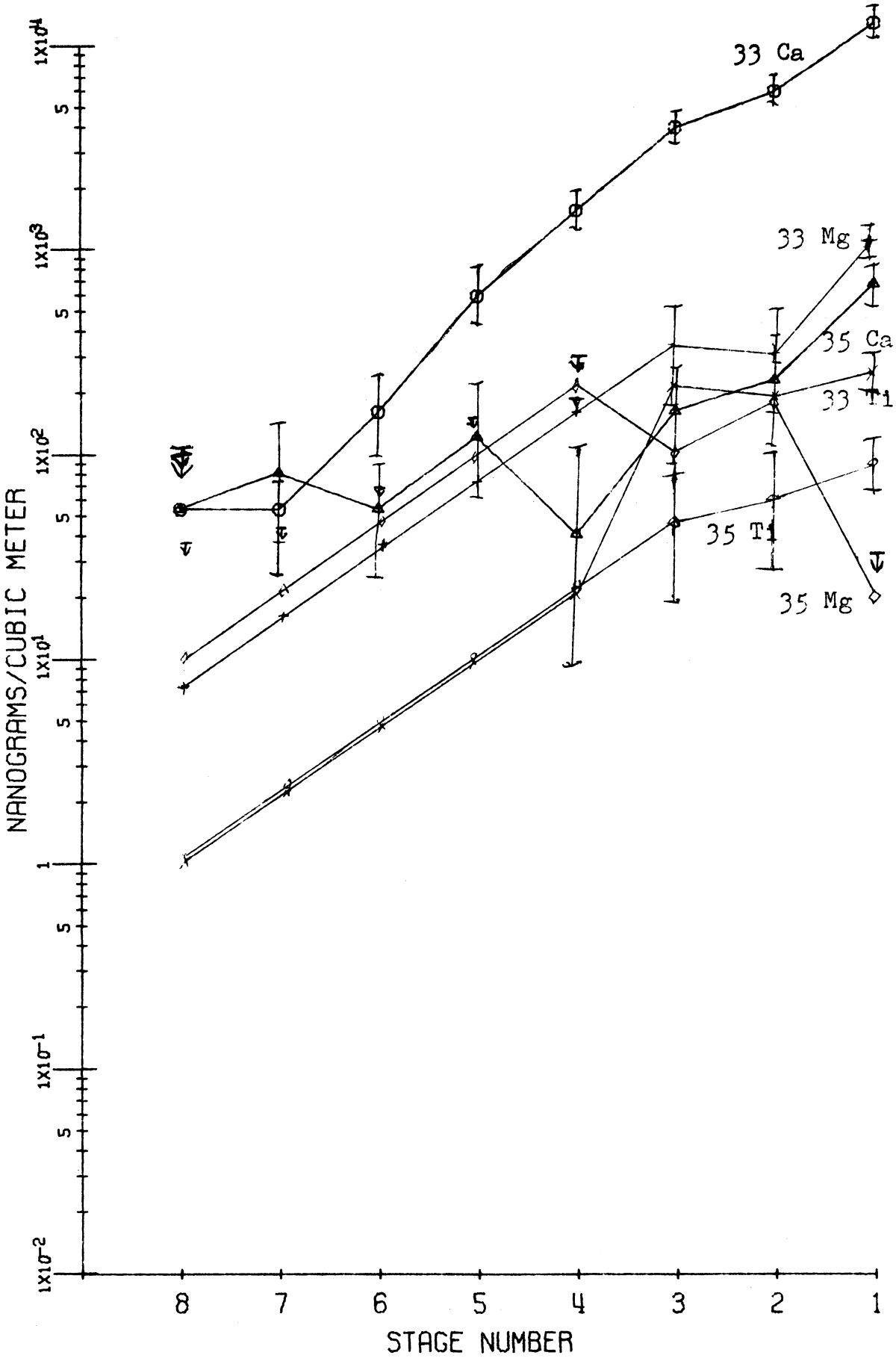

Figure 53. Runs 42 & 43, Lake Michigan.

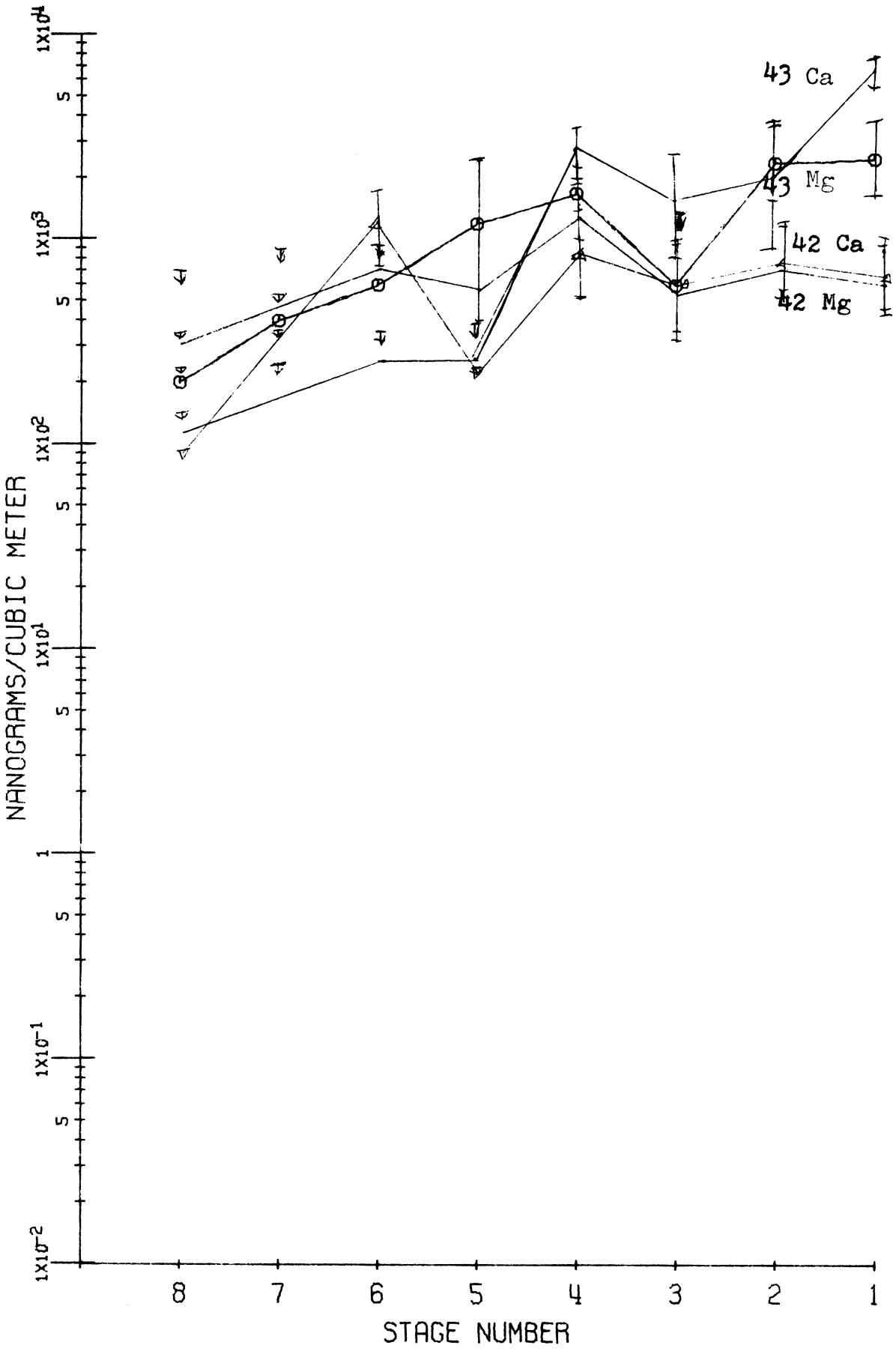

5. Aluminum and Rare Earths

Aluminum and the rare earths (La, Sm, Eu, and Ce) resemble each other in their size distributions, and hence have been grouped together. Most of the mass of these elements appears to be from natural sources, re-entrainment of dust perhaps, but with a certain input of considerable Al pollution from man's activities.

In a relatively non-polluted area (#27) (Figure 54) Al exhibits an even distribution of mass through those particles of sizes impacting on stages 1, 2, and 3, about 300 ng/m^3 per stage. Then the concentration drops fairly smoothly toward the filter with decreasing particle size. This is also true of the rare earths, although in this case La and Ce are more "Junge-distributed" than the others.

But now consider the long-term samples taken in East Chicago (#19, 22) (Figures 55 and 56). In all but one case, concentrations of all elements show increases in at least one stage, usually in several stages, from stage 2 through stage 5. Aluminum is several hundred ng/m^3 per stage associated with larger particles (stages 1-4), dropping to less than 100 ng/m^3 on stage 5, and dropping rapidly on still smaller particles. The rare earths are quite similar, La $\approx$ 1% of Al, Sm $\approx$ 0.1% of Al, Eu $\approx$ 0.01% of Al, and Ce $\approx$ La. But all elements exhibit concentration peaks in stages 2-4. Note that size patterns differ more than concentrations.

Within the steel industry, a maximum concentration on

stages 4-5 is evident for Al and all four rare earths on samples from the open hearth vicinity (#2-5) (Figure 57). This maximum is approximately 2 $\mu g/m^3$ on stage 5 for Al, with the rare earths correspondingly lower. On the sinter plant samples, Al is located on particles impacting on stage 1, as well as on stages 2-6 (Figure 58). Distribution shapes are similar for the rare earths, all decreasing from stage 1 through the filter. Less Al is found near the sinter plant than was present by open hearth operations. It can be concluded that some Al is emitted on particles > 5 μm by sintering operations, but most Al emitted by the steel industry is on smaller particles (1-4 μm) from the open hearth area.

At Markstown Park in East Chicago, a difference in Al spectra between run #20 and run #21 (Figure 59) is noted. Run #20 is the more polluted sample, and not only are size-fraction 1-4 concentrations of Al elevated in #20, but this is particularly true of sizes 3-4. Winds were from steel operations more so during sample #20 than during sample #21.

East Chicago Field School samples (#23, 25) show small concentration maxima for Al on size-fraction-stage 3, imposed on somewhat level distributions from stage 1 to stage 3 (Figure 60). Note similar patterns for La, Sm and Eu on the composite sample (#23-26).

Similar size patterns are noted elsewhere in Northwest Indiana. Note run #17 (Figure 61), the central fire station in East Chicago, and runs #31 and #35 (Figure 62) at the

Gary Airport, where run #31 is downwind and run #35 upwind of the local steel complex.

An Ann Arbor sample (run #49) shows similar results to samples from Northwest Indiana regarding size distribution. Aluminum is lower in concentration in all size ranges, but the rare earths are quite similar (Figure 63).

It seems likely that background Al is present on larger dispersion aerosols to the extent of several hundred ng/m^3 per size-fraction. But pollution Al is mainly emitted on smaller particles, 1 or 2 μm diameter, of concentrations in the immediate source area of approximately 1000 ng/m^3 per size-fraction. Sources are hot processes from the steel industry, and, undoubtedly, coal combustion for power generation.

Figure 54. Run 27, Gary Wirt School

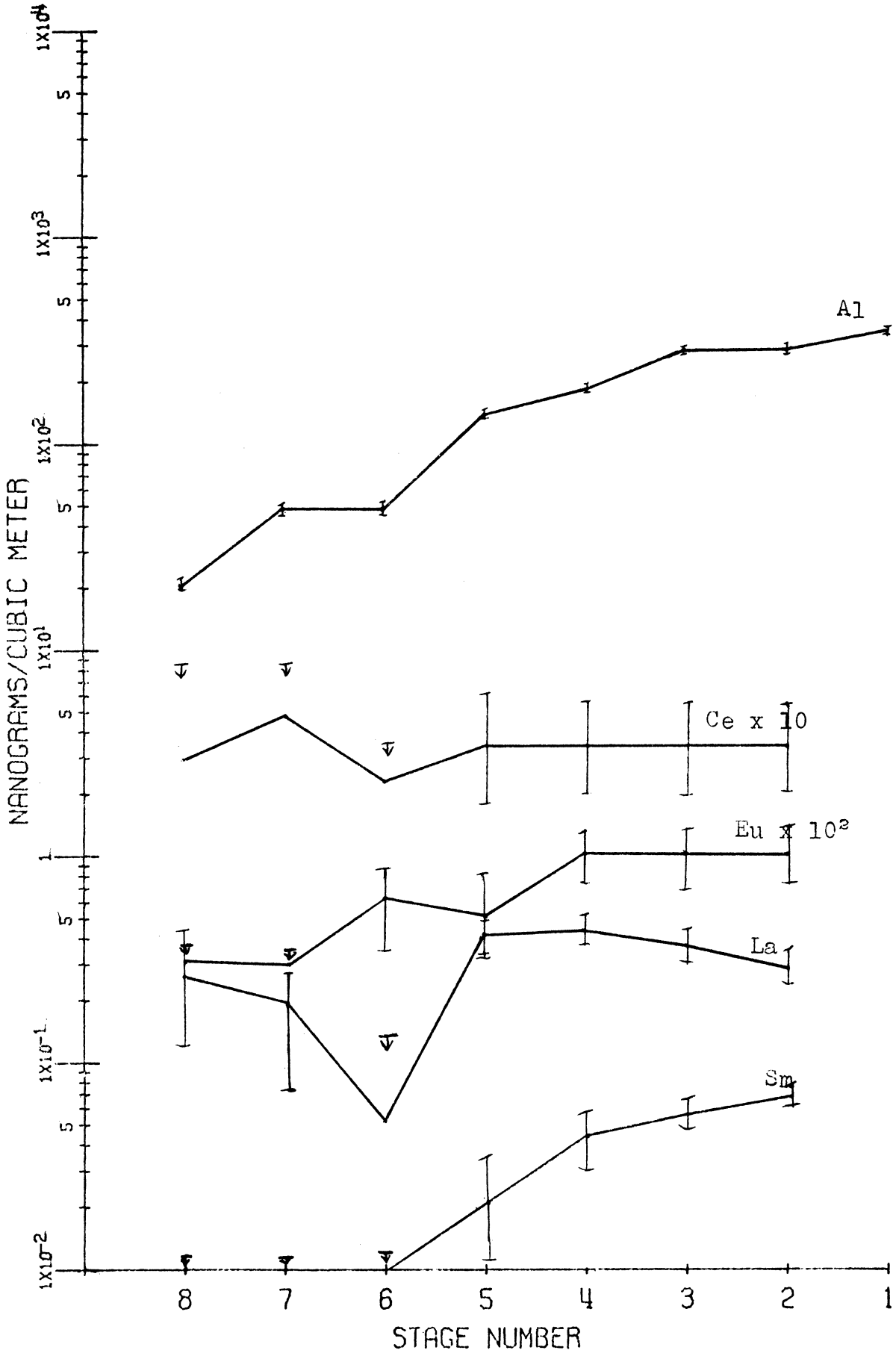

Figure 55. Run 19, East Chicago Central Fire Station.

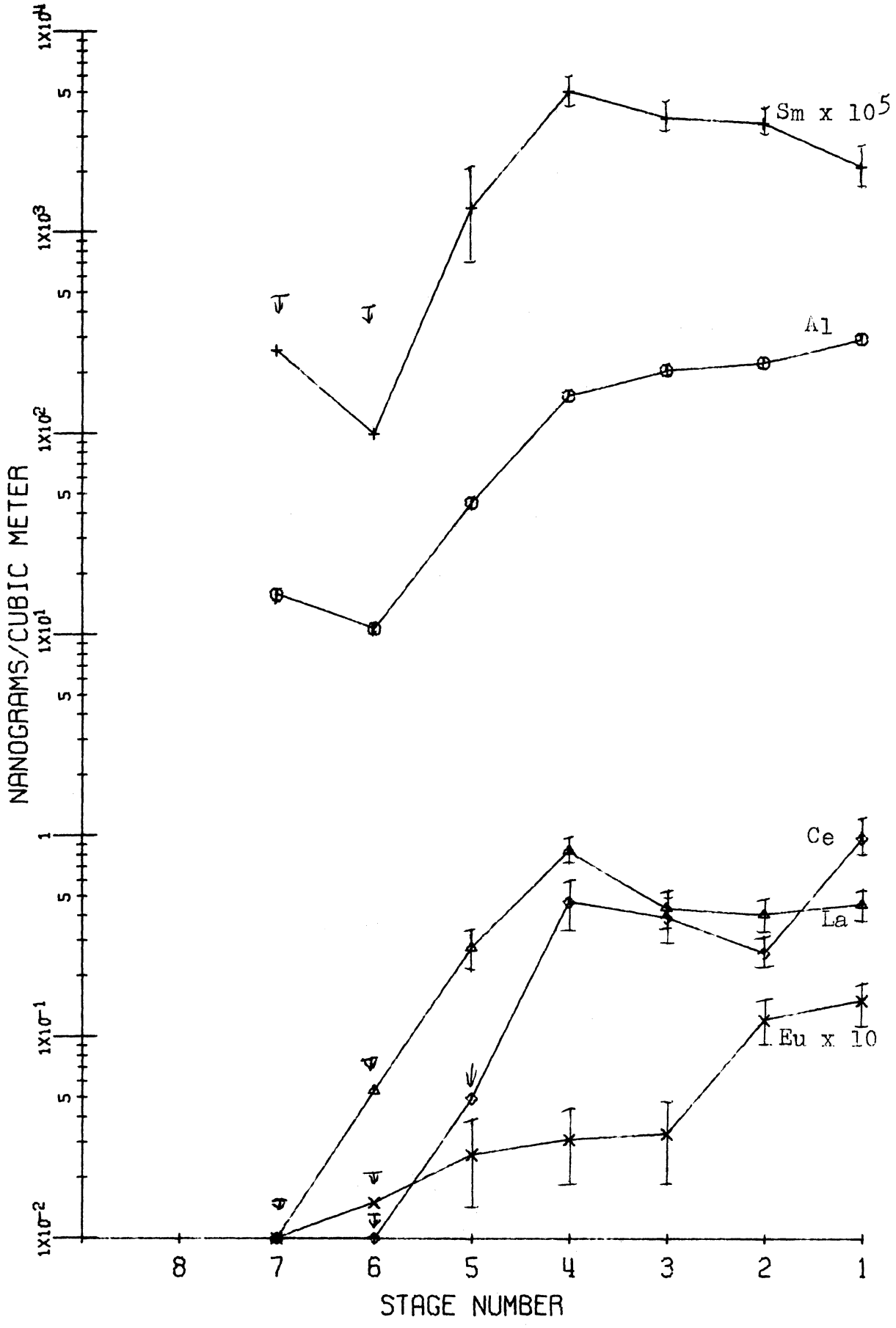

Figure 56. Run 22, East Chicago Markstown Park.

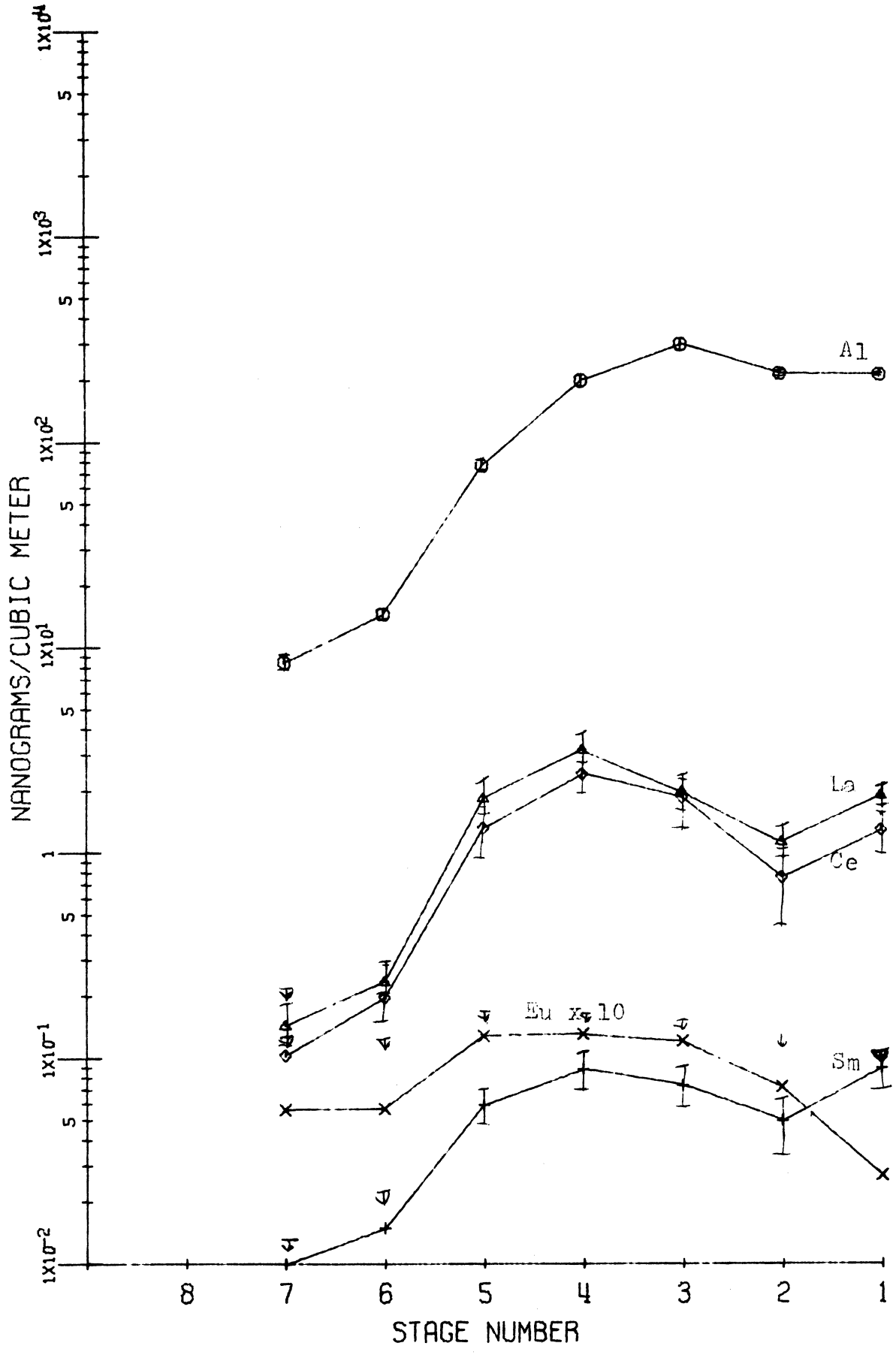

Figure 57. Runs 2-4, Open Hearth Vicinity.

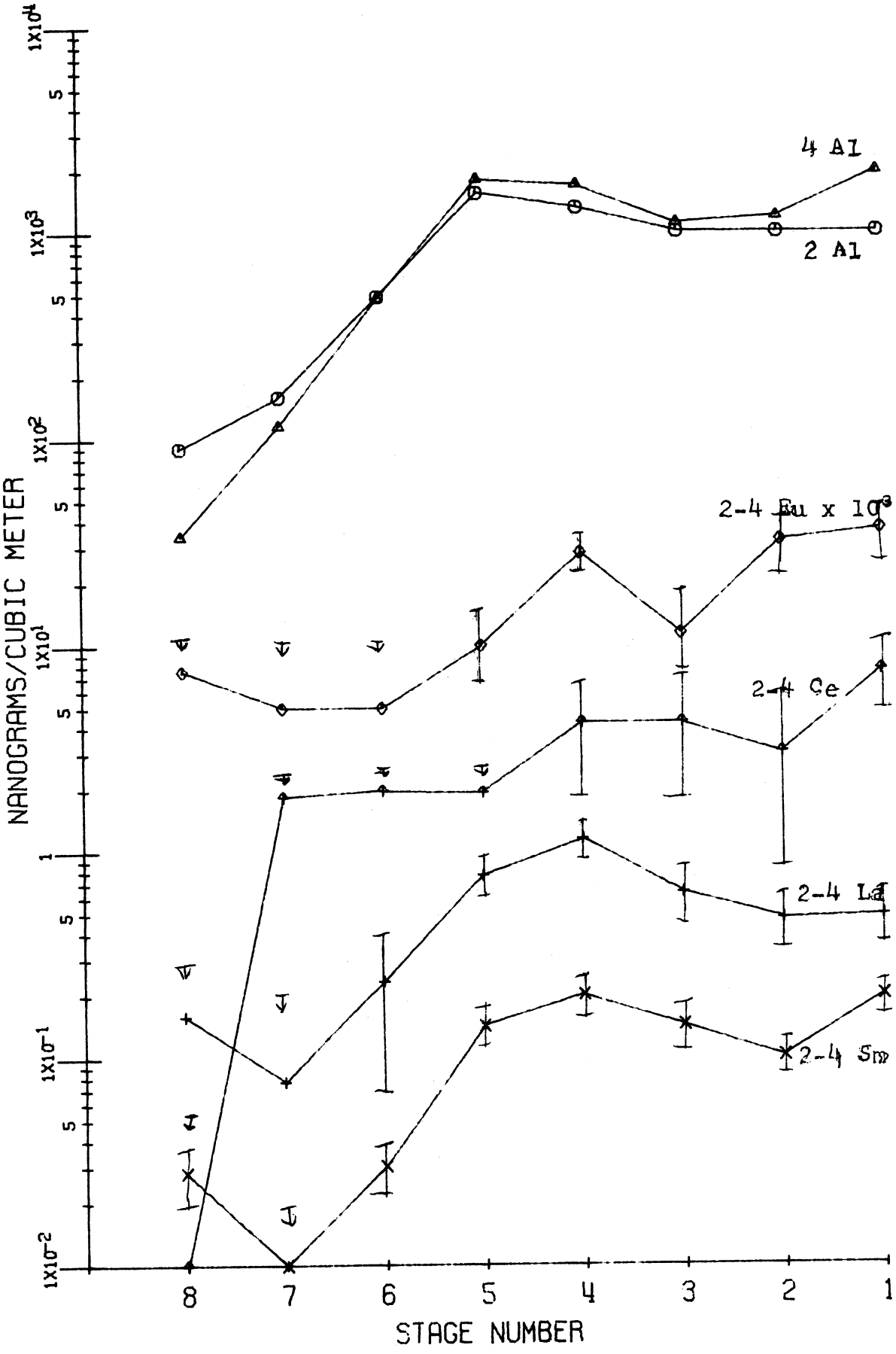

Figure 58. Runs 7-10, Sinter Plant Vicinity.

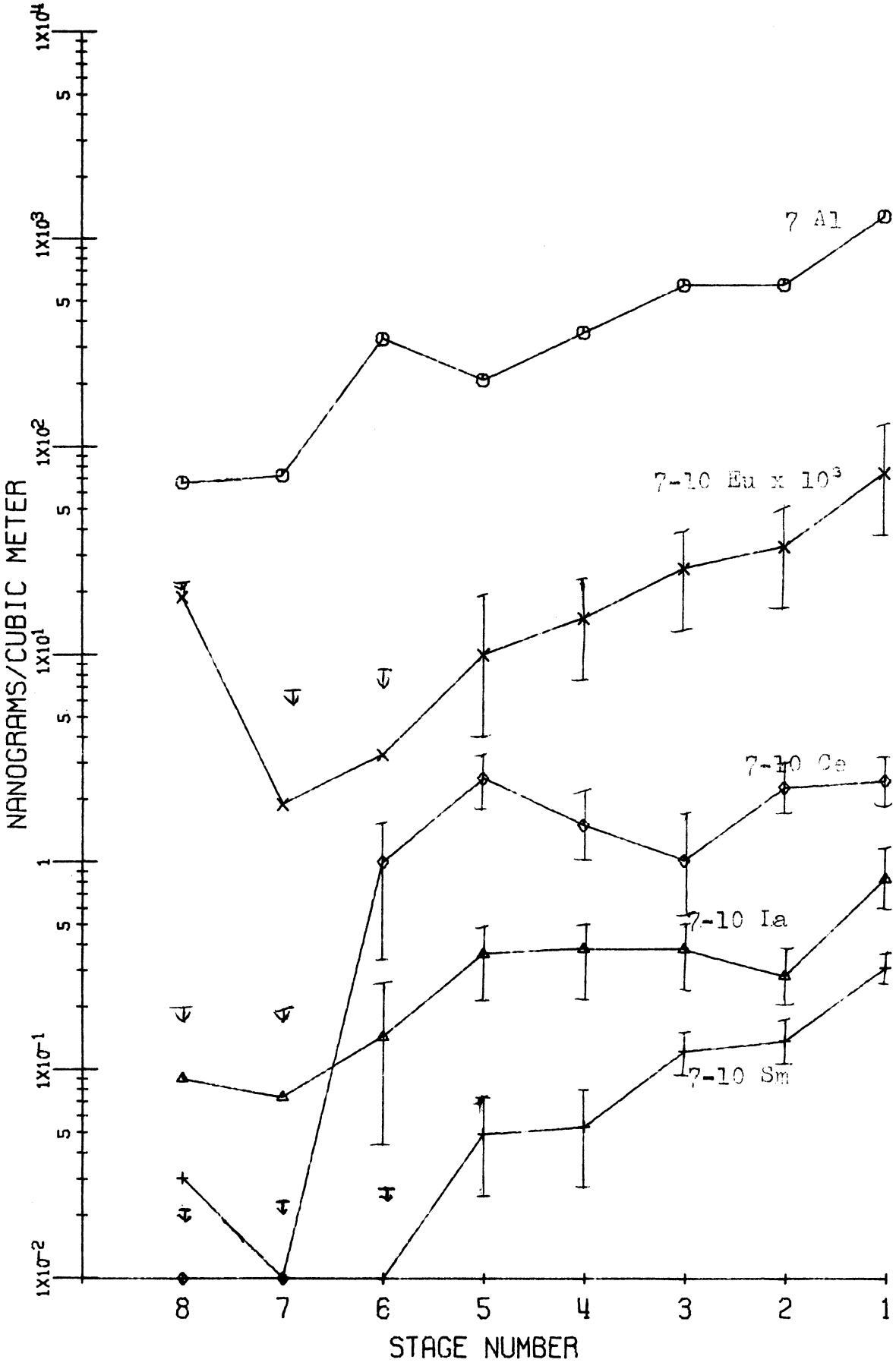

Figure 59, Runs 20 & 21, East Chicago Markstown Park

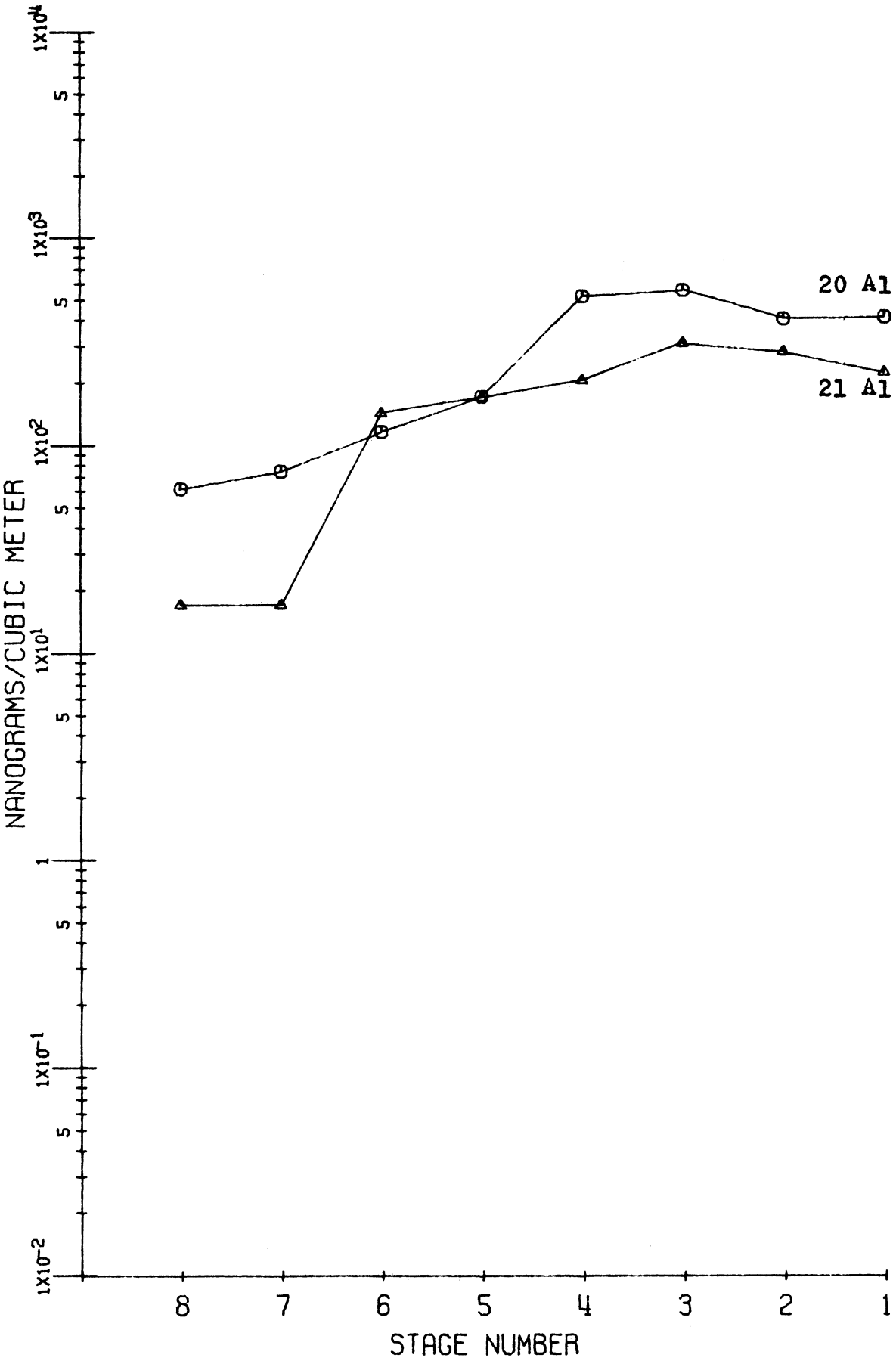

Figure 60. Runs 23-26, East Chicago Field School.

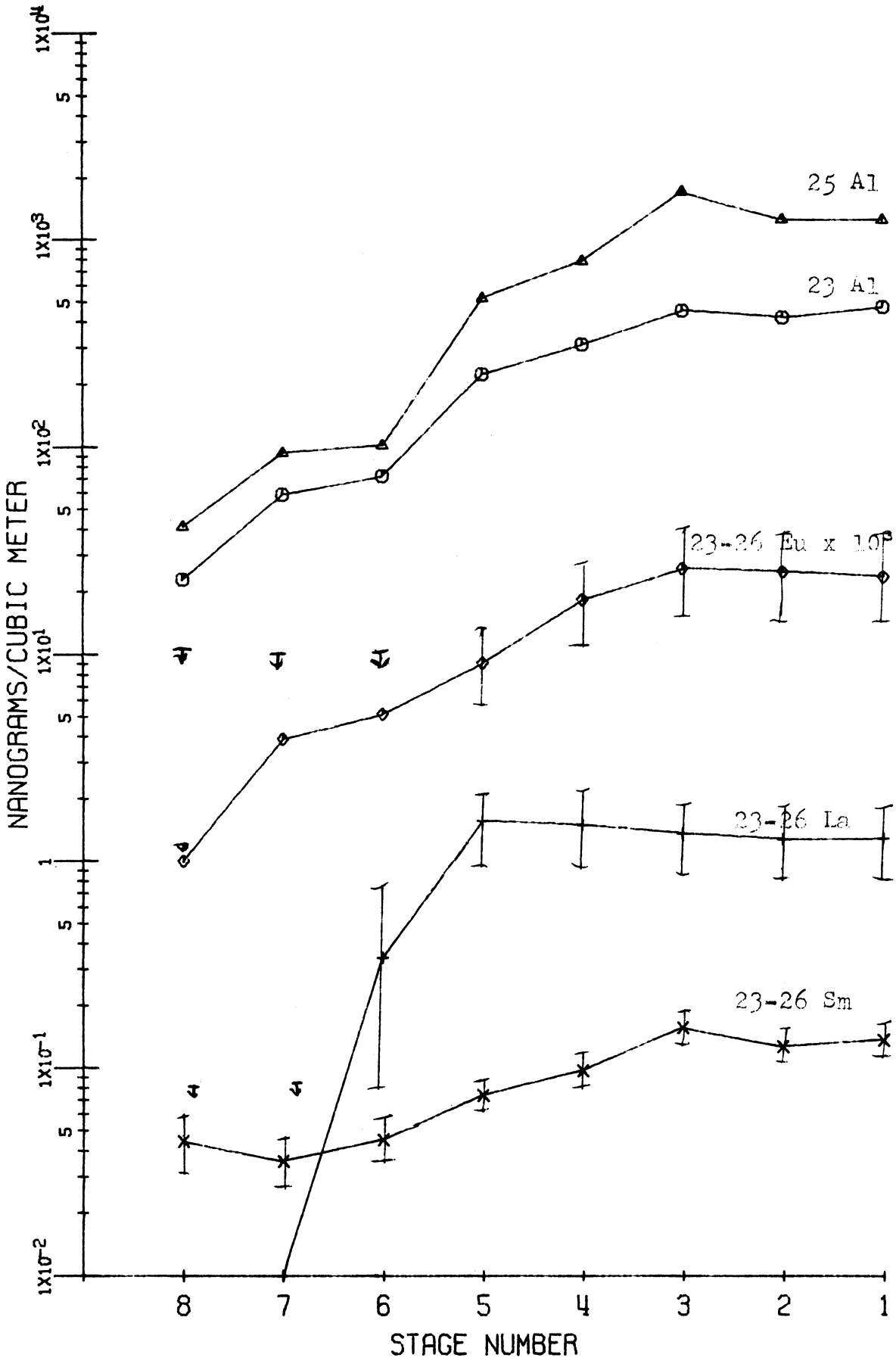

Figure 61. Runs 15-17, East Chicago Central Fire Station.

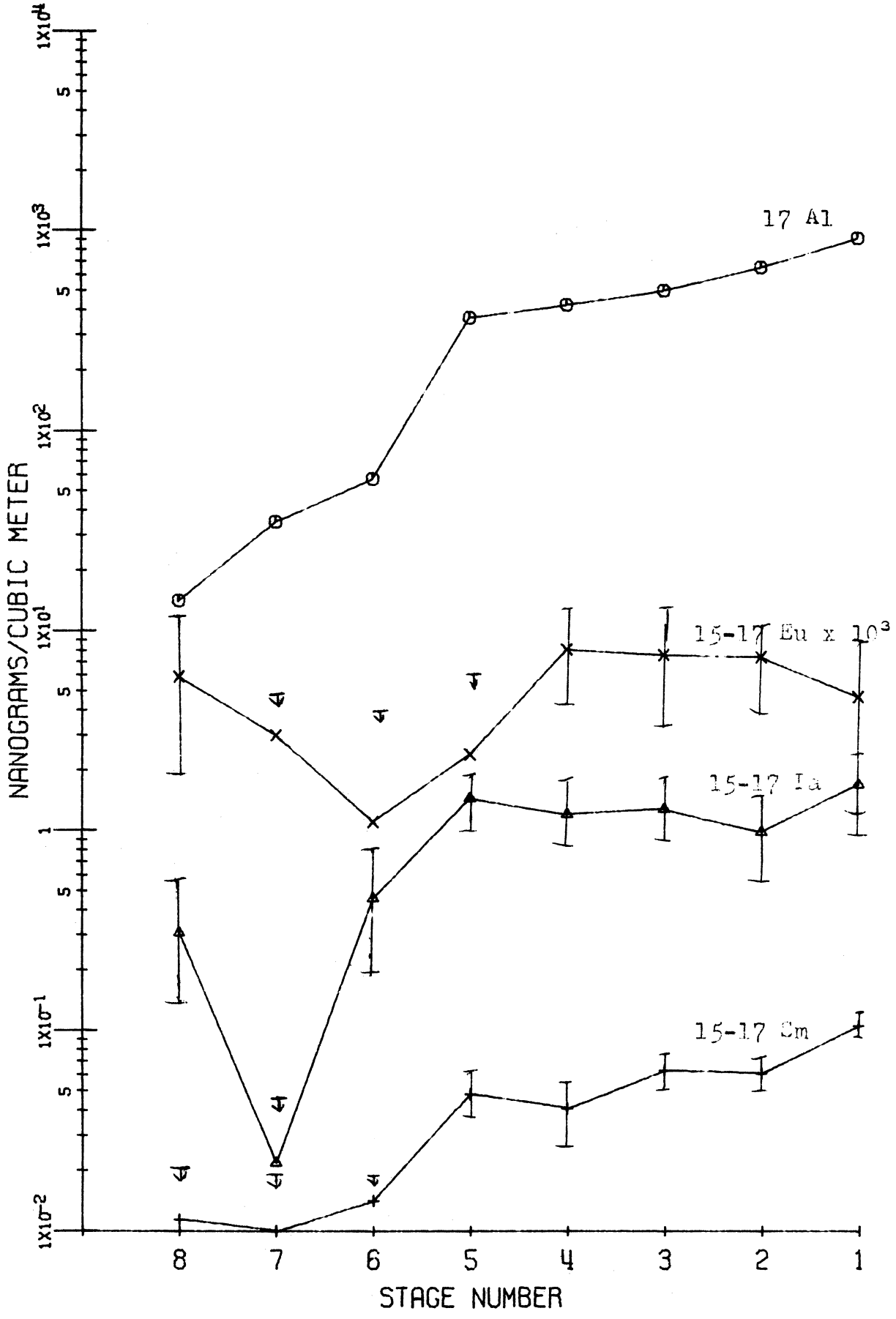

Figure 62. Runs 31-35, Gary Airport.

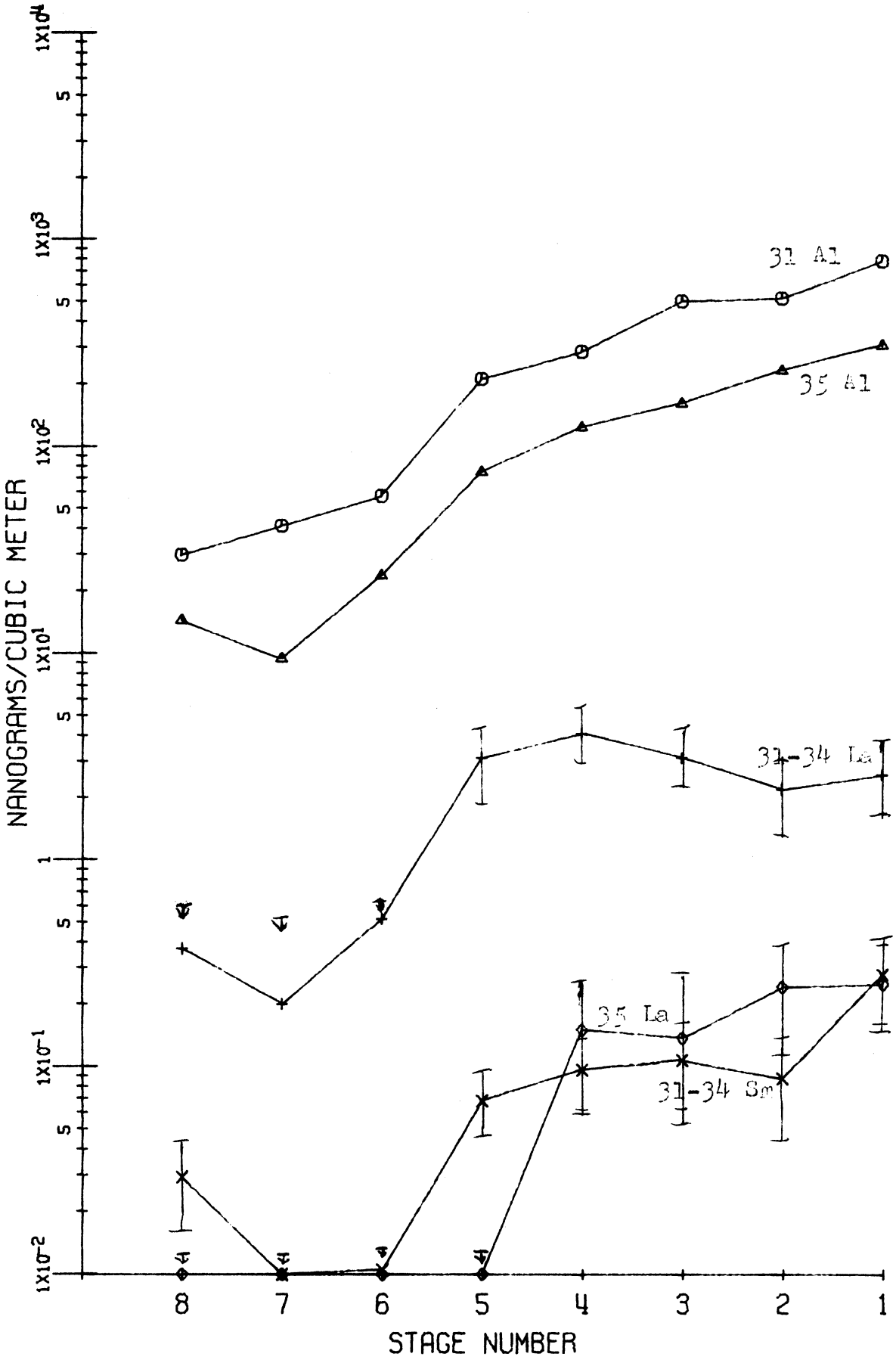

Figure 63. Run 49, Ann Arbor.

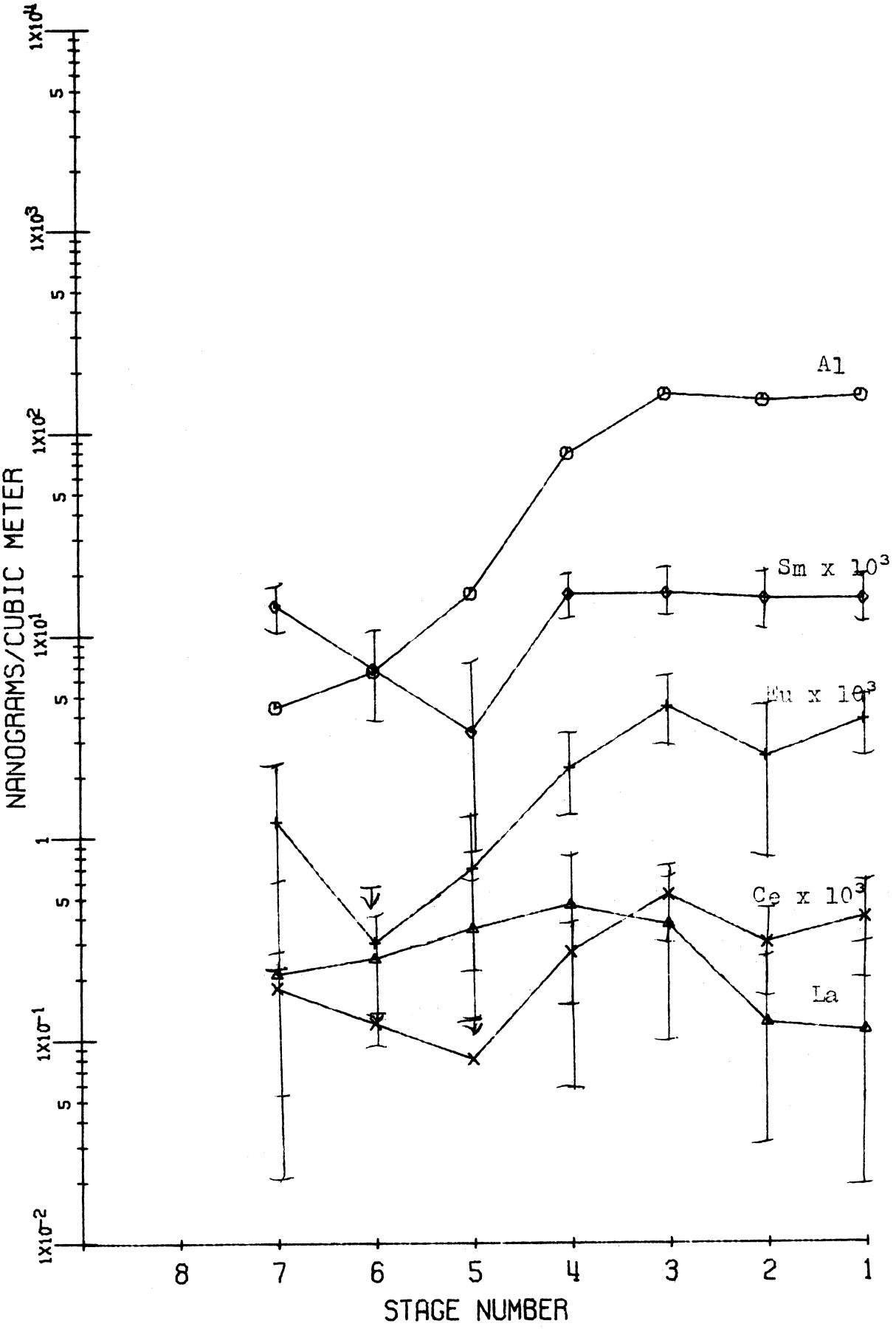

6. Bromine, Gallium, Potassium

Bromine, Ga, and K form a group of elements present on condensation aerosols of intermediate particle size. Aged aerosols show more mass associated with smaller particles than with larger particles, although not to the degree evidenced by the "zinc" group. This association among these three elements is somewhat unusual, and is based on comparisons of spectra, or a grouping by "appearances," and is not based on chemical properties—Br being a halogen, K an alkali metal, and Ga located with the Al family. But perhaps a consideration of possible source processes may provide a clue as to the relationships.

Inspection of runs #19 and 22 from East Chicago shows quite similar distribution curves for Br and Ga. Sample #19 shows a definite concentration maximum on that particle-size range associated with stage 4 (Figure 64). A definite maximum is located at stage 7 on run #22 (Figure 65); this sample being taken much closer to the steel industry. Perhaps this size is more representative of source particle sizes, at least for this industry. Filter data are unavailable for these samples, but based on other samples, it seems most likely that peak concentrations also exist on particles that would have been trapped by a filter. Note that on both runs, especially #22, K is more nearly "Junge-distributed" than most other elements. Concentrations of Br are approximately 10 ng/m^3 per stage, with a decrease of 100-fold for Ga; K is between 20 and 100 ng/m^3 per stage.

Concentrations of Br at Wirt School (#27) are similar to those found at Markstown (#22), again with a rise at stage 7, and an even greater concentration at the filter (Figure 66). Gallium again follows at a magnitude of 1% of Br. Potassium is approximately 100 ng/m^3 per stage, or similar to other samples.

Considering samples taken at a steel industry (#2-4, 6-9) (Figures 67 and 68), Br shows very little change in concentration or in shape of the size spectra—Br again equals about 10 ng/m^3 per stage, with a peak of several 10's of ng/m^3 on the filter. This indicates that, within this industry, ambient Br levels are less! The situation regarding Ga is a bit different. Gallium spectra again resemble Br, but here the concentrations are 5-10% of the Br. Potassium is several hundred ng/m^3 per stage, with a filter peak of nearly 1 ug/m^3, at the open hearth, and similar in the mid-size ranges at the sinter plant. But this latter sample contains sharp K peaks on particles sized by stage 1 and the filter.

To varying degrees, urban locations in East Chicago generally show Br patterns having concentration maxima on particles impacting at about stage 5. With decreasing particle size smaller than that impacted on stage 5, concentrations may increase or decrease slightly, or remain constant except for filter-sized particles. Concentrations per stage range from less than 10 to several hundred ng/m^3. Run #21 (Figure 69) shows a fairly level Br distribution,

paralleled by Ga, at the East Chicago Markstown area. Gallium is less than 1 ng/m^3, and Br approximately 100 ng/m^3, per stage, or Br/Ga $\approx$ 1000. Runs #15-17 show a different pattern for both, with emphasis on the smallest particle size (Figure 70). Magnitudes of Br are 10's to 100's of ng/m^3 per stage, and again Ga is less than 1% of Br. Run #18 (Figure 70) shows an elevation of Br, perhaps caused by a reduction in wind speed, which results in less Br being swept away from the sample site, the East Chicago fire station, located in a commercial area. Wind speed, rather than direction, seems to effect greater changes in Br levels. Essentially K appears less "Junge-distributed," with peaks on large and small particles, when the wind is from industrial, rather than commercial, sources. Its magnitude approximates 100 ng/m^3 per stage.

Runs #36 (north wind) and #38 (south wind) show obvious Br pollution on small particles from downtown Gary (Figure 71).

Runs #42 and 43 on Lake Michigan point out the greater amounts of Br found on small particles near Gary, as contrasted with further offshore (Figure 71).

Based on these results, it appears that Br is produced mainly by transportation sources, with almost no Br associated with the steel industry. This Br is associated with condensation aerosols of very small particle size. Bromine quickly attaches to larger particles of about 0.5-1.0 μm in radius (stages 4-5). Gallium is also emitted

on condensation aerosols, but here primarily by the steel industry, and on particles larger than those emitted by transportation sources. Potassium is emitted by a wider variety of sources, including the steel industry, mostly on condensation, but partly on dispersion, aerosols. Some K, perhaps most, undoubtedly arises from area chemical operations. Because of its high degree of reactivity, and fallout of large particles, K quickly approaches a "Junge distribution."

Figure 64. Run 19, East Chicago Central Fire Station

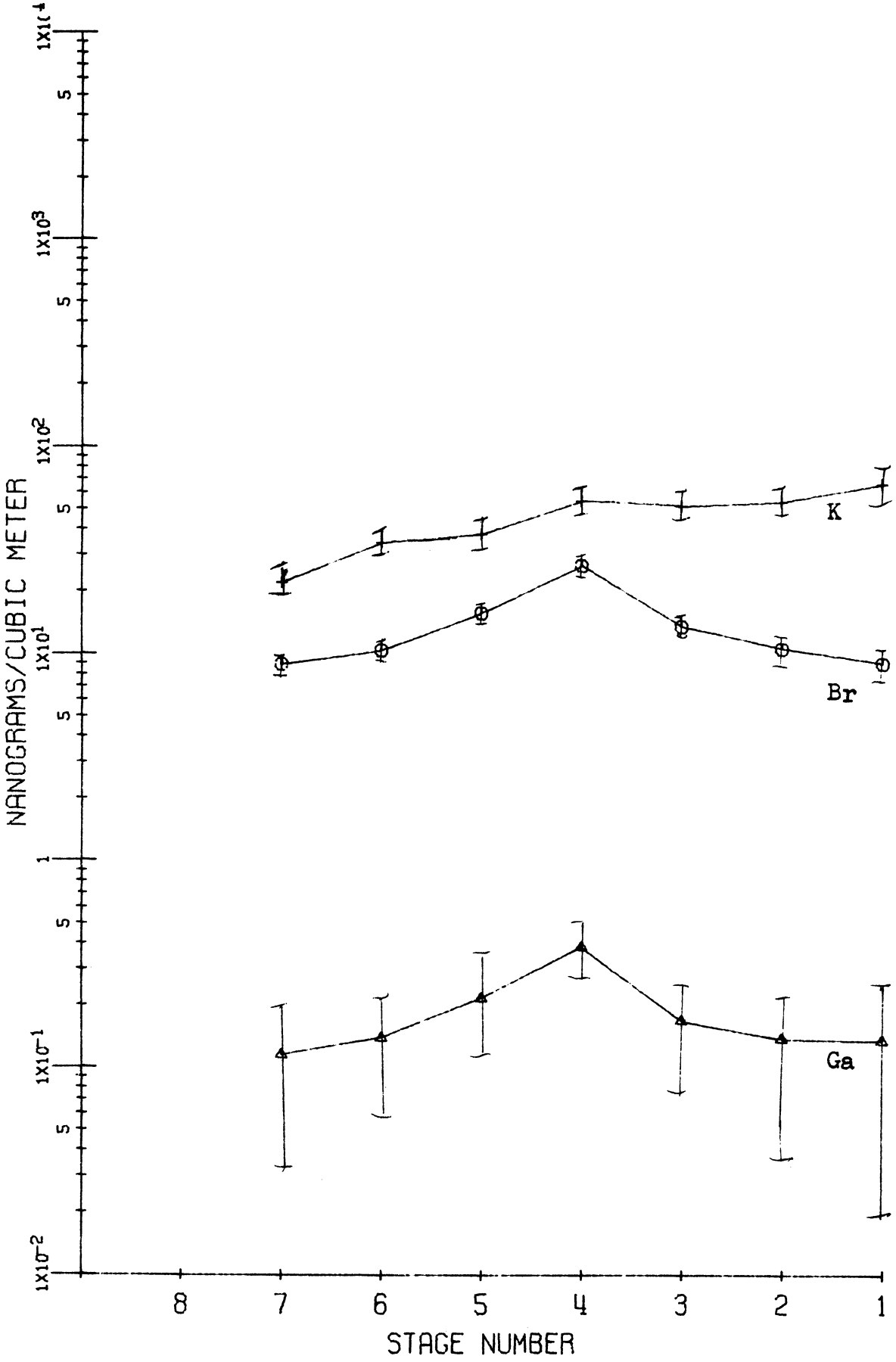

Figure 65. Run 22, East Chicago Markstown Park.

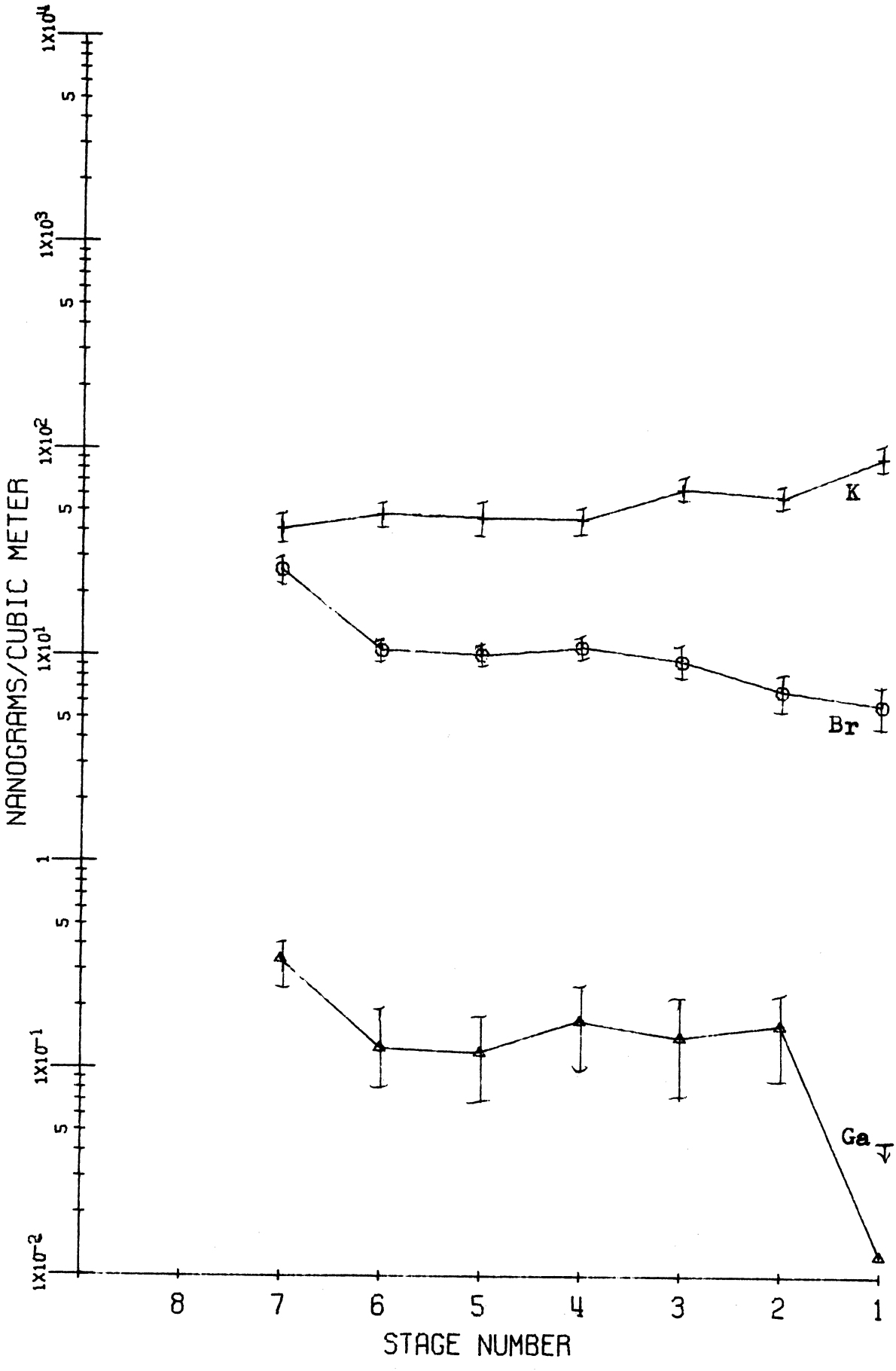

Figure 66. Run 27, Gary Wirt School.

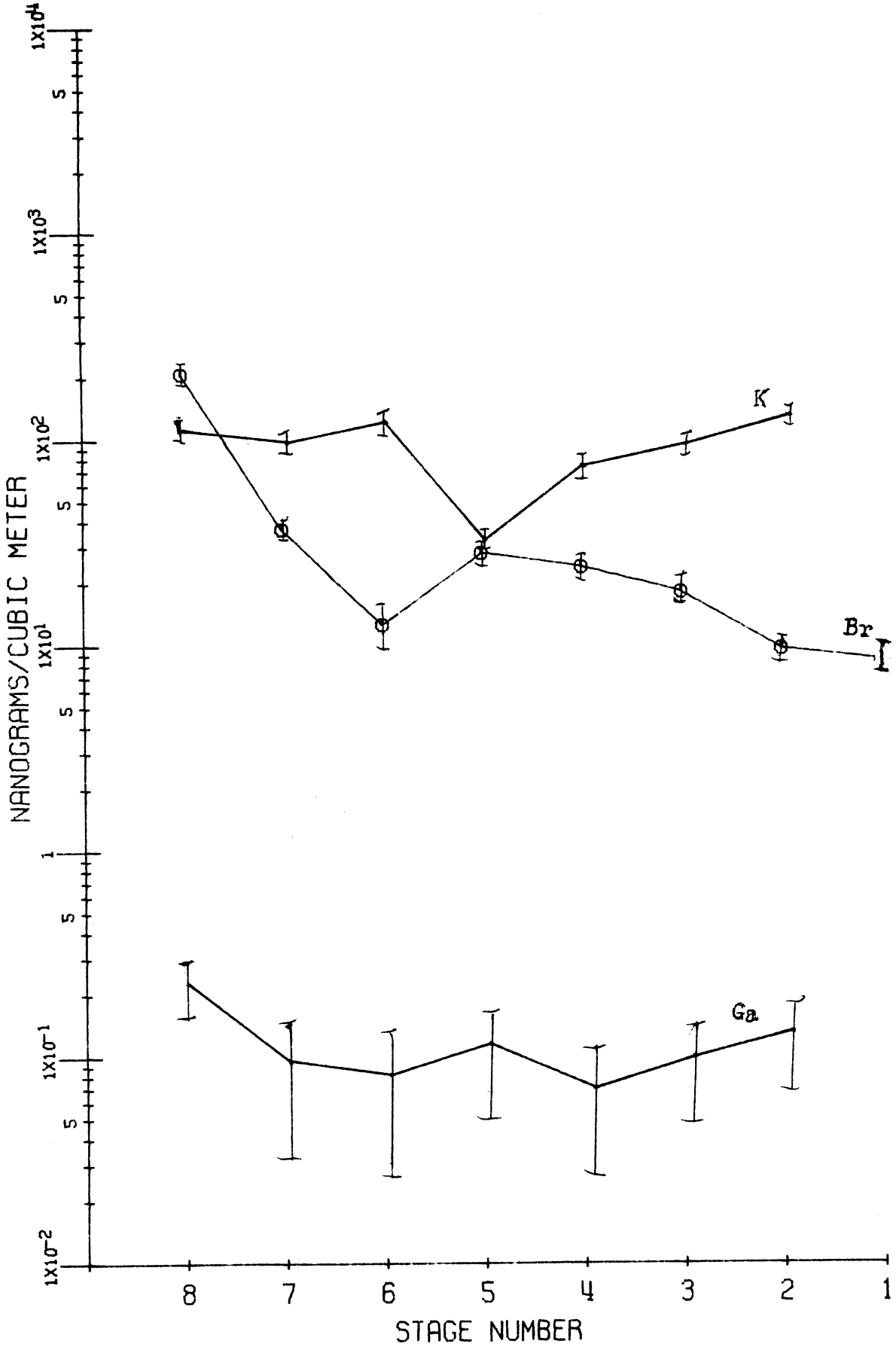

Figure 67. Runs 2-4, Open Hearth Vicinity.

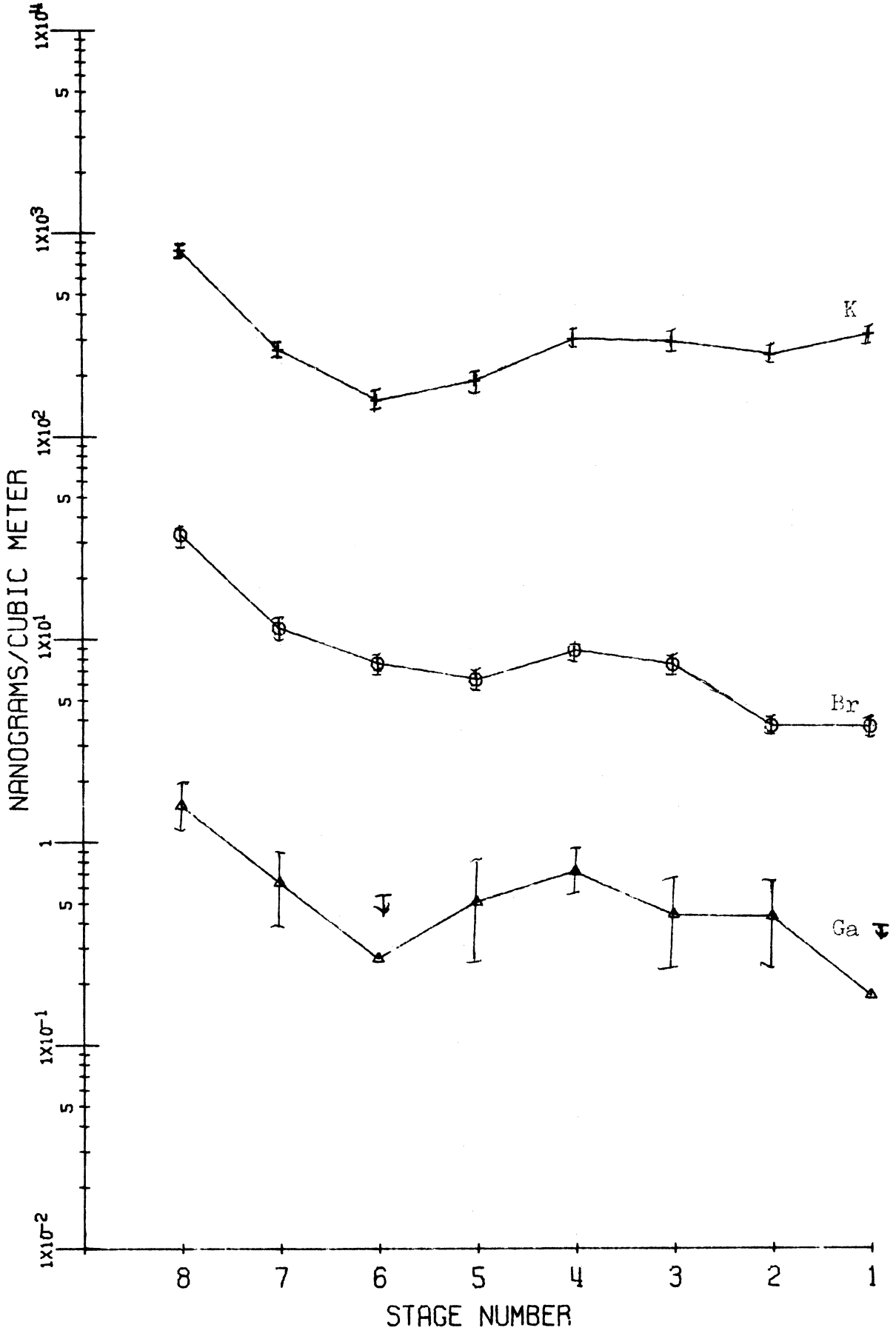

Figure 68. Runs 7-10, Santer Plant Vicinity.

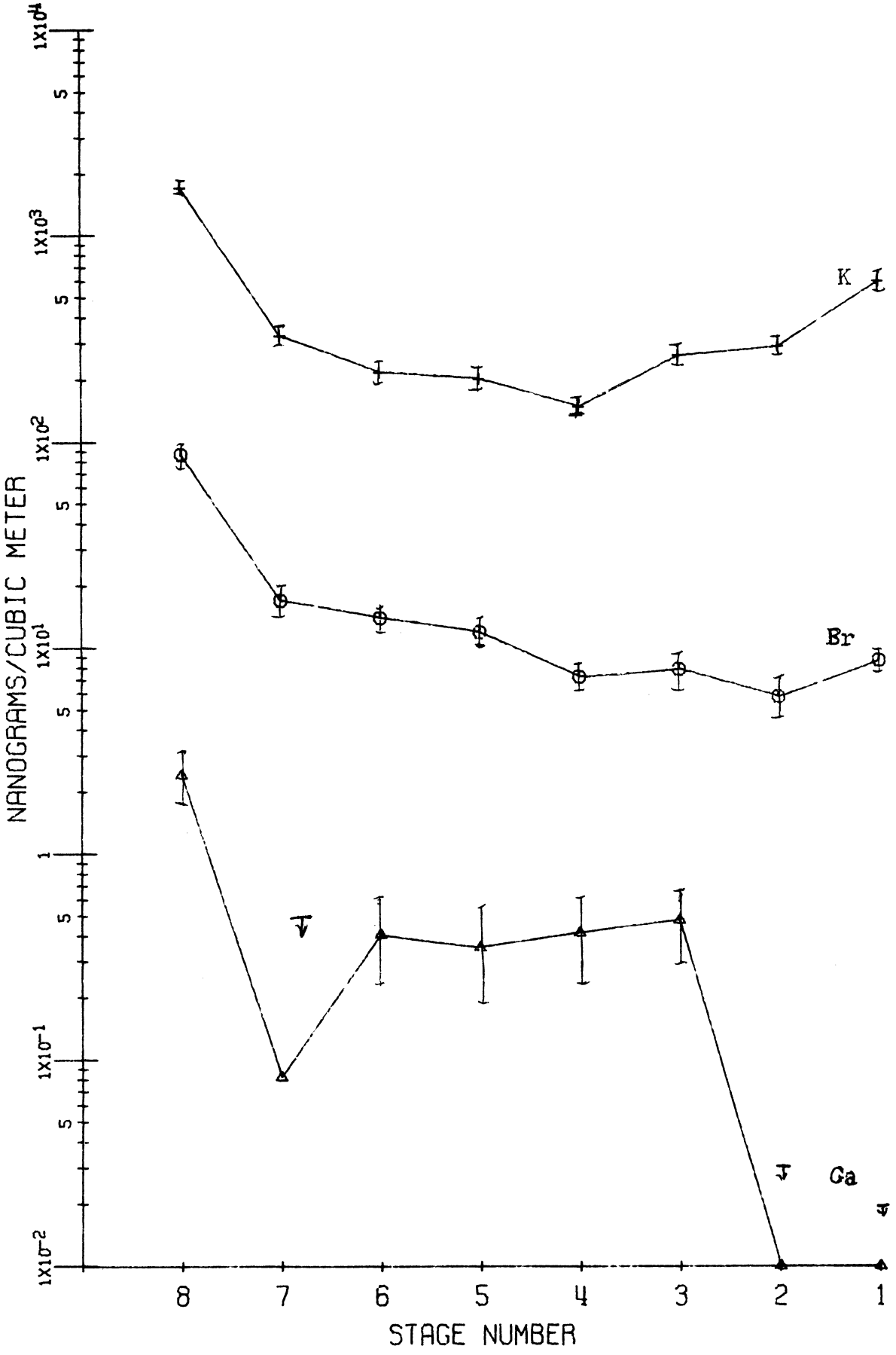

Figure 69. Run 21, East Chicago Markstown Park.

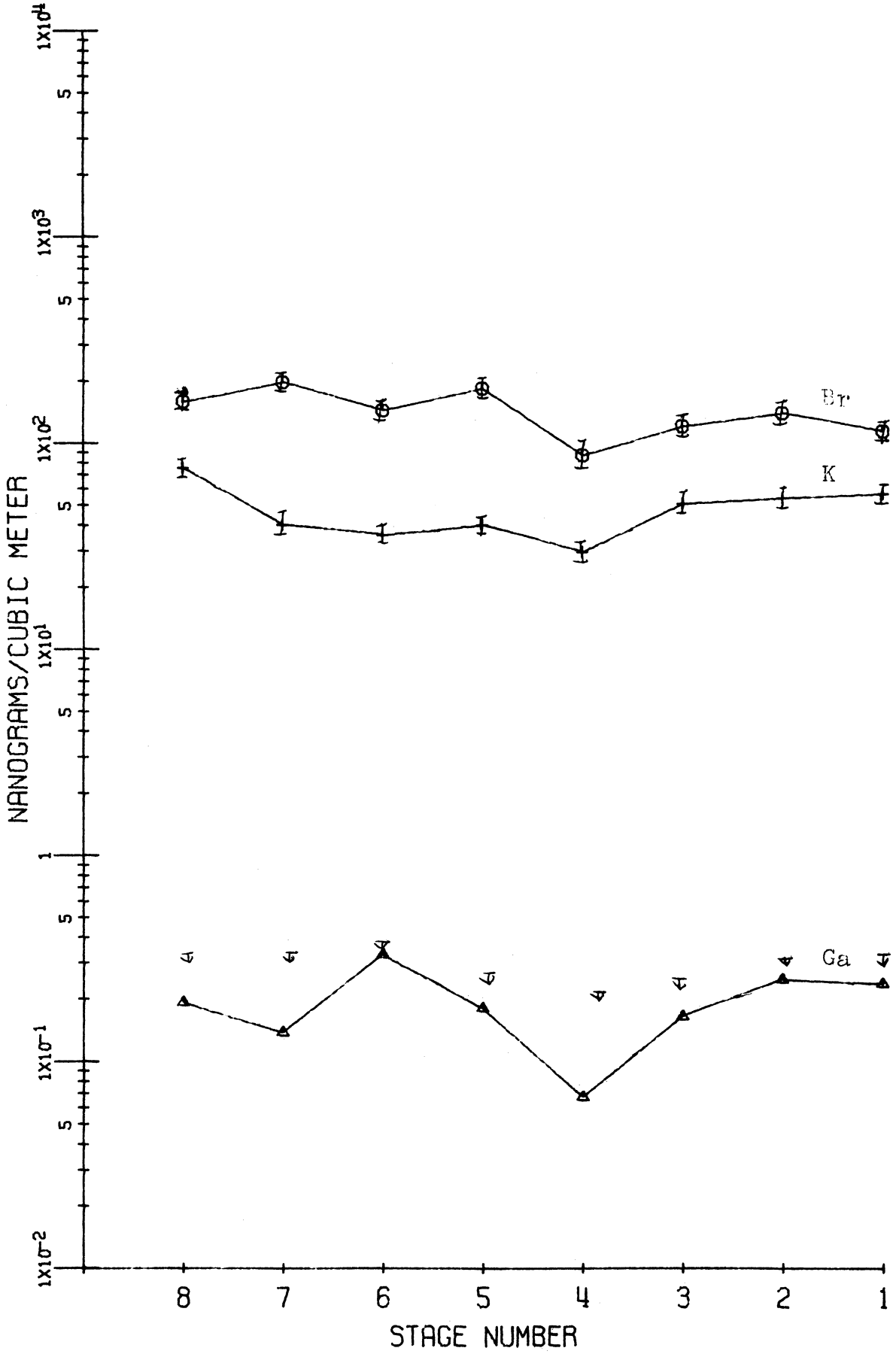

Figure 70. Runs 15-18, East Chicago Central Fire Station.

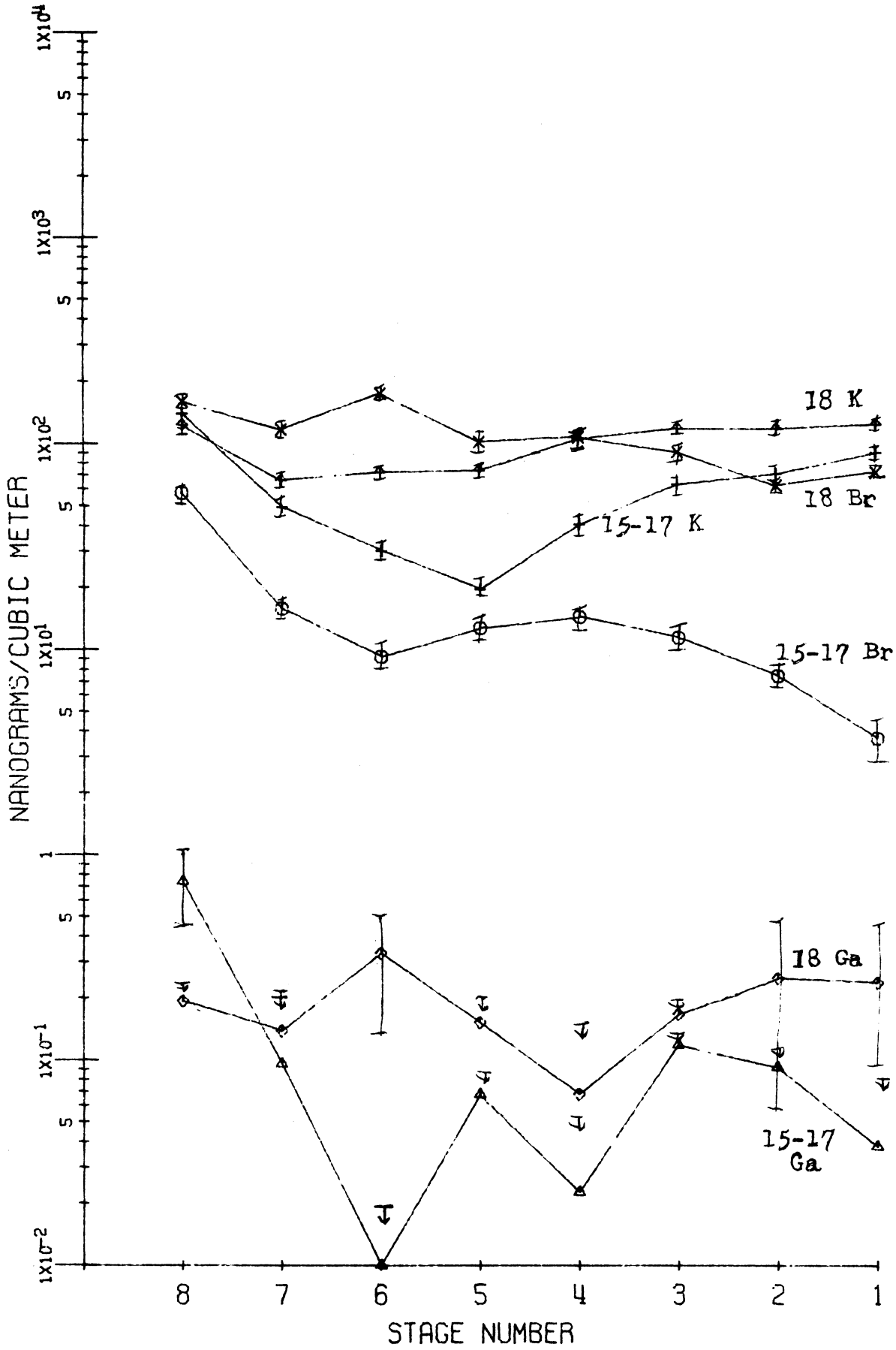

Figure 71. Runs 36 & 38, Gary Central Fire Station; and Runs 42 & 43, Lake Michigan.

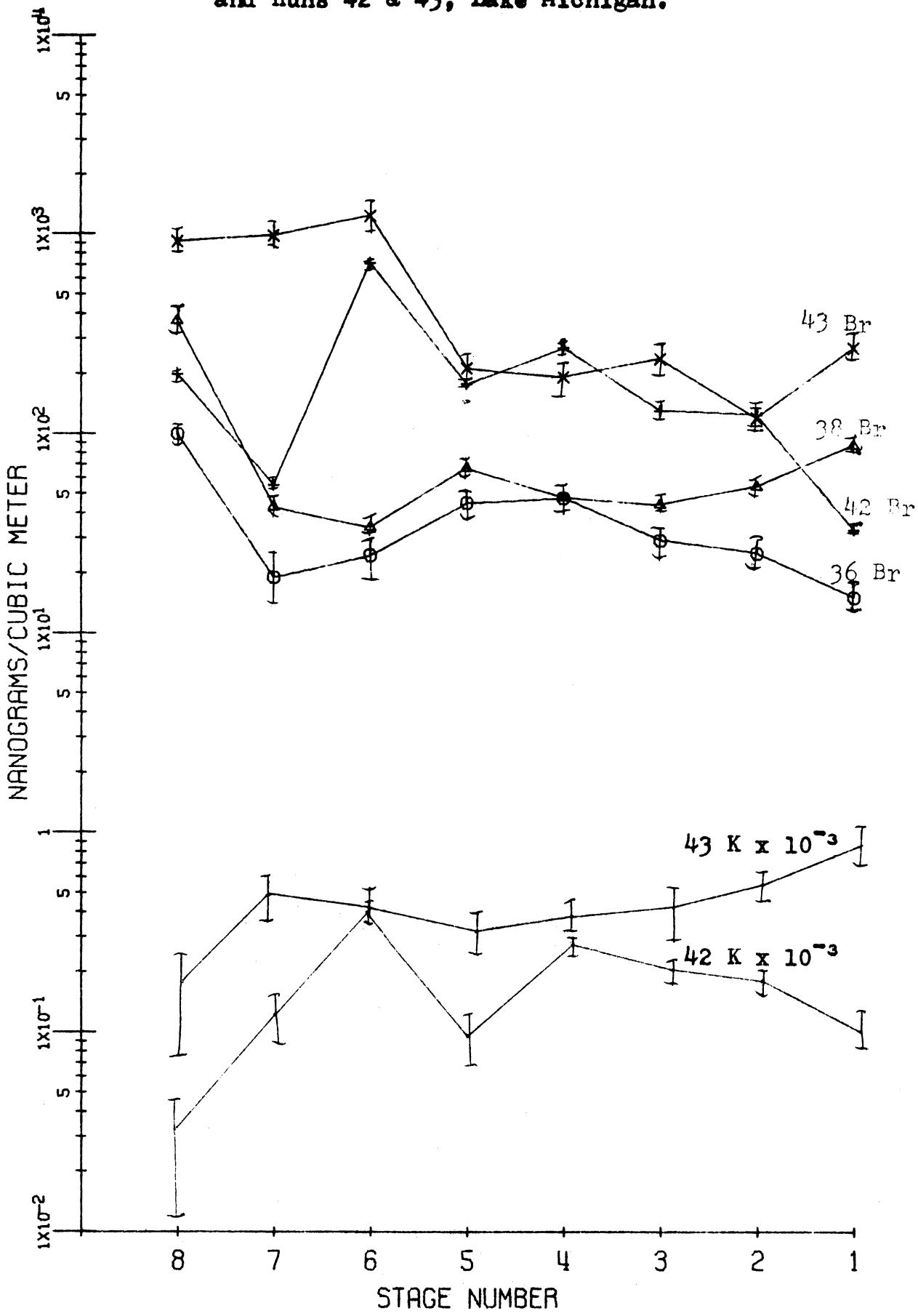

7. Sodium and Chlorine

Sodium and Cl have been grouped together because of their obvious association together in sodium chloride salt crystals. If this association holds true for most aerosol Na and Cl, then not only should their size distributions be parallel, but mass concentration should follow a Cl/Na ratio of 1.5. Also, due to the fallout of large particles, and the chemical reactivity of both Na and Cl, one might expect a "Junge distribution" for urban aerosols to be achieved rather rapidly. In this section these concepts are considered and predominant sizes of fresh Na and Cl pollution aerosol components are determined. Then this group is compared with K and Br from the preceding group, for Na and K are quite similar chemically, as are Cl and Br. Finally Br/Cl ratios are considered.

A two-week sample from East Chicago (#19) shows very smooth size distribution spectra for both Na and Cl at the fire station, with some predominance of mass on larger particles (Figure 72). Sodium concentrations on stage 1 are 200-300 ng/m^3, dropping to about 50 ng/m^3 at the filter. Chloride concentrations are 50-100% higher on larger particles (perhaps salt crystals) as might be expected, but drops more rapidly than does Na with decreasing particle size, until, at filter size, Na exceeds Cl in concentration by a factor of 2-3. Similar features are shown by run #22, Figure 73.

At Wirt School in Gary (#27) the Cl/Na ratios are 1-2

for all size fractions except the filter, where it is 5 (Figure 74). Magnitudes per stage are ≈ 125 ng/m^3 and 80 ng/m^3, respectively, for Cl and Na. But for this sample, concentrations are more uniform over the size ranges than was the case in East Chicago. Similar patterns are seen at the central fire station and airport in Gary (#36-38 and #28-35); again the ratio of Cl/Na on the filter may be somewhat higher than that for the 7 impaction stages. Two runs from the airport are graphed on Figure 75.

In East Chicago on daily samples from the fire station (#12-18) size distributions are again essentially "Junge;" however, the Cl/Na ratio is more variable—from 1 to 5 (Figure 76). Note the Cl peak on stage 5 of run #17. Similar findings arise from samples at Markstown (#20-21) and Field School (#23-26) (Figure 77).

Now note the steel industry (Figure 78). Open hearth samples (#1-5) show the expected pattern and magnitude, except for stage 1. Here Cl and Na are elevated in concentration four-fold. Also some elevation of concentration of both elements is noted on the smaller particle sizes. But a Cl/Na ratio of 1.5 holds well. At the sinter plant (#6-10), Cl concentrations are elevated on all stages, especially the filter. Sodium concentrations are high on both stage 1 and the filter. From stage 3 to stage 7 the Cl/Na is constant, but high—about 5. This ratio increases to ≈ 20 on stage 8, but has a value of 1.2 on stage 1.

Hence it seems likely that the steel industry emits

large NaCl salt particles from both open hearth and sintering operations, some small particles from both sources, but including an aerosol especially rich in condensation Cl from the sinter plant.

Samples from the air over Lake Michigan show fairly parallel Cl/Na distributions, except for high Cl concentrations on size interval-stage 8 (Figure 79).

It has been noted by Loucks and Winchester (1969) that generally the Br/Cl ratio in aerosols increases with decreasing particle size, and it has been postulated that Br leaves larger particles preferentially to Cl, and attaches to smaller particles. These data confirm that the Br/Cl ratio does indeed increase with decreasing particle size on urban aerosols. This effect is masked, however, near sources (such as sintering operations) where there is a large input to the atmosphere of small particles containing Cl. This effect is shown on Figure 80 for urban samples #27 and 30, and for industrial complex samples #4 and 7.

Figure 72. Run 19, East Chicago Central Fire Station.

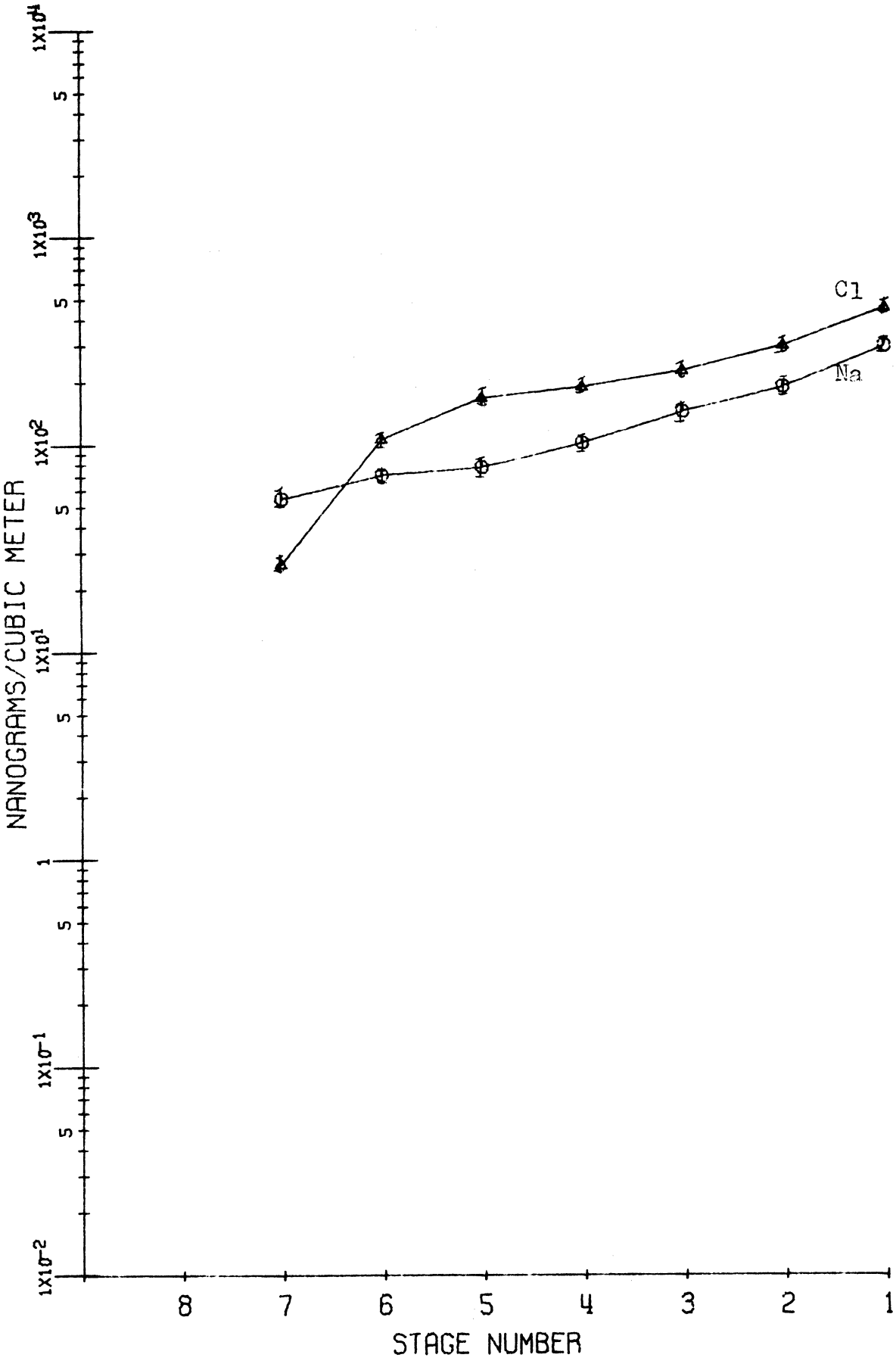

Figure 73. Run 22, East Chicago, Markstown Park.

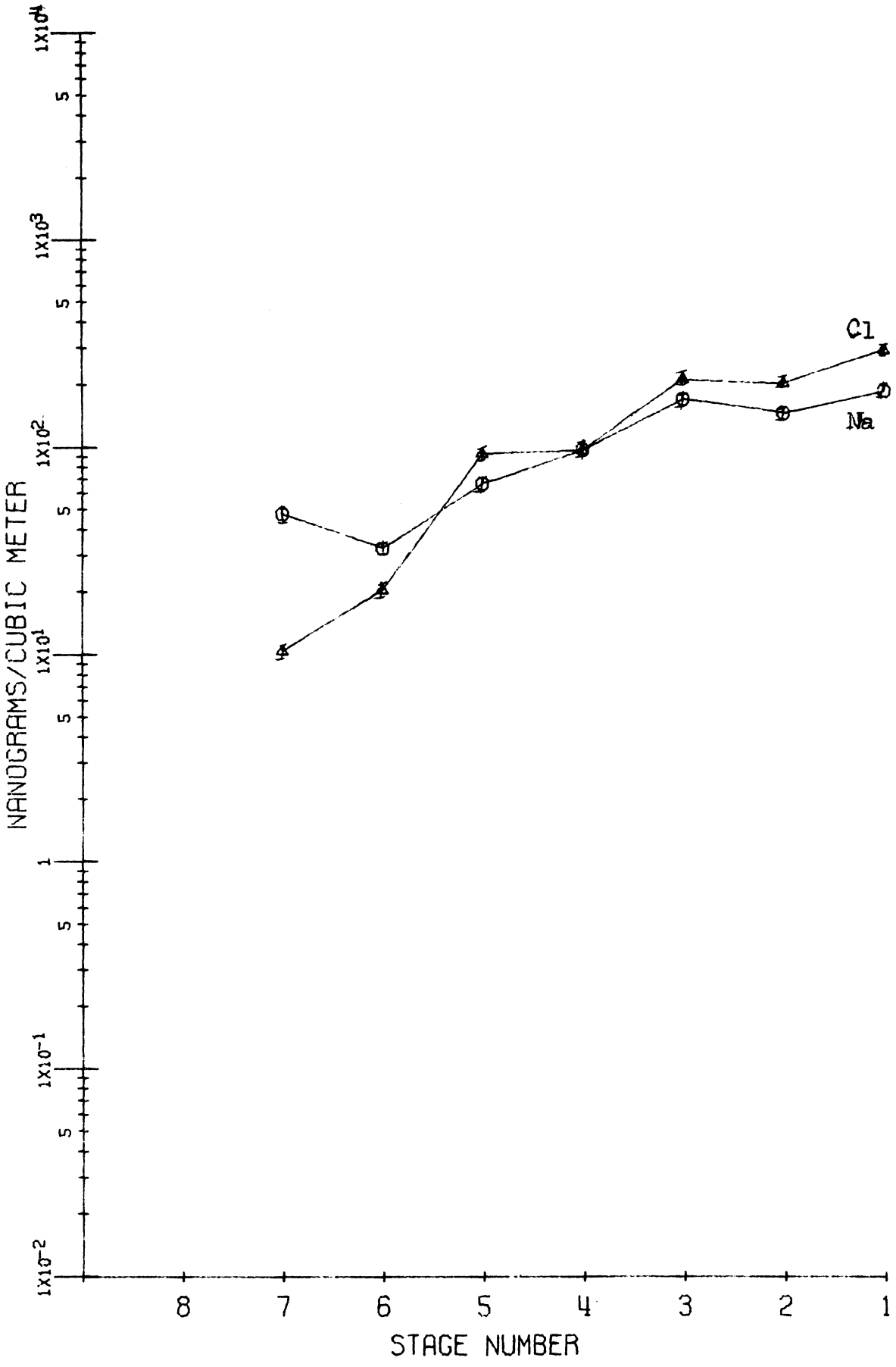

Figure 74. Run 27, Gary Wirt School.

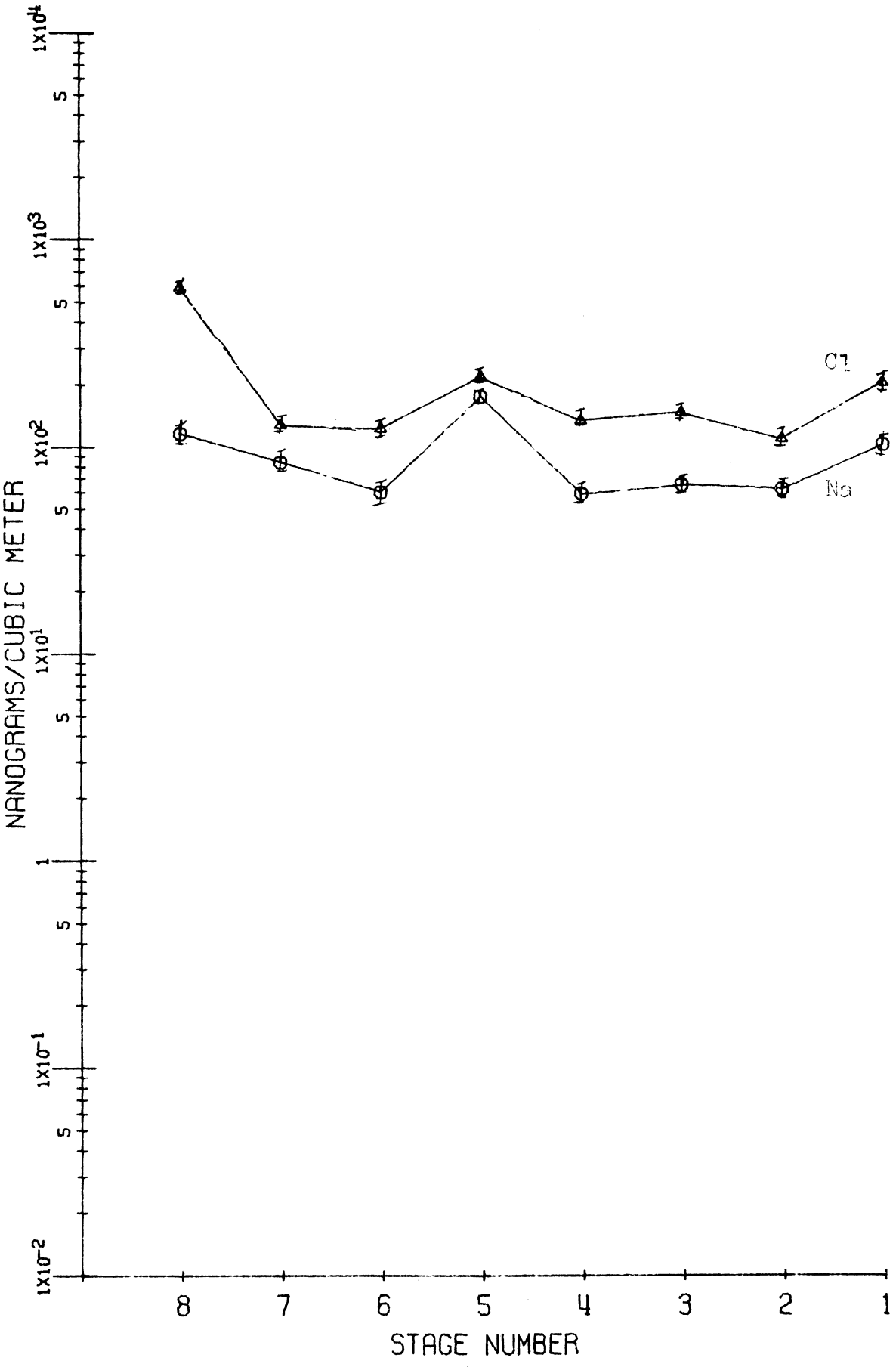

Figure 75. Runs 33 & 35, Gary Airport.

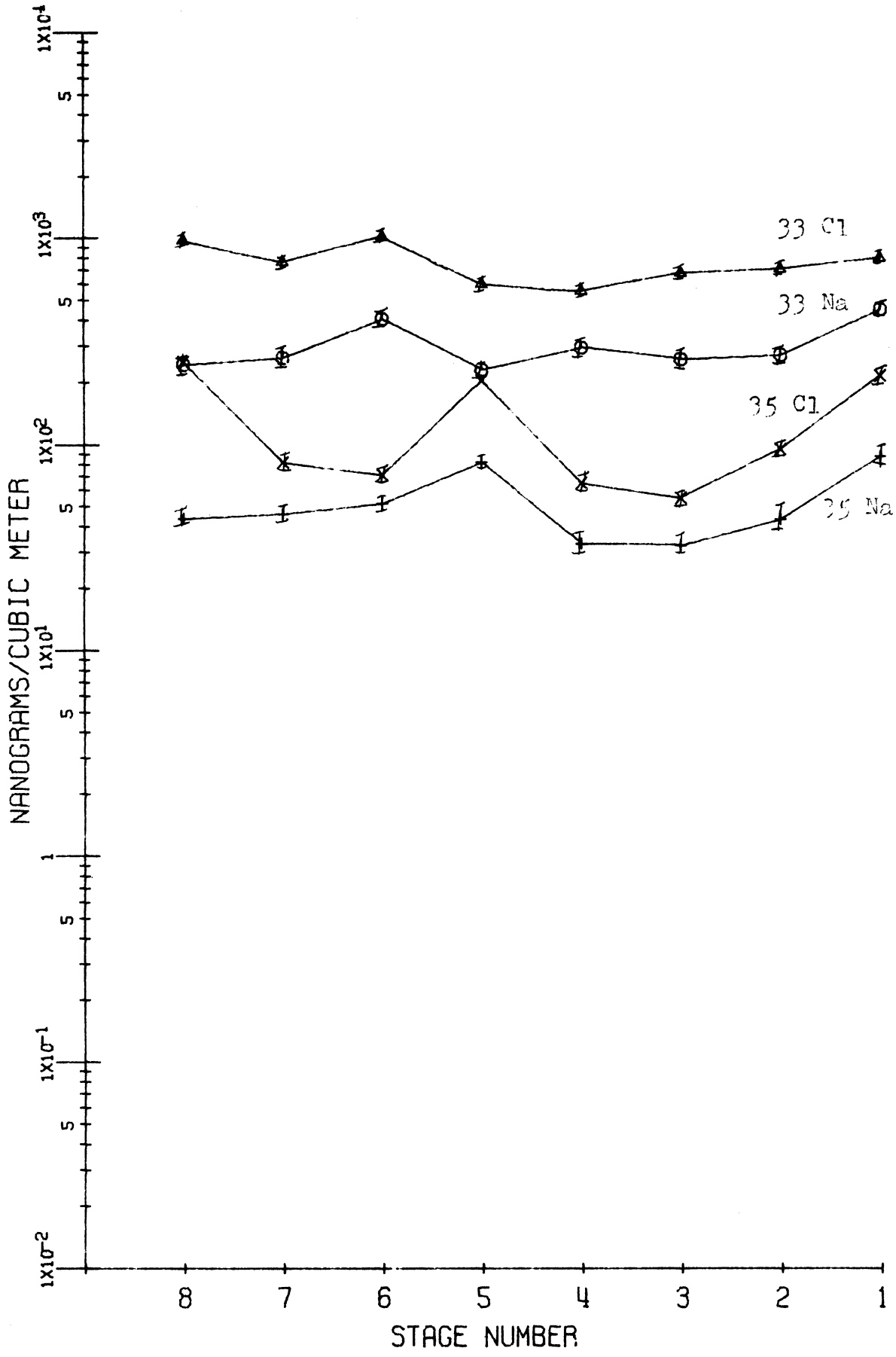

Figure 76. Runs 17 & 18, East Chicago, Central Fire Station.

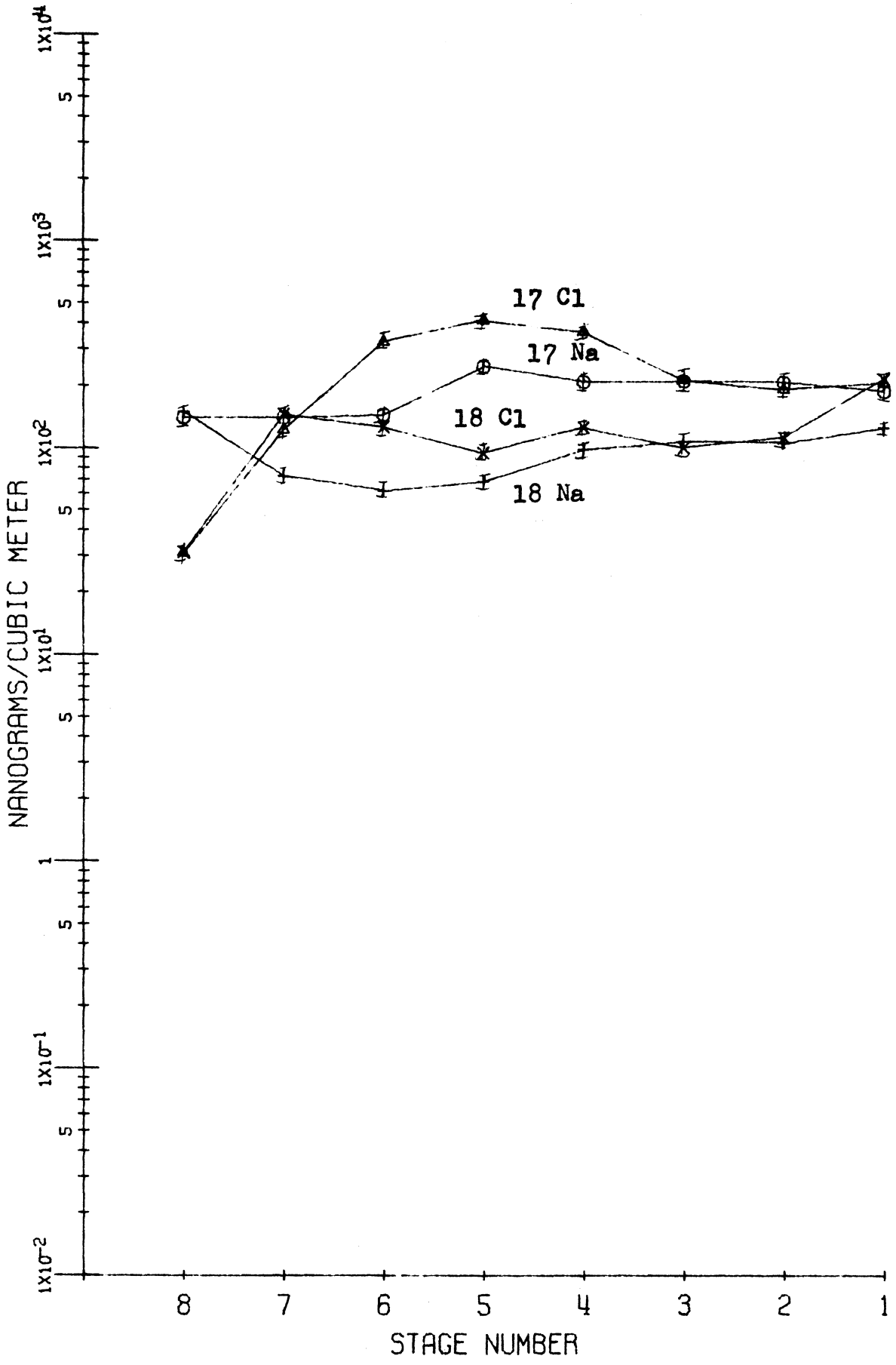

Figure 77. Run 20, East Chicago Markstown Park; and Run 25, East Chicago Field School.

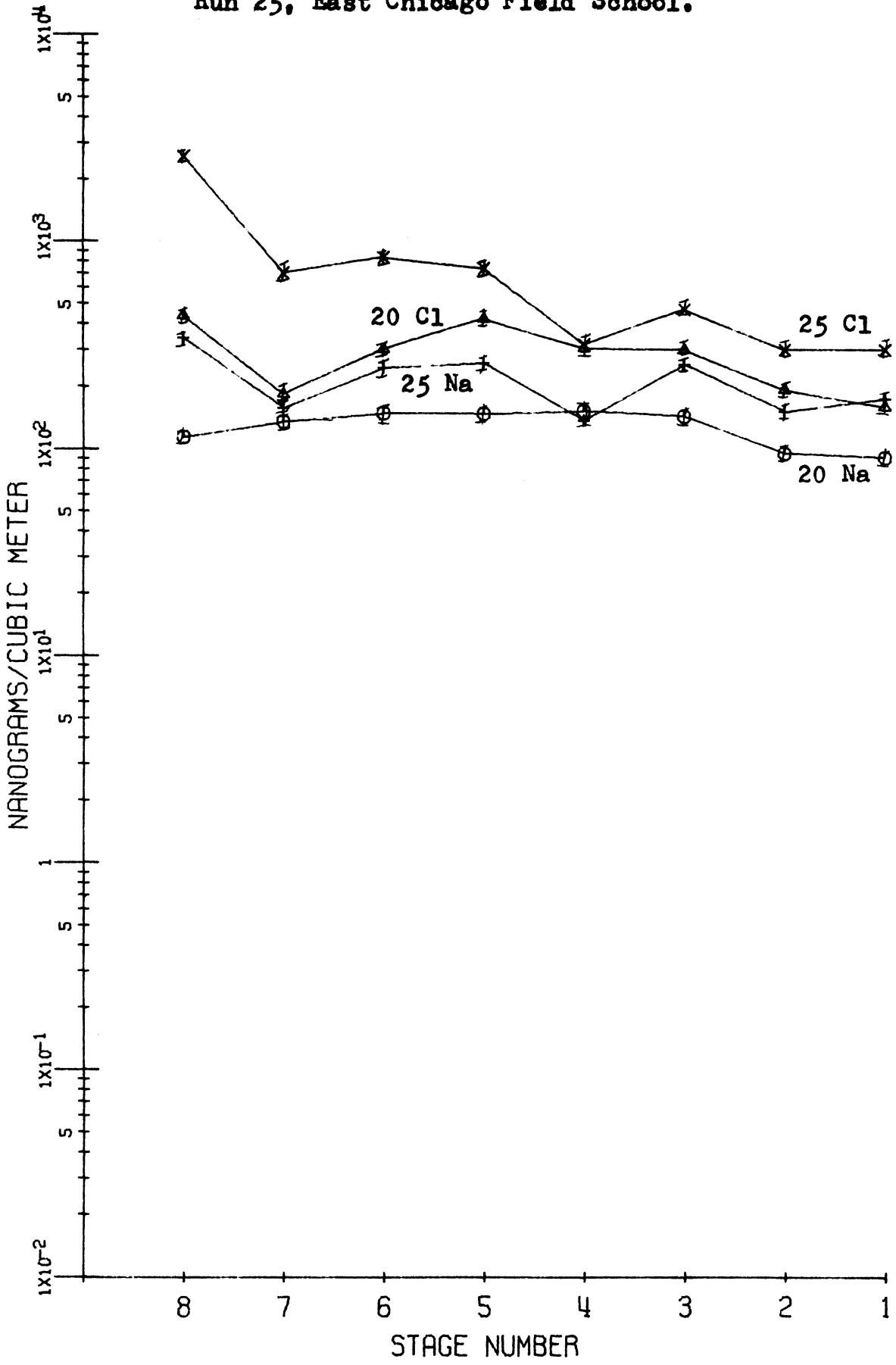

Figure 78. Run 4, Open Hearth Vicinity; and Run 9, Sinter Plant Vicinity.

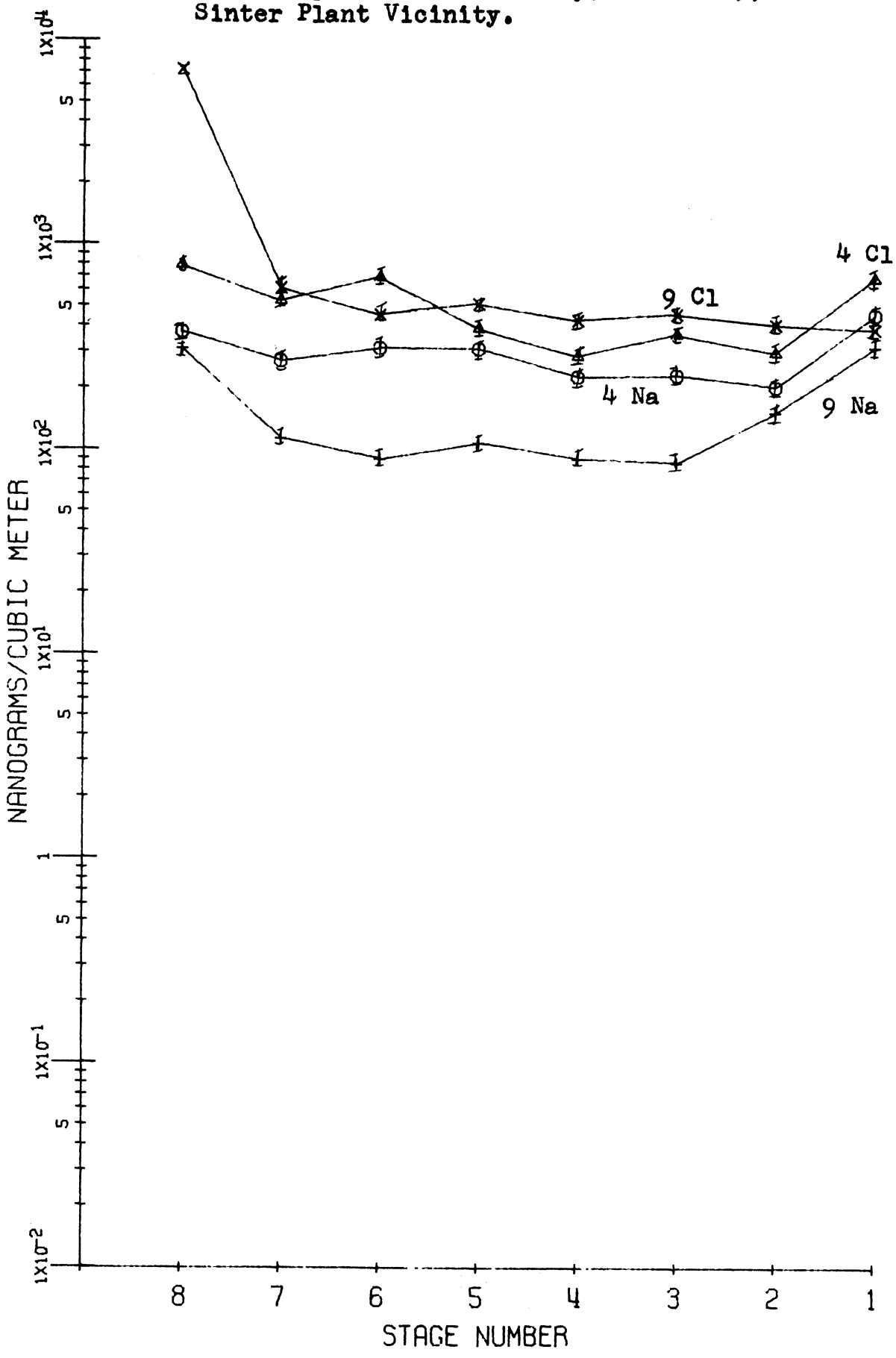

Figure 79. Runs 42 & 44, Lake Michigan.

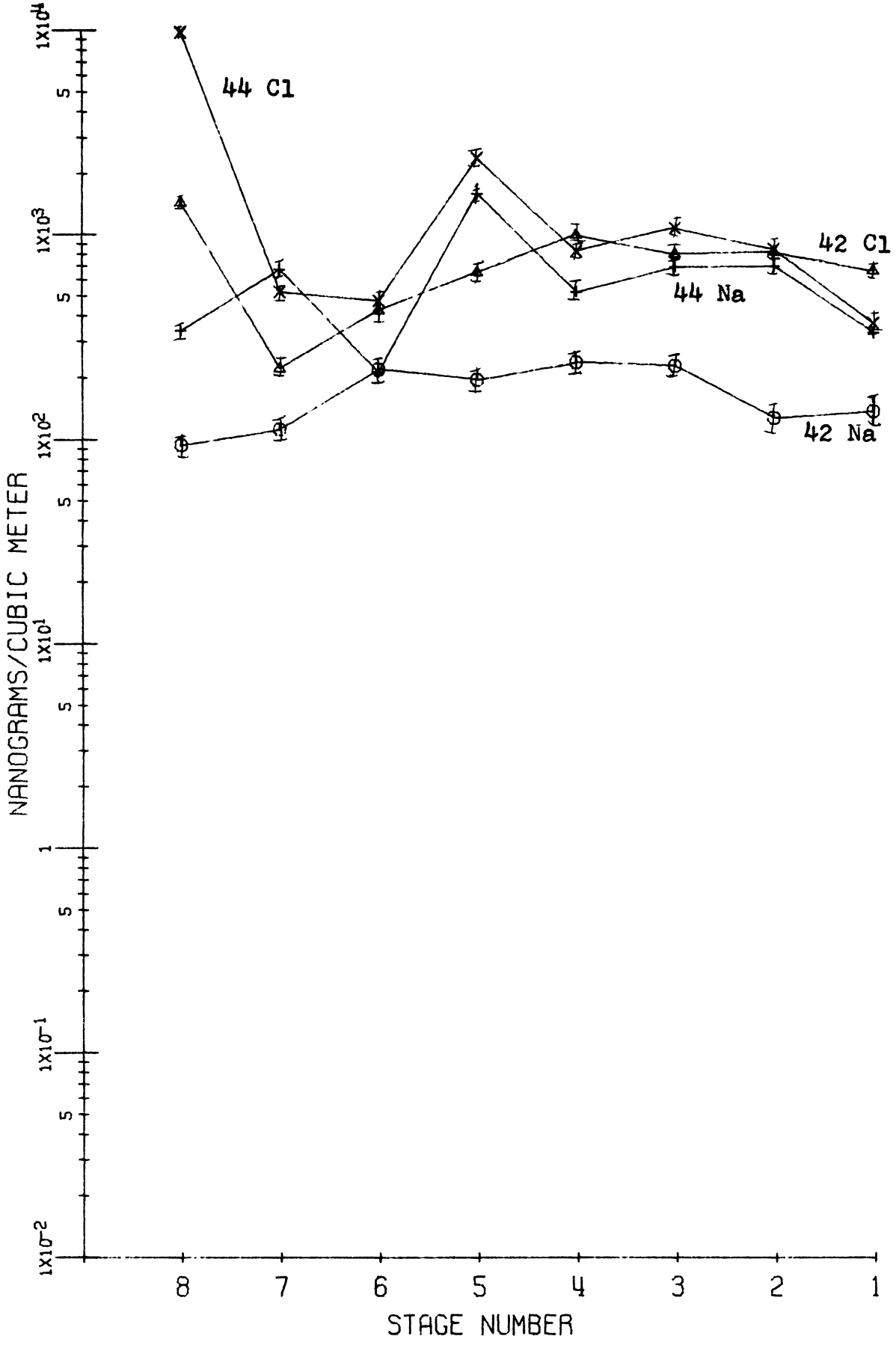

Figure 80. Run 4, Open Hearth Vicinity; Run 7, Sinter Plant Vicinity; Run 27, Gary Wirt School; and Run 30, Gary Airport.

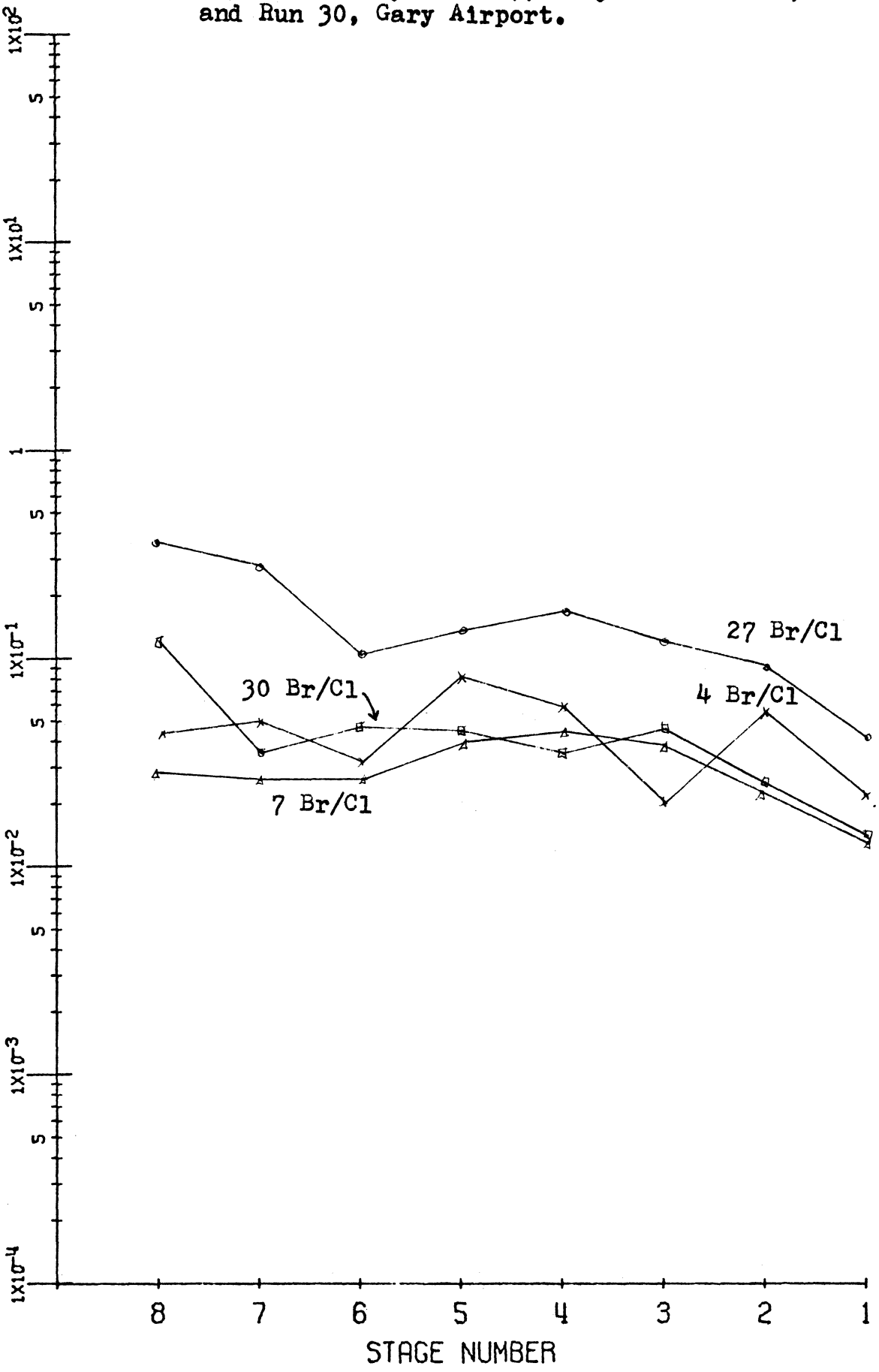

8. Vanadium

Vanadium has been classified by itself due to its having a constant and unique size distribution on nearly all samples. Total concentrations vary more than do the size spectra.

Urban Wirt School in Gary (#27) (Figure 81) shows a typical size distribution for V-containing aerosols. This distribution is nearly uniform over the largest 5 size ranges (stages 1-5), with concentration decreasing in stage 6, but rising to a sharp maximum point at stage 8. Concentrations are several ng/m^3 per size-fraction for larger particle size ranges, dropping to 1 ng/m^3 on stage 6, but rising to 13 ng/m^3 on the filter.

This pattern is essentially repeated on other long samples (#19, 21) from East Chicago, but with higher concentrations per stage (Figure 82).

Similar patterns and magnitudes, but for lower stages 1 and 2 concentrations are found at Markstown (#20, 21), and at Field School (#23-26) (Figure 83).

At Gary Airport results are again similar on runs #31-34, but on run #35 concentrations are lower (Figure 81).

On Lake Michigan, close to the Northwest Indiana shoreline (#43-44), the expected distributions are found, but for run #42, taken much further offshore (Figure 84), patterns and amounts per size-fraction are again similar for stages 1-7, but the sharp filter maximum is absent.

Runs #15-18 in East Chicago, at the fire station, show

lowest levels on run #15, but with a definite filter peak, with winds from commercial areas of East Chicago (Figure 85). Run #17 shows much higher levels overall, and still retains the general curvature of a level distribution on particles at stages 1-4, a decrease to stage 6, and a sharp rise in V concentration on material trapped by the filter. Here winds are from the oil refining industries of East Chicago and Whiting, Indiana. Run #18 shows still higher concentrations per stage, and retains a peak on stage 8, but shows high V on stages 3 and 4. Here winds are from part of the East Chicago chemicals manufacturing complex.

Hence it might be argued that V, used extensively as a catalyst by both types of industries just mentioned, is being emitted by the chemical industry on particles impacting on the mid-size stages of the Andersen. Oil refining operations emit slightly less V, on a more evenly distributed aerosol size range, but with a higher V concentration on smallest particles. Lastly, transportation sources emit V an order of magnitude less in concentration, and essentially on only those particles trapped by the Andersen filter. The even, but lower level, distribution of V on larger sizes in non-manufacturing urban areas is most likely background V. The steel complex does not seem to be a significant source of V.

Figure 81. Run 27, Gary Wirt School; Runs 31-35, Gary Airport.

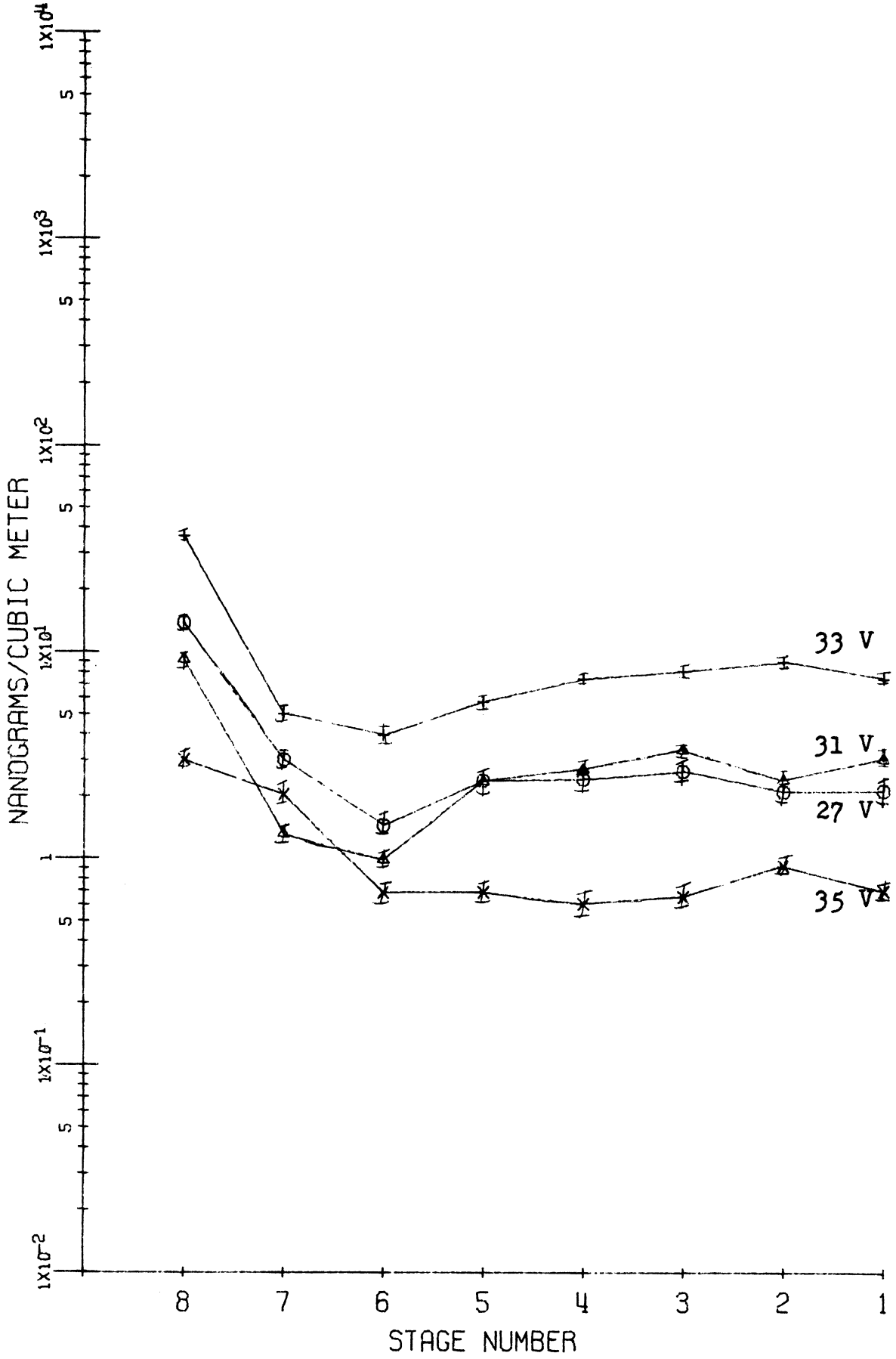

Figure 82. Run 19, East Chicago Central Fire Station; and Run 22, East Chicago Markstown Park.

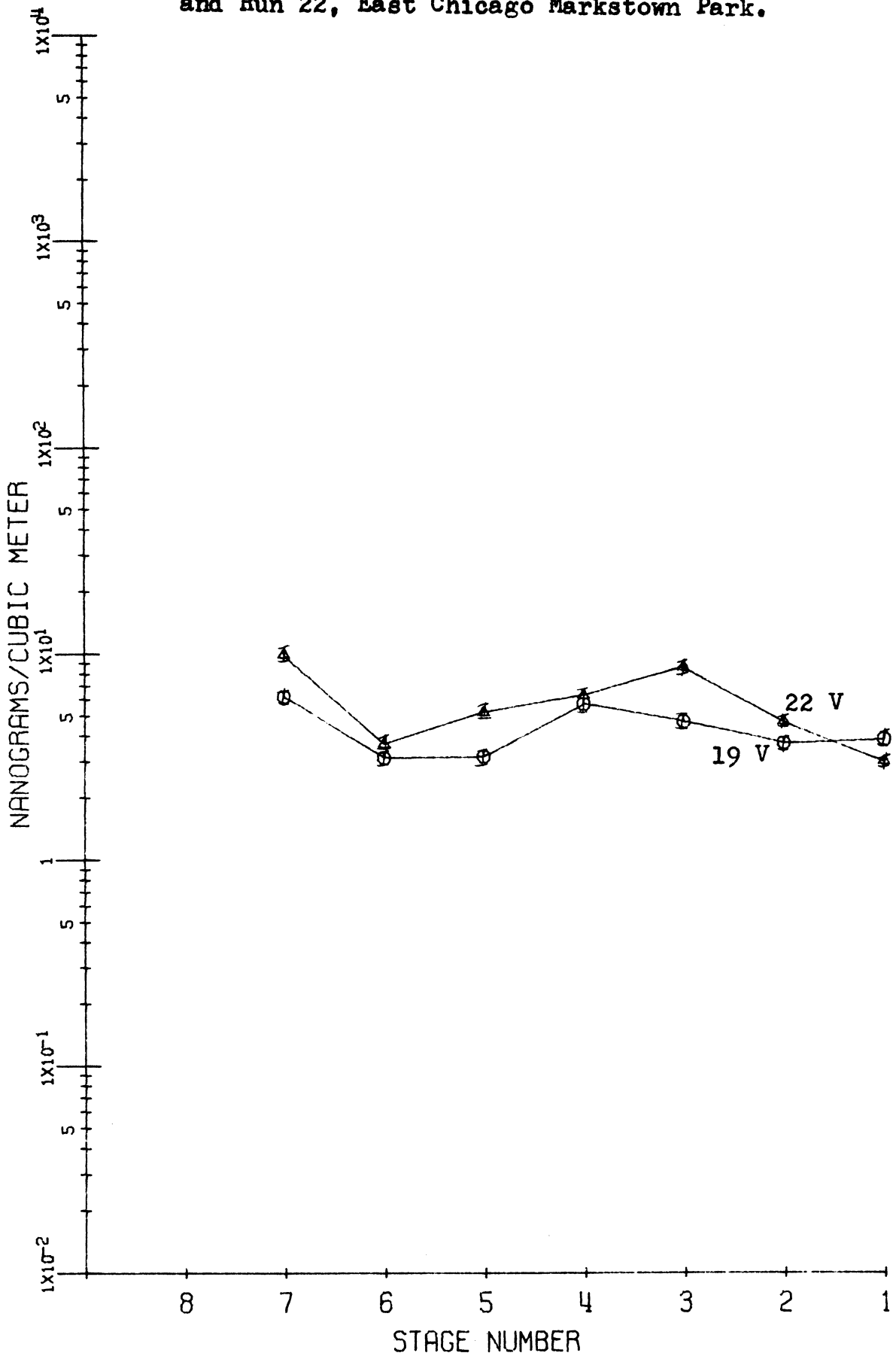

Figure 83. Runs 20 & 21, East Chicago Markstown Park; and Run 23, East Chicago Field School.

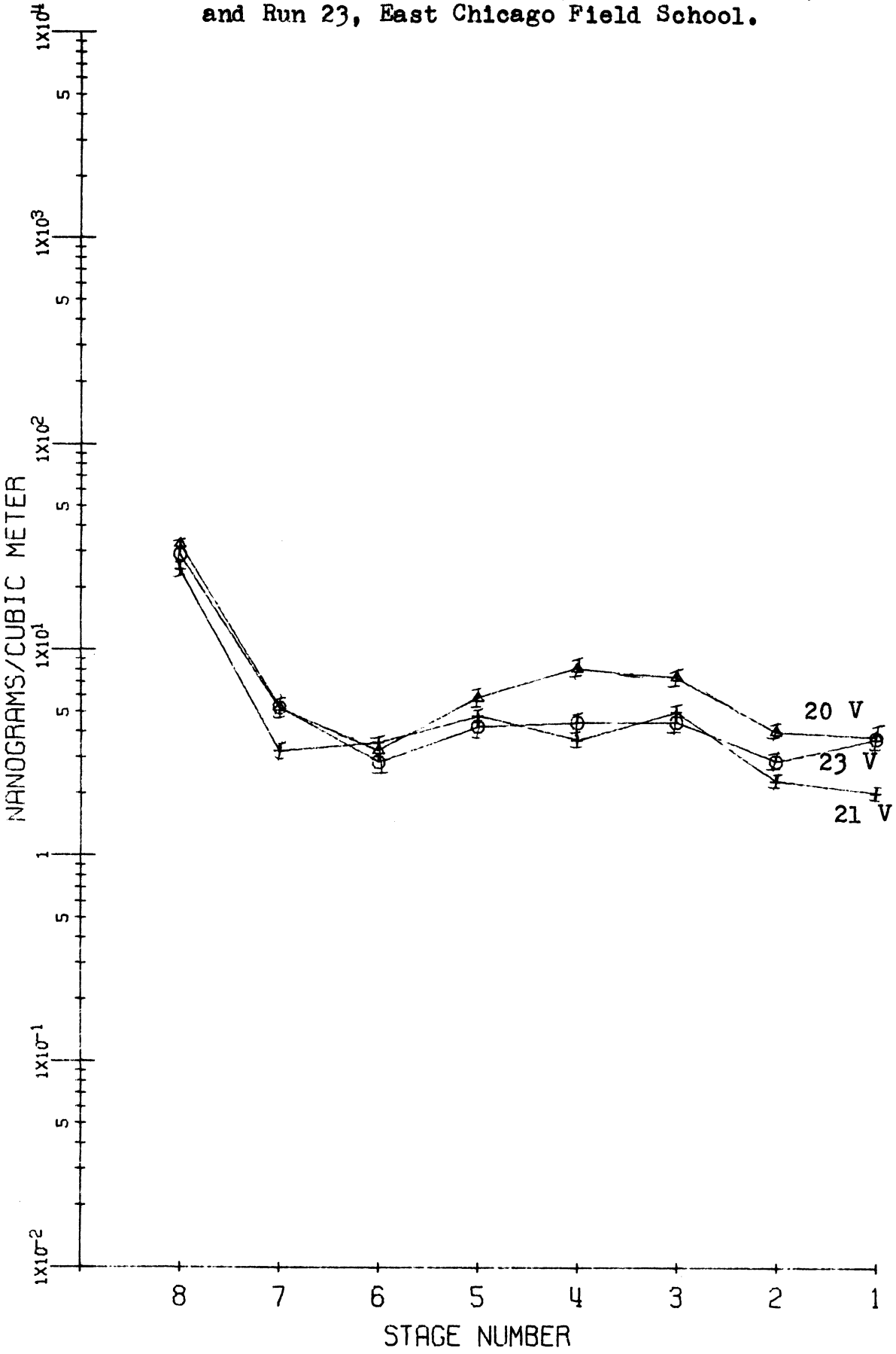

Figure 84. Runs 42 & 44, Lake Michigan

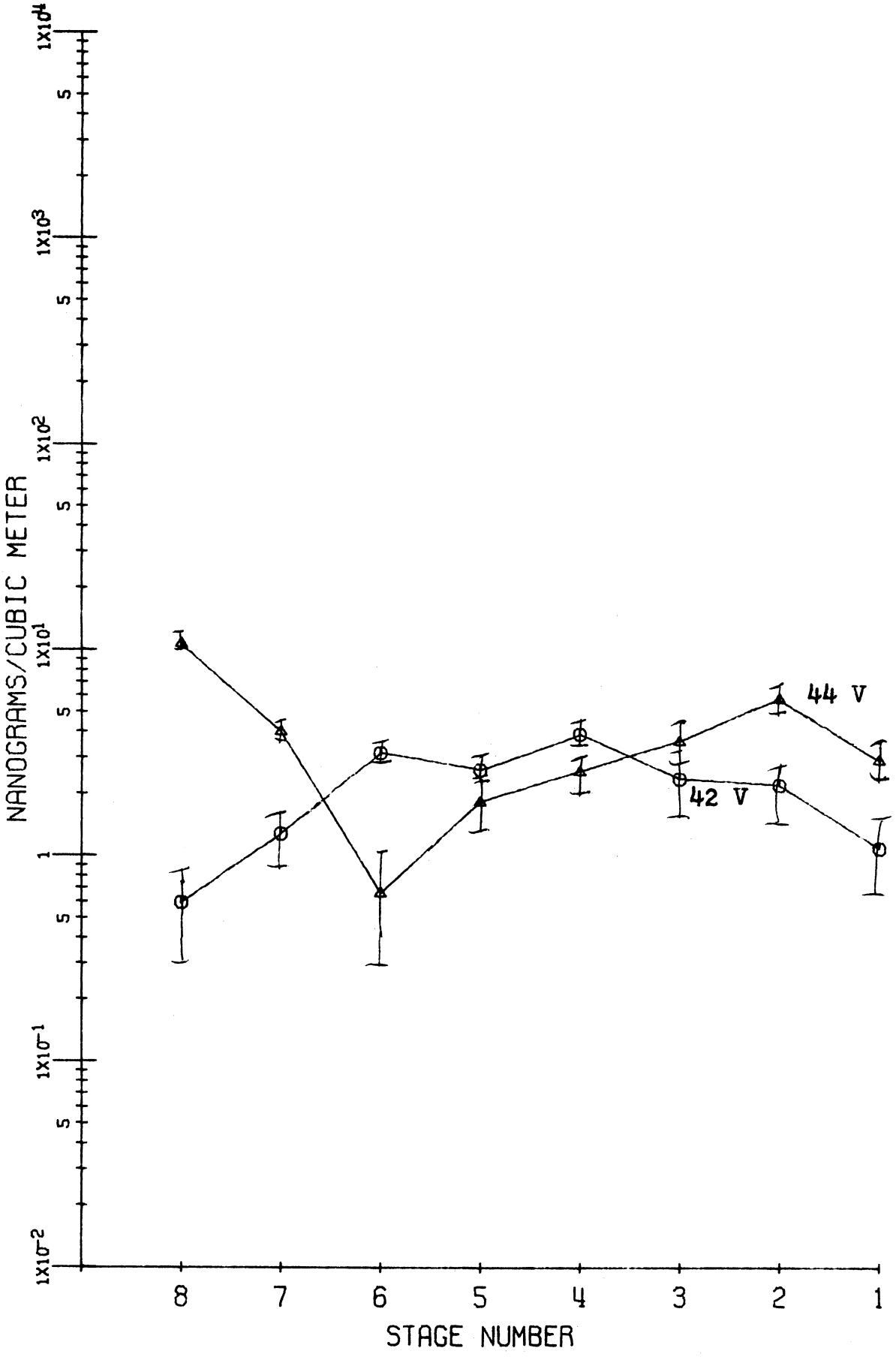

Figure 85. Runs 15, 17 & 18, East Chicago Central Fire Station.

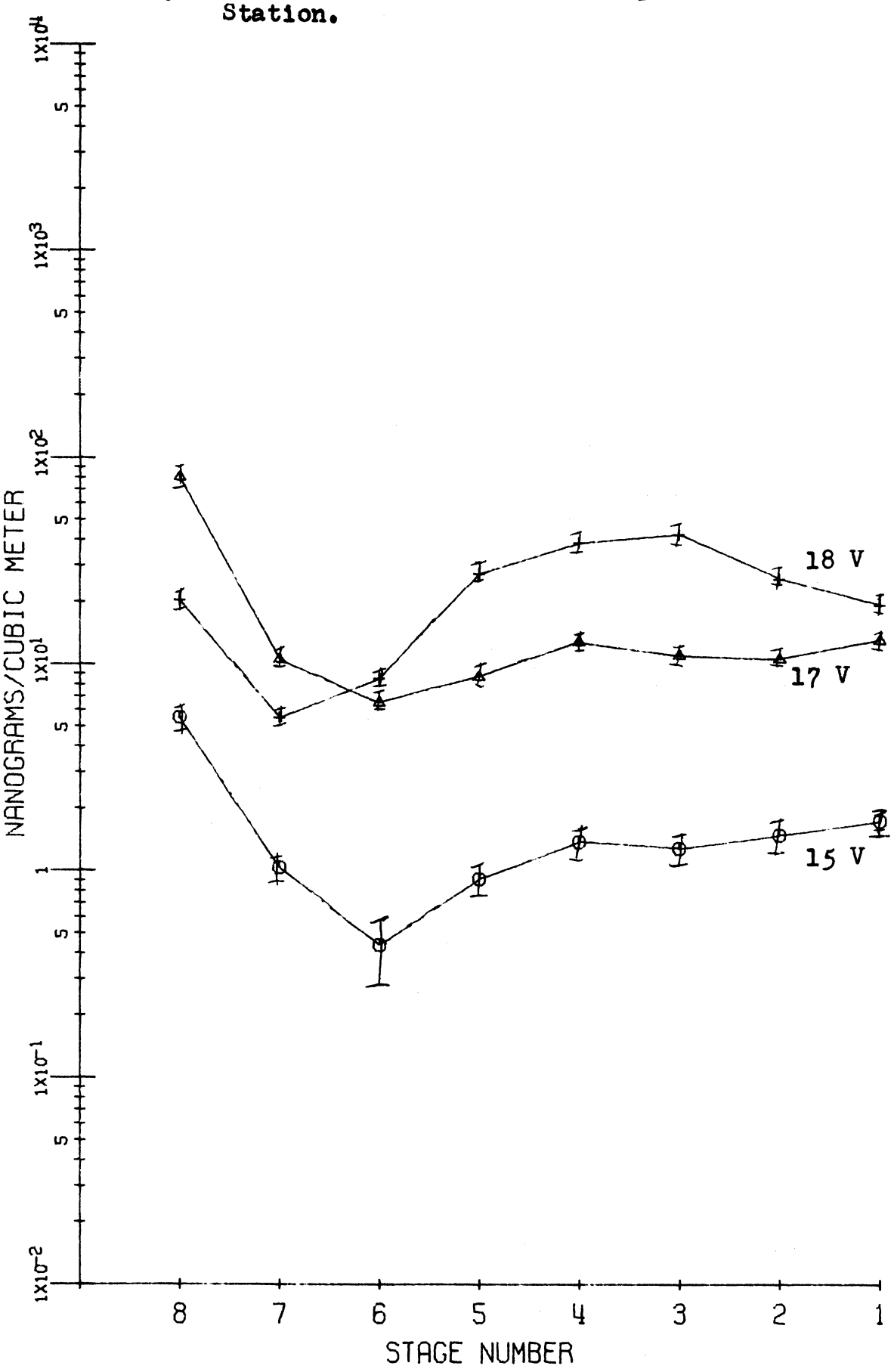

9. Miscellaneous Elements

Data for four other elements identified in this study are included in the Appendix. These are W, Hg, Se and I. But the data are too fragmentary and errors too large to draw definite conclusions as to source processes for these four elements or their behavior when airborne.

One might infer that since W is used as a catalyst by the chemicals industry, and considering the larger chemical complex in Northwest Indiana, this might be a significant W source; perhaps the prevailing size is that aerosol size range associated with the mid-stages of the Andersen. The data are not in conflict with such an argument. Tungsten impurities in Fe ore and steel-tungsten alloy production may also contribute to atmospheric W.

No particular sources of mercury are known. Chemically Hg is related to Zn, and one good sample for Hg size distribution (#19) does show fair size distribution correlation between Zn and Hg (Figure 86).

Selenium has been shown to be related to sulfur, where Se/S is approximately equal to 10^{-4}. Thus electric power production may be the significant source of atmospheric Se. One run (#19) shows a Se distribution not unlike that of Al, a major pollutant from power plant operation (Figure 86).

Concerning I, the data show nothing that may be related to source processes. Iodine may be associated with other halogens in the atmosphere due to chemical properties.

Figure 86. Run 19, East Chicago Central Fire Station.

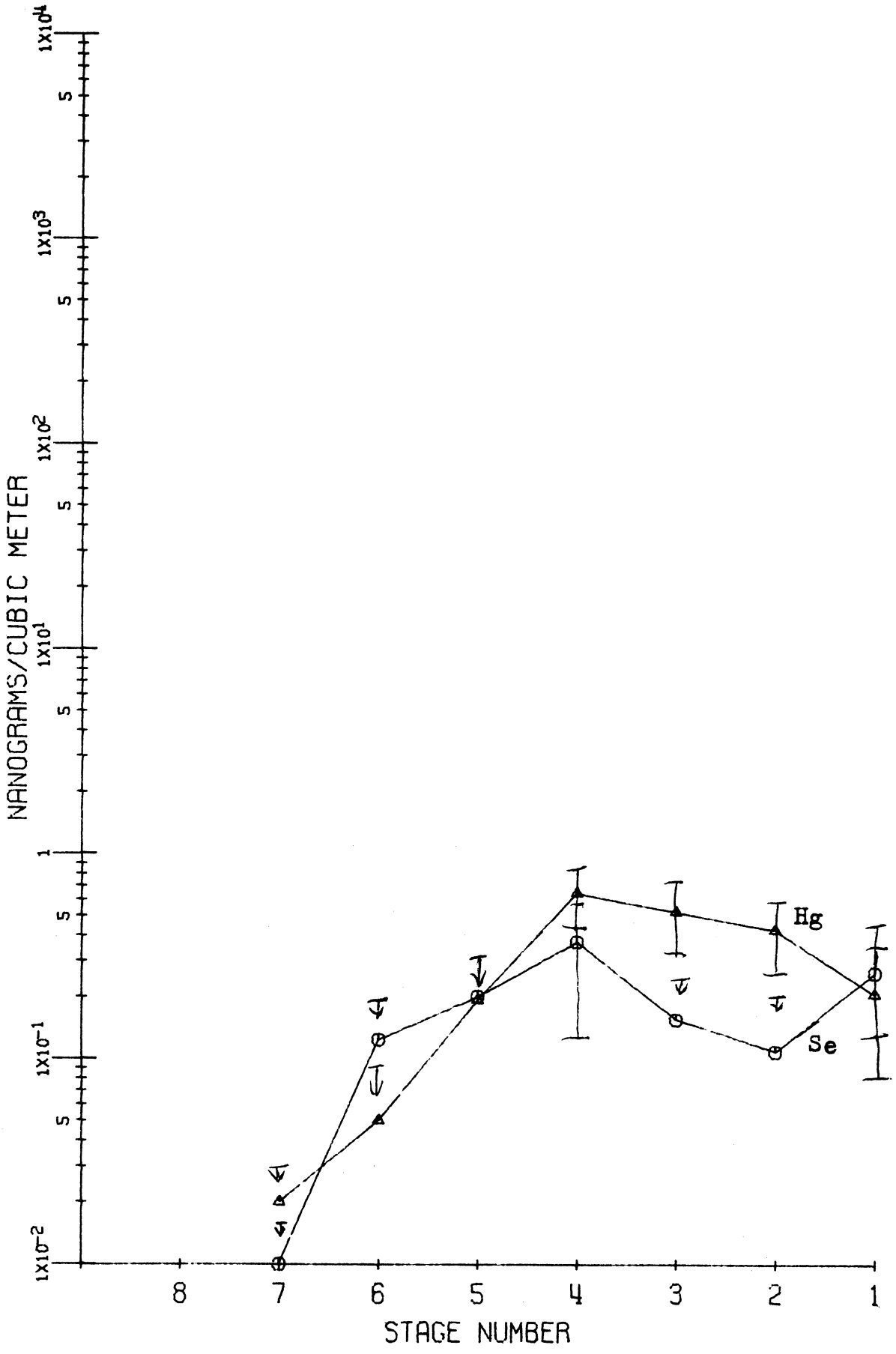

10. Total Aerosol Samples

Sixteen "high volume" air samples were taken during the first week of December, 1969, in conjunction with the samples collected for size-distribution studies during that week. Fourteen of these were collected simultaneously with the size-fraction samples. Only for runs #51 and 52 were sized aerosol samples not taken simultaneously at the same location. Elemental composition of each total aerosol sample was determined by neutron activation analysis and atomic absorption spectrophotometry in the same manner as was elemental composition of each particle size-fraction determined on the samples collected by impactors. The data obtained reinforce well the conclusions reached by examination of the size spectra. Three treatments of the data are presented.

In Table 33 of the Appendix are listed total aerosol concentrations by mass for each of the sixteen samples. The high "suspended" particulate content of the samples taken near steel industry operations, compared with samples taken in the community of East Chicago, is indicative of pollution, particularly by dispersion aerosols, from that operation. Samples from Field School in East Chicago were also high, but this location, on the days of sampling, was downwind of the local steel complex. Of the 16 samples, those from the fire station in East Chicago represent the furthest point from the suspected source, and aerosol levels there are approximately 20% of the levels found within the industry.

A second treatment of the data was to plot average concentrations found during the week for each of the elements against location. Results for 8 representative elements are shown in Figures 87-94. These comparisons especially point out the degree by which the steel industry is responsible for certain pollution elements, but not responsible for others. Iron is emitted by open hearth and sinter plant operations, but sintering emissions are especially rich in Mn. Copper is more strongly associated with the open hearth shop than with the sinter plant; the same is true for Zn, but to a less noticeable extent. The steel complex is only one of several sources of Al. Oil refining operations, which surround the East Chicago Fire Station, account for most V pollution. The data for K and Cl suggest that steel operations are not generally a major source.

A third treatment of the total aerosol composition data involved the calculation of the mass of each element as a per cent of total mass. Total aerosol mass was determined for each sample gravimetrically. Results from each location were averaged, and are presented in Table 10. Consider samples taken close to the steel industry (open hearth and sinter plant) and those taken downwind (fire station and Field School). For those elements emitted as dispersion aerosols from steel operations, the percentage should drop downwind as the larger particles more quickly settle out of the atmosphere. That they do is supported by the trend of data for Fe and Mn. But for condensation elements from the

TABLE 10

AVERAGE MASS OF ELEMENTS AS PER CENT OF TOTAL AEROSOL MASS

	Open Hearth	Sinter Plant	Fire Station	Marks-town	Field School
Fe	4.8	3.1	2.6	2.9	2.7
Mn	.21	.35	.15	.13	.15
Cr	.03	.02	.03	.02	.03
Co	.0007	.0002	.002	.002	.001
Sc	.0005	.001	.001	.0005	.001
Th	.0003	.0002	.0001	.0005	.0003
Cu	.05	.02	.05	.09	.03
Zn	.55	.37	.76	.38	1.4
Sb	.006	.004	.03	.01	.02
As	.005	.004	.01	.007	.01
Ca	2.7	6.2	2.9	1.3	2.8
Mg	1.2	2.1	1.3	0.9	1.2
Al	1.03	.43	1.27	0.83	.51
La	.001	.0002	.007	.006	.002
Sm	.0001	.00003	.0005	.0002	.0002
Ce	.001	.001	.006	.005	.005
Na	.35	.14	.71	.52	.46
Cl	.6	.6	2.7	1.2	2.5
K	.35	.45	.7	.25	.55
Br	.02	.025	.21	.14	.14
V	.005	.005	.08	.04	.02
Hg	.003	.002	.003	.005	.003

same industry, percentages should rise as the larger particles are removed. This interpretation is consistent with the data for Zn, Sb, and As. For elements not associated with steel processing, percentage should rise, as large "steel source" particles fall out. This is shown well by V and Br, as the source of V pollution is indicated well by the high V content of aerosols from the oil refining area (fire station). For elements having multiple sources, the situation is less clear. Aluminum appears more randomly distributed in space, as are K and Cl.

C. PROPERTIES AND USES OF ELEMENTS

The groupings outlined on previous pages may now be related to possible natural groupings, based purely on chemical and physical properties, and to groupings based on major uses of each element. It is found that many groups or parts of groups based on size spectra do agree with groups arising from ordering the elements by chemical properties as suggested by the Periodic Table. Many exceptions occur, but these seem to be associated with a major-use classification of the elements, as may be seen in Table 11. Hence it appears that the source process largely determines the size distribution found for a given element. But, in addition to physical processes such as particle fallout and adsorption, chemical properties may play an indirect role in particle size determination. This arises from a consideration of common salts and/or oxides that may be expected for compounds for the elements. A few common compounds

TABLE 11

CLASSIFICATION OF ELEMENTS BY SIZE, CHEMICAL PROPERTIES, AND USES

Size Distribution	Chemical Properties	Use Categories
1) Fe, Mn, Cr, Co, Se, Th	1) Fe, Co	Metals) Fe, Mn, Cr, Co, Zn, In, Sb, As, Cu, Mg, Ti, Al, Ga, Na, Cl
2) Zn, In, Sb, As, (Hg)	2) Mn, ¦ Br, Cl	
3) Cu	3) Cr	Chemicals) Na, K, V
4) Ca, Mg, Ti	4) V ¦ Sb, As	Power Production) Al
5) Al, Rare Earths (Se)	5) Ti, Th	Cement) Ca, Mg
6) Br, Ga, K	6) Sc, Rare Earths¦ Al, Ga, In	Transportation) Br, Cl
7) Na, Cl	7) Mg, Ca ¦ Zn, Hg	Natural Pollutants) Al, Rare Earths, Na, Cl, Ca, Mg, Ti
8) V	8) Na, K ¦ Cu	

are listed in Table 12 (Handbook of Chemistry and Physics, 1956).

It is obvious from Table 12 that halide and sulfate salts of the elements are more soluble in water and have lower melting points than do the oxides. Because of the solute effect (discussed in Chapter I), small particles of soluble salt may grow to larger sizes more rapidly than would small particles of oxides. Hence these salts, especially the alkali metal halides, and involving Na, K, Cl, and Br, should more quickly approach a "Junge distribution." This is well shown by the data.

Melting points should also be examined. The salts generally melt at much lower temperatures than do the oxides. Therefore, from a high temperature source, condensation aerosols are more likely to result for low melting point materials than for high, and condensation aerosols should more readily approach a "Junge distribution" than should dispersion aerosols. The data indicate that Na, K, Cl, Br, and perhaps V, probably present as salts, readily approach the theoretical "Junge mass distribution;" Cu, Zn, Sb, and As do so more slowly; and Fe, Mn, Cr, Al, Ca, and Mg, probably present as oxides, do so to only a slight degree.

D. ATMOSPHERIC RESIDENCE TIMES

One may now consider the estimated residence times in the atmosphere for selected pollutants. Rainfall occurs in the Midwest about 3-4% of the time. For a constant source

TABLE 12

MELTING POINTS AND SOLUBILITIES IN WATER
FOR COMMON COMPOUNDS

Compound	Melting Point (°C)	Solubility in Water (g/100 ml)
Fe_2O_3	1565	i.
$FeCl_3$	282	74
MnO_2	535	i.
ZnO	> 1800	i.
$ZnCl_2$	262	432
CuO	d.	i.
$CuSO_4$	200	14
CaO	2580	< 1
$CaCl_2$	772	60
Al_2O_3	2050	i.
KCl	776	35
NaCl	801	36
KBr	730	53
NaBr	755	80
V_2O_5	690	< 1

of pollution, therefore, dry sedimentation and impaction may be the major avenues of aerosol removal for the larger particle sizes, 5-10 μm and greater in diameter, even though soluble particles of this size may act as condensation nuclei. Much of this larger-sized material falls within the source region. A smaller percentage of those aerosols less than about 5 μm emitted within the source region also pollutes the same area. Much of this material remains airborne for at least hours, is transported away from the immediate area, and may be activated as cloud-droplet nuclei because of its longer residence time. But consider the particle size range of an aerosol from a major source process. For example, Fe from steel mill sintering operations has a mass median diameter of at least 10 μm. As shown in Chapter I, for a particle of diameter greater than 10 μm, sedimentation is important, where fall velocity (V_s) > 1 cm/sec. Hence a particle originally at 100 m would fall to the ground in about 10,000 seconds, or less than 3 hours. For a wind speed of 5 MPH, probably most particles would impact on the ground within 15 miles of the point of origin. That Fe particulates emitted by a sinter plant do fall out actually much closer than 15 miles to the point of origin appears obvious from the results previously discussed. Hence other fallout mechanisms (turbulence) must operate. A particle 1 μm in diameter has a sedimentation velocity of about 0.01 cm/sec, for a residence time on the order of 300 hours. For a 5 MPH wind, this means a particle could

remain airborne for a range of 1500 miles or more if no other removal mechanisms were in operation. Decreases in concentrations of particles 1-10 μm in diameter are significant even a few miles from a source process, as shown by the data of Chapter IV. The deposition rate, based on observed decreases in concentration, of smaller particles ($d < 10$ μm) is greater than that predicted by sedimentation theory. Stokes' Law is not valid for these smaller particles, where $V_s < 1$ cm/sec. Although deposition rate is proportional to the immediate ground level concentration, dry deposition velocity (V_d) ranges over an order of magnitude and is largely dependent on surface roughness. Thus V_d exceeds V_s for smaller particles.

$$W = V_d \cdot X,$$

where W = amount removed per unit time per unit area,

V_d = deposition velocity,

X = ground level concentration of aerosol.

The Harwell experiments (discussed by Slade, 1968) show that iodine-131 vapor, adsorbed on condensation nuclei too small to have an appreciable gravitational settling velocity, deposit on surfaces due to turbulent impaction, electrostatic, and chemical forces with an average V_d of approximately 2 cm/sec. Other studies (Slade, 1968) show V_d to be much greater under strong lapse conditions than under inversion conditions. Hence the relatively fast dry removal of smaller particles noted in this work, which

cannot be explained by sedimentation alone, does confirm the existence of other dry removal processes, such as turbulent impaction, acting on the aerosol. It appears that elements associated with the largest particles ($d > 10$ μm) emitted in Northwest Indiana tend to fall out in the same general area. But those on smaller particles pollute both the immediate source vicinity and areas further away. This latter class includes, certainly, much Zn and Cu.

Winchester and Nifong (1969) have attempted to predict the extent of pollution of Lake Michigan by aerosol fallout for several elements, and for Cu and Zn the atmospheric contribution may be comparable to that from streams flowing into the lake. Assuming the major source of both elements to be the Chicago area steel complex, and emission heights to be 100 meters, calculated times for settling, according to the Stokes formula, for two sources within the industry for Cu and Zn are tabulated in Table 13.

TABLE 13

ELEMENTAL SETTLING TIMES

Open Hearth	MMD, μm	Settling Time, hrs.
Cu	≈ .75	≈ 300
Zn	≈ .75	≈ 300
Sinter Plant		
Cu	≈ 1-1.5	≈ 200
Zn	> 5	< 10

Due to atmospheric turbulence, surface roughness, and sources closer to the ground, true times for settling may be much shorter than the above table indicates. It does imply, however, that much atmospheric particulate matter, especially that distributed on larger sizes, with certain prevailing wind speeds and directions, finds its way into Lake Michigan by a fallout route.

E. TRACERS

An area of great interest in air pollution studies is the use of tracers to identify a particular source or source process. Hashimoto and Winchester (1967) have investigated the Se/S ratio ($\approx 10^{-4}$) and possible use of Se as an index of S pollution. A knowledge of both concentration and size distribution of certain elements in aerosols, as learned from this project, may enable the investigator to select natural tracers for certain pollution processes.

Mass measurement of a single element associated with an aerosol, even with a knowledge of size distribution, seldom enables the use of that element as a natural tracer. Lead may indicate the combustion of leaded motor fuel, and serve as an index of pollution by transportation sources, and vanadium may be a tracer for emissions from oil refining operations, but generally concentrations of single elements in the atmosphere reveal little about specific source processes producing those elements. A single element may come from several types of sources, and therefore, is

at best an ambiguous tracer. Size and concentration of a single element may be indicative of a specific source process if the air is sampled close to a suspected source. In the data presented, for example, Mn located on large particles ($d > 10$ μm) indicates sinter plant emissions from the steel industry. But further downwind, after removal of these large particles, background Mn found reveals nothing regarding its sources. Thus such use of single-element measurements is quite limited.

But clusters of elements found within a small source region may serve as a tracer if size-distribution ratios and absolute concentrations are determined near to and progressively further from a potential source. East Chicago appears to be such a source region.

Several individual elements may not be components of the same particles, but of different particles, with different removal efficiencies while airborne. Such elements would not be useful as tracers, since different particles usually arise from a variety of sources. If, on the other hand, two or more elements are found having the same size distribution patterns, this would indicate these elements were located on the same particles, and were from the same source process. A spectrum of element-to-element ratios by size-fraction would be a constant, and these elements would tend to have the same removal efficiencies while in transit from their source. Then ratios determined for these elements at locations further from the source would again be

uniform. Such ratios may serve as a very good tracer technique.

The elements were earlier classified into eight groups in this chapter, based on similarities in size distribution spectra found near large source processes in East Chicago, in the belief that such similarities indicated common origin. The degree to which such similarities persist in samples taken further from the suspected source area is an indication of what portion of those elements found at the latter location arose from the specified source. The data suggest that the distribution of antimony-to-zinc ratios is a useful tracer. In Figure 95 are plotted ratios of Sb-to-Zn from a suspected source, open hearth steel operations, from nearby at the East Chicago Fire Station, and from Wirt School in Gary, several miles from East Chicago. Note the constant spectra found for ratios from the first two samples, and the deviation from these found in the last. It is concluded that Zn and Sb in East Chicago air come primarily from open hearth steel making, but that only a small part of Zn and Sb found in Gary is due to the same source process.

Similar examination of manganese-to-iron ratios at the same three locations, and at iron ore sintering operations, shows both these elements are emitted from the two steel industry operations, that most Fe and Mn in East Chicago air is from these sources, and that most of these elements in Gary is also from such operations. Magnitudes of

concentrations indicate sinter production to be the prime source. These ratio distributions are shown in Figure 96.

Sodium and chloride present a situation where, due to the presence of NaCl salt, uniform ratio distributions are extremely prevalent, and do not isolate source processes. But, near suspected sources, departures from Cl/Na = 1.5 indicate pollution processes. In Figure 97, small particle Cl from open hearth facilities and large particle Na from sintering processes are demonstrated. Nearby, at East Chicago Field School, the same trend is shown, but in Gary, at the airport, a 1.5 ratio for Cl/Na is quite uniform over all particle sizes.

It can be concluded that in a few cases comparisons of size distributions of concentrations of a single element may be useful as a tracer technique, but a more powerful concept lies in comparing size distributions of <u>ratios</u> of elemental concentrations. This latter field deserves much consideration in future work of this nature.

Caption to Figures 87-94. Elemental concentrations, averaged, on total aerosol samples taken December 1-5, 1969, East Chicago, Indiana. Sample locations as shown in Figure 1 and described in Chapter II; winds SW-N, as shown in Table 15.

Figure 87. Iron, total aerosol averages.

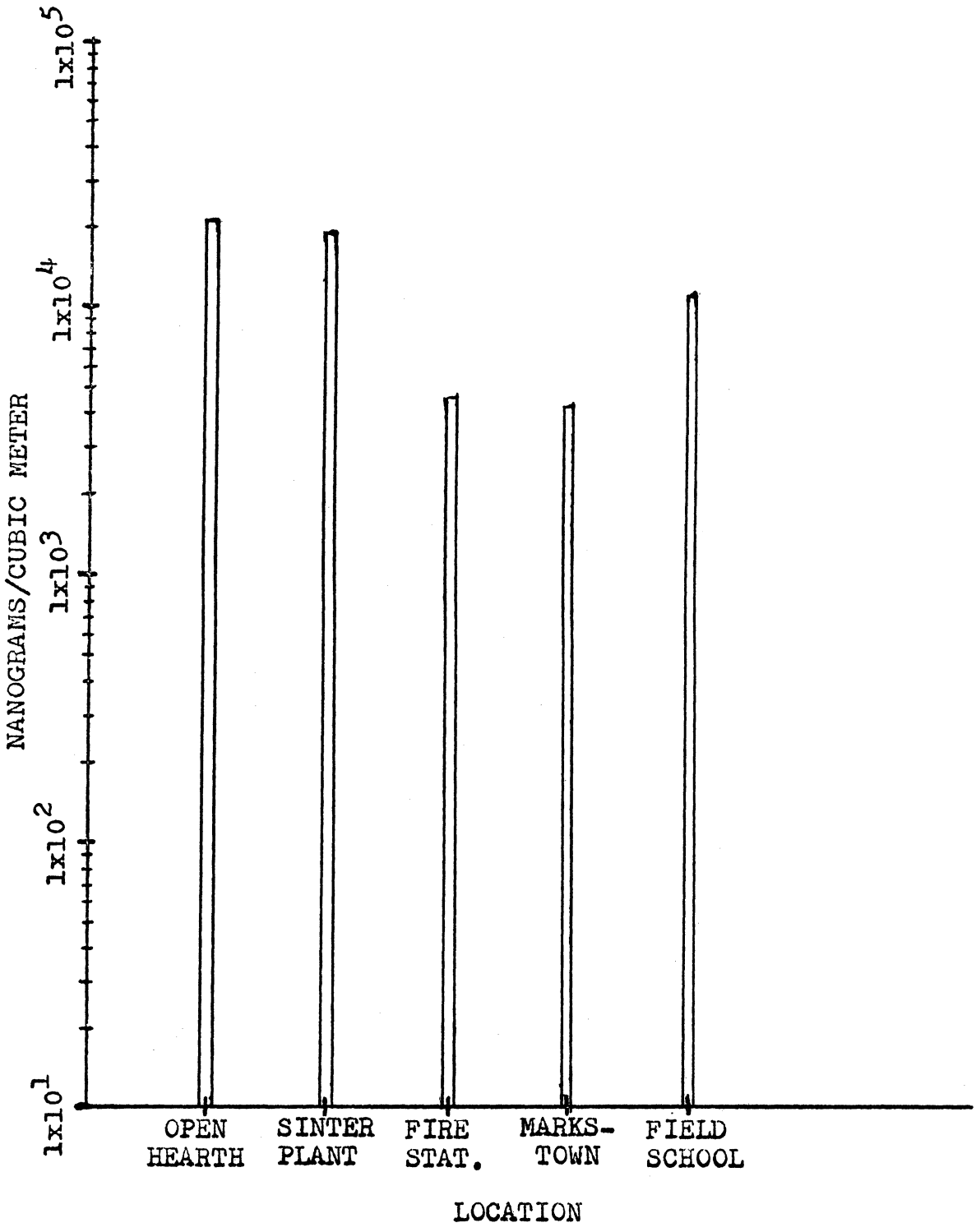

Figure 88. Manganese, total aerosol averages.

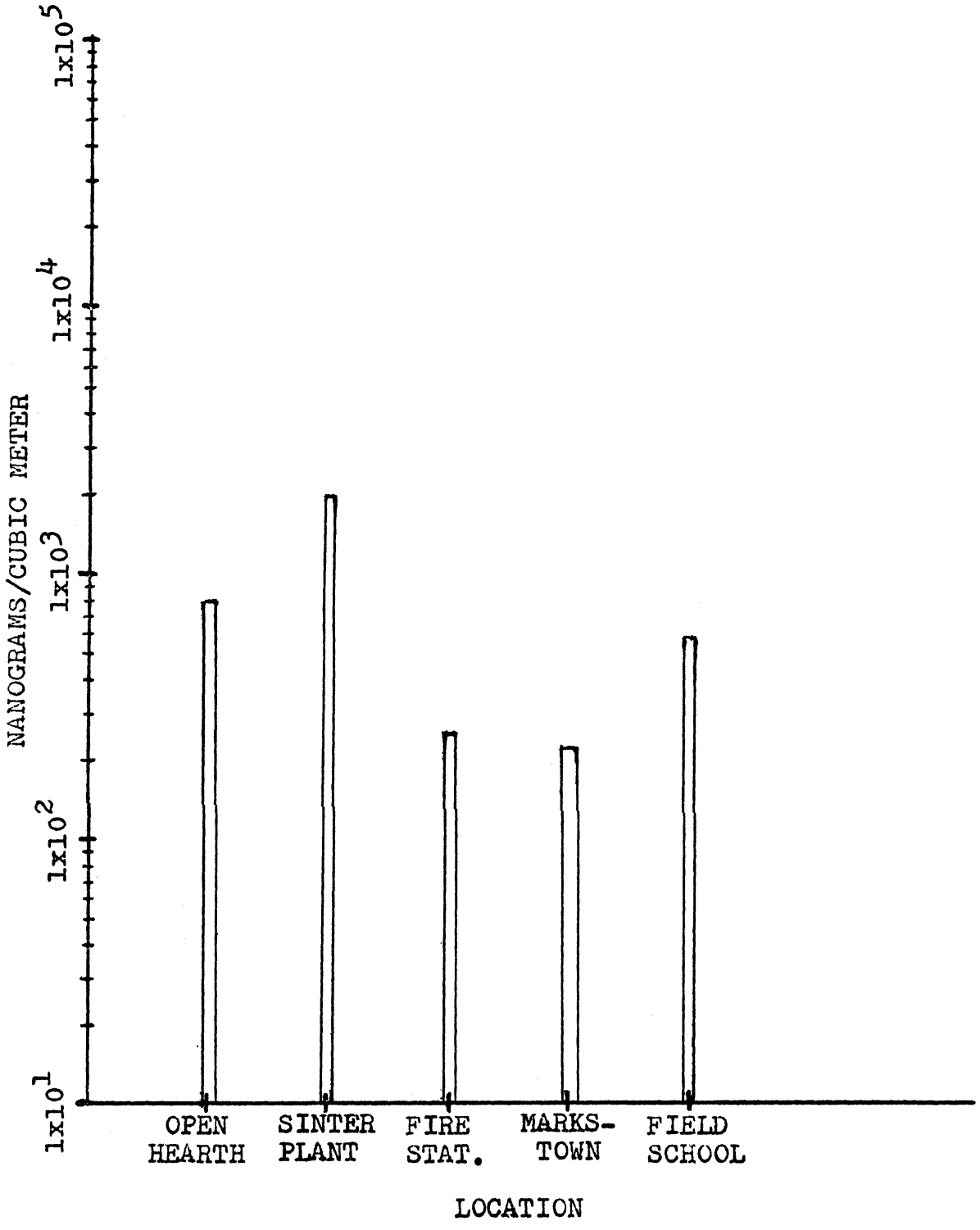

Figure 89. Copper, total aerosol averages.

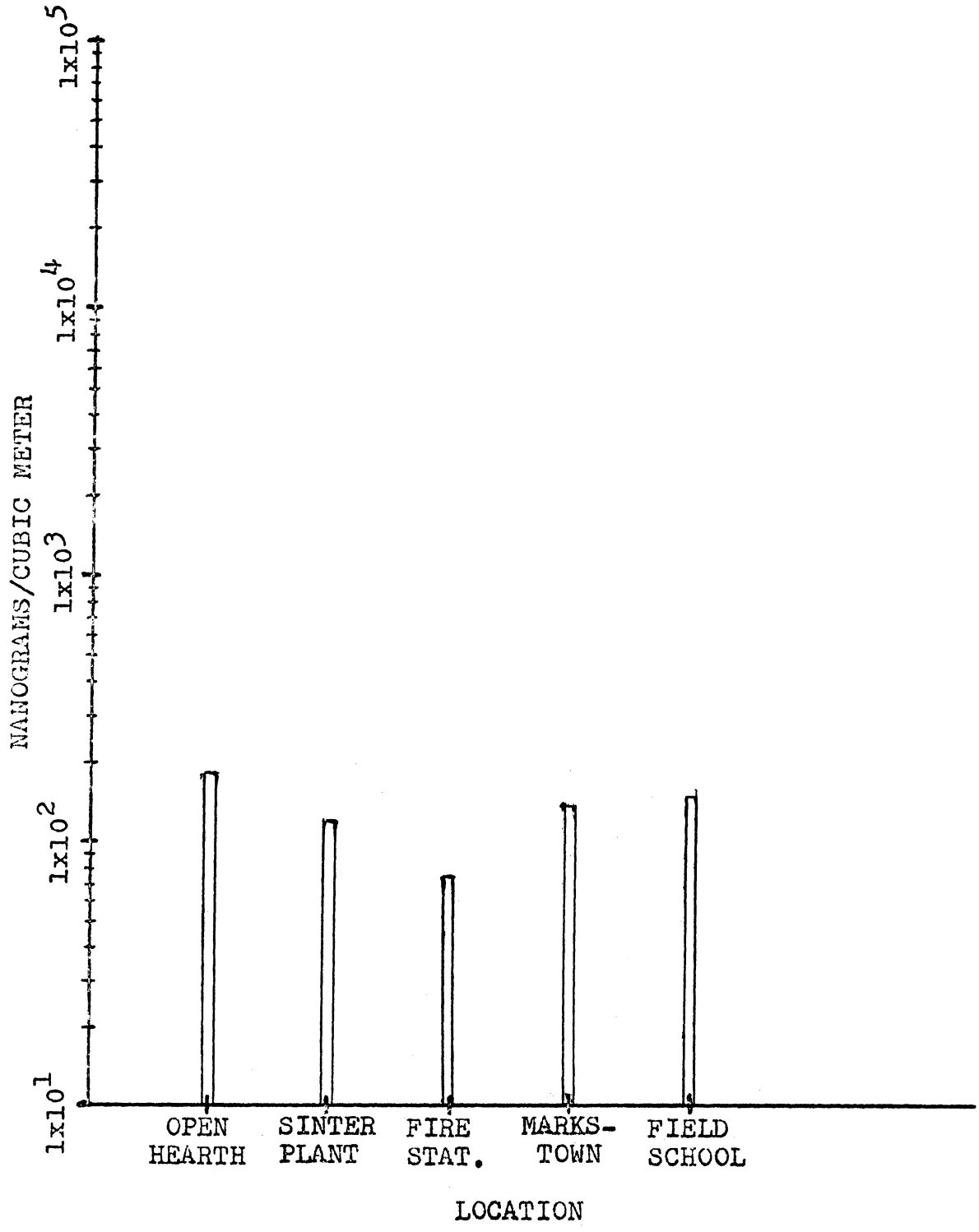

Figure 90. Zinc, total aerosol averages.

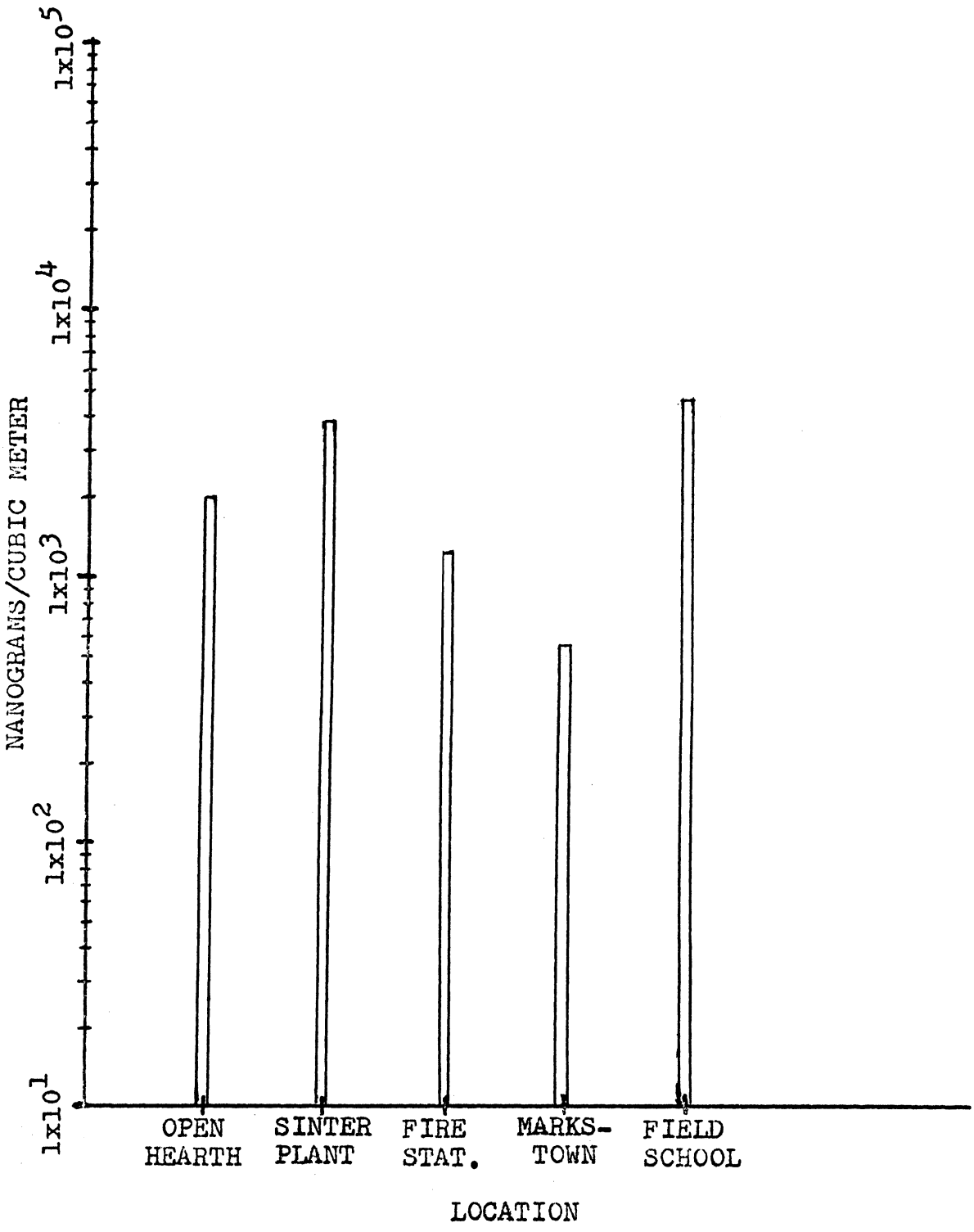

Figure 91. Aluminum, total aerosol averages.

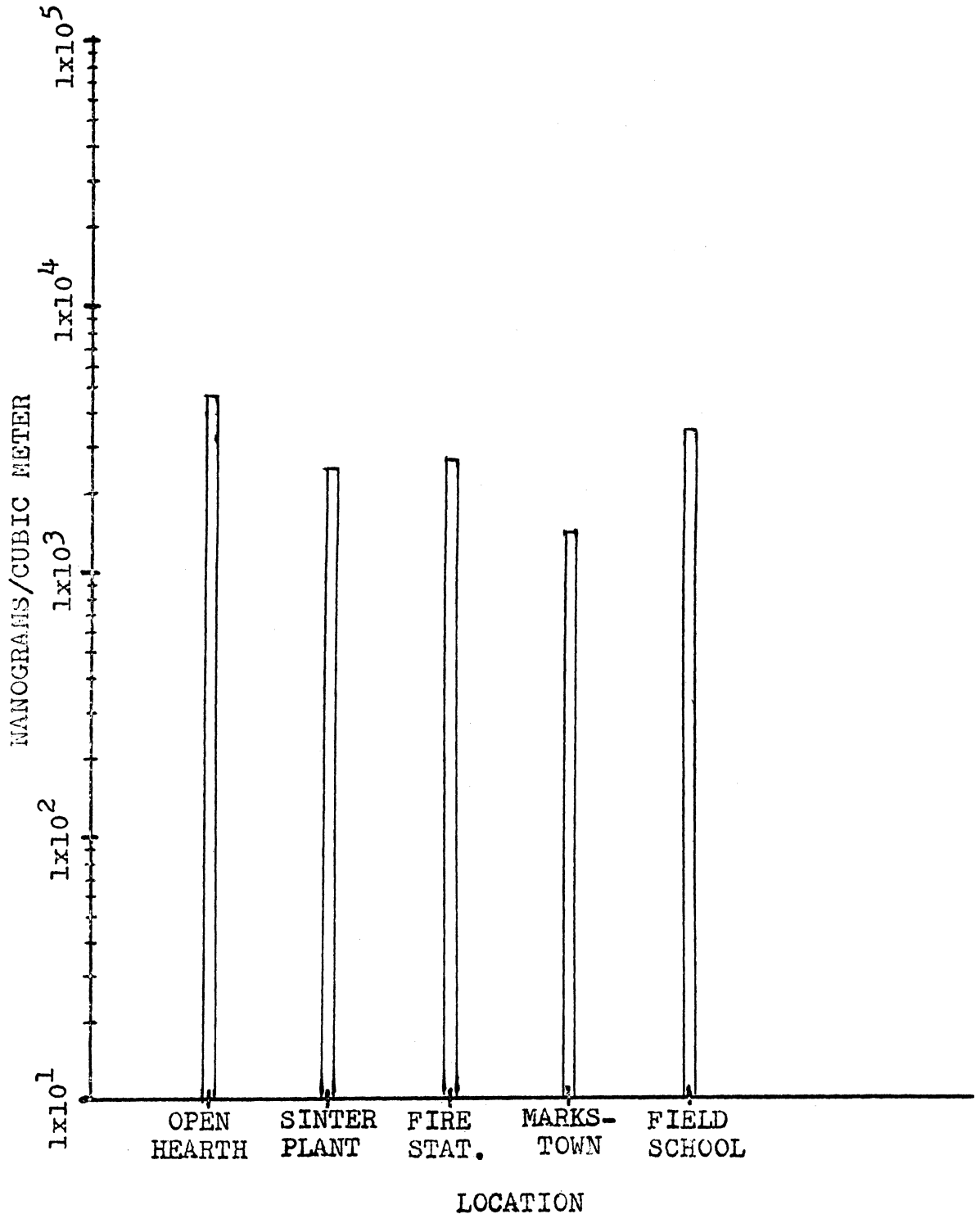

Figure 92. Chlorine, total aerosol averages.

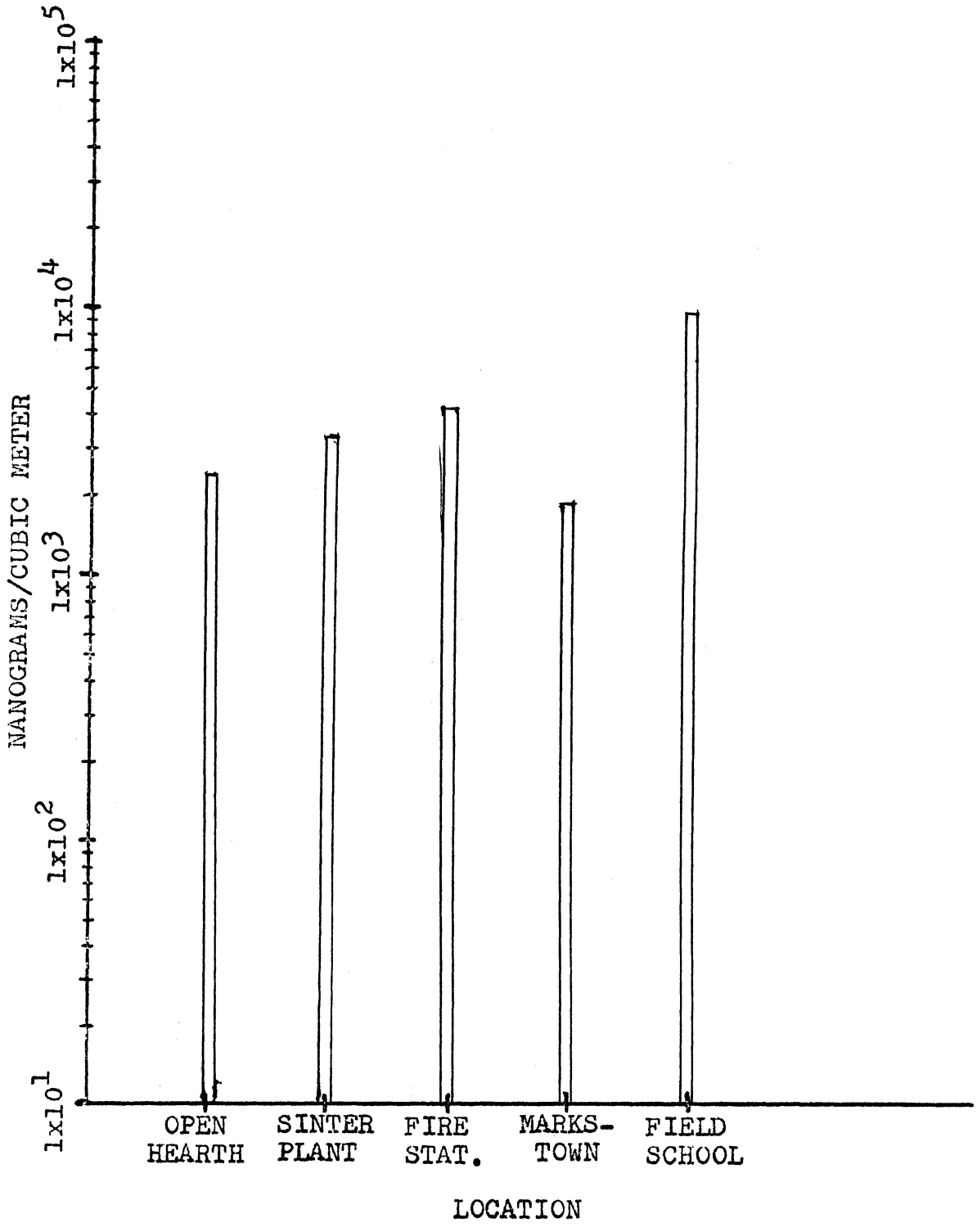

Figure 93. Potassium, total aerosol averages.

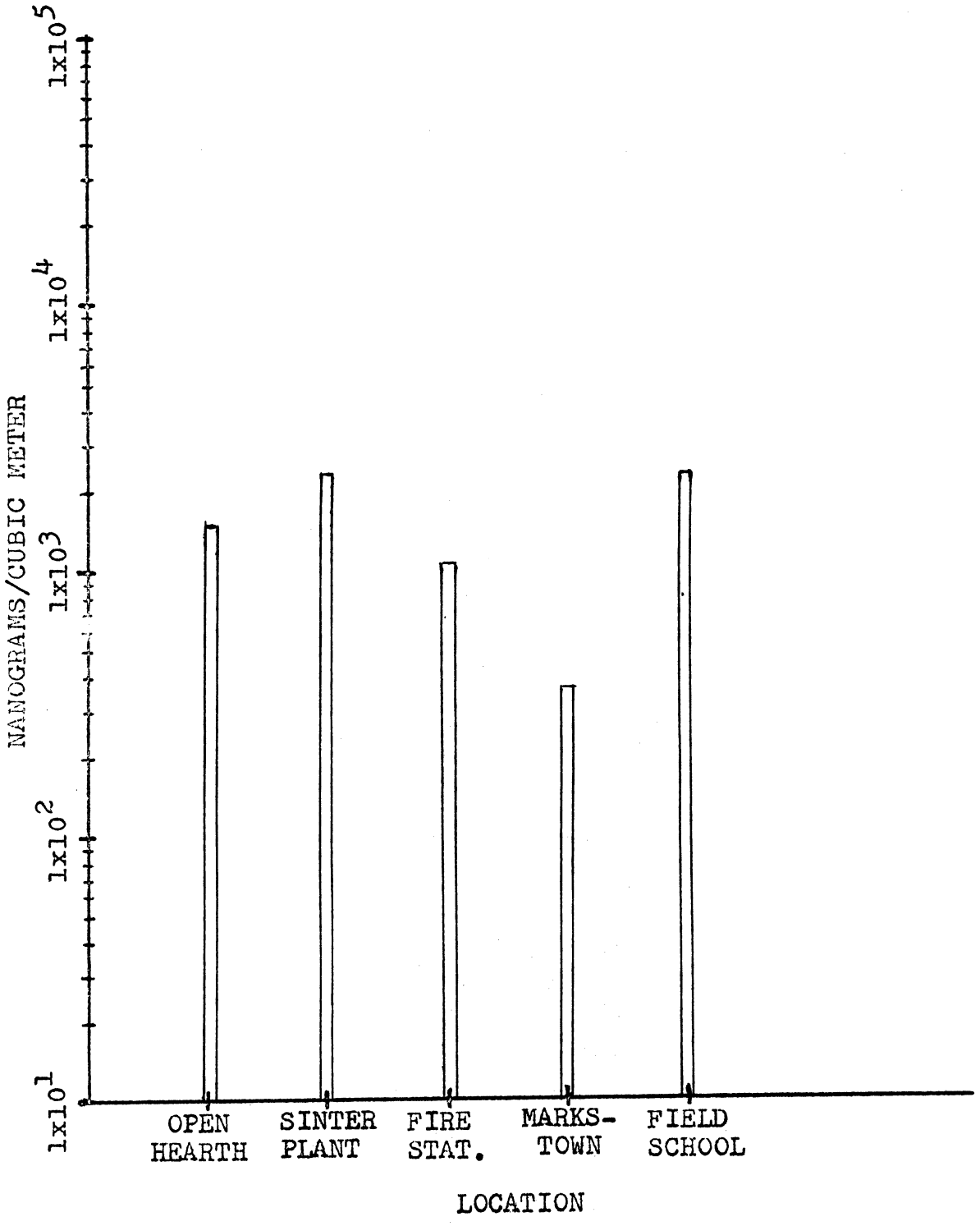

Figure 94. Vanadium, total aerosol averages.

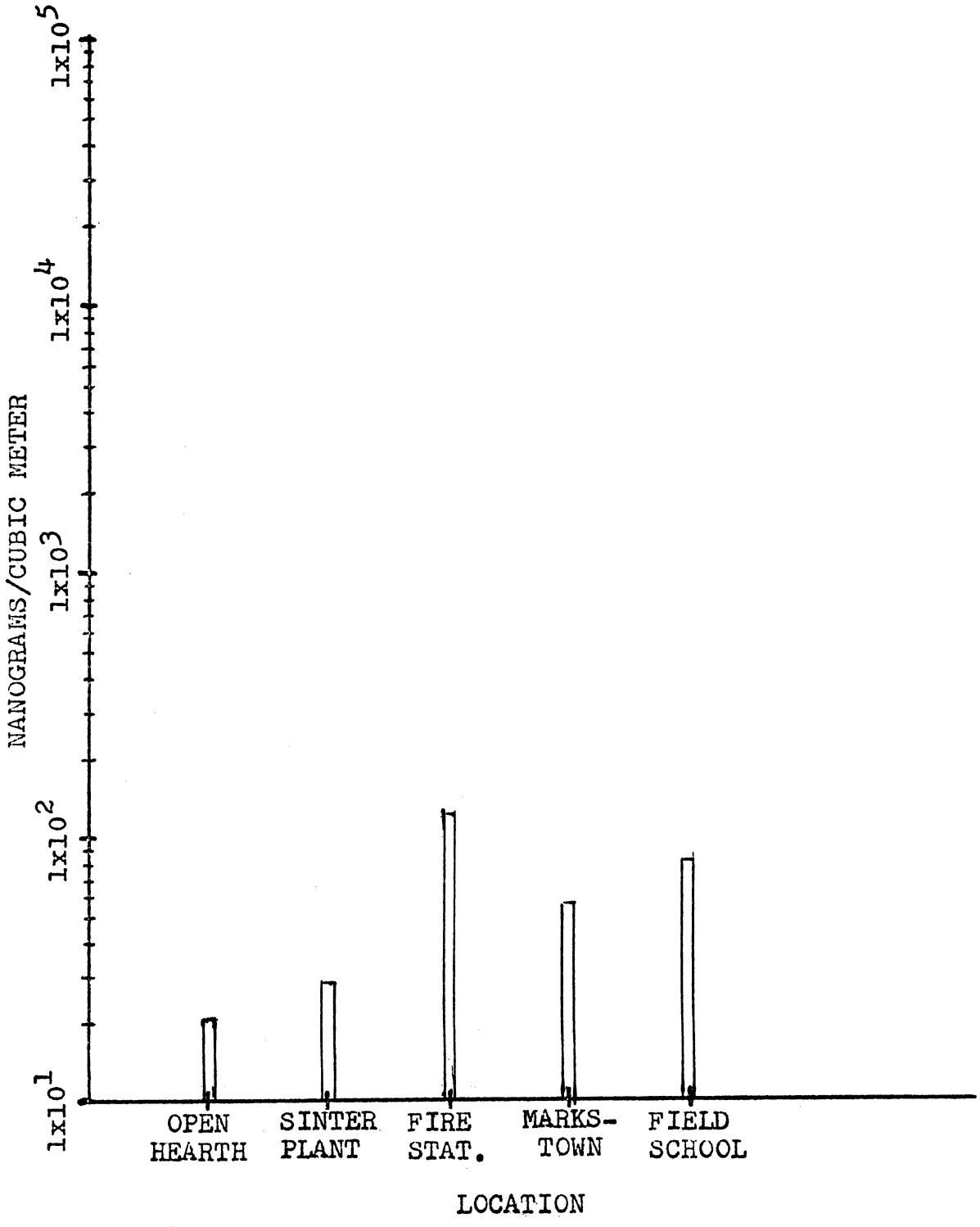

Figure 95. Antimony-to-Zinc ratios—(A) Run 19, East Chicago Central Fire Station; (B) Runs 2-4, Open Hearth Vicinity; (C) Run 27, Gary Wirt School.

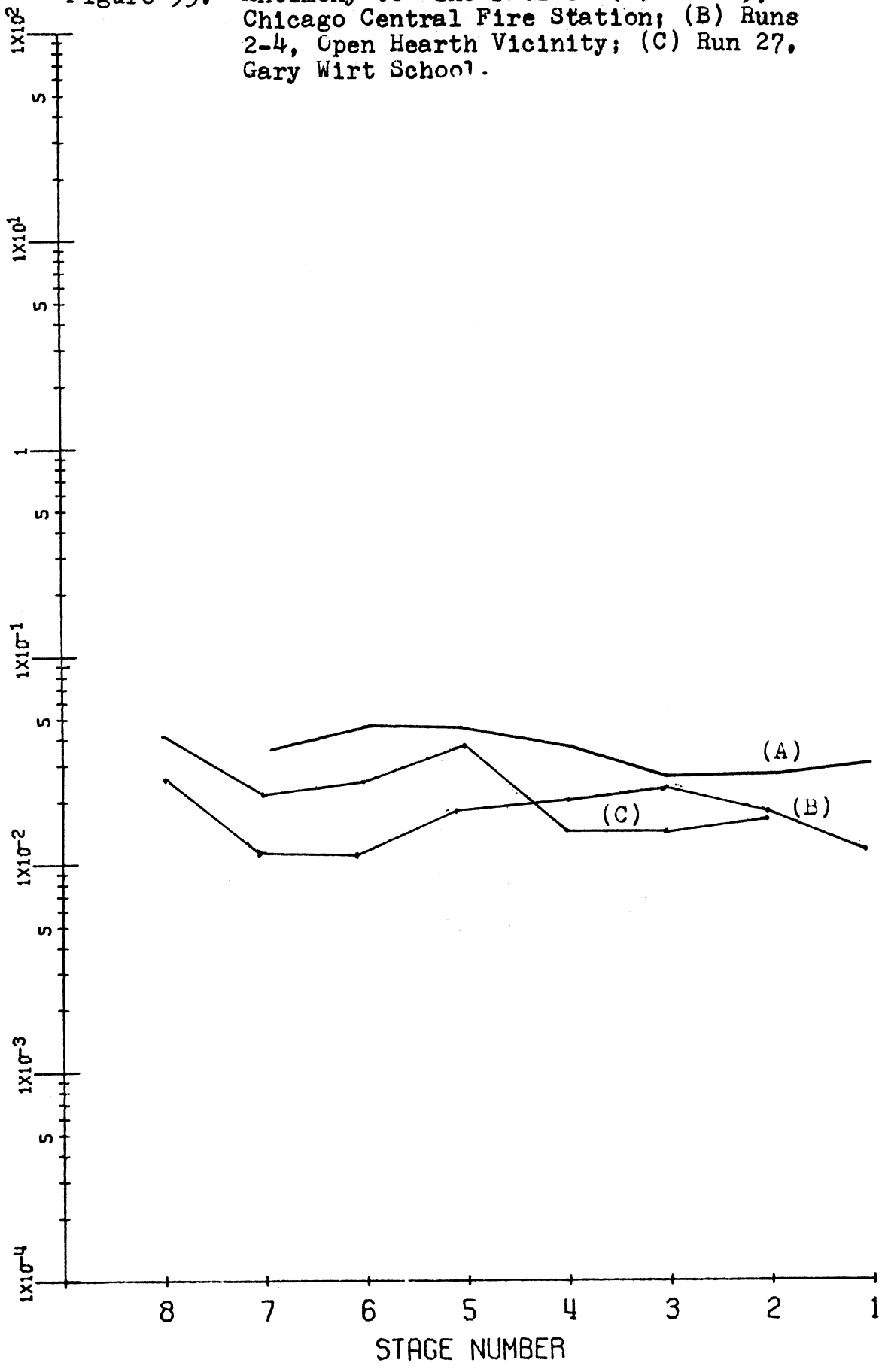

Figure 96. Manganese-to-Iron ratios—(A) Run 27, Gary Wirt School; (B) Run 4, Open Hearth Vicinity; (C) Run 7, Sinter Plant Vicinity; (D) Run 19, East Chicago Central Fire Station.

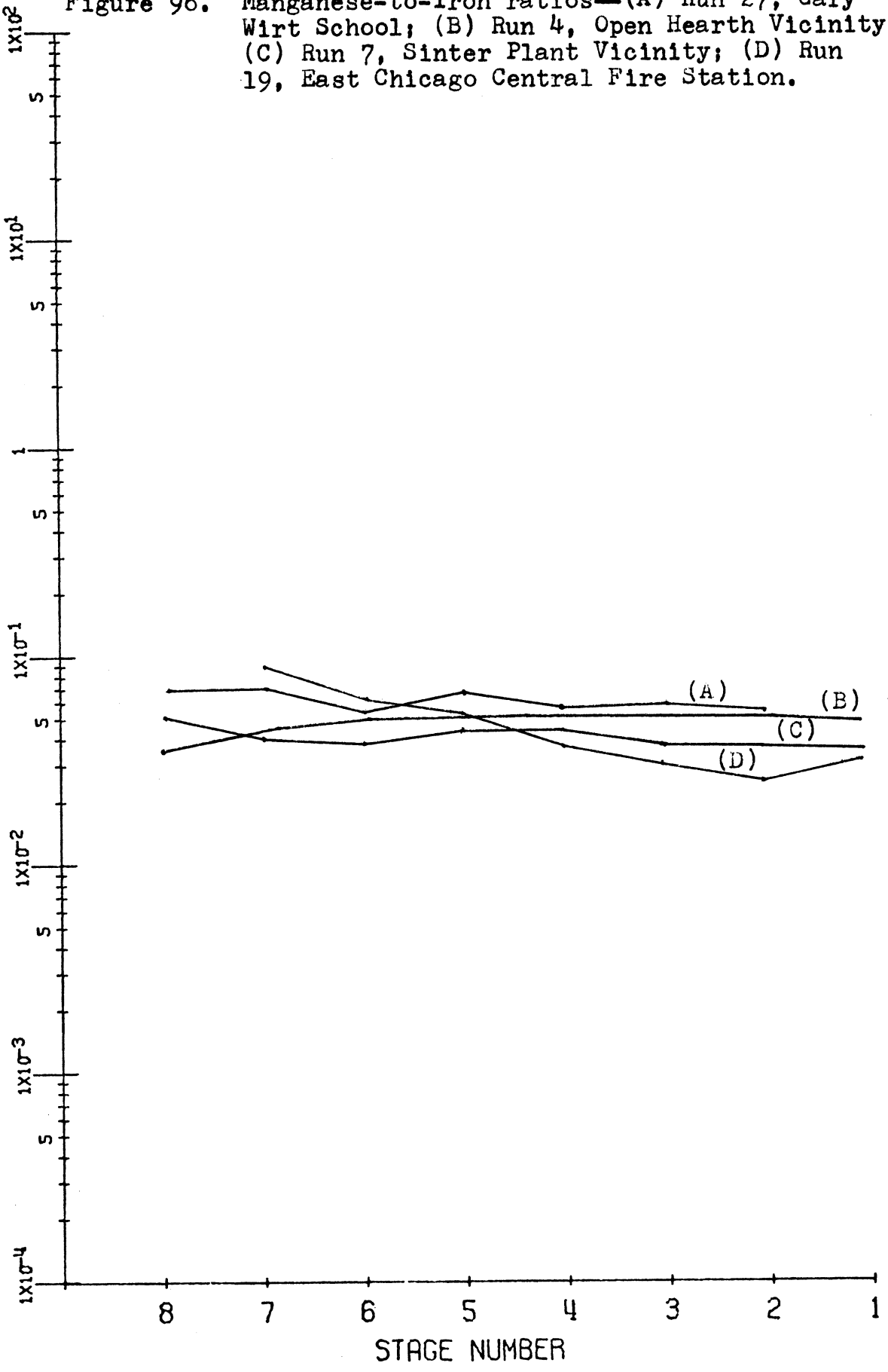

Figure 97. Chloride-to-Sodium ratios—(A) Run 9, Sinter Plant Vicinity; (B) Run 33, Gary Airport; (C) Run 4, Open Hearth Vicinity; (D) Run 25, East Chicago Field School.

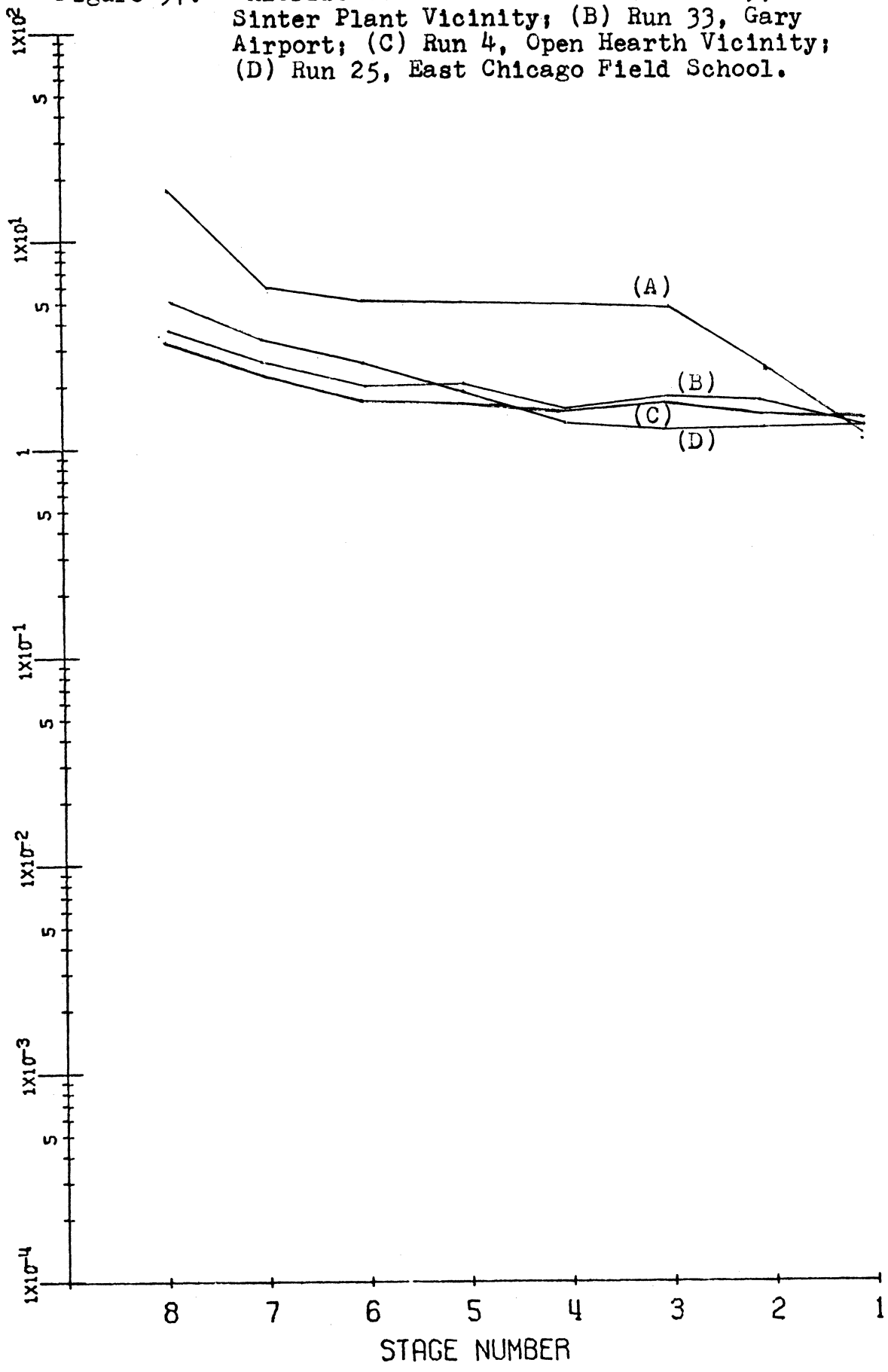

CHAPTER V

CONCLUSIONS

Measurements of trace elements in ambient aerosols from a heavily polluted source area have been extended by this work to include detection and quantitation of 29 trace elements in aerosol size-fractions. These data have been used in an attempt to identify major local source processes by type for as many elemental components of the ambient aerosol as possible, and to distinguish between anthropogenic and natural sources. Changes in particle-size distribution for these elements after emission have been considered, and their differential removal from the atmosphere by dry fallout has been estimated. The situation in the source area studied, Northwest Indiana, is that trace elements in urban aerosols fall into distinct groups.

1) Dispersion aerosols primarily from industrial sources include Fe, Mn, Cr, Co, and perhaps Sc and Th from the steel industry. These elements, as emitted from sintering operations, show a distinct large particle preference, usually occurring on particles greater than 10 μm. As emitted from open hearth and blast furnace operations, they occur on slightly smaller particles and in lower concentrations. In either case, the particle size is large enough that much if not most of this material falls out in the near-source vicinity. There are other local sources (e.g. power generation) for these metals, but based on changes in size distributions found with distance, and on an emissions

inventory (Ozolins and Rehmann, 1968) for the area, the steel industry accounts for most pollution by the elements in this group.

2) Other dispersion aerosols showing distinct large particle preference (d > 10 μm) include Ca, Mg, and Ti. But for these not only is the steel industry a major source, but cement manufacture and power generation, plus natural sources, are quite significant. Again, atmospheric residence times for these elements should be quite short, with dry fallout rapid due to the large particle size. Aluminum and the rare earths (lanthanum, samarium, europium and cerium) constitute an additional group of dispersion elements, also showing a large particle preference. For these, input from natural sources (soil re-entrainment) may be substantial. Pollution Al is emitted in smaller quantities from the steel complex than from power production, but for both source processes, the quantity of Al is small compared to that of natural origin. Aluminum is associated with particles 1-5 μm in diameter from steel operation, and with particles > 5 μm in diameter from power generation sources.

3) The elements zinc, antimony, arsenic and indium show a distinct small particle preference, and arise largely from the steel industry. This suggests a process of vapor condensation at high supersaturation, resulting in a condensation aerosol. The open hearth operation is a main source; sinter plant operations release smaller amounts of these elements, and partly on dispersion aerosols. But

elements in this group have longer atmospheric residence times, and pollute regions far from the source, including Lake Michigan. Copper is related to this group, but has a larger variety of sources. The size distribution of Cu shows both dispersion and condensation aerosol components, but with emphasis on the smaller sizes.

4) Sodium and chlorine showed an apparent grouping more nearly "Junge mass-distributed." The steel industry appeared to be a major source of dispersion Na and small-particle Cl, but these effects on the distribution curve disappear rapidly after emission, due in part to the fallout of the Na and to the reactivity of the condensation Cl. Except near the steel industry, Cl/Na mass ratios for the various size fractions were fairly constant at 1.5, suggesting a NaCl background. The effects of road salting for snow removal could clearly be seen in an elevation of both Na and Cl on larger sized particles, with Cl/Na remaining at 1.5. Potassium, gallium, and bromine also grouped together in their appearance by size distribution. These three elements were also quite "Junge-distributed," perhaps indicated for K and Br by their reactivity. No major source process could be firmly established for the three, but it is likely that combustion of leaded gasoline accounts for most of the Br and the area chemical industry for much K. Vanadium was also investigated and found to have a unique and constant size spectrum, suggestive of vapor condensation as a main source. This may arise from the chemical industry, due to

its frequent use as a catalyst, especially in oil refining, and its presence as a natural constituent in fuel oil.

The goal as stated in Chapter I of predicting source processes based on a knowledge of particle size distributions by mass of trace elements as found in urban aerosols is met in part by this work. It has been feasible in some cases to distinguish man-made pollution from natural pollution by such work. Pollution elements from dispersion source processes have been distinguished from those arising from condensation processes. Since much pollution in the region studied in this project is from sources within the steel industry, samples were taken close to specific source processes in conjunction with samples taken further away. It has been possible to estimate what part of urban pollution aerosol levels are due to this industry, and, in most cases, to isolate a major source process within the industry for the elements attributed to that industry.

It has been feasible to determine which pollution elements were primarily <u>not</u> from steel operations. But specific source processes for this group of elements could only be estimated, based on a knowledge of other sources of pollution in Northwest Indiana, and use patterns of elements. Further research in controlled observation of other types of industrial operations and commercial activities is suggested in order to better determine the relations between source operations and urban pollution aerosols.

Groupings of the elements as established by size

distribution patterns were compared with groups as would occur based on chemical properties, and with groups as would occur based on categories of major usage. For those elements arising from natural sources, groups based on size distribution and on chemical properties agreed well. But for elements arising more from anthropogenic pollution sources, size distribution groups and groups-by-use agreed better, especially near sources. As the aerosol aged, however, size groupings began more to resemble that expected on the basis of similarities in chemical and physical properties.

Particle size distributions by mass of each of the various elements investigated were compared with an expected "Junge mass-distribution,"

$$\frac{dM}{d\ (\log r)} = \text{Constant.}$$

Two theories have been advanced to explain why this distribution (for total aerosols) is found. Junge has held that the smooth mass distribution results from homogeneous mixing of various particle size distributions from many different sources; Friedlander has pointed out that it could be the result of a dynamic system involving input by coagulation of small particles and removal of large particles by sedimentation. This work demonstrates that the "Junge distribution" is followed closely by many elements, despite the fact that in the immediate source vicinity there are only a few major source processes, at most, for each

element. The Friedlander hypothesis therefore, though not fully understood as yet, better accounts for the distributions found. This is especially evident in samples taken close to, and also further downwind from, one specific source. The conclusion is supported by the finding that condensation aerosols more quickly approach the "Junge distribution" than do dispersion aerosols.

This work demonstrates for which elements quick removal from the atmosphere by dry fallout occurs, and demonstrates for elements having longer atmospheric residence times how the particle size distribution changes as the aerosol ages. Dispersion aerosols are shown to have short atmospheric residence times and to pollute the source area by a removal mechanism of mainly dry fallout. The largest of these, $d > 10$ μm, are removed by dry settling as well as turbulent impaction. For particles less than 10 μm in diameter, dry removal is much more efficient than can be explained by the Stokes settling velocity, and surface impaction from turbulent air near the ground is the major removal mechanism in operation. Condensation aerosols may grow by coagulation and adsorption, have much longer residence times, be more active as condensation nuclei, and pollute areas further removed from the immediate source. Pollution of Lake Michigan by dry fallout of pollution aerosols is shown to be significant with regard to certain trace metals emitted to the atmosphere.

Natural tracers are discussed, where use of Mn, Fe, Zn,

and Sb may serve as an index of pollution from steel manufacture; V, oil refining; and Br, transportation. But, except for V and Br, only elemental content per particle size-fraction provides the requisite information; concentration of each element in the total aerosol is usually not sufficient for tracer studies. Element-to-element ratios of size distributions measured close to a possible source and again as the aerosol moves outward from the immediate source area is a most important tracer technique. A smooth ratio of size distributions for two elements indicates that both are on the same particles; hence removal efficiencies for the two should be similar. If the ratio pattern is smooth both near to and downwind from a source, pollution downwind from that source is indicated. Examples of this technique are the use of Mn/Fe ratios to determine steel plant dispersion aerosols, and Sb/Zn to determine condensation aerosols from the same industry.

Finally, it is suggested that toxicologic studies of pollution elements present in ambient air include size of the particles on which the elements are located, as the respirable fraction of particle size spectra of toxic elements is more hazardous than are equivalent masses of the same elements located on larger particles.

SELECTED BIBLIOGRAPHY

American Conference of Governmental Industrial Hygienists, 1966. Air Sampling Instruments for Evaluation of Atmospheric Contaminants, 3rd ed. Cincinnati, Ohio.

Andersen, A. A. 1958. New Sampler for the Collection, Sizing, and Enumeration of Viable Airborne Particles. J. Bacteriology, 76:471.

Andersen, A. A. 1966. A Sampler for Respiratory Health Hazard Assessment. Amer. Ind. Hyg. Assoc. J., 27:160.

Cadle, R. D. 1965. Particle Size-Theory and Industrial Applications. Reinhold, New York.

Corn, M. 1969. Seminar on Aerosol Research, presented at The University of Michigan, April 16.

Cuffe, S. T., and Gerstle, R. W. 1967. Emissions from Coal-Fired Power Plants: A Comprehensive Summary. Publication No. 999-AP-35. National Center for Air Pollution Control, U. S. Department of Health, Education, and Welfare. Cincinnati, Ohio.

Dams, R., and Adams, F. 1968. Gamma-Ray Energies of Radionuclides Formed by Neutron Capture Determined by Ge(Li) Spectrometry. Radiochimica Acta, 10:1.

Dams, R., Rahn, K. A., and Winchester, J. W. 1970. Sampling Aerosols for Nondestructive Neutron Activation Analysis. (Submitted to Env. Sci. and Tech., January 1970).

Dams, R., Robbins, J. A., Rahn, K. A., and Winchester, J. W. 1970. Quantitative Relationships Among Trace Elements in Air Particulates Over the Industrialized Area of Northwest Indiana. (In Preparation).

Davies, C. N., and Aylward, M. 1951. The Trajectories of Heavy Solid Particles in a Two Dimensional Jet of Ideal Fluid Impinging Normally Upon a Plate. Proc. of the Phys. Soc. 64:889.

Duprey, R. L. 1968. Compilation of Air Pollutant Emission Factors. Publication No. 999-AP-42. National Center for Air Pollution Control, U. S. Department of Health, Education, and Welfare. Durham, N. C.

Faith, W. L. 1964. Air Pollution Research—Reflections and Projection. J. Air Poll. Control Assoc., 14:367.

Fleagle, R. G., and Businger, J. A. 1963. An Introduction to Atmospheric Physics. Academic Press, New York.

Flesch, J. P., Norris, C. H., and Nugent, A. E., Jr. 1967. Calibrating Particulate Air Samplers with Monodisperse Aerosols. J. Amer. Indus. Hyg. Assoc., 28:507.

Fletcher, N. H. 1962. The Physics of Clouds. University Press, Cambridge, Mass.

Friedlander, S. K. 1960. Similarity Considerations for the Particle-Size Spectrum of a Coagulating, Sedimenting Aerosol. J. Meteorology, 17:479.

Gillette, D. A. 1970. A Study of Aging of Lead Aerosols. Ph. D. Thesis, The University of Michigan.

Harrison, P. R., and Winchester, J. W. 1970. Area-Wide Distribution of Lead, Copper, and Cadmium in Air Particulates from Chicago and Northwest Indiana. (Submitted to J. Air Poll. Cont. Assoc., April 1970).

Hashimoto, Y., and Winchester, J. W. 1967. Selenium in the Atmosphere. Env. Sci. and Tech., 1:338.

Hewson, E. W. 1964. Industrial Air Pollution Meteorology. Meteorological Laboratories of the College of Engineering, The University of Michigan, Ann Arbor, Michigan.

Hodgman, C. D., Weast, R. C., and Selby, S. M. 1956. Handbook of Chemistry and Physics, 37th Ed. Chemical Rubber Publishing Company, Cleveland, Ohio.

Junge, C. E. 1963. Air Chemistry and Radioactivity. Academic Press, New York.

Junge, C. E. 1969. Comments on "Concentration and Size Distribution Measurements of Atmospheric Aerosols and a Test of the Theory of Self-Preserving Distributions." J. Atmos. Sc., 26:603.

Keane, J. R., and Fisher, E. M. R. 1968. Analysis of Trace Elements in Air-borne Particulates by Neutron Activation and Gamma-Ray Spectrometry. Atm. Env., 2:603.

Kreichelt, T. E., Kemnitz, D. A., and Cuffe, S. T. 1967. Atmospheric Emissions from the Manufacture of Portland Cement. Publication No. 999-AP-17. National Center for Air Pollution Control, U. S. Department of Health, Education, and Welfare, Cincinnati, Ohio.

Lee, R. E., and Patterson, R. K. 1969. Size Determination of Atmospheric Phosphate, Nitrate, Chloride, and Ammonium Particulate in Several Urban Areas. Atm. Env., 3:249.

Lee, R. E., Patterson, R. K., and Wagman, J. 1968. Particle Size Distribution of Metal Components in Urban Air. Env. Sci. and Tech., 2:288.

Loucks, R. H. 1969. Particle Size Distributions of Chlorine and Bromine in Mid-Continent Aerosols from the Great Lakes Basin. Ph. D. Thesis, The University of Michigan.

Lundgren, D. A. 1967. An Aerosol Sampler for Determination of Particle Concentration as a Function of Size and Time. J. Air Poll. Cont. Assoc., 17:225.

Lundgren, D. A. 1969. Atmospheric Aerosol Composition and Concentration as a Function of Particle Size and of Time. Paper presented at the 62nd annual Air Pollution Control Association Meeting, New York, June 1969.

May, K. R. 1945. The Cascade Impactor. J. Scientific Instruments, 22:187.

Mercer, T. T. 1963. On the Calibration of Cascade Impactors. Annals Occupational Hygiene, 6:1.

Mirsky, W. 1969. Seminar on Research Areas in Air Pollution, presented at The University of Michigan, March 5, 1969.

Ozolins, G., and Rehmann, C. 1968. Air Pollutant Emission Inventory of Northwest Indiana, A Preliminary Survey, 1966. Publication APTD-68-4. National Center for Air Pollution Control, U. S. Department of Health, Education, and Welfare. Cincinnati, Ohio.

Ranz, W. E. and Wong, J. B. 1952. Jet Impactors for Determining the Particle-Size Distributions of Aerosols. Ind. Hyg. Occup. Med., 5:464.

Robinson, E., Ludwig, F. L., DeVries, J. E., and Hopkins, T. E. 1963. Variation of Atmospheric Lead Concentrations and Type with Particle Size. Final report to the Stanford Research Institute, Menlo Park, Cal.

Robinson, E. and Ludwig, F. L. 1964. Size Distributions of Atmospheric Lead Aerosols. Final report to the Stanford Research Institute, Menlo Park, Cal.

Schueneman, J. J., High, M. D., and Bye, W. E. 1963. Air Pollution Aspects of the Iron and Steel Industry. Publication No. 999-AP-1. Division of Air Pollution, Public Health Service, U. S. Department of Health, Education, and Welfare, Cincinnati, Ohio.

Sebesta, W. 1968. Ferrous Metallurgical Processes. Air Pollution. Stern, A. C., ed., III. Academic Press, New York.

Slade, D. H. 1968. Meteorology and Atomic Energy 1968. U. S. Atomic Energy Commission Publication No. TID-24190. Washington, D. C.

Slavin, W. 1968. Atomic Absorption Spectroscopy. John Wiley and Sons, Inc., New York.

Smith, W. S. 1962. Atmospheric Emissions from Fuel Oil Combustion, An Inventory Guide. Publication No. 999-AP-2. Division of Air Pollution, Public Health Service, U. S. Department of Health, Education, and Welfare. Cincinnati, Ohio.

Smith, W. S., and Gruber, C. W. 1966. Atmospheric Emissions from Coal Combustion - An Inventory Guide. Publication No. 999-AP-24. Division of Air Pollution, U. S. Public Health Service, U. S. Department of Health, Education, and Welfare. Cincinnati, Ohio.

U. S. Department of Health, Education, and Welfare. 1969. Air Quality Criteria for Particulate Matter. Publication No. 999-AP-49. National Air Pollution Control Administration. Durham, N. C.

U. S. Department of Health, Education, and Welfare. 1966. Air Quality Data from the National Air Sampling Networks and Contributing State and Local Networks, 1964-1965. Division of Air Pollution, U. S. Public Health Service. Cincinnati, Ohio.

U. S. Department of Interior. Monthly Weather Data Summary for Midway Airport, (1950-1959). National Weather Records Center. Ashville, N. C.

Wagman, J. 1966. Current Problems in Atmospheric Aerosol Research. Int. J. Air and Water Poll., 10:777.

Wagman, J. 1967. Aerosol Research at the National Center for Air Pollution Control. J. Air Poll. Cont. Assoc., 17:572.

Whitby, K. T. 1969. Seminar on Aerosol Research, presented at The University of Michigan, April 9.

Wilcox, J. E. 1953. Design of a New Five-Stage Cascade Impactor. AMA Arch. Ind. Hyg. and Occ. Med., 7:5.

Willard, H. H. Merritt, J., L. L., and Dean, J. A. 1965. Instrumental Methods of Analysis, 4th ed. D. Van Nostrand Company, Inc., Princeton, N. J.

Winchester, J. W., and Nifong, G. D. 1969. Water Pollution in Lake Michigan by Trace Elements from Pollution Aerosol Fallout, presented at the Great Lakes Symposium, American Chemical Society annual meeting, Minneapolis, Minn., 1969.

Winchester, J. W., Robbins, J. A., and Dams, R. F. 1969. Sources and Sinks of Air Pollution Trace Metals in Lake Michigan, presented at a conference on Nuclear Techniques in Atmospheric Pollution Studies, American Nuclear Society, San Francisco, Cal., 1969.

APPENDIX

TABLE 14: DETAILS OF SAMPLE RUNS

Run	Start-Stop Times * Hour/Day/Month			Air Volume Sampled (Cubic Meters)		Location Number
1	0945/12/6	-	1400/12/6	7.23		1
2	0914/1/12	-	0634/2/12	36.3		1
3	1200/2/12	-	0705/3/12	32.4		1
4	0845/3/12	-	0735/4/12	38.7		1
5	0945/13/6	-	1332/13/6	6.43		1
6	1028/13/6	-	1350/13/6	5.72		2
7	1005/1/12	-	0635/2/12	34.8		2
8	0850/2/12	-	0632/3/12	36.9		2
9	0855/3/12	-	0740/4/12	38.8		2
10	0855/4/12	-	0753/5/12	39.0		2
11	0925/13/6	-	1325/13/6	6.79		3
12	1230/1/7	-	1245/2/7	41.2		4
13	1220/28/7	-	0940/29/7	36.2		4
14	1335/14/8	-	0953/15/8	34.6		4
15	1510/1/12	-	1335/2/12	38.1		4
16	1335/2/12	-	1345/3/12	41.0		4
17	1345/3/12	-	1335/4/12	40.5		4
18	1335/5/12	-	1055/6/12	36.3		4
19	1030/9/2	-	1030/24/2	459	*,**	4
20	1415/4/12	-	1415/5/12	40.8		5
21	1415/5/12	-	1115/6/12	37.5		5
22	1105/9/2	-	1105/24/2	459	*,**	5
23	1410/1/12	-	1320/2/12	39.3		6
24	1355/2/12	-	1415/3/12	41.4		6
25	1415/3/12	-	1355/4/12	40.2		6
26	1355/4/12	-	1355/5/12	40.8		6
27	1200/1/12	-	1040/5/12	119	**	7
28	0930/1/7	-	0900/2/7	40.0		8
29	1100/28/7	-	1100/29/7	40.8		8
30	1050/14/8	-	0910/15/8	37.9		8
31	1250/1/12	-	0900/2/12	34.3		8
32	1115/2/12	-	1115/3/12	40.8		8
33	1115/3/12	-	0955/4/12	38.5		8
34	0955/4/12	-	0955/5/12	40.8		8
35	1130/5/12	-	1000/6/12	38.3		8
36	1010/1/7	-	1125/2/7	42.9		9
37	1030/28/7	-	1400/29/7	46.7		9
38	1005/14/8	-	1030/15/8	41.5		9
39	1700/1/7	-	0900/2/7	27.2		10
40	1400/28/7	-	0830/29/7	31.4		10

* All samples collected during 1969, except those denoted by *, which were collected during 1970.

** Sample collected intermittently during time interval.

(TABLE 14, continued)

Run	Start-Stop Times * Hour/Day/Month			Air Volume Sampled (Cubic Meters)	Location Number
41	0000/15/8	-	1330/15/8	23.0	10
42	1010/6/10	-	1551/6/10	8.73**	11
43	0640/7/10	-	0751/7/10	2.01	11
44	0758/7/10	-	0935/7/10	2.75	11
45	1700/9/6	-	0900/11/6	68.0	12
46	1130/18/8	-	0830/20/8	76.0	12
47	1005/27/8	-	1315/29/8	87.0	12
48	1000/27/8	-	1310/29/8	87.0	12
49	1000/12/1	-	1600/2/2	867 *	12
50	1400/6/2	-	1300/23/2	692 *	12
51	1335/4/12	-	1335/5/12	40.8	4
52	1440/3/12	-	0000/4/12	15.9	5

TABLE 15: METEOROLOGICAL CONDITIONS FOR SAMPLE RUNS

Run	Wind Extremes Direction	Speed (MPH)	Temp. Range (Degrees F.)	Rel. Humidity %	Ppt. ?
1	S	8-10	-	-	no
2	SW-N	4-16	24-34	50-85	no
3	W-NW	10-16	31-43	40-85	no
4	NW	9-20	19-33	40-85	Tr.
5	S	8-10	-	-	no
6	S	8-10	-	-	no
7	SW-N	4-14	24-32	50-85	no
8	N-NW	10-15	31-43	40-85	no
9	NW	9-20	19-33	40-85	Tr.
10	SW-N	2-6	22-30	40-85	no
11	S	8-10	-	-	no
12	NE-S	4-6	60-95	-	no
13	NW-N	8-20	60-90	-	no
14	S-SW	4-8	50-70	70-90	rain
15	SW-N	4-18	24-41	50-85	no
16	W-NW	10-20	28-43	40-85	no
17	NW	8-16	19-30	40-85	Tr.
18	SE	5-8	27-32	55-80	no
19	-	-	-	-	-
20	SE-N	2-7	26-32	40-85	no
21	SE	5-8	27-35	55-80	no
22	-	-	-	-	-
23	SW-N	4-18	24-41	50-85	no
24	W-NW	10-20	28-43	40-85	no
25	NW	8-16	19-30	40-85	Tr.
26	SE-N	2-7	26-32	40-85	no
27	variable	4-20	19-43	40-85	no
28	NE-S	4-6	60-94	-	no
29	NW-N	8-20	60-90	-	no
30	S-SW	4-8	50-75	70-90	rain
31	SW-N	4-14	24-40	50-85	no
32	W-NW	10-20	28-42	40-85	no
33	NW	8-16	20-30	40-85	Tr.
34	SE-N	2-7	26-32	40-85	no
35	SE	5-8	27-30	55-80	no
36	NE-S	4-6	60-95	-	no
37	NW-N	8-20	60-90	-	no
38	S-SW	4-8	50-75	70-90	rain
39	NE-S	4-6	60-92	-	no
40	NW-N	8-20	60-90	-	no
41	S-SW	4-8	50-75	70-90	rain
42	S	12-14	-	-	rain
43	SW	12-14	-	-	no
44	SW	13-15	-	-	no
45-50	-	-	-	-	-
51	SE-N	2-7	26-32	40-85	no
52	NW	10-16	24-30	40-85	Tr.

TABLE 16: IMPACTOR STAGE AND FILTER MATERIALS USED

Material	Manufacturer's Name	(Key)	?ications
Polyethylene	---	(PE)	ss: 0.025 mm ?: 83 mm
Membrane cellulose ester	MF-Millipore	(AAWP025)	Pore size: 0.8 µm Diameter: 25 mm
Membrane cellulose ester	MF-Millipore	(AAWP047)	Pore size: 0.8 µm Diameter: 47 mm
Polystyrene	Microsorban	(MS)	---

TABLE 17: IMPACTOR STAGE AND FILTER IMPURITY LEVELS, ng/disc.

Element	(PE)	(AAWP025)	(AAWP047)	(MS)
Na	130	2760	6900	400
Mg	45	2100	3400	<7500
Al	360	80	170	100
Cl	400	9000	17000	15000
Ca	400	2650	6400	1500
Ti	550	50	<150	200
V	0.7	<1	<1	0.3
Mn	5.5	10	35	6
Cu	50	450	1000	1500
Br	50	10	20	5000
In	<0.3	<0.2	<0.2	<0.2
I	<10	<10	<10	7
K	65	650	1700	50
Zn	100	50	120	2750
Ga	<2	<2	<2	<2
As	<10	<10	<10	<10
Sb	2	2	17	5
La	<0.5	<2	<3	<0.5
Eu	<0.1	<0.1	<0.1	<0.1
Sm	<0.2	<0.2	<0.2	<0.2
W	<3	<3	<3	<3
Sc	<0.05	<0.05	<0.75	<0.05
Cr	<10	100	250	10
Fe	<1000	425	700	450
Co	<2	2	2	1
Se	<20	<20	<20	<20
Ce	<4	<2	<5	<5
Hg	<10	<5	8	5
Th	<3	<3	<3	<3

TABLE 18: NUCLEAR PROPERTIES AND MEASUREMENT OF SHORT-LIVED ISOTOPES

Element	Isotope	Half-life	$t_{irradiate}$	t_{cool}	t_{count}	Gamma-ray used Kev
Al	^{28}Al	2.31 min.	5 min.	3 min.	400 sec.	1778.9
Ca	^{49}Ca	8.8 min.	"	"	"	3083.0
Ti	^{51}Ti	5.79 min.	"	"	"	320.0
V	^{52}V	3.76 min.	"	"	"	1434.4
Cu	^{66}Cu	5.1 min.	"	"	"	1039.0
Na	^{24}Na	15 hr.	"	15 min.	1000 sec.	1368.4
Mg	^{27}Mg	9.45 min.	"	"	"	1014.1
Cl	^{38}Cl	37.3 min.	"	"	"	1642.0
Mn	^{56}Mn	2.58 hr.	"	"	"	846.9
Br	^{80}Br	17.6 min.	"	"	"	617.0
In	^{116m}In	54 min.	"	"	"	417.0
I	^{128}I	25 min.	"	"	"	442.7

TABLE 19: NUCLEAR PROPERTIES AND MEASUREMENT OF LONG-LIVED ISOTOPES

Element	Isotope	Half-life	$t_{irradiate}$	t_{cool}	t_{count}	Gamma-ray used Kev
K	^{42}K	12.52 hr.	1-2 hr.	20-30 hr.	2000 sec.	1524.7
Cu	^{64}Cu	12.5 hr.	"	"	"	511.0
Zn	^{69m}Zn	13.8 hr.	"	"	"	438.7
Ga	^{72}Ga	14.3 hr.	"	"	"	834.1
As	^{76}As	26.3 hr.	"	"	"	657.0
Br	^{82}Br	35.9 hr.	"	"	"	776.6
Sb	^{122}Sb	2.75 day	"	"	"	564.0
La	^{140}La	40.3 hr.	"	"	"	1595.4
Eu	^{152m}Eu	9.35 hr.	"	"	"	963.5
Sm	^{153}Sm	47.1 hr.	"	"	"	103.2
W	^{187}W	24.0 hr.	"	"	"	685.7

(TABLE 19, continued)

Element	Isotope	Half-life	$t_{irradiate}$	t_{cool}	t_{count}	Gamma-ray used Kev
Sc	^{46}Sc	83.9 day	1-2 hr.	20-30 day	4000 sec.	889.4
Cr	^{51}Cr	27.8 day	"	"	"	320.0
Fe	^{59}Fe	45.1 day	"	"	"	1291.5
Co	^{60}Co	5.2 yr.	"	"	"	1332.4
Zn	^{65}Zn	245 day	"	"	"	1115.4
Se	^{75}Se	121 day	"	"	"	264.6
Sb	^{124}Sb	60.9 day	"	"	"	602.6
Ce	^{141}Ce	32.5 day	"	"	"	145.4
Hg	^{203}Hg	46.9 day	"	"	"	279.1
Th	^{233}Pa	27.0 day	"	"	"	311.8

TABLE 20: LIMITS OF DETECTION FOR DETERMINATION OF TRACE ELEMENTS IN AEROSOLS

Element	Neutron Activation		
	Decay Time*	Detection Limit (ug)	Minimum Detectable Concentration in Urban Air (ug/m^3) 24 hours sample
Al	3 min.	0.04	0.008
Ca	"	1.0	0.2
Ti	"	0.2	0.04
V	"	0.001	0.002
Cu	"	0.1	0.02
Na	15 min.	0.2	0.04
Mg	"	3.0	0.6
Cl	"	0.5	0.1
Mn	"	0.003	0.0006
Br	"	0.02	0.004
In	"	0.0002	0.00004
I	"	0.1	0.02
K	20-30 hr.	0.075	0.0075
Cu	"	0.05	0.005
Zn	"	0.2	0.02
Ga	"	0.01	0.001
As	"	0.04	0.004
Br	"	0.025	0.0025
Sb	"	0.03	0.003
La	"	0.002	0.0002
Eu	"	0.0001	0.00001
Sm	"	0.00005	0.000005
W	"	0.005	0.0005
Sc	20-30 day	0.003	0.000004
Cr	"	0.02	0.00025
Fe	"	1.5	0.02
Co	"	0.002	0.000025
Zn	"	0.1	0.001
Se	"	0.01	0.0001
Sb	"	0.08	0.001
Ce	"	0.02	0.00025
Hg	"	0.01	0.0001
Th	"	0.003	0.00004

	Atomic Absorption Spectroscopy	
	Detection Limit (ug/ml)	Minimum Detectable Concentration in Urban Air (ug/m^3) 24 hours sample
Fe	0.1	0.0125
Zn	0.03	0.00375

* Decay time before counting.

TABLE 21: OPEN HEARTH VICINITY, Concentrations and Standard Deviations #

Element	Stage 1	2	3	4	5	6	7	8
Run 1								
Na	130(60)	150(60)	150(60)	170(70)	170(65)	210(70)	300(75)	-
Mg	1.5(1)*	1.6(1)*	1.6(1)*	1.7(1)*	1.5(1)*	1.0(1)*	0.9(1)*	-
Al	560(16)	670(15)	580(15)	580(15)	490(16)	100(10)	20(13)	-
Cl	400(90)	410(90)	400(90)	330(85)	300(80)	550(95)	970(110)	-
Ca	2600(500)	2300(500)	2400(500)	2100(450)	600(400)	<400	<400	-
V	2.7(.4)	3.3(.4)	4.0(.4)	4.2(.4)	4.1(.4)	1.9(.4)	2.3(.4)	-
Mn	50(4)	47(4)	46(4)	44(4)	25(3)	14(3)	17(3)	-
Cu	110(50)	60(50)	60(50)	80(50)	40(50)	50(50)	40(50)	-
In	.05(.03)	.03(.03)	.03(.03)	<.04	.03(.03)	.03(.03)	.04(.03)	-
I	<5	<5	<5	<5	<5	<5	<5	-
Fe (AA)	2.1(.5)*	1.1(.5)*	0.7(.5)*	<.5*	<.5*	<.5*	<.5*	.8(.5)*
Zn (AA)	460(100)	340(100)	370(100)	440(100)	900(100)	1080(100)	1780(100)	1630(100)
Run 2								
Na	220(22)	220(15)	225(15)	190(15)	290(15)	225(15)	190(15)	630(30)
Mg	1.0(.4)*	<600	680(280)	340(250)	<600	<550	<600	<900
Al	994(11)	994(11)	1000(11)	1320(12)	1560(14)	490(8)	160(5)	91.1(4.5)
Cl	355(40)	265(30)	360(25)	215(25)	660(30)	1000(35)	980(35)	2900(60)
Ca	4.0(.4)*	2.3(.3)*	1.8(.2)*	570(140)	260(110)	<170	<170	<140
Ti	<100	90(30)	50(20)	<50	<40	<30	<35	40(30)
V	6.4(.3)	7.5(.3)	7.1(.3)	7.6(.4)	6.6(.4)	2.4(.2)	2.7(.2)	20.4(.4)
Mn	268(1)	141(1)	77.1(.6)	61.1(.5)	72.6(.6)	60.0(.5)	79.9(6)	145(1)
Cu	<30	<30	16(14)	17(16)	23(17)	<20	21(10)	<30
Br	15(6)	4.5(4.4)	5.6(3.4)	<6.4	12.3(3.3)	8.9(3.1)	13.0(3.5)	120(5)
In	<.09	<.06	<.05	<.05	<.05	<.05	<.05	<.08
I	<11.5	<8.3	<6.6	<5.7	<6.5	<6.2	<6.7	<10

All values in ng/m^3, except values denoted by an asterisk(*), which are in ug/m^3.

(TABLE 21, continued)

Element	Stage 1	2	3	4	5	6	7	8
Run 2								
Fe (AA)	7600(550)	2920(440)	2780(440)	2390(440)	3470(440)	2500(440)	3600(440)	2500(440)
Zn (AA)	290(20)	130(20)	170(20)	310(20)	630(25)	770(25)	940(25)	520(25)
Run 3								
Fe (AA)	4960(490)	1880(490)	1840(490)	1510(490)	1340(490)	1100(490)	830(490)	1110(490)
Zn (AA)	320(20)	130(20)	140(20)	140(20)	190(20)	180(20)	140(20)	150(20)
Run 4								
Na	460(25)	200(15)	230(15)	225(15)	310(20)	315(20)	270(15)	375(20)
Mg	2.0(.5)*	1.3(.3)*	660(300)	925(275)	370(300)	680(310)	350(320)	<600
Al	1950(15)	1180(12)	1110(11)	1710(14)	1830(15)	478(8)	116(4)	35(3)
Cl	690(50)	300(25)	365(30)	285(30)	390(30)	690(30)	530(30)	790(40)
Ca	6.0(.4)*	3.6(.3)*	2.7(.3)*	2.5(.3)*	910(160)	500(110)	190(110)	<200
Ti	.65(.05)*	100(30)	90(30)	100(30)	130(30)	<45	<40	<45
V	8.4(.4)	4.3(.3)	3.9(.3)	4.3(.3)	4.0(.3)	1.9(.2)	1.8(.2)	7.9(.3)
Mn	415(1)	147(1)	113(1)	118(1)	113(1)	118(1)	131(1)	151(1)
Cu	40(21)	16(15)	<30	<35	25(17)	29(12)	<17	37(10)
Br	17(3)	17(4)	6.6(3.8)	16(4)	32(4)	22(4)	27(4)	33(4)
In	<.11	<.07	<.06	<.06	<.06	<.06	.10(.03)	.08(.03)
I	7.2(7.0)	<8.2	<6.2	<7.7	<7.7	<7.7	<6.2	<8.8
Fe (AA)	9050(620)	2610(420)	1750(420)	1750(420)	2040(420)	2020(420)	2870(420)	4050(420)
Zn (AA)	310(20)	150(20)	130(20)	150(20)	260(20)	290(20)	370(20)	420(20)

(TABLE 21, continued)

Element	Stage 1	2	3	4	5	6	7	8
Run 4 Duplicate Analyses								
Na	495(30)	190(12)	240(15)	205(12)	300(25)	310(20)	260(15)	390(20)
Mg	2.0(.6)*	1.1(.4)*	600(300)	900(300)	320(300)	650(350)	300(350)	<650
Al	1990(17)	1020(10)	1000(10)	1605(13)	1720(15)	460(8)	112(5)	32(3)
Cl	750(55)	260(25)	390(30)	305(25)	375(30)	670(30)	500(30)	810(35)
Ca	6.0(.4)*	3.2(.3)*	2.2(.4)*	2.0(.4)*	800(200)	400(150)	160(150)	<200
Ti	.55(.05)*	90(30)	75(35)	90(30)	100(30)	<40	<40	<40
V	7.6(.4)	4.4(.3)	3.2(.3)	4.0(.3)	4.1(.3)	1.8(.2)	1.8(.2)	7.9(.3)
Mn	425(1)	127(1)	110(1)	108(1)	108(1)	117(1)	118(1)	161(1)
Cu	36(20)	14(16)	<25	<30	26(14)	31(13)	<16	40(10)
Br	19(4)	16(4)	6.0(3.0)	15(5)	30(4)	23(4)	27(5)	35(5)
In	<.12	<.09	<.07	<.06	<.06	<.06	.10(.04)	.08(.04)
I	6.4(7.1)	<8.4	<6.1	<7.9	<7.8	<7.7	<7.1	<8.9
Run 2, 3, 4 Composite								
K	320(28)	250(20)	290(21)	300(22)	190(20)	150(20)	265(20)	820(30)
Cu	26.9(.6)	9.4(.5)	10.8(.5)	13.6(.5)	10.7(.5)	20.3(.5)	19.0(30)	41.5(.6)
Zn	456(35)	177(24)	148(25)	256(27)	406(26)	661(27)	685(30)	647(25)
Ga	.17(.32)	.42(.24)	.43(.25)	.71(.27)	.50(.25)	.26(.26)	.63(.29)	1.5(.3)
As	<2.4	<1.7	1.5(1.7)	1.0(1.8)	2.5(1.6)	3.1(1.7)	4.0(1.8)	20.9(2.0)
Br	3.7(.4)	3.7(.3)	7.4(.3)	8.8(.3)	6.3(.3)	7.5(.3)	11.3(.3)	32.6(.9)
Sb	5.5(.5)	4.0(.4)	5.1(.4)	5.6(.4)	5.0(.4)	5.5(.4)	6.5(.4)	15.9(.5)
La	.48(.18)	.47(.13)	.63(.13)	1.1(.1)	.77(.13)	.23(.13)	.08(14)	.16(31)
Eu	.036(.02)	.032(.01)	.011(.01)	.03(.01)	.01(.01)	<.01	<.01	.008(.01)
Sm	.20(.02)	.10(.02)	.14(.02)	.20(.02)	.14(.02)	.03(.02)	.003(.02)	.03(.02)
W	<.4	<.3	<.3	.17(.31)	<.3	.31(.28)	<.3	.12(.27)

(TABLE 21, continued)

Element	1	2	3	4	5	6	7	8
Run 2, 3, 4 Composite								
Sc	.83(.20)	.81(.16)	.78(.18)	1.0(.2)	.54(.2)	.16(.17)	.30(.16)	<.27
Cr	80(7)	18(5)	20(5)	15(5)	16(5)	8.6(6.0)	3.5(6.1)	2.7(6.6)
Fe	9450(900)	3385(750)	2970(700)	4900(800)	3500(800)	2040(700)	2800(700)	1670(800)
Co	.6(.7)	.81(.61)	.9(.8)	1.1(.8)	1.8(.8)	1.1(.8)	0.9(0.7)	1.0(1.2)
Zn	35(25)	240(30)	240(30)	290(35)	450(40)	650(45)	680(40)	725(60)
Se	.8(3.2)	<3.0	<2.9	<3.1	3.1(2.9)	.8(2.8)	1.4(2.8)	3.4(3.0)
Sb	5.3(1.3)	6.3(1.2)	5.7(1.1)	5.3(1.1)	7.0(1.2)	8.7(1.3)	6.5(1.3)	9.5(1.7)
Ce	7.4(2.1)	3.0(1.9)	4.2(2.0)	4.2(2.0)	1.9(2.0)	2.0(1.9)	1.8(2.0)	<3.0
Hg	2.6(4.3)	1.7(4.0)	.7(3.2)	.6(3.7)	<4.0	<4.1	2.6(3.8)	<3.0
Th	.36(.27)	.06(.22)	.30(.24)	.03(.22)	.19(.24)	.13(.23)	.16(.24)	<.40
Run 5								
Fe (AA)	10.1(.5)*	4.4(.5)*	2.0(.5)*	1.0(.5)*	<.5*	<.5*	<.5*	<.5*
Zn (AA)	580(100)	280(80)	230(75)	260(80)	220(75)	260(75)	190(70)	560(85)

TABLE 22: SINTER PLANT VICINITY, Concentrations and Standard Deviations #

Element	Stage 1	2	3	4	5	6	7	8
Run 6								
Fe (AA)	13.3(.6)*	6.3(.5)*	1.1(.4)*	<.5*	<.5*	<.5*	<.5*	<.5*
Zn (AA)	660(95)	400(85)	260(80)	220(80)	230(80)	140(80)	120(75)	330(100)
Run 7								
Na	200(25)	130(15)	95(15)	99(12)	135(15)	195(20)	170(15)	350(35)
Mg	850(580)	360(300)	<550	<470	<500	<600	<500	<1200
Al	1310(15)	604(9)	602(9)	356(7)	209(5)	363(7)	73.5(3.6)	67(5)
Cl	510(45)	310(30)	350(25)	305(25)	830(35)	1640(45)	1130(35)	10.2(.1)*
Ca	4.9(.4)*	1.6(.2)*	1.6(.2)*	540(150)	1.0(90)	<300	<200	<200
Ti	110(40)	60(20)	<50	<40	<40	<45	<35	<60
V	10.9(.4)	8.4(.3)	12.6(.4)	13.7(.3)	11.2(.3)	8.0(.3)	4.3(.2)	22(.5)
Mn	408(1)	106(1)	78.3(.6)	53.1(.5)	49.7(.5)	46.9(.5)	34.9(.4)	47.2(.5)
Cu	37(21)	<26	37(14)	32(11)	22(11)	36(12)	25(9)	19(18)
Br	6(5)	7(4)	14(4)	14(3)	32(3)	43(4)	30(3)	300(6)
In	<.12	<.06	<.05	<.05	<.05	<.05	.05(.02)	.15(.04)
I	<15	<7.8	<6.9	<5.6	<5.9	<6.2	<5.4	<9.5
Fe (AA)	16.1(.5)*	4050(350)	3620(350)	2610(350)	1750(350)	1580(350)	2040(350)	1060(350)
Zn (AA)	860(40)	470(20)	440(20)	270(20)	490(20)	860(20)	300(20)	400(20)
Run 8								
Fe (AA)	19.8(15)*	6300(320)	4000(320)	2770(320)	3300(320)	3580(320)	3550(320)	3360(320)
Zn (AA)	7730(30)	4230(30)	1870(30)	620(30)	380(30)	290(30)	320(30)	400(30)

All values in ng/m^3, except values denoted by an asterisk(*), which are in ug/m^3.

(TABLE 22, continued)

Element	Stage 1	2	3	4	5	6	7	8
Run 9								
Na	320(35)	150(25)	86(25)	90(15)	110(12)	90(10)	115(10)	310(30)
Mg	3.8(.8)*	2.7(.5)*	2.2(.5)*	0.8(.3)*	0.3(.2)*	<370	<350	<970
Al	1280(13)	864(11)	655(9)	350(7)	183(5)	39.7(2.7)	34.4(2.6)	19.2(3.8)
Cl	390(65)	410(50)	460(40)	425(30)	510(30)	450(25)	610(25)	7250(85)
Ca	12.3(.6)*	7.2(.5)*	6.4(.4)*	2.8(.3)*	1.0(.2)*	110(80)	50(50)	190(110)
Ti	130(55)	125(45)	<80	<30	<35	<25	20(15)	<30
V	9.1(.5)	6.7(.4)	5.4(.3)	3.2(.2)	2.2(.2)	1.1(.1)	1.4(.1)	17.5(.4)
Mn	906(.2)	480(.1)	348(.1)	155(.8)	57.4(.5)	23.8(.3)	25.5(.3)	26.5(.4)
Cu	<50	17(17)	59(15)	17(11)	9(7)	10(6)	6(6)	20(15)
Br	33(11)	19(8)	20(7)	26(4)	17(3)	7.6(1.9)	20(2)	110(4)
In	<.11	<.11	<.13	<.07	<.04	<.03	.02(.02)	.04(.03)
I	<21	<15	<16	<8.5	<5.5	<3.7	<2.5	<7.3
Fe (AA)	20000(460)	5270(310)	3360(310)	1700(310)	1110(310)	640(310)	880(310)	390(310)
Zn (AA)	3110(30)	550(30)	400(30)	180(30)	160(30)	1650(30)	200(30)	250(30)
Run 10								
Fe (AA)	21600(460)	6400(310)	5180(310)	3020(310)	2980(310)	2670(310)	1230(310)	1200(310)
Zn (AA)	760(30)	520(30)	480(30)	250(30)	420(30)	590(30)	490(30)	570(30)
Run 7, 8, 9, 10 Composite								
K	600(20)	290(13)	260(12)	150(10)	200(12	215(12)	325(12)	1715(25)
Cu	23.5(.4)	11.1(.3)	16.8(.3)	7.6(.2)	12.1(.2)	11.1(.2)	10.2(.2)	32.3(.5)
Zn	3720(28)	1020(17)	914(16)	380(12)	620(14)	563(14)	345(13)	472(22)
Ga	<.3	<.2	.47(.16)	.41(.13)	.34(.14)	.40(.14)	.08(.13)	2.4(.2)
As	7.1(1.9)	2.4(1.1)	3.5(1.1)	2.6(.9)	1.3(1.1)	3.8(1.0)	3.4(1.0)	11.8(1.6)
Br	8.7(.4)	5.8(.2)	7.8(.2)	7.2(.2)	11.9(.2)	13.9(.2)	16.9(.2)	87(1)

(TABLE 22. continued)

Element	Stage 1	2	3	4	5	6	7	8
Run 7, 8, 9, 10 Composite								
Sb	3.1(.6)	2.4(.4)	3.3(.4)	2.8(.3)	5.7(.3)	3.2(.3)	3.0(.3)	7.0(.3)
La	.83(.10)	.28(.07)	.38(.06)	.38(.05)	.36(.06)	.14(.06)	.07(.05)	.09(.24)
Eu	.075(.008)	.033(.005)	.030(.010)	.015(.005)	.010(.010)	.003(.005)	.002(.005)	.02(.01)
Sm	.31(.02)	.14(.01)	.12(.01)	.053(.011)	.049(.011)	.01(.01)	<.01	.03(.02)
W	.16(.24)	<.1	<.1	<.1	.09(.14)	.14(.13)	.21(.12)	.17(.21)
Sc	1.4(.3)	.62(.21)	.47(.20)	.31(.17)	<.21	<.2	<.18	<.20
Cr	45(7)	12(5)	12(5)	7.8(6.0)	6.7(6.1)	3.6(5.9)	12.4(5.9)	12.6(5.4)
Fe	26.8(1.8)*	7.8(1.2)*	6.3(1.1)*	2.4(.8)*	1.9(.8)*	2.6(.9)*	1.5(.8)*	.9(.6)*
Co	3.9(1.1)	1.3(1.0)	.7(1.1)	1.3(1.0)	,6(1.0)	.3(.9)	.4(1.0)	1.1(1.0)
Zn	2940(90)	780(50)	665(45)	250(35)	380(35)	395(38)	260(33)	555(50)
Se	3.5(4.1)	.5(3.0)	<3.3	<3.1	<3.0	<3.0	<2.7	3.0(2.5)
Sb	5.0(1.6)	1.9(1.2)	1.9(1.1)	2.5(1.1)	5.2(1.3)	3.2(1.1)	2.4(1.1)	9.1(1.3)
Ce	2.5(2.3)	2.3(1.9)	1.0(2.0)	1.5(1.7)	2.5(1.7)	<1.9	<1.8	<2.2
Hg	5.6(5.2)	1.8(3.8)	1.8(3.9)	1.2(3.6)	<3.8	<3.7	1.6(3.6)	<2.5
Th	.30(.50)	.26(.40)	.20(.38)	.32(.36)	<.37	.20(.37)	<.4	<.33

TABLE 23: BLAST FURNACE VICINITY, Concentrations and Standard Deviations #

Element	Stage 1	2	3	4	5	6	7	8
Run 11								
Cl	440(90)	200(80)	200(80)	190(80)	70(70)	180(80)	1070(150)	-
Mn	265(10)	80(5)	80(5)	55(4)	50(4)	35(5)	90(6)	-
Fe (AA)	19.2(.5)*	3.1(.5)*	1.0(.5)*	<.5*	<.5*	<.5*	<.5*	-
Zn (AA)	1300(100)	250(100)	310(100)	300(90)	270(90)	210(90)	550(100)	1190(110)

All values in ng/m^3, except values denoted by an asterisk(*), which are in ug/m^3.

TABLE 24: CENTRAL FIRE STATION, EAST CHICAGO, INDIANA. Concentrations and Standard Deviations #

Element	Stage 1	2	3	4	5	6	7	8
Run 12								
Na	56(6)	64(6)	59(6)	33(5)	28(5)	55(6)	62(6)	-
Mg	580(200)	330(200)	330(200)	110(100)	<100	<100	<100	-
Al	619(5)	406(4)	465(5)	500(5)	192(3)	129(2)	70(2)	-
Cl	140(10)	210(20)	170(15)	150(15)	170(15)	210(20)	320(25)	-
Ti	<10	27(12)	48(14)	14(12)	14(12)	<10	<10	-
V	1.8(.2)	1.4(.1)	2.3(.2)	1.7(.2)	1.4(.1)	1.0(.1)	0.8(.1)	-
Mn	31.5(.2)	16.2(.2)	22.4(.2)	20.1(.2)	24.7(.2)	35.0(.3)	34.2(.3)	-
Cu	7(4)	6(5)	7(5)	8(5)	5(4)	4(4)	4(4)	-
Br	7(2)	6(1)	14(2)	20(2)	17(2)	15(2)	14(2)	-
Fe (AA)	850(65)	240(60)	220(50)	120(50)	60(50)	<50	<50	<50
Zn (AA)	180(30)	130(30)	130(30)	130(30)	180(30)	230(35)	210(35)	190(35)
Run 13								
Fe (AA)	460(25)	210(20)	170(15)	170(15)	150(15)	110(15)	110(15)	120(25)
Zn (AA)	55(10)	41(8)	66(10)	83(10)	140(12)	120(12)	110(12)	64(10)

All values in ng/m^3, except values denoted by an asterisk(*), which are in ug/m^3.

(TABLE 24, continued)

Element	Stage 1	2	3	4	5	6	7	8
Run 14								
Na	135(10)	145(10)	100(7)	125(8)	100(7)	135(8)	160(9)	175(9)
Mg	300(150)	260(160)	340(150)	<150	<150	<150	<150	<150
Al	441(17)	508(20)	610(10)	490(10)	225(5)	90(3)	60(2)	50(2)
Cl	125(15)	190(15)	130(12)	195(20)	110(11)	112(15)	200(15)	290(20)
Ca	885(125)	760(120)	620(110)	240(80)	300(80)	<80	<80	<80
Ti	25(10)	38(12)	50(13)	13(10)	<12	<10	<10	<12
V	1.5(.1)	1.4(.1)	1.3(.1)	1.1(.1)	0.7(.1)	0.4(.1)	0.9(.1)	1.0(.1)
Mn	18(1)	21(1)	21(2)	15(2)	28(2)	43(3)	52(3)	24(2)
Cu	45(10)	64(11)	39(8)	43(7)	31(6)	26(6)	64(6)	40(6)
Br	9(1)	21(2)	19(2)	19(2)	20(2)	17(2)	24(2)	92(2)
In	<.1	<.1	<.1	<.1	<.1	<.1	<.1	<.1
Fe (AA)	490(100)	320(50)	300(50)	210(25)	170(25)	110(25)	90(25)	80(25)
Zn (AA)	87(10)	78(10)	90(10)	105(10)	235(20)	490(20)	1000(25)	720(25)
Run 15								
Na	140(8)	67(6)	60(5)	73(6)	78(6)	58(6)	92(7)	36(7)
Mg	450(120)	<180	220(120)	<140	250(160)	<200	<300	<225
Al	317(4)	285(4)	224(4)	163(3)	108(3)	61.8(2.2)	18.0(1.4)	10.7(1.2)
Cl	360(15)	240(10)	160(10)	310(15)	340(15)	245(15)	220(15)	235(15)
Ca	710(110)	410(80)	410(80)	330(70)	120(50)	55(40)	25(25)	<50
Ti	<40	21(15)	43(18)	22(14)	24(17)	26(12)	<20	<50
V	1.7(.1)	1.5(.1)	1.3(.1)	1.4(.1)	.9(.1)	.4(.1)	1.0(.1)	5.5(.1)
Mn	14.7(.2)	15.2(.2)	10.7(.2)	8.9(.1)	9.2(.1)	16.4(.2)	24.8(.2)	17.1(.2)
Cu	32(6)	27(6)	24(6)	18(6)	10(6)	4.7(4.5)	15(5)	14(5)
Br	3.7(1.1)	7.4(.9)	11(1)	14(1)	13(1)	9.2(1.2)	16(1)	57(2)
In	<.015	<.02	<.01	<.02	<.02	.02(.01)	.02(.01)	<.02
I	<2.3	<2.1	<1.9	<2.1	<2.2	<2.2	<2.8	<2.8

(TABLE 24, continued)

Element	Stage 1	2	3	4	5	6	7	8
Run 15								
Fe (AA)	1190(310)	480(310)	320(240)	290(240)	220(240)	320(240)	340(240)	340(240)
Zn (AA)	20(13)	21(13)	26(13)	29(13)	115(13)	105(13)	81(13)	92(13)
Run 16								
Fe (AA)	1560(290)	460(290)	300(220)	230(220)	160(220)	300(220)	160(220)	380(220)
Zn (AA)	51(10)	20(10)	36(10)	51(10)	88(10)	97(10)	44(10)	44(10)
Run 17								
Na	185(15)	205(15)	210(20)	210(15)	250(15)	145(12)	140(10)	140(10)
Mg	470(260)	1.1(.3)*	290(200)	230(230)	255(220)	200(180)	<500	<220
Al	918(10)	654(9)	499(7)	425(7)	367(6)	57(3)	35(2)	14(1)
Cl	205(20)	190(25)	215(25)	360(25)	410(25)	325(20)	125(20)	31(21)
Ca	2.3(.2)*	2.1(.3)*	1.0(.2)*	640(130)	770(130)	180(80)	80(50)	<75
Ti	70(20)	55(20)	28(25)	<25	<25	<25	<25	<35
V	12.9(.3)	10.5(.3)	11.0(.3)	12.7(.3)	8.6(.3)	6.5(.2)	10.5(.2)	80.6(.7)
Mn	59.6(.5)	125(1)	46.3(.4)	59.2(.5)	47.2(.4)	35.5(.4)	20.0(.3)	15.7(.2)
Cu	14(13)	31(12)	10(9)	14(11)	<14	<14	<14	26(15)
Br	6.4(2.7)	18(4)	14(2)	14(3)	47.2(.4)	14(2)	7.2(1.8)	16(2)
Ir	<.04	<.06	<.04	<.04	.04(.02)	.03(.02)	.01(.01)	.06(.02)
I	<5.5	<7.5	8.1(2.6)	<2.8	3.8(2.6)	<4.2	<3.1	1.7(1.7)
Fe (AA)	2000(300)	960(300)	610(220)	510(220)	500(220)	350(220)	310(220)	150(220)
Zn (AA)	163(13)	87(13)	94(13)	151(13)	235(13)	284(13)	244(13)	185(13)

(TABLE 24, continued)

Element	Stage 1	2	3	4	5	6	7	8
Run 15, 16, 17 Composite								
K	91(10)	71(8)	63(9)	40(8)	20(8)	30(7)	49(7)	140(14)
Cu	7.6(.2)	7.0(.2)	6.9(.2)	4.7(.2)	3.2(.2)	4.1(.2)	4.9(.2)	15.9(.3)
Zn	31(10)	20(9)	37(10)	37(10)	83(9)	115(9)	78(8)	86(9)
Ga	.04(.13)	.09(.11)	.12(.10)	.02(.10)	.07(.09)	<.1	.10(.10)	.74(.17)
As	1.2(.8)	.89(.74)	1.0(.7)	.44(.76)	.61(.74)	.71(.71)	1.12(.74)	3.2(1.2)
Br	11.2(.5)	13.6(.4)	21.9(.5)	30.9(.5)	15.1(.4)	14.0(.4)	13.9(.4)	19.3(.6)
Sb	2.4(.1)	1.0(.1)	1.5(.1)	2.9(.1)	1.3(.1)	1.3(.1)	1.8(.1)	5.5(.2)
La	1.7(.1)	.98(.11)	1.3(.1)	1.2(.1)	1.4(.1)	.45(.10)	.02(.09)	.31(.18)
Eu	.004(.004)	.007(.004)	.007(.004)	.008(.004)	.002(.004)	.001(.003)	<.003	.006(.007)
Sm	.10(.01)	.06(.01)	.06(.01)	.04(.01)	.05(.01)	.015(.01)	.007(.01)	.01(.01)
W	.03(.08)	.13(.09)	.02(.09)	.12(.09)	<.09	<.09	.10(.09)	.08(.14)
Sc	.39(.19)	.14(.14)	.13(.16)	.10(.16)	.09(.19)	.03(.16)	.02(17)	.05(.19)
Cr	15.7(5.4)	6.7(4.3)	7.9(4.4)	6.3(4.3)	5.6(4.2)	4.9(4.2)	214(5.6)	4.4(5.1)
Fe	1365(670)	1270(670)	680(670)	585(650)	680(660)	585(660)	195(660)	220(440)
Co	.3(.9)	.3(.9)	.1(1.0)	.26(.90)	.26(.90)	.26(.90)	.26(.90)	.40(.93)
Zn	39(31)	22(25)	31(32)	27(31)	93(33)	118(40)	105(35)	95(30)
Se	.8(3.4)	<3.6	<3.6	<3.6	1.4(3.6)	1.8(3.3)	1.6(3.2)	2.9(2.1)
Sb	3.0(1.1)	2.5(.9)	2.6(1.0)	4.1(1.0)	2.1(1.0)	1.8(1.0)	1.6(1.1)	5.3(1.0)
Ce	2.3(1.7)	1.4(1.8)	.8(2.0)	.7(1.8)	.3(2.0)	<2.0	<2.0	<2.5
Hg	.5(2.2)	.6(2.2)	<2.1	<2.6	<2.5	.9(2.6)	.3(2.8)	.6(2.1)
Th	.15(.23)	<.28	<.29	<.26	<.26	<.26	<.30	<.30
Run 18								
Na	125(10)	105(10)	108(10)	98(8)	68(8)	62(8)	73(8)	150(12)
Mg	470(290)	320(160)	450(215)	240(160)	<330	<330	<300	<390
Al	606(9)	569(8)	687(9)	547(8)	215(5)	125(4)	55(3)	30(2)
Cl	215(20)	112(12)	100(15)	125(15)	95(12)	125(12)	145(15)	31(18)

(TABLE 24, continued)

Element	Stage 1	2	3	4	5	6	7	8
Run 18								
Ca	920(170)	600(140)	720(140)	510(140)	60(85)	60(60)	<150	<100
Ti	70(20)	40(15)	30(20)	45(25)	30(20)	18(20)	<25	<100
V	19.2(.4)	25.7(.4)	42.2(.5)	38.5(.5)	27.2(.4)	8.5(.2)	5.5(.2)	20.5(.4)
Mn	15.8(.3)	7.1(.2)	12.3(.2)	15.6(.3)	6.3(.2)	6.9(.2)	14.1(.2)	13.7(.2)
Cu	<16	<20	<22	<20	<15	<10	<10	12(9)
Br	73(3)	63(2)	92(3)	108(3)	102(3)	175(3)	115(3)	160(3)
In	<.04	<.03	<.03	<.04	<.03	.02(.02)	.03(.02)	<.04
I	<4.2	<3.4	<4.3	<4.4	<3.5	<4.2	<3.8	<4.4
Fe (AA)	510(160)	250(160)	530(160)	550(160)	440(160)	360(160)	300(160)	150(160)
Zn (AA)	243(19)	185(19)	226(19)	165(19)	149(19)	138(19)	127(19)	97(19)
K	125(16)	118(14)	118(14)	105(11)	73(13)	72(11)	66(11)	122(14)
Cu	6.9(.4)	6.4(.4)	8.1(.4)	7.4(.4)	9.5(.4)	10.2(.4)	12.5(.4)	5.1(.4)
Zn	240(20)	163(21)	144(20)	93(19)	165(24)	84(23)	58(20)	54(16)
Ga	.24(.23)	.24(.22)	.16(.20)	.07(.20)	<.24	.33(.21)	.14(.20)	.19(.19)
As	3.2(2.4)	<2.3	<2.2	.95(2.3)	1.6(2.7)	<2.6	<2.6	<2.3
Br	112(1)	102(1)	84(1)	102(1)	202(2)	195(1)	161(1)	135(1)
Sb	2.4(.5)	2.1(.4)	2.2(.5)	3.3(.5)	2.7(.6)	3.8(.6)	5.6(.6)	7.4(.6)
La	2.0(.2)	1.4(.2)	1.2(.2)	1.4(.2)	1.2(.2)	.05(.21)	.14(.20)	.05(.22)
Eu	.04(.01)	.04(.01)	.03(.01)	.03(.01)	.02(.01)	.01(.01)	<.01	<.01
Sm	.19(.02)	.20(.02)	.20(.02)	.15(.02)	.11(.02)	.09(.02)	.01(.02)	.03(.02)
W	.31(.24)	.20(.22)	.08(.24)	<.26	<.31	.08(.26)	.19(.27)	.13(.24)

(TABLE 24, continued)

Element	Stage 1	2	3	4	5	6	7	8
Run 18								
Sc	.69(.31)	.51(.29)	.48(.31)	.27(.26)	.29(.28)	.19(.21)	.05(.28)	<.33
Cr	73(10)	7.6(10.1)	7.0(10.6)	2.5(9.1)	3.2(9.1)	6.3(7.8)	7.0(9.8)	<10.0
Fe	800(1200)	265(1200)	1340(1100)	1330(1200)	800(1200)	535(1200)	800(1200)	<1300
Co	1.0(1.9)	1.1(1.8)	1.3(1.9)	.6(2.0)	.3(1.6)	.3(1.6)	.3(1.6)	<2.1
Zn	305(70)	145(60)	112(60)	117(65)	143(65)	74(52)	51(53)	58(54)
Se	<5.0	<5.1	<5.1	<5.0	<5.0	1.6(5.0)	<5,1	<4.8
Sb	2.3(2.2)	2.7(2.2)	2.8(2.1)	3.0(2.1)	3.0(2.1)	3.6(2.1)	5.2(2.2)	6.5(1.6)
Ce	2.9(5.4)	3.0(4.9)	3.2(5.3)	1.5(4.6)	2.9(4.6)	2.9(4.3)	<6.0	<6.0
Hg	.6(4.1)	<3.9	<3.8	<3.6	<3.8	<4.0	<3.9	<3.9
Th	<.86	<.81	<.80	<.79	<.78	<.81	<.80	<.74
Run 19								
Na	300(4)	190(3)	145(3)	103(3)	78(2)	72(2)	55(2)	-
Mg	160(60)	100(45)	160(40)	45(40)	30(40)	15(35)	10(30)	-
Al	295(3)	225(3)	206(3)	154(2)	45(1)	10.7(.7)	15.9(.8)	-
Cl	450(7)	300(5)	228(5)	190(4)	170(4)	106(4)	26(2)	-
Ca	440(60)	360(55)	230(50)	200(40)	45(25)	15(15)	15(8)	-
Ti	10(7)	14(4)	7.6(6.0)	6.2(5.9)	4.8(4.8)	1.3(4.8)	2.6(4.8)	-
V	3.8(.1)	3.7(.1)	4.7(.1)	5.7(.1)	3.1(.1)	3.1(.1)	6.2(.1)	-
Mn	13.0(.1)	7.5(.05)	8.0(.05)	10.6(.06)	12.8(.07)	13.5(.07)	8.1(.05)	-
Cu	2.0(4.3)	6.0(3.8)	9.3(3.8)	5.0(3.6)	3.4(2.6)	3.0(2.1)	7.3(2.8)	-
Br	8.2(.5)	8.5(.4)	13.2(.4)	21.1(.5)	14.0(.5)	11.9(.4)	10.6(.4)	-
In	<.02	.003(.003)	.02(.003)	.06(.004)	.10(.004)	.08(.004)	.04(.003)	-
I	6.8(4.6)	<.73	<.74	<.83	<.84	<.80	<.66	-
Fe (AA)	540(40)	440(40)	400(30)	270(30)	230(30)	160(30)	80(130)	-
Zn (AA)	31(4)	37(4)	79(4)	145(4)	248(4)	137(4)	76(4)	

(TABLE 24, continued)

Element	Stage 1	2	3	4	5	6	7	8
Run 19								
K	66(6)	54(5)	52(4)	55(5)	38(4)	34(3)	22(3)	-
Cu	4.30(.14)	3.25(.11)	3.56(.10)	3.88(.11)	3.62(.10)	2.95(.09)	2.46(.08)	-
Zn	26(7)	34(5)	69(5)	146(6)	200(5)	135(4)	47(3)	-
Ga	.13(.11)	.14(.08)	.17(.05)	.38(.07)	.21(.05)	.14(.04)	.11(.03)	-
As	<.52	<.41	.64(.36)	1.4(.4)	3.6(.3)	2.25(.3)	1.7(.2)	-
Br	9.0(.3)	10.6(.2)	13.5(.1)	26.7(.2)	15.7(.1)	10.3(.1)	8.9(.1)	-
Sb	1.9(.1)	1.7(.1)	2.3(.1)	5.8(.1)	7.4(.1)	3.6(.1)	1.7(.1)	-
La	.45(.09)	.40(.07)	.43(.04)	.84(.05)	.28(.04)	.05(.03)	<.03	-
Eu	.014(.004)	.011(.003)	.003(.002)	.003(.002)	.003(.002)	.002(.002)	<.001	-
Sm	.022(.006)	.035(.005)	.037(.004)	.051(.004)	.013(.004)	.001(.003)	.002(.003)	-
W	<.1	<.1	.03(.06)	.08(.08)	.08(.06)	.02(.05)	<.05	-
Sc	.31(.02)	.13(.01)	.10(.01)	.11(.01)	.035(.02)	.02(.03)	.011(.02)	-
Cr	5.3(0.5)	3.9(.5)	2.0(.5)	3.0(.5)	3.2(.6)	.22(.50)	.70(.5?)	-
Fe	655(65)	415(60)	325(55)	300(55)	310(60)	40(50)	30(50)	-
Co	.39(.10)	.25(.10)	.15(.10)	.23(.10)	.08(.10)	.12(.10)	.06(.10)	-
Zn	45(3)	39(3)	62(3)	175(5)	300(?)	200(5)	65(4)	-
Se	.26(.19)	.11(.18)	.15(.18)	.37(.22)	.20(.28)	.12(.23)	<.4	-
Sb	1.5(.1)	1.9(.1)	2.7(.1)	6.7(.2)	7.9(.2)	4.7(.2)	2.1(.2)	-
Ce	.96(.19)	.26(.18)	.39(.18)	.47(.21)	.05(.22)	<.2	<.4	-
Hg	.21(.18)	.42(.17)	.52(.18)	.64(.20)	.19(.24)	<.2	<.4	-
Th	.029(.026)	.020(.02)	.071(.02)	.049(.03)	.016(.03)	<.03	<.05	-
Run 12 Duplicate Analyses								
Fe (AA)	570(4)	460(40)	410(30)	250(30)	240(30)	200(30)	60(30)	-
Zn (AA)	30(4)	39(4)	84(4)	150(4)	250(4)	129(4)	84(4)	-

TABLE 25: MARKSTOWN PARK, EAST CHICAGO, INDIANA, Concentrations and Standard Deviations #

Element	Stage 1	2	3	4	5	6	7	8
Run 20								
Na	90(10)	95(10)	140(10)	150(10)	145(10)	150(10)	135(10)	115(12)
Mg	330(210)	175(190)	300(190)	175(200)	<320	<380	<400	<450
Al	417(7)	408(7)	560(8)	525(7)	172(4)	117(4)	75(3)	62(3)
Cl	160(20)	190(20)	300(20)	300(20)	420(25)	300(20)	185(20)	440(30)
Ca	1.2(.2)*	920(180)	1.1(.2)*	770(150)	460(100)	130(80)	50(50)	<75
Ti	<25	<23	35(17)	26(18)	<28	<20	<20	<35
V	3.8(.2)	4.0(.2)	7.4(.3)	8.1(.3)	5.8(.2)	3.2(.2)	5.2(.2)	32.7(.4)
Mn	49.4(.4)	32.8(.4)	41.5(.4)	40.4(.4)	39.5(.4)	40.6(.4)	42.3(.4)	37.6(.4)
Cu	34(11)	30(10)	40(11)	89(12)	17(8)	<10	<10	14(12)
Br	4.0(2.6)	13(2)	37(3)	56(3)	55(3)	31(3)	39(3)	205(4)
In	<.02	.02(.02)	.03(.02)	.02(.02)	.13(.02)	.12(.02)	.15(.02)	.14(.02)
I	<5.0	<4.4	<4.9	<5.0	<5.1	<4.8	<4.9	<5.6
Fe (AA)	1080(150)	710(150)	320(150)	290(150)	150(150)	<150	<150	<150
Zn (AA)	113(18)	83(18)	113(18)	130(18)	357(18)	299(18)	216(18)	226(18)
K	185(15)	80(13)	110(22)	80(18)	46(14)	39(12)	42(9)	75(20)
Cu	65(1)	41(1)	38.2(.3)	11.6(.3)	8.3(.3)	3.0(.3)	2.6(.3)	3.0(.3)
Zn	69(16)	10.2(20.1)	20(14)	67(15)	184(20)	242(18)	152(18)	52(20)
Ga	<.17	<.13	<.14	<.13	<.16	<.15	<.15	.30(.26)
As	<1.5	<1.4	.7(1.4)	1.2(1.5)	1.0(1.4)	1.3(1.5)	1.2(.9)	3.6(1.5)
Br	4.6(.6)	11.3(.7)	32.2(.4)	50.1(.4)	54.1(.5)	28.8(.3)	24.0(.4)	80(8)
Sb	1.9(.3)	1.9(.2)	3.4(.2)	4.3(.2)	10.5(.3)	12.4(.4)	4.4(.2)	3.3(.2)
La	.52(.17)	.51(.16)	.30(.19)	.18(.20)	.08(.22)	.06(.23)	<.27	<.25
Eu	.02(.006)	.01(.004)	.007(.006)	.006(.006)	<.006	<.006	<.006	<.01
Sm	.16(.01)	.12(01)	.13(.01)	.08(.01)	.09(01)	.09(.01)	<.01	<.02
W	.06(.15)	.13(.17)	.17(.17)	.11(.2)	.14(.18)	.07(.16)	.36(.27)	.09(.26)

All values in ng/m^3, except values denoted by an asterisk(*), which are in ug/m^3.

(TABLE 25, continued)

Element	Stage 1	2	3	4	5	6	7	8
Run 20								
Sc	.29(.11)	.10(.11)	.14(.11)	.08(.12)	.04(.12)	<.13	.01(.12)	.07(.32)
Cr	13.0(4.0)	12.7(4.1)	19.0(4.1)	8.3(3.9)	5.7(3.9)	4.3(3.8)	1.7(4.0)	3.7(9.0)
Fe	1380(500)	950(500)	310(550)	320(550)	200(550)	<500	<500	<1000
Co	.1(.6)	.1(.6)	.1(.7)	.1(.7)	.1(.7)	<.6	.1(.6)	.2(2.0)
Zn	62(20)	12(17)	25(20)	51(19)	110(26)	240(31)	102(27)	67(45)
Se	1.3(1.1)	.4(1.0)	.5(1.0)	<1.1	.2(1.0)	.1(1.1)	.4(1.0)	1.0(3.0)
Sb	2.1(1.0)	5.5(1.1)	7.2(1.2)	6.5(1.1)	6.6(1.1)	9.5(1.2)	8.0(1.1)	4.5(2.1)
Ce	1.8(1.3)	1.9(1.3)	2.3(1.4)	2.5(1.4)	4.5(1.4)	.6(1.3)	.2(1.2)	<2.0
Hg	.4(2.6)	2.3(2.8)	2.4(2.7)	2.0(2.8)	0.7(2.8)	1.8(2.9)	2.0(2.7)	.3(4.2)
Th	.13(.20)	.12(.19)	.27(.18)	.24(.19)	.22(.18)	.13(.18)	<.20	<.35
Run 21								
Na	71(8)	47(8)	55(8)	68(8)	84(9)	98(10)	62(8)	88(7)
Mg	<380	<380	<360	130(160)	<380	<380	<400	<400
Al	225(5)	283(6)	312(6)	206(5)	170(5)	143(4)	17(2)	17(2)
Cl	53(11)	95(12)	56(13)	73(12)	140(16)	135(15)	92(12)	120(12)
Ca	350(115)	350(120)	320(90)	175(120)	<120	<110	<100	<115
Ti	<40	<20	<25	<30	<35	<35	<35	<35
V	2.0(.2)	2.3(.2)	5.0(.2)	3.6(.2)	4.8(.2)	3.5(.2)	3.2(.2)	24.7(.4)
Mn	13.2(.2)	10.9(.2)	16.1(.3)	13.6(.2)	26.3(.3)	27.4(.4)	14.8(.3)	14.3(.2)
Cu	53(9)	59(10)	33(10)	18(9)	18(8)	5(8)	6(6)	10(11)
Br	114(3)	140(3)	120(3)	87(3)	185(4)	144(3)	200(4)	160(4)
In	.05(.02)	<.04	<.03	<.03	<.04	<.04	<.04	<.04
I	<4.0	<4.5	<3.9	<4.1	<5.0	<5.0	<5.1	<4.5
Fe (AA)	660(170)	420(170)	170(170)	120(170)	30(170)	<170	<170	<170
Zn (AA)	227(17)	87(17)	70(17)	84(17)	134(17)	121(17)	109(17)	165(17)

(TABLE 25, continued)

Element	Stage 1	2	3	4	5	6	7	8
Run 21								
K	57(16)	54(17)	51(16)	29(14)	40(14)	36(16)	40(14)	76(16)
Cu	80.8(.6)	64.8(.6)	27.6(.5)	24.3(.4)	18.9(.5)	9.0(.4)	12.0(.5)	9.7(.5)
Zn	13(15)	11(12)	16(10)	41(22)	104(20)	94(20)	58(20)	157(21)
Ga	.16(.20)	.11(.21)	.13(.20)	.08(.21)	.10(.24)	.11(.21)	.13(.23)	.38(.24)
As	<2.2	<2.5	<2.1	<2.2	2.8(2.6)	2.1(2.0)	3.2(2.7)	3.6(.6)
Br	112(1)	188(1)	122(1)	122(1)	247(2)	172(1)	350(2)	71(1)
Sb	4.0(.4)	3.1(.5)	1.2(.4)	3.2(.5)	4.7(.6)	5.8(.6)	5.0(.6)	4.1(.6)
La	2.7(.2)	3.1(.2)	5.1(.2)	7.3(.2)	5.2(.3)	.59(.20)	<.20	<.3
Eu	.012(.01)	.014(.01)	.02(.01)	.02(.01)	.01(.01)	<.01	<.01	<.008
Sm	.08(.02)	.12(03)	.17(.02)	.28(.02)	.14(.02)	.09(.02)	.008(.02)	<.02
W	.11(.23)	.08(.24)	.11(.23)	.06(.20)	<.27	<.25	<.27	<.3
Sc	.37(.37)	.27(.32)	.11(.37)	.08(.35)	.08(.37)	.11(.37)	.19(.37)	.08(.36)
Cr	3.9(10.1)	6.8(8.3)	2.9(8.1)	2.9(7.9)	2.9(7.5)	1.9(8.3)	2.4(8.7)	2.8(8.1)
Fe	660(640)	330(640)	495(640)	495(790)	330(790)	330(790)	165(790)	320(790)
Co	.7(1.6)	1.5(1.3)	1.5(1.3)	.8(1.3)	.8(1.3)	.5(1.7)	.5(1.3)	.5(1.3)
Zn	16(56)	11(54)	16(56)	38(46)	127(64)	94(60)	70(60)	95(60)
Se	<4.3	<4.2	<4.2	<4.1	<4.7	2.0(4.7)	<4.7	1.4(4.2)
Sb	9.1(3.3)	12.6(3.4)	6.0(2.4)	6.0(2.3)	7.9(2.4)	10.5(3.5)	14.0(3.6)	10.7(3.3
Ce	5.6(4.1)	4.3(4.1)	9.2(4.1)	9.9(4.1)	1.6(4.1)	.5(4.1)	<4.1	<4.0
Hg	1.8(3.6)	.8(3.6)	2.0(3.2)	.6(3.6)	.8(3.5)	1.4(3.5)	1.0(3.8)	.8(4.2)
Th	.51(.44)	.40(.43)	.08(.43)	<.4	<.5	<.6	<4.4	.30(.44)

(TABLE 25, continued)

Element	Stage 1	2	3	4	5	6	7	8
Run 21 Duplicate Sample								
Na	66(6)	51(10)	50(8)	66(8)	91(10)	99(10)	52(7)	80(7)
Mg	<350	<350	<325	130(150)	<350	<360	<400	<400
Al	205(5)	270(6)	298(6)	200(5)	160(5)	125(4)	37(3)	30(4)
Cl	48(10)	100(15)	51(15)	70(12)	150(18)	126(15)	81(10)	102(12)
Ca	300(110)	300(100)	280(80)	160(80)	<125	<110	<100	<110
Ti	8(35)	<25	<20	<25	<30	<35	<35	<35
V	2.0(.2)	2.0(.2)	4.6(.3)	3.5(.3)	4.4(.3)	3.8(.3)	3.0(.2)	29.0(.6)
Mn	11.6(.2)	8.6(.2)	16.0(.3)	13.1(.3)	27.9(.4)	29.9(.4)	14.4(.4)	12.8(.3)
Cu	49(8)	51(9)	30(9)	18(8)	17(8)	6(8)	6(6)	12(7)
Br	100(4)	125(4)	105(4)	81(3)	190(5)	141(4)	190(5)	150(5)
In	.07(.03)	<.04	<.02	<.03	<.04	<.04	<.05	<.05
I	<4.0	<4.0	<3.6	<3.7	<4.7	<4.9	<5.2	<6.0
Fe (AA)	620(150)	400(150)	190(150)	130(150)	50(150)	50(150)	<150	<150
Zn (AA)	230(17)	90(17)	70(17)	75(17)	120(17)	130(17)	130(17)	175(17)
Run 22								
Na	185(3)	145(3)	170(3)	97(2)	66(2)	32(1)	47(2)	-
Mg	170(50)	55(40)	90(45)	45(30)	45(35)	25(25)	<60	-
Al	212(3)	215(3)	298(3)	200(2)	76(2)	14.5(.7)	8.4(.6)	-
Cl	290(5)	200(4)	211(5)	96(3)	92(3)	20(2)	10(2)	-
Ca	385(60)	285(50)	280(50)	170(40)	40(15)	<15	<15	-
Ti	12(6)	13(6)	20(8)	7.2(5.6)	<11	<8	<10	-
V	3.0(.1)	4.6(.1)	8.6(.1)	6.2(.1)	5.2(.1)	3.6(.1)	9.9(.1)	-
Mn	13.9(.06)	9.7(.05)	15.6(.1)	15.4(.1)	14.7(.1)	6.7(.05)	6.7(.05)	-
Cu	23(4)	20(4)	53(5)	54(4)	66(4)	29(3)	34(3)	-
Br	3.6(.4)	4.6(.4)	9.0(.5)	7.2(.4)	7.7(.4)	7.1(.3)	9.1(.3)	-
In	.004(.003)	.006(.003)	.005(.004)	.012(.003)	.03(.003)	.01(.002)	.006(.002)	-
I	<.87	<.77	<.89	<.73	<.86	.05(3)	.69(.31)	-

(TABLE 25, continued)

Element	Stage 1	2	3	4	5	6	7	8
Run 22								
Fe (AA)	790(40)	400(40)	390(30)	300(30)	280(30)	190(30)	70(30)	-
Zn (AA)	21(4)	28(4)	45(4)	90(4)	173(4)	102(4)	77(4)	-
K	92(12)	59(9)	64(9)	46(9)	47(8)	49(8)	41(8)	-
Cu	39.5(.3)	22.6(.3)	40.2(.3)	68.6(.3)	93.9(.4)	47.1(.3)	25.7(.2)	-
Zn	15(10)	27(9)	44(9)	82(9)	161(10)	107(8)	70(9)	-
Ga	.01(.18)	.16(.12)	.14(.12)	.17(.10)	.12(.10)	.12(.08)	.34(.09)	-
As	.32(.98)	.52(.68)	1.2(.6)	1.0(.6)	2.8(.5)	1.7(.4)	1.3(.5)	-
Br	5.8(.4)	6.8(.3)	9.5(.3)	11.0(.2)	10.1(.2)	10.7(.2)	26.0(.4)	-
Sb	1.1(.2)	.62(.20)	.9(.2)	1.6(.2)	2.8(.2)	2.4(.2)	1.9(.2)	-
La	1.9(.1)	1.1(.1)	2.0(.1)	3.1(.1)	1.8(.1)	.23(.07)	.14(.07)	-
Eu	.002(.01)	.007(.01)	.01(.01)	.01(.01)	.01(.01)	.005(.01)	<.01	-
Sm	.09(.01)	.05(.01)	.07(.01)	.09(.01)	.06(.01)	.02(.01)	<.01	-
W	<.13	<.10	.14(.09)	.06(.07)	.07(.07)	.09(.07)	.08(.07)	-
Sc	.20(.01)	.18(.01)	.15(01)	.093(.02)	.057(.02)	.007(.03)	.005(.02)	-
Cr	6.5(.5)	4.2(.5)	5.0(.6)	3.8(.5)	2.8(.6)	.92(.49)	.70(.51)	-
Fe	920(75)	565(80)	460(75)	235(70)	210(70)	40(65)	40(65)	-
Co	.34(.09)	.14(.09)	.26(.09)	.10(.10)	.12(.09)	.04(.09)	.04(.09)	-
Zn	23(3)	23(3)	39(3)	78(4)	135(4)	86(4)	54(4)	-
Se	.17(.19)	<.19	<.19	<.20	<.21	.05(.19)	.67(.21)	-
Sb	.80(.13)	.72(.13)	1.2(.1)	1.4(.2)	4.5(.3)	1.4(.2)	1.7(.2)	-
Ce	1.3(.2)	.75(.17)	1.8(.2)	2.4(.2)	1.3(.2)	.20(.16)	.1(.2)	-
Hg	<.22	<.22	.19(.22)	.21(.22)	.16(.24)	.07(.22)	.25(.24)	-
Th	.072(.02)	.048(.02)	.072(.02)	.033(.028)	.02(.02)	.015(.02)	.011(.02)	-

TABLE 26: FIELD SCHOOL, EAST CHICAGO, INDIANA, Concentrations and Standard Deviations #

Element	Stage 1	2	3	4	5	6	7	8
Run 23								
Na	160(10)	250(13)	120(10)	150(12)	370(15)	225(15)	195(15)	350(20)
Mg	620(220)	<380	<400	<250	350(250)	315(270)	<500	<700
Al	475(7)	421(7)	455(7)	312(6)	225(6)	72(3)	59(3)	23(3)
Cl	490(25)	540(25)	380(25)	335(20)	600(25)	700(30)	690(30)	2170(50)
Ca	780(180)	650(100)	520(130)	470(105)	500(130)	155(80)	155(80)	155(105)
Ti	45(20)	30(15)	<20	<20	<25	<30	<35	<45
V	3.7(.2)	2.9(.2)	4.4(.2)	4.4(.2)	4.2(.2)	2.8(.2)	5.2(.2)	29.1(.4)
Mn	42.6(.4)	26.4(.3)	31.5(.4)	25.6(.3)	37.5(.4)	42.5(.4)	61.5(.5)	70.1(.5)
Cu	16(10)	13(10)	11(10)	19(9)	15(12)	20(9)	<10	40(13)
Br	5.5(2.5)	5.8(2.1)	22(2)	24(2)	30(3)	24(3)	38(3)	225(5)
In	.03(.02)	.03(.02)	.02(.02)	<.02	.02(.02)	.06(.02)	.05(.02)	.08(.03)
I	<4.5	<4.2	<4.4	<4.0	<4.9	<5.0	<6.0	<7.7
Fe (AA)	2160(460)	630(300)	800(300)	690(300)	810(300)	820(300)	740(300)	610(300)
Zn (AA)	400(50)	190(50)	240(50)	300(50)	700(50)	660(50)	680(50)	650(50)
Run 24								
Fe (AA)	4960(430)	1260(290)	1210(290)	1100(290)	1100(290)	960(290)	520(290)	560(290)
Zn (AA)	255(13)	250(13)	244(13)	238(13)	655(13)	643(13)	604(13)	510(13)
Run 25								
Na	175(15)	150(15)	250(15)	135(12)	260(15)	245(15)	160(15)	340(20)
Mg	<320	330(260)	620(275)	160(210)	560(280)	170(210)	210(230)	<700
Al	1260(12)	1265(12)	1730(14)	790(9)	521(6)	102(4)	93(3)	41(3)
Cl	300(25)	300(25)	465(30)	320(25)	740(30)	830(30)	700(30)	2590(55)
Ca	3.1(.4)*	1.8(.2)*	4.2(.3)*	1.6(.2)*	830(155)	180(100)	230(100)	180(100)

All values in ng/m^3, except values denoted by an asterisk(*), which are in ug/m^3.

(TABLE 26, continued)

Element	Stage 1	2	3	4	5	6	7	8
Run 25								
Ti	60(20)	70(25)	120(30)	80(20)	65(20)	<20	<30	<40
V	4.9(.3)	5.5(.3)	8.2(.4)	4.7(.3)	6.5(.3)	4.8(.2)	6.1(.2)	28.5(.4)
Mn	92.9(.6)	78.4(.5)	103(.6)	46.7(.4)	62.7(.5)	47.3(.4)	39.2(.4)	53.6(.5)
Cu	22(15)	20(14)	12(12)	20(12)	<20	15(9)	22(8)	21(14)
Br	12(3)	11(3)	13(3)	12(2)	26(3)	24(3)	16(3)	103(4)
In	<.04	.06(.02)	.02(.02)	<.04	.09(.02)	.08(.02)	.05(.02)	.16(.02)
I	<6.8	4.3(3.1)	<7.1	<4.9	<5.8	<5.5	<5.1	<7.0
Fe (AA)	7550(220)	3210(150)	1900(150)	1500(150)	2020(150)	1100(150)	950(150)	<150
Zn (AA)	65(25)	48(25)	52(25)	57(25)	137(25)	129(25)	104(25)	87(25)
Run 26								
Fe (AA)	1910(220)	850(150)	730(150)	530(150)	490(150)	460(150)	370(150)	300(150)
Zn (AA)	172(15)	152(15)	162(15)	179(15)	461(15)	523(15)	383(15)	285(15)
Run 23, 24, 25, 26 Composite								
K	155(10)	175(8)	225(10)	195(10)	175(10)	250(10)	345(10)	795(20)
Cu	10.3(.2)	11.7(.2)	14.7(.2)	13.2(.2)	17.5(.2)	14.3(.2)	16.1(.2)	33.7(.4)
Zn	344(12)	341(12)	376(12)	395(12)	1000(15)	1200(12)	964(14)	685(20)
Ga	.44(.13)	.69(.13)	.60(.12)	.76(.14)	.48(.13)	.60(.12)	.52(.12)	1.9(.2)
As	<1.1	1.0(1.0)	.7(1.1)	4.1(1.2)	6.1(1.3)	3.8(1.2)	.33(1.3)	11.9(1.4)
Br	5.3(.2)	11.1(.2)	18.0(.2)	20.1(.2)	20.1(.2)	16.7(.2)	21.2(.2)	165(2)
Sb	.79(.10)	1.07(.11)	2.9(.1)	4.6(.1)	9.1(.1)	7.3(.1)	4.6(.1)	12.1(.2)
La	1.3(.1)	1.3(.1)	1.4(.1)	1.5(.1)	1.6(.1)	.34(.12)	<.12	<.2
Eu	.02(.004)	.02(.004)	.03(.004)	.02(.004)	.01(.004)	.005(.004)	.004(.004)	<.01
Sm	.14(.01)	.13(.01)	.15(.01)	.10(.01)	.07(.01)	.05(.01)	.04(.01)	.05(.01)
W	.04(.12)	<.11	<.13	<.13	.03(.14)	<1.4	<.14	.35(.17)

(TABLE 26, continued)

Element	Stage 1	2	3	4	5	6	7	8
Run 23, 24, 25, 26 Composite								
Sc	.49(.18)	.43(.17)	.53(.17)	.14(.16)	.31(.19)	.11(.17)	<.17	.05(.17)
Cr	13.1(5.1)	9.0(5.0)	7.1(5.0)	5.5(5.2)	10.6(5.6)	7.1(5.4)	9.9(5.1)	9.2(4.9)
Fe	5.1(1.0)*	1370(750)	2740(900)	1660(800)	1470(800)	200(800)	1170(750)	950(550)
Co	.4(.9)	.5(.9)	.5(.9)	.4(.9)	.8(.9)	.2(.9)	.1(.8)	.2(.9)
Zn	445(65)	350(60)	470(60)	440(60)	1080(100)	1430(100)	1340(95)	700(50)
Se	<2.5	<2.5	<2.5	<2.5	<2.6	<2.6	<2.6	3.2(2.3)
Sb	1.3(.9)	1.2(.9)	4.2(.9)	3.6(.9)	11.9(1.2)	10.3(1.1)	7.7(1.0)	15.6(1.3)
Ce	2.6(2.0)	1.8(1.9)	1.8(1.9)	1.7(2.0)	0.8(2.2)	0.4(2.2)	<2.3	<2.1
Hg	.5(2.4)	<2.4	<2.6	<2.6	<2.6	<2.8	<2.7	2.3(2.2)
Th	<.28	<.27	<.28	<.27	<.30	<.30	<.30	<.33

TABLE 27: WIRT SCHOOL, GARY, INDIANA, Concentrations and Standard Deviations #

Element	Stage 1	2	3	4	5	6	7	8
Run 27								
Na	100(6)	62(5)	65(5)	60(5)	175(7)	60(4)	84(5)	115(7)
Mg	200(100)	220(90)	125(90)	<150	<200	<125	<150	<240
Al	328(4)	281(3)	283(3)	169(3)	123(2)	45(1)	46(1)	20(1)
Cl	200(10)	110(8)	145(10)	135(8)	220(10)	125(8)	130(8)	590(15)
Ca	1.1(.1)*	840(90)	840(90)	350(60)	220(45)	90(20)	96(35)	26(9)
Ti	20(8)	<15	<15	<15	<20	<25	<20	<20
V	2.1(.1)	2.1(.1)	2.7(.1)	2.4(.1)	2.4(.1)	1.4(.1)	3.0(.1)	13.8(.2)
Mn	39.3(.2)	24.5(.2)	23.2(.2)	16.6(.2)	30.7(.2)	14.3(.1)	17.8(.2)	14.1(.1)
Cu	7(5)	<9	15(4)	3.8(3.2)	8.5(3.2)	<4.3	3.9(3.2)	13(5)
Br	8.3(1.3)	9.5(1.1)	18(1)	24(1)	28(1)	13(1)	37(1)	210(2)
In	<.02	<.02	<.02	<.01	<.03	<.01	<.01	<.02
I	1.4(1.2)	<2.0	<2.2	<1.9	<3.4	<1.7	<2.0	<2.5
Fe (AA)	-	530(50)	350(50)	270(50)	280(50)	290(50)	220(50)	230(50)
Zn (AA)	-	29(6)	40(6)	53(6)	80(6)	45(6)	34(6)	25(6)
K	-	120(5)	93(5)	70(4)	30(5)	107(5)	94(8)	105(10)
Cu	-	2.23(.10)	2.32(.11)	2.51(.10)	2.51(.11)	1.86(.11)	2.55(.18)	4.27(.20)
Zn	-	38(6)	53(6)	68(6)	135(6)	102(6)	73(8)	44(9)
Ga	-	.12(.06)	.10(.06)	.07(.05)	.11(.06)	.08(.06)	.09(.08)	.22(.09)
As	-	.28(.36)	.30(.35)	.30(.34)	.35(.40)	.30(.36)	1.0(.6)	1.2(.6)
Br	-	9.0(.1)	11.5(.1)	14.2(.1)	17.2(.1)	12.6(.1)	42(.4)	145(2)
Sb	-	1.0(.1)	.90(.10)	.80(.10)	3.7(.1)	2.1(.1)	1.7(.1)	1.6(.1)
La	-	.27(.03)	.35(.03)	.43(.03)	.41(.36)	.05(.03)	.19(.08)	.25(.09)
Eu	-	.01(.002)	.01(.003)	.01(.002)	.005(.002)	.006(.002)	.001(.004)	.003(.004)
Sm	-	.066(.005)	.053(.005)	.042(.004)	.025(.005)	.004(.004)	.01(.01)	.01(.01)
W	-	.08(.05)	.10(.05)	.12(.05)	.10(.05)	.04(.04)	.03(.08)	.07(.08)

All values in ng/m^3, except values denoted by an asterisk(*), which are in ug/m^3.

(TABLE 27, continued)

Element	Stage 1	2	3	4	5	6	7	8
Run 27								
Sc	-	.19(.01)	.10(.01)	.07(.01)	.035(.01)	.015(.01)	.04(.09)	.024(.09)
Cr	-	4.3(.4)	3.0(.4)	2.8(.4)	2.5(.4)	2.2(.4)	1.9(2.5)	2.5(2.6)
Fe	-	670(65)	560(65)	400(60)	270(60)	265(55)	155(40)	75(35)
Co	-	.05(.06)	.05(.06)	.06(.06)	.04(.06)	.03(.07)	.07(.57)	.21(.56)
Zn	-	35.4(2.6)	45.3(2.6)	56.1(2.6)	100(3)	75.2(3.0)	63.1(17.9)	39.4(17.0)
Se	-	.40(.20)	.09(.21)	.04(.19)	.26(.22)	.22(.21)	.60(1.1)	.88(.98)
Sb	-	.93(.10)	.62(.09)	.71(.09)	2.6(.5)	1.7(1.0)	2.3(0.7)	2.0(0.7)
Ce	-	.24(.16)	.24(.16)	.24(.15)	.24(.15)	.12(.16)	.37(.99)	.17(.96)
Hg	-	.09(.33)	.17(.33)	.26(.34)	.36(.34)	.42(.33)	<1.4	<1.4
Th	-	.027(.02)	.021(.02)	.010(.02)	.022(.02)	.02(.02)	<.18	<.18

TABLE 28: GARY AIRPORT, GARY, INDIANA, Concentrations and Standard Deviations #

Element	Stage 1	2	3	4	5	6	7	8
Run 28								
Na	14(4)	12(4)	17(4)	16(4)	9(3)	14(4)	28(4)	-
Mg	140(50)	160(50)	60(40)	<50	<50	<50	<50	-
Al	410(5)	364(4)	291(4)	161(3)	98(3)	18(2)	18(2)	-
Cl	100(10)	80(8)	56(6)	55(6)	65(6)	80(8)	195(11)	-
Ti	59(20)	27(20)	34(20)	<20	20(20)	<20	<20	-
V	1.5(.1)	1.7(.1)	1.4(.1)	1.4(.1)	1.2(.1)	0.4(.1)	0.3(.1)	-
Mn	8.8(.2)	8.2(.2)	7.0(.2)	4.1(.1)	3.8(.1)	3.2(.1)	2.5(.1)	-
Cu	<10	<10	<10	<10	<10	<10	<10	-
Br	10(1)	12(1)	18(2)	23(2)	28(2)	23(2)	22(2)	-
Fe (AA)	1350(65)	460(50)	400(50)	180(50)	120(50)	<50	<50	<50
Zn (AA)	200(30)	80(20)	50(20)	40(20)	90(20)	130(20)	150(25)	80(20)
Run 29								
Fe (AA)	1.4(.2)*	0.7(.2)*	0.8(.2)*	0.5(.15)*	0.5(.15)*	0.3(.2)*	0.3(.2)*	0.2(.15)*
Zn (AA)	56(10)	29(10)	69(10)	74(10)	220(20)	160(20)	220(20)	290(25)
Run 29 Duplicate Analyses								
Fe (AA)	1.4(.2)*	0.7(.2)*	0.8(.1)*	0.5(.1)*	0.5(.1)*	0.4(.1)*	0.3(.1)*	0.2(.1)*
Zn (AA)	60(10)	30(10)	61(10)	72(10)	210(20)	150(20)	120(20)	270(25)

All values in ng/m^3, except values denoted by an asterisk(*), which are in ug/m^3.

(TABLE 28, continued)

Element	Stage 1	2	3	4	5	6	7	8
Run 30								
Na	335(40)	155(20)	150(20)	170(25)	200(25)	150(25)	250(30)	130(20)
Mg	780(350)	420(240)	240(220)	450(270)	830(300)	175(200)	<300	<300
Al	940(10)	920(9)	610(6)	632(6)	523(5)	347(4)	288(3)	107(11)
Cl	1425(150)	685(75)	530(60)	855(90)	750(80)	730(80)	995(100)	815(90)
Ca	1.1(.2)*	0.6(.1)*	0.7(.1)*	0.6(.1)*	0.4(.1)*	<0.1*	001(.1)*	<0.1*
Ti	40(20)	70(20)	50(20)	60(20)	40(20)	20(15)	10(15)	20(15)
V	2.0(.2)	2.0(.2)	2.0(.2)	1.5(.2)	1.1(.1)	0.5(.1)	0.4(.1)	2.0(.2)
Mn	42(4)	24(2)	25(2)	27(3)	52(5)	41(4)	23(2)	6(1)
Cu	60(17)	48(15)	28(12)	65(15)	15(11)	15(12)	18(9)	13(8)
Br	22(4)	20(3)	25(4)	27(4)	32(4)	32(4)	31(4)	89(10)
Fe (AA)	1940(200)	680(100)	720(100)	500(50)	540(50)	210(50)	180(30)	<10
Zn (AA)	71(10)	55(9)	69(9)	53(8)	67(8)	52(8)	62(8)	8(8)
Run 31								
Na	235(15)	150(10)	230(15)	235(15)	200(15)	180(12)	225(15)	190(15)
Mg	<400	250(175)	<400	<400	<550	<350	<400	<400
Al	797(10)	521(8)	503(8)	288(6)	213(6)	57.7(3.0)	41.4(2.8)	30(3)
Cl	530(25)	290(20)	460(25)	420(25)	680(30)	320(20)	560(25)	770(30)
Ca	1.5(.2)*	1.3(.2)*	1.2(.2)*	500(150)	640(150)	330(120)	<180)	<300
Ti	30(20)	40(15)	<30	<25	<30	<20	<25	<30
V	3.0(.3)	2.4(.2)	3.4(.2)	2.7(.2)	2.4(.2)	1.0(.1)	1.3(.1)	9.2(.3)
Mn	17.5(.3)	13.8(.3)	13.1(.3)	10.3(.2)	38.8(.4)	12.9(.2)	19.9(.3)	22(.4)
Cu	13(12)	<21	<20	<20	<20	7.8(6.0)	8(7)	<80
Br	7.5(1.9)	15.7(1.9)	24(2)	25(2)	28(3)	14(2)	31(2)	50(4)
In	<.03	<.03	<.03	<.03	<.04	<.03	<.03	<.03
I	<3.5	<3.5	<3.5	<3.4	<5.3	<3.3	<4.1	<4

(TABLE 28, continued)

Element	Stage 1	2	3	4	5	6	7	8
Run 31								
Fe (AA)	2050(350)	530(260)	470(260)	330(260)	280(260)	190(260)	190(260)	270(260)
Zn (AA)	64(23)	52(23)	82(23)	87(23)	250(23)	230(23)	150(23)	200(23)
Run 32								
Fe (AA)	1690(290)	740(220)	760(220)	540(220)	590(220)	510(220)	330(220)	220(220)
Zn (AA)	93(12)	71(12)	83(12)	91(12)	140(12)	137(12)	100(12)	108(12)
Run 33								
Na	450(20)	270(15)	260(15)	295(15)	230(15)	405(20)	260(15)	245(15)
Mg	1.1(.3)*	0.4(.3)*	310(240)	340(230)	<420	<480	<400	<500
Al	2040(15)	1260(12)	869(10)	559(8)	240(6)	50(3)	25(2)	32(2)
Cl	800(35)	710(30)	680(30)	550(25)	600(25)	1015(35)	760(30)	970(35)
Ca	12.9(.6)*	6.0(.4)*	4.0(.3)*	1.6(.2)*	600(135)	160(80)	55(30)	<130
Ti	85(30)	65(30)	75(20)	<20	<25	<20	<20	<30
V	7.5(.4)	9.0(.3)	8.1(.3)	7.5(.3)	5.8(.2)	4.0(.2)	5.0(.2)	36.5(4.7)
Mn	110(1)	52.4(.5)	37.6(.4)	35.7(.4)	21.6(.3)	22.1(.3)	19.7(.3)	20.5(.3)
Cu	<50	13(15)	12(12)	<23	<18	<15	<15	25(14)
Br	16(4)	18(3)	19(2)	15(2)	16(2)	23(2)	22(2)	36(3)
In	<.06	<.04	<.04	<.04	<.03	<.03	<20	0.4(.2)
I	<7.7	<5.4	<5.1	<4.6	<3.8	<4.4	2.1(2.0)	<3.4
Fe (AA)	1150(230)	690(160)	740(160)	570(160)	570(160)	420(160)	290(160)	240(160)
Zn (AA)	78(13)	67(13)	104(13)	140(13)	445(13)	370(13)	229(13)	132(13)

(TABLE 28, continued)

Element	Stage 1	2	3	4	5	6	7	8
Run 34								
Fe (AA)	830(150)	570(150)	510(150)	370(150)	240(150)	120(150)	150(150)	<150
Zn (AA)	96(15)	89(15)	140(15)	170(15)	282(15)	253(15)	172(15)	206(15)
Run 31, 32, 33, 34 Composite								
K	310(12)	150(9)	140(10)	105(10)	120(10)	355(10)	245(10)	425(20)
Cu	9.1(.3)	4.5(.2)	5.6(.2)	4.8(.2)	4.9(.2)	4.7(.2)	5.5(.2)	14.2(.4)
Zn	97(12)	42(10)	81(11)	107(11)	295(11)	256(11)	157(10)	162(18)
Ga	<.17	<.12	<.13	<.13	<.12	.04(.12)	.11(.12)	.97(.2)
As	1.4(.8)	.71(.65)	.45(.74)	.30(.76)	.22(.73)	.39(.74)	1.1(.7)	4.6(1.4)
Br	22.1(.3)	17.0(.2)	27.0(.3)	29.0(.3)	30.0(.3)	27.6(.3)	33.6(.3)	86(1)
Sb	3.2(.2)	1.1(.1)	1.4(.1)	1.5(.1)	2.1(.1)	1.8(.1)	1.1(.1)	2.3(.2)
La	2.6(.2)	2.2(.1)	3.1(.1)	4.1(.1)	3.1(.1)	.52(.11)	.20(.10)	.37(.21)
Eu	.041(.01)	.02(.005)	.02(.005)	.02(.005)	.01(.005)	<.006	<.006	<.01
Sm	.28(.01)	.08(.01)	.11(.01)	.10(.01)	.07(.01)	.01(.01)	.01(.01)	.03(.01)
W	<.14	<.11	<.12	<.13	<.12	<.12	.05(.12)	<.18
Sc	.76(.11)	.30(.09)	.23(.08)	.17(.08)	.095(.09)	.035(.09)	.01(.1)	<.23
Cr	9.3(3.9)	3.6(3.5)	2.4(1.9)	4.0(1.9)	1.4(1.9)	1.6(1.9)	1.4(1.8)	1.3(5.5)
Fe	1620(500)	875(450)	745(440)	525(470)	440(450)	220(460)	395(440)	525(700)
Co	.57(.56)	.76(.61)	.38(.51)	.38(.58)	.32(.60)	.19(.58)	.32(.58)	.72(1.2)
Zn	105(20)	54(19)	71(19)	103(20)	312(26)	245(25)	153(21)	168(36)
Se	<3	<2.9	<2.8	<2.9	<2.9	<2.9	<2.8	4.6(2.8)
Sb	2.8(.6)	1.2(.6)	1.0(.6)	1.7(.6)	2.1(.6)	1.8(.6)	1.4(.6)	2.8(1.4)
Ce	3.2(1.4)	2.6(1.2)	1.7(1.2)	3.7(1.1)	1.2(1.2)	.5(1.2)	<1.4	<2.6
Hg	.22(1.4)	<1.2	<1.4	<1.2	<1.3	<1.2	.2(1.2)	<2.9
Th	.049(.16)	.07(.16)	<.18	.02(16)	<.16	<.16	<.17	<.39

(TABLE 28, continued)

Element	Stage 1	2	3	4	5	6	7	8
Run 35								
Na	88(8)	43(4)	32(4)	33(4)	82(6)	51(4)	46(5)	44(7)
Mg	<300	180(75)	100(65)	220(80)	<200	<130	<170	<230
Al	309(6)	233(4)	161(3)	124(3)	75(2)	24(1)	9.4(1.1)	15(1)
Cl	215(15)	94(7)	55(6)	65(6)	205(10)	71(7)	82(8)	250(15)
Ca	680(140)	230(70)	160(40)	40(30)	120(50)	55(40)	80(55)	55(55)
Ti	30(15)	20(15)	20(10)	<15	<25	<20	<15	<15
V	.7(.1)	.9(.1)	.7(.1)	.6(.1)	0.7(.1)	0.7(.05)	2.0(.1)	3.0(.1)
Mn	10.4(.2)	3.4(.1)	2.7(.1)	3.2(.1)	6.2(.1)	5.5(.1)	10.1(.1)	6.5(.1)
Cu	12(7)	5(4)	<4	<4	<8	<3	<4	<6
Br	98(3)	82(2)	66(2)	88(2)	280(3)	108(2)	86(2)	82(2)
In	<.03	<.02	<.02	<.02	<.03	<.02	<.02	<.02
I	<3.2	<2.1	<1.7	<1.8	<3.3	<2.6	<2.2	<2.3
Fe (AA)	370(230)	210(150)	190(150)	120(150)	90(150)	80(150)	100(150)	80(150)
Zn (AA)	81(16)	83(16)	89(16)	97(16)	151(16)	141(16)	117(16)	89(16)
K	79(10)	77(11)	29(10)	24(8)	40(9)	26(10)	50(10)	30(10)
Cu	3.30(.31)	2.94(.31)	1.31(.31)	1.75(.32)	6.10(.41)	1.67(.33)	4.0(.3)	3.0(.3)
Zn	13.9(9.6)	18.1(11.9)	21.5(11.3)	34.4(14.0)	92(20)	53(14)	49(12)	14.2(11.1)
Ga	<.16	<.15	.11(.12)	.06(.11)	<.2	<.15	.016(.16)	.44(.17)
As	<1.2	<1.2	.60(1.0)	<1.1	<1.5	<1.1	.09(1.2)	.58(1.1)
Br	150(1)	115(1)	67(1)	99(1)	330(2)	130(1)	128(1)	114(1)
Sb	2.0(.3)	0.6(0.2)	.80(.21)	.25(.31)	1.0(.4)	.72(.33)	3.7(.3)	3.8(.3)
La	.25(.11)	.24(.11)	.14(.10)	.15(.10)	<.13	<.12	<.13	<.13
Eu	<.01	.003(.01)	.002(.004)	.006(.005)	<.01	.005(.006)	.002(.006)	.001(.01)
Sm	.04(.01)	.03(.01)	.03(.01)	.008(.01)	.03(.01)	.01(.01)	<.02	<.01
W	<.20	<.07(.18)	<.16	<.18	<.24	<.19	<.19	.07(.18)

(TABLE 28, continued)

Element	Stage 1	2	3	4	5	6	7	8
Run 35								
Sc	.09(.29)	.07(.29)	.04(.29)	.06(.29)	.06(.29)	.02(.29)	.04(.29)	.02(.29)
Cr	4.1(3.2)	2.1(2.9)	1.4(2.8)	.4(3.6)	1.4(2.8)	1.4(2.8)	1.4(1.8)	<3.8
Fe	700(200)	280(400)	140(380)	140(380)	<760	<760	<760	<760
Co	.2(1.1)	.4(1.1)	.2(.9)	.2(1.2)	<1.9	.5(1.4)	.5(1.3)	<1.4
Zn	15(18)	26(25)	30(25)	36(26)	88(27)	50(26)	42(26)	15(25)
Se	<5.1	<4.3	<5.0	<5.2	<3.4	<3.4	<4.4	<4.4
Sb	1.5(1.4)	1.2(2.7)	.4(2.3)	.9(2.3)	2.6(2.4)	2.8(2.4)	3.1(2.4)	4.2(1.4)
Ce	1.2(3.0)	1.2(2.8)	<3.0	<3.0	<3.1	<3.0	<3.0	<3.1
Hg	<3.0	.6(2.7)	<3.6	<2.9	<2.9	.3(2.9)	.1(2.9)	.3(2.9)
Th	.06(.42)	.04(.22)	<.4	<.32	.16(.32)	.06(.32)	<.4	.04(.32)
Run 35 Duplicate Sample								
Na	100(9)	44(6)	35(5)	40(5)	105(10)	45(5)	42(5)	50(8)
Mg	<400	175(85)	110(70)	250(100	<250	<100	<120	<100
Al	350(10)	235(5)	170(4)	130(3)	105(3)	20(2)	9(2)	5(2)
Cl	240(17)	100(8)	65(6)	80(7)	220(12)	50(8)	77(8)	280(15)
Ca	700(160)	240(90)	160(60)	<150	120(80)	<50	<50	<50
Ti	35(20)	20(15)	20(20)	<20	<20	<20	<20	<15
V	.8(.1)	.9(.1)	.8(.1)	.7(.1)	.7(.1)	.7(.05)	1.5(.1)	2.6(.1)
Mn	11.1(.2)	3.1(.1)	2.9(.1)	3.8(.1)	8.6(.1)	4.9(.1)	10.9(.1)	6.8(.1)
Cu	14(8)	6(4)	4(6)	<4	<6	<3	<4	<4
Br	108(4)	81(2)	67(2)	98(3)	300(5)	68(4)	80(4)	89(4)
In	<.04	<.03	<.03	<.025	<.03	<.02	<.02	<.02
I	<4.0	<3.0	<2.5	<2.5	<3.5	<2.0	<2.5	<2.4
Fe (AA)	370(230)	200(150)	200(150)	150(150)	100(150)	75(150)	100(150)	70(150)
Zn	85(17)	86(17)	90(17)	100(18)	150(18)	131(18)	106(17)	100(17)

TABLE 29: CENTRAL FIRE STATION, GARY, INDIANA, Concentrations and Standard Deviations #

Element	Stage 1	2	3	4	5	6	7	8
Run 36								
Na	26(7)	19(6)	29(6)	21(5)	21(4)	24(3)	34(5)	-
Mg	240(90)	320(95)	240(95)	220(90)	180(90)	120(80)	80(70)	-
Al	337(4)	269(4)	244(3)	164(3)	93(2)	50(2)	34(1)	-
Cl	120(10)	110(10)	140(10)	160(15)	160(15)	180(15)	210(20)	-
Ti	70(15)	20(15)	27(16)	<15	<20	<15	<15	-
V	2.1(.2)	1.9(.1)	1.9(.1)	1.7(.1)	1.4(.1)	0.6(.1)	0.8(.1)	-
Mn	71(.4)	47(.3)	39(.3)	23(.2)	13(.2)	12(.2)	13(.2)	-
Cu	<12	<12	<12	<12	<12	<12	<12	-
Br	15(2)	26(2)	29(2)	48(2)	45(1)	24(1)	19(1)	-
Fe (AA)	2.0(.3)*	0.9(.2)*	1.1(.2)*	0.3(.2)*	<.2*	<.2*	<.2*	-
Zn (AA)	50(20)	30(15)	50(20)	60(20)	110(25)	110(25)	120(25)	140(25)
Run 37								
Fe (AA)	1.0(.2)*	0.5(.2)*	0.4(.2)*	0.2(.2)*	0.5(.2)*	0.7(.2)*	0.7(.2)*	0.7(.2)*
Zn (AA)	24(10)	17(10)	15(12)	21(12)	110(20)	140(20)	110(15)	160(20)
Run 38								
Na	450(20)	90(10)	70(10)	100(10)	70(10)	50(10)	55(10)	160(20)
Mg	1900(800)	500(200)	250(120)	220(180)	260(240)	160(120)	<200	<250
Al	1100(40)	870(30)	400(70)	320(10)	370(10)	90(10)	35(5)	78(9)
Cl	1200(30)	480(20)	320(10)	650(20)	540(20)	200(10)	185(25)	525(55)
Ti	89(28)	52(14)	35(10)	26(10)	<15	<15	<15	<15
V	3.3(.3)	2.0(.2)	1.4(.1)	1.0(.1)	0.8(.1)	0.7(.1)	1.0(.1)	2.0(.2)
Mn	73(1)	26(1)	16(1)	18(1)	19(1)	14(1)	26(3)	14(1)

All values in ng/m^3, except values denoted by an asterisk(*), which are in ug/m^3.

(TABLE 29, continued)

Element	Stage 1	2	3	4	5	6	7	8
Run 38								
Cu	170(30)	9(10)	<10	26(9)	11(8)	7(5)	5(5)	6(6)
Br	88(4)	54(2)	43(2)	49(2)	69(2)	35(1)	43(5)	370(40)
In	<.1	<.1	<.1	<.1	<.1	<.1	<.1	<.1
I	<2.5	<1	<1	<1	<1	<1	<1	<1
Fe (AA)	1200(200)	650(200)	430(100)	380(100)	230(100)	<100	130(100)	<100
Zn (AA)	105(15)	60(10)	41(10)	43(10)	65(10)	50(10)	48(10)	19(10)

TABLE 30: CITY HALL, HAMMOND, INDIANA, Concentrations and Standard Deviations #

Element	Stage 1	2	3	4	5	6	7	8
Run 39								
Na	105(10)	130(10)	135(10)	135(10)	120(10)	120(10)	125(10)	-
Al	800(10)	610(10)	540(10)	360(10)	170(10)	120(10)	70(10)	-
Cl	150(15)	200(20)	210(20)	160(15)	150(15)	120(12)	100(10)	-
Ti	30(10)	80(20)	30(15)	30(20)	<15	<10	<10	-
V	3.3(.1)	3.7(.1)	4.2(.2)	1.7(.1)	2.6(.1)	3.4(.1)	4.2(.2)	-
Mn	50(.5)	36(.4)	31(.4)	23(.3)	24(.3)	14(.3)	7(.2)	-
Cu	<10	<10	<10	14(11)	25(13)	19(12)	<10	-
Br	11(2)	21(3)	31(3)	31(3)	29(3)	33(3)	39(4)	-
Fe (AA)	890(100)	370(100)	380(95)	230(95)	240(95)	230(95)	<130	160(120)
Zn (AA)	70(30)	30(20)	40(20)	70(25)	150(30)	140(30)	60(20)	40(20)
Run 40								
Fe (AA)	320(20)	260(20)	260(20)	130(20)	140(15)	110(15)	130(15)	140(15)
Zn (AA)	35(10)	25(7)	25(7)	41(11)	70(12)	48(10)	64(12)	29(10)
Run 41								
Na	260(20)	200(15)	200(15)	195(12)	150(12)	150(12)	90(10)	255(20)
Mg	1300(400)	850(350)	790(350)	260(200)	220(210)	210(200)	<300	305(290)
Al	1280(50)	1140(45)	1000(40)	530(18)	370(16)	110(6)	115(6)	170(8)
Cl	915(35)	610(30)	1120(35)	535(20)	360(20)	240(20)	135(15)	1110(35)
Ca	2000(250)	1300(200)	720(140)	270(90)	200(70)	<50	60(35)	60(60)

All values in ng/m^3, except values denoted by an asterisk(*), which are in ug/m^3.

(TABLE 30, continued)

Element	Stage 1	2	3	4	5	6	7	8
Run 41								
Ti	60(20)	30(20)	40(20)	16(14)	25(15)	<15	<15	20(15)
V	2.0(.2)	2.0(.2)	1.7(.2)	1.5(.2)	1.4(.2)	1.1(.2)	1.0(.1)	1.0(.1)
Mn	60(3)	24(1)	20(1)	19(1)	20(1)	16(1)	10(1)	6(1)
Cu	19(18)	20(18)	10(17)	32(11)	11(10)	<10	<10	16(11)
Br	28(3)	27(2)	48(3)	34(2)	27(2)	25(2)	20(2)	125(3)
Fe (AA)	450(75)	390(75)	320(50)	170(50)	70(50)	70(50)	60(50)	<50
Zn (AA)	74(10)	61(10)	65(10)	61(10)	100(12)	64(10)	52(10)	17(10)

TABLE 31: LAKE MICHIGAN, Concentrations and Standard Deviations #

Element	Stage 1	2	3	4	5	6	7	8
Run 42								
Na	140(20)	130(20)	230(30)	240(30)	190(25)	220(20)	110(15)	94(26)
Mg	<400	<500	<450	1400(600)	550(400)	730(490)	430(410)	<900
Al	590(13)	1035(17)	1570(20)	2540(25)	561(9)	1220(18)	552(12)	52.9(4.8)
Cl	660(40)	820(45)	800(60)	1000(60)	650(40)	420(40)	220(30)	1440(80)
Ca	540(240)	710(240)	540(240)	770(240)	120(120)	1550(350)	<100	<100
Ti	<20	15(15)	25(12)	20(18)	12(10)	<25	<20	<20
V	1.1(.3)	2.2(.4)	2.3(.5)	3.9(.6)	2.6(.4)	3.1(.4)	1.3(.3)	.60(.26)
Mn	29.9(.5)	43.4(.6)	38.9(.5)	139(1)	56.6(.6)	58.3(.7)	39.2(.6)	11.8(.4)
Cu	<25	26(21)	25(25)	33(32)	23(14)	310(30)	<30	79(16)
Br	33(4)	125(5)	130(6)	270(9)	180(7)	720(10)	55(4)	200(6)
In	<.05	<.06	<.07	<.1	<.06	<.11	<.06	<.07
I	<6.6	<8.0	<9.2	<14	<7.8	<13	<7.3	<8.5
K	107(28)	195(35)	240(45)	335(45)	86(28)	315(50)	120(30)	30(27)
Cu	2.01(.93)	1.48(1.1)	11.5(1.1)	21.2(1.6)	11.8(1.0)	180(5)	13.1(1.0)	67(2)
Zn	84(34)	104(56)	100(65)	102(77)	115(50)	255(40)	56(40)	235(65)
Ga	3.4(2.4)	3.9(2.8)	2.0(2.1)	7.3(3.9)	6.0(3.5)	6.3(3.6)	1.8(2.1)	7.4(12)
As	1.8(2.5)	1.4(3.6)	1.3(2.6)	1.5(4.8)	1.7(5.2)	2.1(6.2)	4.7(2.7)	12(11)
Br	26(4)	135(15)	171(18)	260(30)	92(11)	635(70)	46(6)	165(20)
Sb	1.9(.5)	4.8(.8)	2.1(.6)	6.7(1.2)	1.6(.7)	5.4(1.6)	2.4(.6)	1.3(1.1)
La	.35(.25)	.56(.31)	.98(.26)	1.8(.4)	.92(.27)	.89(.38)	.53(.45)	.42(2.4)
Eu	.02(.02)	<.03	.02(.02)	.04(.03)	.02(.02)	.01(.03)	.02(.02)	.02(.02)
Sm	.017(.02)	.025(.03)	.051(.03)	.11(.05)	.04(.03)	.06(.07)	.03(.02)	<.04
W	1.2(.8)	.89(.47)	.57(.34)	1.3(.6)	.22(.80)	1.3(1.0)	.37(.32)	.25(.55)

Values in ng/m^3, except values denoted by an asterisk(*), which are in ug/m^3.

(TABLE 31, continued)

Element	Stage 1	2	3	4	5	6	7	8
Run 43								
Na	770(95)	495(65)	140(45)	130(60)	225(55)	435(60)	505(70)	<125
Mg	2.6(2.0)*	2.6(1.2)*	<1.5*	1.8(1.2)*	1.2(1.1)*	<2.0*	<2.1*	<4000
Al	4390(68)	2680(55)	1100(35)	7710(80)	5610(80)	2490(55)	6935(90)	66.8(17.7)
Cl	2850(200)	975(120)	655(90)	2650(165)	1460(130)	1440(120)	2610(170)	7000(350)
Ca	7.0(1.5)*	2.1(.8)*	1.5(1.0*	2.8(1.5)*	260(260)	260(260)	<500	<500
Ti	165(50)	80(70)	<40	<100	<90	<90	<105	<80
V	12(2)	5.2(1.3)	6.2(1.0)	6.1(2.2)	2.5(1.7)	<1.5	5.2(1.9)	9.2(1.1)
Mn	308(3)	45.9(1.4)	45.6(1.4)	31.1(1.1)	56.3(1.6)	32.7(1.2)	44.0(1.4)	11.2(1.1)
Cu	<115	<140	<40	<150	<90	<140	<200	370(80)
Br	270(23)	120(12)	240(14)	190(13)	215(14)	1245(26)	990(25)	920(24)
In	<.33	<.17	<.18	<.17	<.21	<.28	<.18	<.19
I	<42	<21	<22	<21	<26	<36	<32	<9.0
K	830(150)	500(140)	375(95)	350(100)	310(100)	405(135	495(135)	200(120)
Cu	35(5)	12(4)	11(4)	7.8(3.0)	<4.3	5.2(6)	4.9(5.4)	380(15)
Zn	330(190)	180(190)	90(170)	550(205)	500(200)	515(355)	750(350)	1710(365)
Ga	8.1(11)	14(12)	4.4(6.9)	5.9(11)	6.4(8.5)	5.8(9.4)	10(10)	12(12)
As	14(12)	17(12)	12(10)	4.9(13)	3.0(10)	3.1(18)	5.1(8.1)	10(6)
Br	220(25)	210(25)	230(30)	245(30)	285(35)	1240(135)	770(85)	1050(115)
Sb	28(3)	14(3)	13(2)	9.8(2.8)	6.2(2.6)	6.9(4.5)	8.0(5.1)	21(5)
La	1.9(1.1)	1.4(1.1)	3.3(.9)	3.7(1.2)	3.0(.9)	3.8(3.7)	4.1(3.1)	.42(.86)
Eu	.08(.09)	.03(.09)	.12(.07)	.09(.09)	.10(.08)	.12(.11)	.12(.11)	.13(.11)
Sm	.14(.11)	.13(.11)	.08(.10)	.06(.12)	.10(.11)	.10(.18)	.08(.15)	.08(.18)
W	1.6(1.5)	1.5(1.6)	.57(1.4)	1.8(1.6)	2.3(1.4)	1.6(1.7)	1.4(1.9)	1.7(2.2)
Run 43 Duplicate Analyses								
Na	690(90)	495(65)	110(40)	145(65)	215(55)	415(55)	465(65)	95(60)
Mg	2.7(2.1)*	2.4(1.1)*	<1.2*	<1.4*	1.2(1.2)*	<1.9*	<2.0*	<4.0*

(TABLE 31, continued)

Element	Stage 1	2	3	4	5	6	7	8
Run 43 Duplicate Analyses								
Al	4120(61)	2600(50)	1050(36)	7900(90)	5410(80)	2400(50)	6600(80)	72(19)
Cl	2760(190)	955(110)	620(85)	2920(175)	1325(125)	1295(115)	2790(170)	7500(400)
Ca	6.1(1.4)*	1.8(.7)*	1.6(1.0)*	3.0(1.6)*	275(290)	230(260)	<500	<600
Ti	150(50)	50(70)	<50	<100	<90	<95	<110	<100
V	10(2)	5.0(1.2)	6.1(1.0)	5.6(2.4)	3.0(1.8)	<1.5	5.0(2.0)	10.0(1.4)
Mn	300(3)	41.3(1.2)	43.2(1.4)	33.3(1.6)	48.3(1.4)	30.9(1.1)	44.0(1.4)	12.2(1.2)
Cu	<100	<140	<40	<140	<95	<150	<195	390(100)
Br	290(25)	110(10)	210(15)	195(15)	225(15)	1140(24)	890(30)	900(25)
In	<.30	<.16	<.18	<.21	<.23	<.30	<.19	<.22
I	<42	<20	<20	<23	<29	<36	<30	<33
Run 44								
Na	330(45)	700(60)	690(50)	520(45)	1590(80)	210(35)	680(50)	340(90)
Mg	1.0(.7)*	3.4(.8)*	<1400	<1600	1.4(1.2)*	<1300	<1600	<3300
Al	1030(30)	2160(40)	954(28)	787(26)	1950(40)	1300(35)	219(17)	80(15)
Cl	370(65)	850(95)	1080(90)	830(85)	2.38(.13)*	470(65)	525(75)	9.8(.3)*
Ca	570(380)	950(570)	1130(570)	570(380)	1100(550)	570(380)	570(380)	<700
Ti	<40	<55	<45	<50	<50	<40	<40	<70
V	2.9(.7)	5.7(1.0)	3.6(.7)	2.5(.7)	1.8(1.0)	<1.4	4.0(.6)	10.7(1.0)
Mn	42.5(1.1)	76.6(1.5)	12.2(.7)	13.1(.7)	26.2(.9)	22.4(.8)	18.2(.8)	11.9(.9)
Cu	65(42)	<80	<90	<80	<100	<80	<80	480(60)
Br	65(8)	315(15)	1500(25)	380(13)	245(11)	40(7)	200(10)	1130(20)
In	<.12	<.17	<.23	<.14	<.15	<.11	<.13	<.16
I	<15	<22	<30	<17	<19	<13	<17	<30

(TABLE 31, continued)

Element	Stage 1	2	3	4	5	6	7	8
Run 44								
K	260(95)	280(100)	325(140)	140(115)	390(200)	190(90)	475(135)	65(85)
Cu	35(4)	5.8(3.5)	15(6)	7.7(4.1)	5.9(4.6)	10(3)	15(4)	235(10)
Zn	140(125)	285(170)	645(360)	275(215)	365(240)	190(120)	300(180)	830(270)
Ga	11(9)	26(30)	20(19)	16(11)	17(18)	15(16)	11(10)	1.5(60)
As	11(8)	11(9)	12(11)	14(12)	9.4(15)	6.6(6.9)	10(11)	5.7(12)
Br	84(12)	240(30)	1450(160)	430(50)	240(30)	67(11)	180(20)	675(75)
Sb	4.5(1.6)	3.7(2.1)	12(4)	5.2(2.5)	4.1(2.9)	3.1(1.4)	12(2)	60(4)
La	1.1(.7)	1.5(.8)	1.0(.9)	1.7(1.2)	2.6(1.5)	1.2(.6)	1.6(1.0)	.61(.58)
Eu	.07(.07)	.07(.07)	.11(.12)	.08(.09)	.07(.07)	.03(.06)	.11(.10)	.12(.09)
Sm	.14(.07)	.09(.08)	.08(.09)	.07(.11)	.09(.12)	.05(.06)	.04(.07)	<.04
W	2.3(1.1)	2.1(1.2)	3.8(2.4)	2.6(1.5)	1.3(1.9)	1.0(1.1)	1.2(1.3)	1.2(1.4)

TABLE 32: SCHOOL OF PUBLIC HEALTH, UNIVERSITY OF MICHIGAN, ANN ARBOR, MICHIGAN
Concentrations and Standard Deviations #

Element	Stage 1	2	3	4	5	6	7	8
Run 45								
Fe (AA)	330(40)	240(40)	260(30)	130(30)	70(30)	50(30)	<30	<30
Zn (AA)	70(5)	21(5)	25(5)	16(5)	31(5)	62(5)	90(5)	50(5)
Run 46								
Fe (AA)	190(30)	180(30)	80(20)	60(20)	40(20)	40(20)	40(20)	20(20)
Zn (AA)	220(15)	220(15)	215(15)	210(15)	160(15)	70(10)	40(10)	80(10)
Run 47								
Andersen #2								
Fe (AA)	1040(50)	1050(50)	1120(50)	480(30)	250(25)	70(25)	50(25)	-
Zn (AA)	615(20)	610(20)	600(20)	465(20)	335(20)	145(15)	65(10)	-
Andersen #1								
Fe (AA)	20(20)	<20	<20	<20	<20	<20	<20	<20
Zn (AA)	10(10)	10(10)	10(10)	15(10)	<10	10(10)	20(10)	15(10)

All values in ng/m^3, except values denoted by an asterisk(*), which are in ug/m^3.

(TABLE 32, continued)

Element	Stage 1	2	3	4	5	6	7
Run 48							
Fe (AA) "upper"	1030(40)	1260(40)	630(20)	280(20)	130(20)	60(20)	<20
Fe (AA) "lower"	-	390(20)	160(20)	70(20)	30(20)	<20	<20
Zn (AA) "upper"	630(30)	625(30)	540(20)	370(20)	240(20)	100(20)	30(20)
Zn (AA) "lower"	-	440(20)	250(20)	110(20)	60(20)	20(20)	<20
Run 49							
Na	102(5)	70(4)	65(3)	37(2)	27(2)	35(4)	20.0(1.0)
Mg	<23	14(16)	18(17)	19(14)	13(13)	3(15)	4.8(9)
Al	151(7)	146(7)	158(8)	79(4)	16(1)	6.9(.4)	4.5(.3)
Cl	170(11)	101(7)	88(6)	41(3)	11.5(1)	20(3)	14(1.)
Ca	183(25)	67(16)	24(16)	37(18)	11(3)	8.0(3.7)	5.5(2.5)
Ti	15(3)	11(3)	12(3)	8.5(2.5)	1.8(.9)	2.8(1.5)	1.3(1.4)
V	.41(.05)	.38(.05)	.55(.06)	.45(.05)	.33(.02)	.57(.06)	.70(.07)
Mn	4.2(.3)	2.6(.2)	4.4(.3)	5.6(.3)	7.2(.4)	11.1(1.1)	5.9(.3)
Cu	103(10)	18(3)	11(2)	4.2(1.3)	1.3(.5)	1.4(.6)	1.7(.6)
Br	5.1(.6)	7.0(.9)	10.3(1.3)	10.2(1.3)	8.8(1.1)	14.5(1.5)	13.6(1.7)
In	.002(.001)	.002(.001)	.005(.001)	.004(.001)	.009(.001)	.010(.002)	.006(.001)
I	-	-	<.06	.13(.07)	.15(.07)	-	.43(.11)
K	41(9)	26(2)	40(4)	26(3)	13.5(2.0)	24(2)	33(3)
Cu	119(10)	15.5(1.2)	11.8(.3)	4.8(.1)	2.1(.1)	2.1(.07)	1.9(.1)
Zn	172(30)	82(7)	105(6)	66(4)	30(3)	28(3)	16(3)
Ga	0.11(.11)	0.14(.03)	0.16(.03)	0.11(.02)	0.09(.03)	0.09(.02)	0.18(.03)
As	0.57(.39)	0.40(.25)	0.61(.20)	0.81(.20)	0.70(.15)	0.72(.18)	1.1(.18)
Br	7.4(1.0)	9.6(1.2)	16(2)	14(2)	11(1.5)	14(2)	21(3)
Sb	0.14(.11)	0.18(.08)	0.30(.13)	0.37(.13)	0.44(.13)	.84(.13)	1.16(.18)

(TABLE 32, continued)

Element	Stage 1	2	3	4	5	6	7
Run 49							
La	.11(.03)	.11(.03)	.39(.04)	.47(.04)	.35(.03)	.25(.03)	.21(.02)
Eu	<.009	.0025(.001)	.004(.002)	.0023(.001)	.0002(.001)	.0003(.001)	.0013 .001)
Sm	.015(.004)	.015(.003)	.076(.005)	.016(.003)	.0033(.002)	.0068(.002)	.014(.001)
W	.23(.09)	.16(.06)	.15(.06)	.06(.09)	.04(.03)	.03(.03)	.01(.03)
Sc	.14(.07)	.093(.010)	.16(.01)	.077(.010)	.018(.003)	.0085(.001)	.005(.002)
Cr	2.0(.2)	1.0(.15)	1.6(.2)	1.3(.15)	.82(.11)	.70(.10)	.42(.10)
Fe	400(30)	185(20)	320(20)	175(20)	87(15)	54(10)	30(10)
Co	.14(.04)	.095(.025)	.19(.04)	.073(.015)	.03(.01)	.036(.020)	.045(.020)
Zn	145(10)	70(4)	95(6)	49(3)	25(2)	12(1)	12(.5)
Se	<.05	.06(.04)	.10(.07)	.89(.04)	.12(.03)	.25(.04)	.25(.04)
Sb	.16(.03)	.12(.02)	.30(.04)	.30(.02)	.37(.05)	.65(.10)	.75(.05)
Ce	.40(.10)	.30(10)	.53(.08)	.28(.05)	.08(.04)	.13(.05)	.18(.05)
Hg	.12(.10)	<.07	<.10	<.07	.1(.08)	.09(.07)	.17(.09)
Th	.03(.01)	.010(.005)	.034(.010)	.017(.084)	.004(.003)	.003(.004)	.003(.004)
Run 50							
Na	610(30)	290(20)	208(10)	77(4)	50(3)	16(1)	14.5(.9)
Mg	90(7)	55(30)	18(29)	12(20)	27(21)	<13	--
Al	200(10)	165(8)	186(9)	97(5)	39(2)	4.7(.4)	2.9(.3)
Cl	900(60)	420(30)	280(20)	98(6)	22(2)	6(1)	5.2(.8)
Ca	290(60)	200(40)	185(30)	73(17)	33(11)	9,3(3.3)	8(3)
Ti	18(7)	14(2)	19(4)	6(3)	3(3)	.9(.9)	1.1(.9)
V	.53(.08)	.55(.06)	.86(.09)	.67(.07)	1.2(.1)	.93(.06)	1.1(.1)
Mn	3.5(.3)	2.6(.2)	3.8(.2)	5.2(.3)	12.5(.8)	4.3(.3)	3.3(.2)
Cu	17(4)	7(2)	10(3)	5.0(1.7)	4.6(1.5)	1.4(.5)	.95(.52)
Br	6.5(.9)	8.2(1.0)	11.7(1.5)	10.3(1.3)	14(2)	6.4(.8)	8.6(1.1)
In	.005(.003)	.003(.002)	.008(.002)	.009(.002)	.033(.003)	.015(.002)	.01(.001)
I	.39(.18)	0.33(.07)	--	--	.29(.12)	.33(.10)	.36(.10)

TABLE 33: "HIGH VOLUME" SAMPLE RUNS,
Concentrations and Standard Deviations, ng/m³

Element	Sample Run			
	3	4	8	9
Na	1310(80)	1480(8)	750(70)	975(95)
Mg	<1000	5100(1200)	6500(1500)	20800(2000)
Al	3900(20)	4540(30)	2390(25)	2980(30)
Cl	2230(180	2800(160)	2280(140)	5080(165)
Ca	12200(1300)	9800(850)	15900(850)	53800(2100)
Ti	<10	<15	<15	45(15)
V	17(1)	25(1)	25(1)	35(1)
Mn	754(4)	888(3)	1550(4)	2150(5)
Cu	195(50)	200(50)	75(70)	87(43)
Br	59(8)	80(17)	136(20)	136(22)
In	0.096(.06)	<0.12	<0.15	<0.09
K	640(130)	2300(165)	1690(115)	3410(140)
Cu	170(3)	185(3)	99(3)	129(4)
Zn	1480(125)	2910(165)	6180(150)	2420(125)
Ga	0.9(1.2)	3.2(1.8)	0.4(1.1)	1.0(1.1)
As	16(7)	22(10)	26(6)	24(6)
Br	46(3)	69(4)	131(3)	153(3)
Sb	19(2.5)	40(4)	24(2)	18(2)
La	3.6(.9)	4.1(1.2)	1.6(.8)	0.72(.85)
Eu	0.03(.04)	0.11(.08)	0.02(.05)	<0.05
Sm	0.21(.09)	0.84(.10)	0.19(.08)	0.20(.08)
W	0.4(1.3)	6.7(1.9)	0.3(1.2)	0.5(1.2)
Sc	1.2(.8)	3.2(.8)	0.56(.81)	0.7(.8)
Cr	82(24)	185(26)	23(23)	40(21)
Fe	18800(4100)	29700(4800)	10350(3950)	21900(3900)
Co	1.8(3.5)	3.9(3.4)	1.7(3.5)	1.7(3.2)
Zn	1510(175)	3000(195)	6400(210)	2400(165)
Se	10.4(12.2)	<12	9.1(11.9)	8.2(11)
Sb	18(4.3)	24(5)	27(5)	17(5)
Ce	1.8(10.2)	30(9)	5.8(9.8)	6.3(9.1)
Hg	14(11)	11(10)	10(10)	1.2(9.5)
Th	1.0(1.6)	2.1(1.7)	2.4(1.5)	0.6(1.4)
Fe(AA)	12400(500)	18100(650)	13000(500)	22400(900)
Zn(AA)	1290(25)	2460(25)	7650(100)	1890(30)
(Total Aero-sol)	398000	430000	562000	705000

(TABLE 33, continued)

Element	Sample Run			
	10	15	16	17
Na	850(75)	685(45)	440(40)	1005(60)
Mg	11100(600)	950(900)	1100(900)	1500(1000)
Al	2320(30)	777(22)	874(21)	1710(27)
Cl	2950(120)	2160(100)	450(60)	1510(105)
Ca	43800(3400)	1930(330)	1550(300)	5000(700)
Ti	<20	<15	<20	17(8)
V	23(1)	20(1)	110(2)	130(2)
Mn	2170(4)	153(2)	188(2)	275(2)
Cu	100(40)	39(24)	15(40)	25(40)
Br	137(7)	175(8)	36(7)	88(12)
In	<0.06	0.54(.05)	<0.05	<0.09
K	2220(190)	775(130)	425(115)	790(115)
Cu	128(4)	67(3)	18.1(2.5)	32(2)
Zn	2510(105)	940(135)	340(115)	955(125)
Ga	1.8(1.0)	0.5(1.2)	2.2(1.1)	2.4(1.3)
As	25(6)	15(7)	4.2(6.3)	10.9(6.7)
Br	137(2)	160(4)	36(3)	76(3)
Sb	20(2)	18(2)	7.5(2.2)	15(2)
La	1.3(.7)	2.7(.8)	14(1)	17(1)
Eu	<0.05	0.05(.06)	0.05(.05)	0.05(.05)
Sm	0.08(.07)	0.20(.09)	0.55(.08)	0.65(.08)
W	0.14(.83)	2.1(1.4)	<1.3	1.1(1.3)
Sc	0.8(.8)	1.1(.8)	0.24(.79)	1.0(.7)
Cr	17(20)	47(26)	15(22)	102(25)
Fe	15900(3100)	2380(1200)	3230(1400)	5330(1840)
Co	<9.1	0.8(3.1)	1.6(3.3)	2.1(3.1)
Zn	2395(165)	1330(340)	325(140)	1030(150)
Se	<14	9.9(12.4)	10(11)	<11
Sb	14(5)	21(5)	11(4)	14(4)
Ce	4.8(10)	4.6(10.1)	14(9)	<8
Hg	<15	11.7(10.3)	3.6(9.3)	1.1(9.2)
Th	0.8(1.3)	0.5(1.5)	2.1(1.9)	0.4(1.3)
Fe(AA)	11650(600)	2110(310)	2530(290)	4130(400)
Zn(AA)	1290(25)	1000(20)	400(15)	980(20)
(Total Aero-sol)	514000	108000	98000	145000

(TABLE 33, continued)

Element	Sample Run			
	18	20	21	23
Na	880(45)	885(45)	535(35)	1785(95)
Mg	3050(1750)	<1000	<1200	4700(1600)
Al	2340(30)	1541(18)	989(16)	2810(35)
Cl	1070(170)	1910(65)	1800(75)	10300(210)
Ca	10000(1100)	1900(500)	1070(290)	4900(800)
Ti	42(15)	14(12)	<13	60(45)
V	206(4)	53(1)	41(1)	79(2)
Mn	142(2)	265(1)	108(1)	538(3)
Cu	110(65)	100(45)	120(40)	180(60)
Br	640(20)	160(7)	410(8)	535(20)
In	<0.12	0.22(.05)	0.05	0.53(.15)
K	850(120)	385(90)	270(90)	1790(140)
Cu	80(3)	140(3)	162(2)	151(3)
Zn	950(150)	750(110)	330(100)	3260(170)
Ga	6.3(1.5)	1.9(1.1)	2.4(.9)	4.0(1.5)
As	9.7(8.4)	14(6)	3.6(6.1)	35(8)
Br	490(4)	135(3)	490(2)	530(4)
Sb	32(2)	32(2)	7.8(2.3)	45(3)
La	9.2(1.1	3.1(.8)	15.6(.8)	6.6(1.1)
Eu	0.27(.06)	0.06(.04)	0.03(.04)	0.07(.07)
Sm	1.25(.09)	0.42(.07)	0.54(.07)	0.74(.10)
W	0.7(1.1)	0.76(.89)	0.98(.88)	2.2(1.6)
Sc	6.1(.8)	0.64(.60)	0.81(.60)	2.4(.8)
Cr	65(26	51(21)	20(21)	95(26)
Fe	4400(2600)	4900(2400)	2230(2300)	8980(1300)
Co	4.9(4.7)	2.6(3.4)	2.0(4.1)	2.1(3.2)
Zn	1080(165)	750(110)	345(110)	4220(420)
Se	<15	5.3(12)	<14	1.9(13)
Sb	35(6)	40(5)	2.4(5.3)	225(15)
Ce	<10	7.0(8.5)	16(9)	16(10)
Hg	1.6(12)	6.4(10)	11(12)	11(11)
Th	1.1(1.4)	0.9(1.2)	0.7(1.2)	0.5(1.6)
Fe(AA)	3740(350)	3330(300)	2000(300)	6040(600)
Zn(AA)	1070(25)	610(25)	370(20)	2500(50)
(Total Aero-sol)	180000	159000	125000	303000

(TABLE 33, continued)

Element	Sample Run			
	25	26	51	52
Na	2120(120)	1645(80)	2900(110)	890(45)
Mg	<4000	4200(1400)	4100(1900)	1800(700)
Al	5120(55)	2640(35)	4920(45)	1170(16)
Cl	13300(260)	6510(180)	17200(270)	1705(65)
Ca	23000(1650)	5400(800)	11600(1100)	2700(450)
Ti	65(16)	25(12)	45(15)	<14
V	106(2)	71(2)	160(2)	74(1)
Mn	890(5)	432(3)	480(3)	227(1)
Cu	190(60)	110(50)	165(80)	160(30)
Br	380(25)	980(20)	940(20)	85(7)
In	<0.06	<0.14	0.57(.16)	<0.06
K	3980(145)	890(100)	2135(155)	350(195)
Cu	190(4)	62(3)	260(4)	140(5)
Zn	12200(190)	2340(145)	3280(185)	480(110)
Ga	10(2)	1.6(1.4)	8.2(2.2)	0.8(2.0)
As	62(9)	28(7)	59(10)	14(12)
Br	295(4)	525(4)	800(6)	68(5)
Sb	41(2)	64(2)	210(4)	32(4)
La	9.6(1.3)	11(1)	15(1)	4.2(1.6)
Eu	0.22(.07)	<0.06	0.32(.08)	0.11(.10)
Sm	1.24(.10)	0.64(.08)	1.4(.1)	0.26(.15)
W	1.9(1.2)	0.6(1.0)	0.9(1.3)	0.8(1.7)
Sc	8.5(.8)	1.5(.8)	3.9(.7)	1.0(1.6)
Cr	155(27)	85(22)	155(29)	42(33)
Fe	17800(3600)	8300(2300)	7650(2850)	6250(4550)
Co	9.9(4.5)	2.6(3.7)	9.8(4.3)	<9.4
Zn	12300(200)	2290(150)	2720(160)	520(110)
Se	26(15)	5.3(13)	<18	23.1
Sb	61(6)	55(6)	215(8)	40(13)
Ce	26(11)	20(9)	33(11)	17(20)
Hg	4.0(12)	9.7(13)	9.7(14)	27(26)
Th	2.5(1.3)	<1.4	2.5(1.6)	2.6(2.5)
Fe(AA)	19100(750)	5950(550)	6810(650)	4850(500)
Zn(AA)	9600(110)	2600(50)	2740(50)	580(40)
(Total Aero-sol)	645000	237000	304000	157000

ABSTRACT

WATER POLLUTION IN LAKE MICHIGAN BY TRACE ELEMENTS FROM POLLUTION AEROSOL FALLOUT

by

J. W. Winchester
G. D. Nifong

Presented at a conference on Nuclear Techniques in Atmospheric Pollution Studies, American Nuclear Society, San Francisco, Cal., 1969.

Certain trace elements which are strongly associated with air pollution sources in the Lake Michigan basin may be contributing significantly to lake water pollution by an atmospheric fallout route. In this paper a partial inventory of air pollution emissions for 30 trace elements is presented for the Chicago, Milwaukee, and northwest Indiana metropolitan areas, based on available published information, and compared with natural and pollution stream trace element inputs. Evidence indicates that the atmosphere may be the major source of Zn in Lake Michigan, and atmospheric inputs of Cu and Ni are also considerable. Moreover, the evidence suggests that air pollution probably exceeds expected unpolluted stream inputs for many additional elements in Lake Michigan, highlighting the need for more comprehensive chemical data to quantify the evaluation.